

https://dspace.org/

Characterisation of South African indigenous microalgae for biofuel production potential

Grobler, Jasper

2019

https://hdl.handle.net/10539/29670

Grobler, Jasper Jan Hendrik. (2019). Characterization of South African indigenous microalgae for Biofuel production potential. University of the Witwatersrand, https://hdl.handle.net/10539/29670

Downloaded from a DSpace repository. https://dspace.org/

UNIVERSITY OF THE WITWATERSRAND, JOHANNESBURG

CHARACTERISATION OF SOUTH AFRICAN INDIGENOUS MICROALGAE FOR BIOFUEL PRODUCTION POTENTIAL

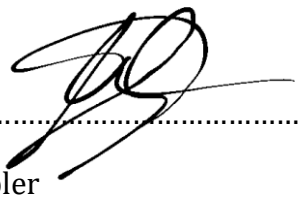
JASPER GROBLER

A dissertation submitted to the Faculty of Engineering and the Built Environment, University of the Witwatersrand, in fulfilment of the requirements for the degree of Master of Science in Engineering.

Johannesburg, 13 August 2019

DECLARATION

I , Jasper Grobler (student no 1776234), declare in accordance of Rule G27 that this dissertation is my own unaided work. It is being submitted to the Degree of Master of Science in Engineering to the University of the Witwatersrand, Johannesburg. It has not been submitted before for any degree or examination to any other University.



……

Jasper Grobler

13 August 2019

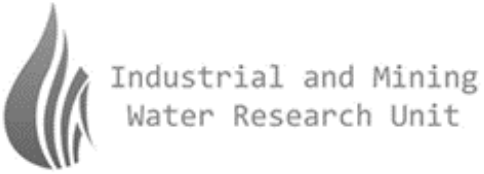
ACKNOWLEDGEMENTS

- Main supervision and support by Doctor Michelle Low and Professor Kevin Harding at the Industrial and Mining Water Research Unit (IMWaRU), University of Witwatersrand, Johannesburg, South Africa.
- Facilities and funding by the Council for Industrial and Scientific Research (CSIR), Pretoria, South Africa
- Supervision and support by Doctor Santosh Ramchuran and Monique Smit at Biosciences, CSIR, Pretoria, South Africa.
- Supervision and support by Doctor Pierre Durand and genetic work performed by his team at the Evolutionary Complexity Laboratory, University of Witwatersrand, Johannesburg, South Africa.
- Funding by the South African National Energy Development Institute (SANEDI).
- Funding by the Department of Science and Technology.











ABSTRACT

Bio-energy has been widely studied as a renewable energy source. One of the main challenges of traditional bio-energy is that it competes with local food and agriculture industries for feedstock and arable land. Bio-energy derived from a microalgal biomass feedstock has the potential to be used without competing with agriculture and food industries. Bio-diesel and bio-ethanol can be generated from cellular lipids and carbohydrates, respectively, isolated from microalgal biomass. In this study we evaluated the potential of South African indigenous microalgae for use in bio-diesel and bio-ethanol production by firstly identifying an isolate suitable for biofuel production, suitable cultivation medium and analysing bio-fuel properties.

Fifteen South African indigenous microalgal isolates from the Microalgal Culture Collection of South Africa (MiCCSA) were cultivated at 2 L scale and characterised to derive their bio-fuel production potential. The isolate referred to as WCB 4.1, identified as *Acutodesmus bajacalifornicus*, showed good potential for use in bio-energy production, and was used in subsequent studies throughout the work.

To explore the potential of increasing lipid, carbohydrate and yield rates of WCB 4.1, eleven potential microalgal cultivation mediums were identified. WCB 4.1 showed the highest growth rate in the JG medium (in-house formulation), with a competitive growth rate of 0.47 d^{-1}. WCB 4.1 showed the highest biomass productivity in the Hase medium, with a relatively low productivity of 53.1 mg/L/d.

To be able to fully understand the effect different cultivation mediums have on the cultivation of WCB 4.1, the effect of medium variation on biomass biochemical composition was considered. The bio-diesel yield rate of WCB 4.1 grown in four of the cultivation mediums was superior to that of first-generation bio-energy crops. However, the bio-ethanol yield rate from WCB 4.1 was inferior to first generation bio-energy crops. Utilising bio-diesel property predictive formulas it was possible to predict the properties of bio-diesel generated from WCB 4.1 biomass cultivated in eleven different mediums. It was found that WCB 4.1 biomass from eight of the mediums adhered to South African summer grade bio-diesel standards.

WCB 4.1 shows potential to become a commercially competitive strain for bio-energy production, which can produce more bio-diesel per hectare annually than traditional food crops. The bio-energy yield rates of WCB 4.1 do however need some improvement to be able to have bio-energy productivities similar or higher than microalgal bio-energy productivities described by other sources. The key to unlock the potential of WCB 4.1 would be in further process development and improvement.

TABLE OF CONTENTS

DECLARATION I

ACKNOWLEDGEMENTS II

ABSTRACT III

LIST OF FIGURES VI

LIST OF TABLES IX

NOMENCLATURE XI

CHAPTER 1: INTRODUCTION AND MOTIVATION ..... - 1 -

1.1 INTRODUCTION AND MOTIVATION ..... - 1 -

1.2 PROBLEM STATEMENT ..... - 6 -

1.3 STUDY AIM AND OBJECTIVES ..... - 7 -

CHAPTER 2: LITERATURE REVIEW ..... - 8 -

2.1 MICROALGAL BIOLOGY ..... - 8 -

2.2 MICROALGAL CULTIVATION ..... - 13 -

2.3 BIOMASS HARVESTING ..... - 24 -

2.4 COMMERCIAL PURPOSES FOR MICROALGAL CULTIVATION ..... - 25 -

CHAPTER 3: CHARACTERISATION OF ISOLATES FOR BIOENERGY PRODUCTION POTENTIAL AND SELECTION ..... - 36 -

3.1 INTRODUCTION ..... - 36 -

3.2 METHODS ..... - 36 -

3.3 RESULTS AND DISCUSSION ..... - 43 -

3.4 CONCLUSION ..... - 51 -

CHAPTER 4: PRE-CULTIVATION AND MEDIUM STUDY OF SELECTED ISOLATE WCB 4.1- 52 -

4.1 INTRODUCTION ..... - 52 -

4.2 METHODS ..... - 52 -

4.3 RESULTS AND DISCUSSION ..... - 57 -

4.4 CONCLUSION ..... - 67 -

CHAPTER 5: LIPID AND CARBOHYDRATE FRACTIONAL EXTRACTION ..... - 68 -

5.1 INTRODUCTION ..... - 68 -

5.2 METHODS ..... - 68 -

5.3 RESULTS AND DISCUSSION ..... - 72 -

5.4 CONCLUSIONS ..... - 82 -

CHAPTER 6: CONCLUSION AND RECOMMENDATION ..... - 83 -
REFERENCES ..... - 86 -
APPENDIX A ..... - 99 -
APPENDIX B ..... - 145 -
APPENDIX C ..... - 158 -

List of Figures

Figure 1: Global distribution of oil reserves between the Middle East and the rest of the world. - 2 -

Figure 2: Diagrammatic representation of the fatty acid methyl transesterification reaction for the production of biodiesel. - 4 -

Figure 3: Simple depiction of the bioethanol production process. - 5 -

Figure 4: Comparison between microalgae and macroalgae. - 8 -

Figure 5: Microalgal growth phases: Microalgal cell concentration over time. - 9 -

Figure 6: Representation of a natural logarithm growth curve with accompanying growth phases. The slope of the linear trend line in the exponential phase is indicative of the intrinsic growth rate. - 11 -

Figure 7: Demonstration of how yield rate slopes can vary depending on the time points at which they are taken. - 12 -

Figure 8: Balanced chemical reaction for the generation of microalgal biomass. - 13 -

Figure 9: Growth rate of *Mycobacterium tuberculosis* in Dubos' medium as a function of glucose concentration. - 14 -

Figure 10: Relationship between pentachlorophenol concentration and microbial growth rate calculated using the Haldane modification of the Monod equation. - 15 -

Figure 11: Number of algal species in each lipid content category under Nitrogen replete and deficient conditions. - 16 -

Figure 12: Growth profiles of three microalgal strains cultivated under increased nitrogen (+N) and reduced nitrogen (-N) Chu medium No. 10. - 17 -

Figure 13: Biomolecule content (ash, carbohydrate, total lipid and protein) of three microalgal strains cultivated under +N and −N Chu medium No. 10.. - 17 -

Figure 14: Fluctuation of CO_2, HCO_3^{-1} and CO_3^{-2} concentrations vs pH. - 19 -

Figure 15: Representation of different types of cultivation systems and photobioreactors - 23 -

Figure 16: Neon light and magnetic stirrer setup for the flask study, under the work benches. - 38 -

Figure 17: Biomass yield rate of the fifteen isolates. The error bars indicate the standard deviation. - 45 -

Figure 18: Lipid yield rate of the fifteen isolates. The error bars indicate the standard deviation. - 46 -

Figure 19: Comparison between literature lipid yield rates of microalgal strains and lipid yield rates measured in this study. The error bars indicate the standard deviation... - 47 -

Figure 20: Carbohydrate yield rate of the fifteen isolates. The error bars indicate the standard deviation. - 48 -

Figure 21: Average specific biomass, lipid and carbohydrate yield rates for the fifteen microalgal isolates. The error bars indicate the standard deviation. - 49 -

Figure 22: Bar graph indicating the matrix score of each respective studied isolate from the highest to the lowest from left to right. - 50 -

Figure 23: Diagrammatic depiction of the autoclavable filtration rig. - 55 -

Figure 24: Diagrammatic depiction of the incubation setup including the light rigs and orbital shaker. - 56 -

Figure 25: Mono septic culture of WCB 4.1 resulting from microscope assisted micro tube single cell isolation. - 57 -

Figure 26: A photographic image of an agarose gel indicating the amplification of the 18S target region. - 58 -

Figure 27: Biomass over time curves for the cultivation of WCB 4.1 in six different mediums (A) and five different mediums (B) over 17 days. - 59 -

Figure 28: The specific maximum growth rate of WCB 4.1 in each medium with the error bars depicting the standard deviation. - 60 -

Figure 29: Comparison between microalgal growth rates from literature sources and the current study - 62 -

Figure 30: Bar graph depicting the biomass yield rate of WCB 4.1 in all eleven mediums, with error bars depicting the standard deviation. - 63 -

Figure 31: Biomass yield rates of different microalglal strains from literature in comparison with WCB 4.1 biomass yield rates - 63 -

Figure 32: Respective medium growth rate over nitrogen (A) and phosphorus (B) concentration plots. The grey dotted line is a visual aid to recognise the potential Monod-Haldane trend. - 65 -

Figure 33: Growth rate over Nitrogen to phosphorous ratio plot for each medium. .. - 66 -

Figure 34: Medium specific lipid yield of WCB 4.1 biomass after 17 days cultivation.- 72 -

Figure 35: Medium specific lipid and biomass yield of WCB 4.1 after 17 days of cultivation. - 73 -

Figure 36: Medium specific carbohydrate yield of WCB 4.1 over 17 days including each replicate and the average yield. The error bars represent the standard deviation. - 77 -

Figure 37: Medium specific carbohydrate percentage with the error bars representing the standard deviation. - 77 -

Figure 38: Combined medium respective biomass, lipid and carbohydrate yield at g/L scale. ..... - 78 -

Figure 39: Comparison between bioethanol yields from different crop sources with that from WCB 4.1 cultivated in different mediums. The error bars represents the standard deviation. ..... - 80 -

Figure 40: Comparison between biodiesel yields from different crop sources with that from WCB 4.1 cultivated in different mediums. The error bars represents the standard deviation. ..... - 80 -

List of Tables

Table 1: Typical properties of HVO, European EN 590:2004 diesel fuel, Gas-To-Liquid and FAME. - 4 -

Table 2: Growth rates and doubling times of microalgae reported by different literature sources. - 11 -

Table 3: Microalgal biomass production rates according to different literature sources - 13 -

Table 4: The benefits and limitations of a few different cultivation systems - 22 -

Table 5: Biomass and lipid yield rates with accompanying cellular lipid contents for different microalgal species - 27 -

Table 6: Comparison of different oil sources for biodiesel productivity. - 28 -

Table 7: European bio-diesel standards EN 14214 for vehicle use and EN 14213 for heating oil use . - 30 -

Table 8: Tmi and ΔHmi values. - 32 -

Table 9: CN and CFPP values predicted for biodiesel generated from an array of microalgal species. - 33 -

Table 10: Carbohydrate content as percentage of dry biomass of microalgal strains. - 33 -

Table 11: Biomass and carbohydrate yield rates of different microalgal strains - 34 -

Table 12: Bioethanol yield from different carbon sources . - 34 -

Table 13: Summary of some advantages and disadvantages related to different biomass measures. - 39 -

Table 14: Summary of some advantages and disadvantages related to different lipid content measures - 40 -

Table 15: Summary of some advantages and disadvantages related to different carbohydrate content measures. - 42 -

Table 16: Presumptive morphological presumptive ID and sequence data ID of fifteen isolates . - 44 -

Table 18: Scoring matrix of the specific isolate yield rates. - 50 -

Table 19: Medium composition of the JG medium. - 54 -

Table 20: Doubling times of WCB 4.1 in 11 different mediums. - 61 -

Table 21: Tmi and ΔHmi values. . - 70 -

Table 22: Nitrogen content of each respective medium. - 73 -

Table 23: Biodiesel yield and productivity of WCB 4.1 biomass cultivated in eleven different mediums. - 74 -

Table 24: Specie specific lipid yield rates with accompanying growth rates, biomass yield rates and cellular lipid contents. - 75 -

Table 25: Estimated CN, CP and CFPP values for biodiesel generated from WCB 4.1 biomass cultivated in eleven different mediums. - 76 -

Table 26: Estimated biodiesel and bioethanol productivities from WCB 4.1 biomass cultivated in eleven different mediums. - 79 -

NOMENCLATURE

AF6	Artificial fresh water 6 medium
BBM	Bold basal medium
BLAST	Basic Local Alignment Support Tool
CFPP	Cold filter plug point
CP	Crystallisation point
CN	Cetane number
CSIR	Council for Scientific and Industrial Research, South Africa
DHA	Docosahexaenoic acid
EPA	Eicosapentanoic acid
FAME	Fatty acid methyl ester
FAME-GC	Fatty acid methyl ester gas chromatography
GC	Gas chromatography
HCl	Hydrochloric acid
HPAEC	High performance anion exchange chromatography
HVO	Hydro-treated vegetable oil
IV	Iodine value
KH_2PO_4	Potassium dihydrogen phosphate
MES	2-(N-morpholino) ethanesulfonic acid
MiCCSA	Microalgal Culture Collection of South Africa
MgSO4	Magnesium Sulphate
NaOH	Sodium hydroxide
$NaNO_3$	Sodium nitrate
NO_3	Nitrate ions
OD	Optical density
PCR	Polymerase chain reaction
PO_4	Phosphate ions
rpm	Rotations per minute

Chapter 1: Introduction and Motivation

In this section, different energy sources will be discussed in order to highlight the relevance of microalgal bioenergy. This will set the scene and motivation as to why identifying a microalgal strain for bioenergy production purposes is of such importance. This chapter will ultimately conclude with the project problem statement, aim and objectives.

1.1 Introduction and Motivation

An increase in global energy demand has been seen since the start of civilisation, with global energy demand expected to spike within the next decade to support modernisation, urbanisation and increase in populations, especially in developing countries (Asif and Muneer, 2007). It has been predicted that the human population will double between 2000 to 2050 (Dincer and Rosen, 1999), which will lead to a constant increase in demand for energy.

Global energy sources are mainly classified as fossil, renewable and nuclear energy. In 2007 the world was estimated to be 80% dependent on fossil fuel energy, 13.5% dependent on renewable energy and 6.5% dependent on nuclear energy (Asif and Muneer, 2007).

1.1.1 Fossil energy

Fossil energy refers to energy derived from fossil energy deposits like petroleum, oil, coal and fossil gas. In 2007, fossil fuel contributed to approximately 80% of the world's energy supply. Depletion of fossil fuel reserves, global warming, energy security concerns and rising energy cost are four main concerns regarding the global dependence on fossil fuels (Asif and Muneer, 2007).

Fossil energy is one of the main contributors to global warming and greenhouse gas emissions. University of Uppsala, Sweden, predicted oil supplies to peak soon after 2010, and gas supplies not long afterwards (Arthur, 2003). This predicts the escalation of petrol and other fuel prices, which can adversely affect economies worldwide with high dependence on fossil fuels (Asif and Muneer, 2007, Arthur, 2003). Fossil energy sources are finite, and depletion of energy sources have been predicted by multiple sources (Shafiee and Topal, 2009, Hoel and Kverndokk, 1996). Depletion of fossil fuel reserves will lead to reduced fossil fuel supply, creating an "energy gap", which should be filled with alternative energy sources (Salameh, 2004). The depletion of fossil fuel reserves creates a challenge of energy security where the availability of fossil fuel sources become limiting. Of the trillion barrels of global oil reserves currently estimated, 66% are distributed amongst Middle Eastern countries compared to the 44% in the rest of the world (Figure 1) (IAGS, 2004). If the Middle East becomes the sole global supplier of oil,

an oil energy bottleneck is likely to form due to logistics. The reliance on the Middle East for oil is a great threat to energy security for the rest of the world.

Due to global conflict and reducing oil reserves the oil price has escalated in the last few years and is predicted to continue to do so. In such a case, the use of fossil energy would slowly become too expensive to be economically feasible (Asif and Muneer, 2007).

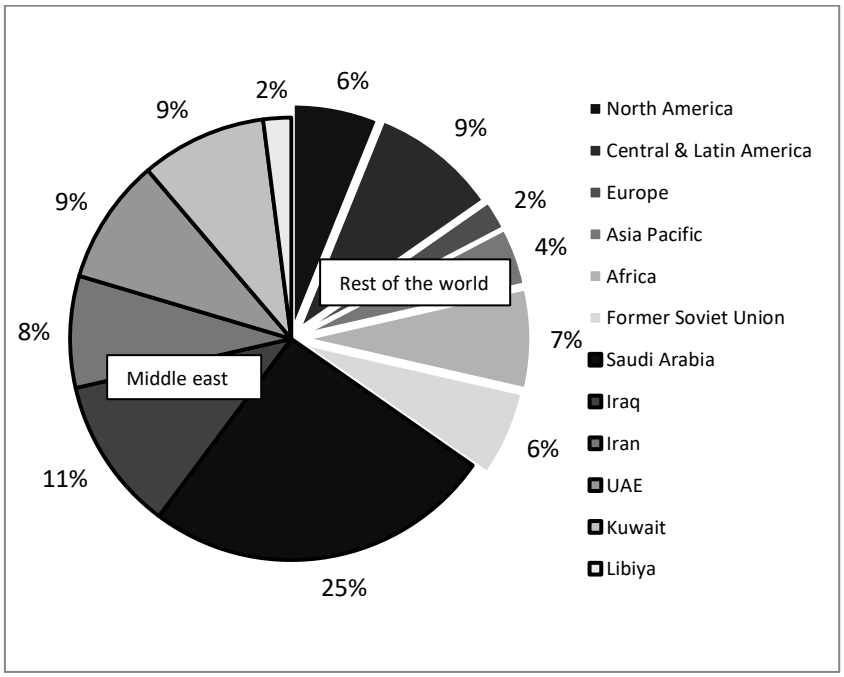


Figure 1: Global distribution of oil reserves between the Middle East and the rest of the world (IAGS, 2004).

Considering the negative impact fossil fuels have on the world and that an ultimate depletion of these sources is possible in the future, alternative energy sources are required. For this reason, alternative energy sources have received increasing attention in the last decade.

1.1.2 Nuclear energy

Nuclear energy is one of the main energy sources in some first world countries and contributes to about 6.5% of the global energy supply (Asif and Muneer, 2007). Nuclear energy refers to the utilisation of energy released by nuclear reactions such as nuclear fission, nuclear decay and nuclear fusion. Nuclear energy is considered as a possible alternative to fossil energy and has been implemented worldwide with great success. Drawbacks of nuclear energy include cost, radiation contamination, safety and proliferation of weapons material (Sackett, 2001). Additionally, nuclear energy is one of the most expensive energy sources to establish and maintain. This is predominantly due to extensive staffing requirements and increasing complexity of plant design to ensure safety (Sackett, 2001).

1.1.3 Renewable energy

Renewable energy refers to energy derived from sources, which cannot be depleted such as wind, hydro, solar, biomass and geothermal energy sources. The renewable energy sector is the fastest growing energy sector worldwide. In 2003, the renewable sector investment showed a distribution of 38%, 24%, 21% and 17% between wind power, solar PV, solar thermal and other renewable sources (small hydropower, bio-energy and geothermal power) respectively (Asif and Muneer, 2007). Renewable energy solutions can be tailor-made to consider the potential and requirements of a specific country. This study is focused on renewable energy in the form of bio-energy, the other renewable energy sources will not be discussed in detail.

Bio-energy

Bio-energy is a form of renewable energy derived from biomass. Bio-energy can be stored in the form of chemical potential energy as combustible liquids, gas or solids which can be utilised at demand (Nigam and Singh, 2011). Examples of bio-energy include combustible solids (wood, agricultural waste), bio-diesel, bio-ethanol, bio-acetone, bio-butanol, bio-methane and bio-hydrogen. Bio-diesel and bio-ethanol are the most common forms being used industrially.

Bio-diesel

Bio-diesel refers to the liquid derived from oil sourced from renewable biomass with properties similar to that of commercial diesel. There are two main forms of bio-diesel namely; fatty acid methyl esters (FAMEs) and hydro treated vegetable oils (HVOs).

FAMEs are generated when neutral fatty acids undergo a reaction referred to as “fatty acid methyl transesterification” (Van Gerpen, 2009). In this reaction a strong alcohol, such as methanol, esterifies the fatty acid chains of triglycerides in the presence of a strong alkaline or acidic catalyst. The products of this reaction are glycerol and FAMEs as depicted in the chemical formula in Figure 2 (Van Gerpen, 2009).

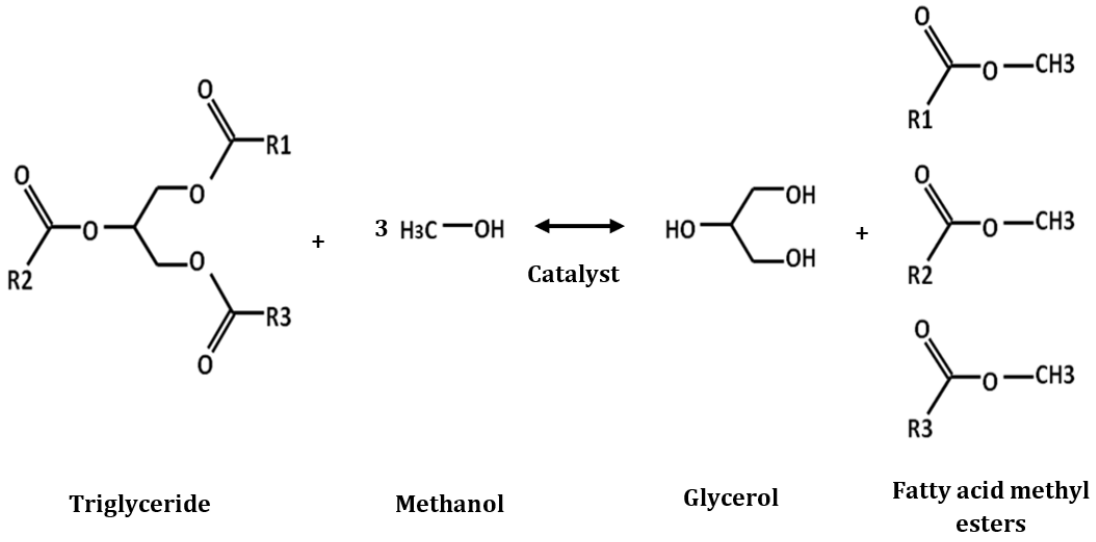


Figure 2: Diagrammatic representation of the fatty acid methyl transesterification reaction for the production of bio-diesel drawn from the reaction as described by (Liu, 1994).

HVOs are generated in a reaction that takes place when neutral fatty acids react in the presence of hydrogen gas to produce hydrocarbon chains, water and propane (Satyarthi *et al*., 2013). The production of HVO is more expensive than that of FAMEs. An advantage of using HVO production is that two bio-energy products are being produced; diesel like hydrocarbons and propane. Another advantage of HVO fuel is that it has near perfect fuel properties: high oxidative stability compared to conventional diesel (EN 590) and FAMEs as displayed in Table 1 (Satyarthi *et al*., 2013). EN 590 can be used as the gold standard for ideal diesel properties.

Table 1: Typical properties of HVO, European EN 590:2004 diesel fuel, Gas-To-Liquid and FAME (Satyarthi *et al*., 2013).

Property	EN 590 (summer grade)	HVO	Gas-To-Liquid	FAME (from rape seed oil)
Density at 15 °C (kg/m³)	~835	775 – 785	770 – 785	~885
Viscosity at 40 °C (mm²/s)	~3.5	2.5 – 3.5	3.2 – 4.5	~4.5
Cetane number	~53	~80 – 99	~73 – 81	~51
Distillation range (°C)	~180 – 360	~180 – 320	~190 – 330	~350 – 370
Cloud point (°C)	~ -5	-5 – -25	-0 – -25	~-5
Heating value, lower (MJ/kg)	~42.7	~44	~43.0	~37.5
Heating value, lower (MJ/l)	~35.7	~34.4	~34.0	~33.2

Property	EN 590 (summer grade)	HVO	Gas-To-Liquid	FAME (from rape seed oil)
Total aromatics (wt-%)	~30	0	0	0
Polyaromatics (wt-%)	~4	0	0	0
Oxygen content (wt-%)	0	0	0	~11
Sulfur content (mg/kg)	<10	<10	<10	<10
Lubricity HFRR at 60 °C (mm)	<460(2)	<460(2)	<460(2)	<460
Storage stability	Good	Good	Good	Very challenging

Bioethanol

Bio-ethanol refers to ethanol produced via a biological fermentation process (Bai *et al.*, 2008). *Saccharomyces cerevisiae* (brewer's yeast) fermentation coupled with fractional distillation is the most common process used for bio-ethanol production (Figure 3) (Bai *et al.*, 2008). *S. cerevisiae* utilises monosaccharide sugars as an energy and carbon source to grow (Bai *et al.*, 2008). Under anaerobic conditions, *S. cerevisiae* switches to an anoxic metabolism where glucose is converted to ethanol (Bai *et al.*, 2008). The ethanol yield from fermentation can be predicted as a 90-93% (w/v) conversion of glucose to ethanol (Bai *et al.*, 2008). With the ethanol tolerance of yeast going up to ~15%, the ideal concentration of glucose to avoid residual sugar and low yield should be ~17% (w/v) in the fermentation cultivation media.

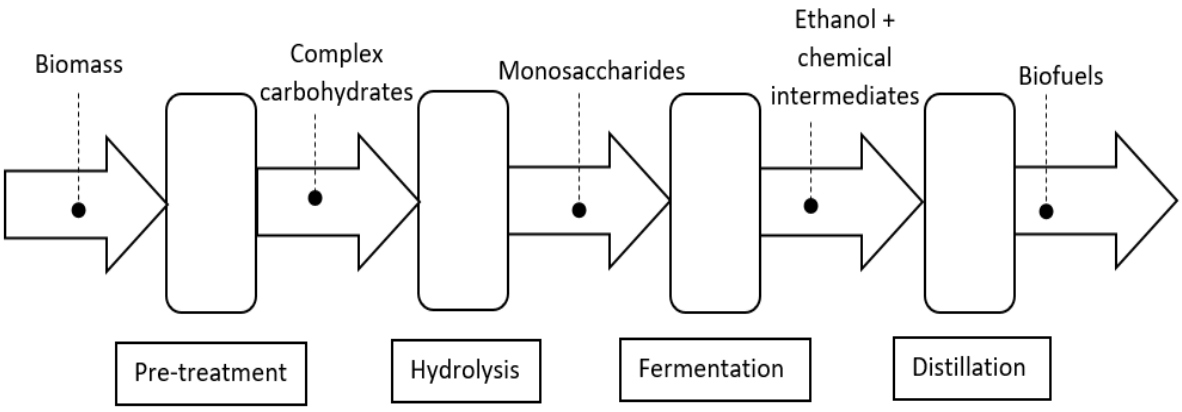


Figure 3: Simple depiction of the bioethanol production process(Van der Cruys, 2014).

Bio-energy biomass sources

Bio-energy can be divided into different generations depending on the type of biomass used.

- First generation bio-energy refers to bio-energy from food crops such as corn grown on arable land.
- Second generation bio-energy is derived from non-food crops and lingo-cellulosic biomass such as wood and agricultural waste.
- Third generation bio-energy is derived from algal biomass (Ahmad et al., 2011)

Microalgae are microscopic single cellular algae. Due to their single celled nature, fast growth rate and high lipid and carbohydrate contents, microalgae have become the focus for third generation bio-energy (Nigam and Singh, 2011). Microalgal biomass show great potential as a bio-energy biomass source.

Microalgae have a few distinct advantages making it a great potential biomass source for bio-fuel production purposes:

- Does not compete with the food industry (Ahmad *et al*., 2011).
- Does not compete for arable land required for food crops (Huang *et al*., 2010).
- Can be cultivated in dams or bioreactors making its implementation versatile (Janaun and Ellis, 2010).
- Can provide high oil or carbohydrate yields (Chisti, 2007) (Rodolfi *et al*., 2009).
- Has fast growth rates and can be harvested multiple times a year (Chisti, 2007).
- Can produce valuable co-products for the pharmaceutical or cosmetic industry including: decosahexanoic acid (DHA), eicosapentaenoic acid (EPA), laminarins, beta-carotene and astaxanthin (Chauton *et al*., 2015, Borowitzka, 1995).
- Can utilise atmospheric carbon dioxide (Chisti, 2007).
- Can be used for bio-remediating waste water (Pittman *et al*., 2011).
- Can be cultivated in saltwater or low-quality fresh water.

1.1.4 The Microalgal Culture Collection of South Africa

The Council for Scientific and Industrial Research (CSIR), South Africa, launched a bio-prospecting programme to collect indigenous microalgae with the aim to identify high-lipid yielding isolates in 2009. The programme resulted in the isolation of microalgae from all 9 South African provinces. In 2011 the culture collection was consolidated with the South African National Phycology Culture Collection (SANPCC) slightly increasing the number of isolates in the collection. The expanded and consolidated collection was renamed to the Microalgae Culture Collection of South Africa (MiCCSA) and contains over 500 isolates that are housed in two locations. The culture collection is maintained in duplicate by the CSIR and the University of Witwatersrand. A standardised maintenance procedure was developed for the culture collection, mainly using AF6 cultivation media. All isolate information is captured electronically for upload onto an online database at the following web address: https://sanpcc.org.za/miccsa. The online database is also

configured for upload of any future research data including data generated from this study.

1.2 Problem statement

Microalgae have been identified as a potential bioenergy source that do not compete with the food or agriculture industry. Part of the National Development Plan of South Africa 2030, is to exploit cleaner energy sources (Commission, 2012). With that been said, South Africa is home to many algal species, and therefore there is a need to find an indigenous microalgal strain and a corresponding cultivation medium that will yield competitive production rates (Smit *et al*., 2017a). Finding and characterising a suitable microalgal strain would act as a stepping stone to process development for that strain. This will be able to contribute to the vision of using microalgae as feedstock for a cleaner bio-energy production process.

1.3 Study aim and objectives

1.3.1 Aim

The aim of this work was to evaluate the potential of South African indigenous microalgae for use as biomass source for the production of both bio-diesel and bio-ethanol.

1.3.2 Study objectives

The following four objectives were used to address the aim of this project:

1. Characterise 15 microalgal isolates from the Microalgal Culture Collection of South Africa (MiCCSA) for bio-diesel and ethanol production potential, and identify the strain with the most potential.
2. Identify and characterise the performance of different cultivation media for a specific microalgal strain.
3. Evaluate combined lipid and carbohydrate extraction from a single biomass source.
4. Theoretically investigate the feasibility of simultaneous microalgal biodiesel and bioethanol production.

Chapter 2: Literature review

2.1 Microalgal biology

In this section, the different types of algae, their metabolism, growth and growth rate equations will be discussed.

2.1.1 Algae

Algae is a term used to refer to all non-plant photosynthetic organisms. Algae occur across an array of taxonomic kingdoms and phyla. Most types of algae are aquatic but some exist within lichens. Algae are grouped as macroalgae or microalgae (Figure 4). Macroalgae are multi cellular and commonly referred to as sea weed. Microalgae are microscopic single celled algae (Bellinger and Sigee, 2015).

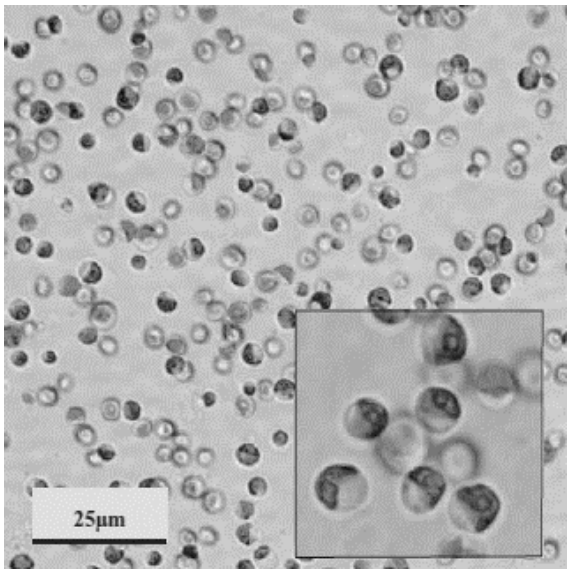
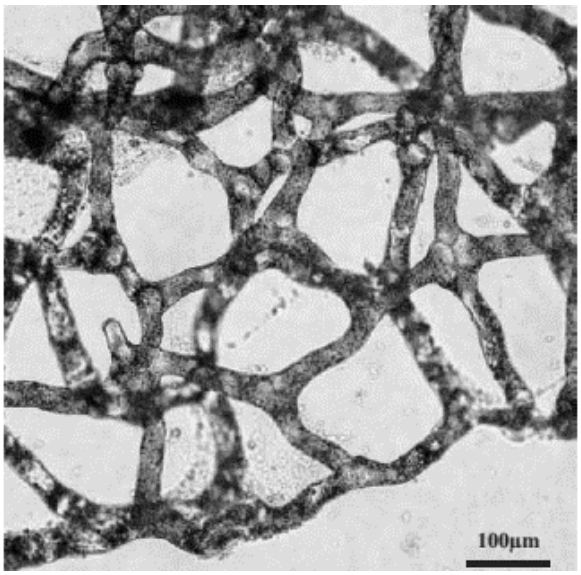
Microalgae: *Chlorella*	**Macroalgae:** *Hydrodictyon*
	

Figure 4: Comparison between microalgae and macroalgae (Bellinger and Sigee, 2015).

Microalgae can have autotrophic, mixotrophic or heterotrophic metabolisms. Autotrophic microalgae, through photosynthesis, utilise light as an energy source and inorganic carbon such as carbon dioxide as carbon source. Mixotrophic microalgae can utilise both light and organic carbon as an energy source. Heterotrophic microalgae utilise organic carbon as an energy and carbon source and can thrive in complete darkness. Heterotrophic microalgae can be phagocytotic or osmotrophic by engulfing whole organic particles/smaller organisms or by absorbing soluble nutrient through the plasma membrane respectively (Lee, 2018). It has been shown that microalgae cultivated in heterotrophic and mixotrophic conditions have higher growth rates than microalgae cultivated in purely autotrophic conditions (Yang *et al*., 2000). The dilemma regarding

the use of heterotrophic and mixotrophic microalgae for microalgal biomass production is that an organic carbon source is required for the cultivation. Common types of carbon sources utilised include glucose and acetate (Nagarajan *et al*., 2018). Unless using waste material as carbon source, the other main path way for supplying organic carbon for heterotrophic or mixotrophic cultivation is from carbon sources derived from agriculture (Nagarajan *et al*., 2018). This creates a dilemma, where resources from the agricultural and food industries will be required for the generation of microalgal bio-energy. Less carbon fixation takes place during heterotrophic and mixotrophic microalgal cultivation, compared to autotrophic cultivation. The use of waste organic carbon such as glycerol and municipal waste can be possibilities for mixotrophic microalgal cultivation to increase biomass yields, bio-remediate waste and utilise sunlight for atmospheric carbon fixation (Liang *et al*., 2009). Autotrophic microalgal cultivation is the more sustainable option for microalgal cultivation as it does not require an organic carbon source.

Microalgae commonly replicate by mitosis (Andersen, 2005). They generate logarithmic growth curves, similar to bacterial growth curves, with the difference that algal growth rates are substantially lower than bacteria. Microalgal growth rates are typically expressed as a function of days and bacterial growth rates as a function of hours (Andersen, 2005). Similar to bacteria, microalgal growth has five phases, namely: Lag phase, exponential growth phase, declining relative growth phase, stationary phase and death phase (Figure 5) (Price and Farag, 2013). Two measures commonly used to quantify microalgal growth include maximum growth rate (d^{-1}) and productivity ($mg.L^{-1}.d^{-1}$).

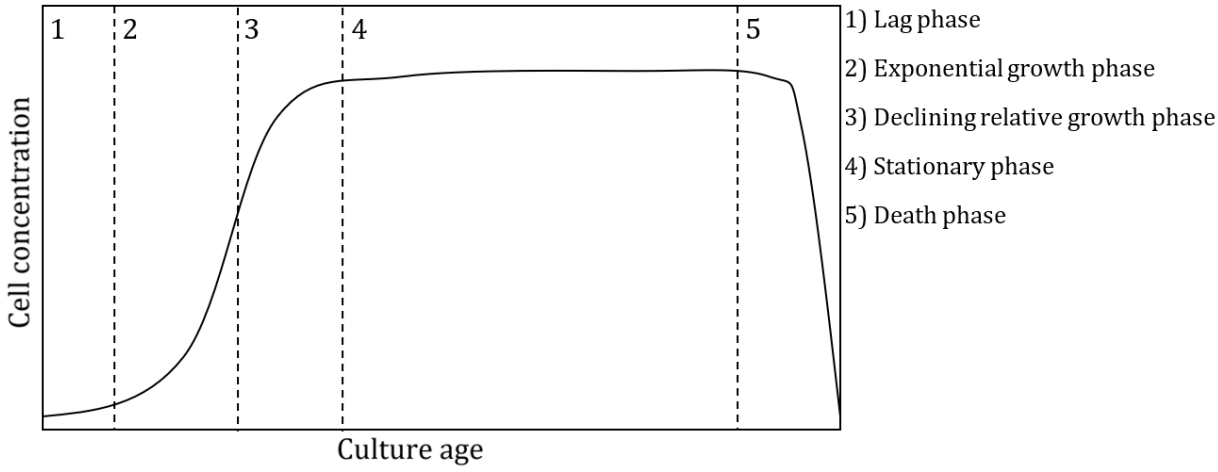


Figure 5: Microalgal growth phases: Microalgal cell concentration over time (Price and Farag, 2013).

Growth rate determination

The maximal specific growth rate (d^{-1}) can be calculated using growth curves generated from biomass, optical density (OD) and cell concentration data. During the exponential

growth phase, the increase of population size per time interval is dependent on the population size at the start of the time interval. A constant proportional increase of population size between set time intervals can be determined during exponential phase. The proportional increase can be expressed by Equation 1 as described by Guillard (Janet *et al.*, 1973).

$$\frac{\Delta n}{\Delta t} = \mu N \qquad 1$$

Where:

- Δn = the change in population size
- Δt = the change in time
- μ = growth rate (d^{-1})
- N = population size

Equation 2, the classic growth equation, can be derived from Equation 1 to determine the population size (Janet *et al.*, 1973, Andersen, 2005).

$$N_t = N_0 e^{\mu t} \qquad 2$$

Where:

- N_0 = population size at the start of a time interval
- N_t = is the population size at the end of the time interval

Equation 2 can be used to derive Equation 3 for calculating the intrinsic growth rate, considering that the intrinsic growth rate is always expressed as a function of time (t^{-1}) (Janet *et al.*, 1973, Andersen, 2005).

$$\mu = \frac{\ln(\frac{N_t}{N_0})}{\Delta t} = \frac{\ln(N_t) - \ln(N_0)}{\Delta t} \qquad 3$$

Equation 3 is similar to the calculation of the slope of a linear trend line. Microalgal growth following a logarithmic growth curve can present a near linear curve when the natural logarithmic values of the cell concentration measure are used (Choi and Lee, 2015). The intrinsic growth rate can thus be calculated by the slope of the linear trend line generated when plotting the natural logarithms of the cell concentration over time as depicted in Figure 6.

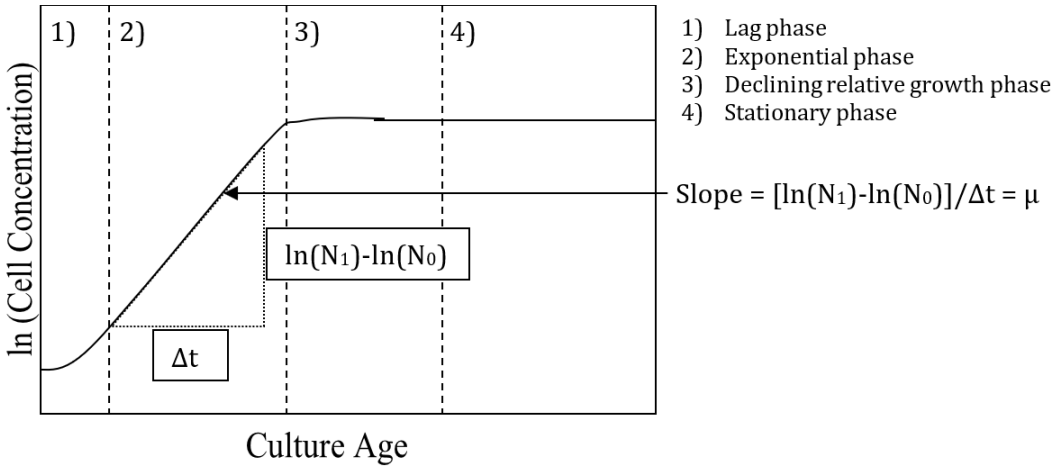


Figure 6: Representation of a natural logarithm growth curve with accompanying growth phases. The slope of the linear trend line in the exponential phase is indicative of the intrinsic growth rate (Monod, 1949).

Intrinsic growth rates of cultures can be used as a measure to compare the growth rates of different microalgal cultures. The intrinsic growth rate can be used to determine the doubling time of a culture, which is also a measure used to compare growth rates of different cultures. The doubling time of a culture (T_2) can be calculated using Equation 4 (Janet *et al.*, 1973, Andersen, 2005):

$$T_2 = \frac{ln(2)}{\mu} \qquad 4$$

Growth rates from literature differ between species, strains and growth conditions (Table 2). Certain strains of microalgae under the right conditions can obtain population doubling rates of almost twice a day.

Table 2: Growth rates and doubling times of microalgae reported by different literature sources.

Species	Growth rate (d^{-1})	Doubling time (doublings.d^{-1})	Source
Neochloris oleabundans	0.34	2.03	Choi and Lee (2015)
Dunaliella sp.	0.31	2.27	
Botryococcus braunii	0.30	2.30	
Chlorella vulgaris	0.38	1.82	Cabanelas *et al.*, (2013)
Rhodomonas sp	0.27	2.57	Renaud *et al.*, (2002)
Cryptomonas sp.	0.33	2.10	
Chaetoceros sp	0.87	0.80	
Isochrysis sp.	0.97	0.71	
Nannochloropsis sp	0.41	1.69	Huerlimann *et al.*, (2010)
Isochrysis sp.	0.25	2.77	
Tetraselmis sp.	0.24	2.89	
Rhodomonas sp.	0.30	2.31	
Scenedesmus sp.	1.11	0.62	Rhee and Gotham (1981)

Biomass yield rate determination

Biomass production rate is a quantitative measure of the rate at which biomass is generated. Production rate can be displayed as an increase of cell number per day or increase of biomass per day. Production rate can also be referred to as the yield rate (Andersen, 2005). The yield rate can be determined using Equation 5.

$$Y = \frac{(N_1 - N_0)}{\Delta t} \qquad 5$$

Where:

Y = yield rate

Equation 5 is similar to the calculation of the slope of a linear trend. Given the growth curve of a microalgal culture, as a function of biomass, the yield rate at any point of the cultivation can be determined using the slope of the curve between any two points on the curve. The slope and subsequent yield rate can vary depending on the time points used to determine the slope (Figure 7). Due to this there are different measures of yield rates such as maximal yield rate and average yield rate. Due to this, the manner by which yield rates are calculated should always be considered before comparing data from different studies and cultures.

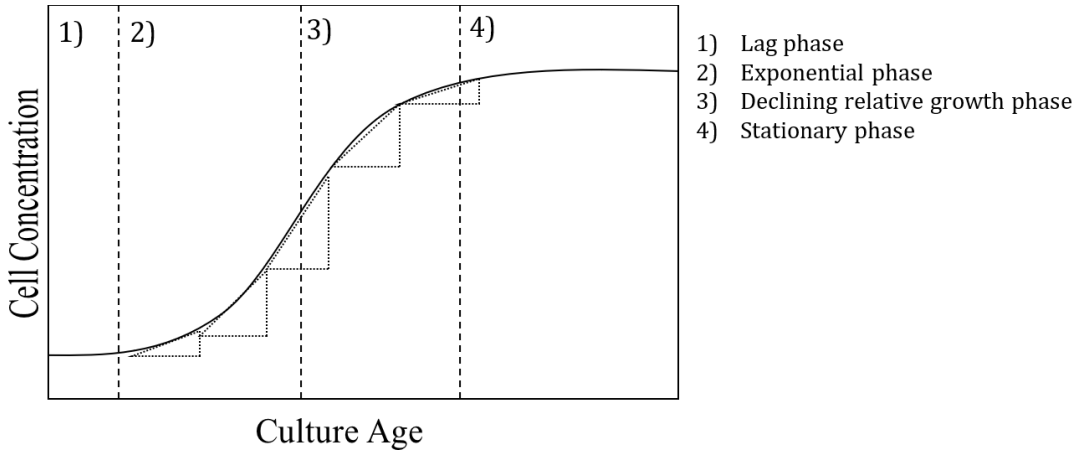


Figure 7: Demonstration of how yield rate slopes can vary depending on the time points at which they are taken.

Yield rates can vary greatly between different species and cultivation conditions. A biomass yield rate for a strain in a cultivation condition can almost be seen as a unique yield rate. The variation of yield rates between strains can be seen in Table 3.

Table 3: Microalgal biomass production rates according to different literature sources.

Species	Biomass yield rate (mg/L/d)	Source
Nannochloropsis oceanica	783	Sandnes *et al.*, (2005)
Spirulina maxima	210	Gouveia and Oliveira (2009)
Chlorella vulgaris	180	
Dunaliella tertiolecta	120	
Neochloris oleabundans	227	Choi and Lee (2015)
Dunaliella sp.	231	
Botryococcus braunii	271	
Ankistrodesmus falcatus	340	Nascimento *et al.*, (2013)
Ankistrodesmus fusiformis	240	
Kirchneriella lunaris	140	
Chlamydomonas sp.	240	
Chlamydocapsa bacillus	320	
Coelastrum microporum	110	
Desmodesmus brasiliensis	130	
Scenedesmus obliquus	160	
Pseudokirchneriella subcapitata	80	
Chlorella vulgaris	730	
Botryococcus braunii	250	
Botryococcus terribilis	200	
Chlorella vulgaris (CCAP 211/11B)	37	Illman *et al.*, (2000)
Chlorella vulgaris (P12)	485	Dragone *et al.*, (2011)
Chlamydomonas reinhardtii UTEX 90	507	Nguyen *et al.*, (2009)
Chlamydomonas reinhardtii	484	Kim *et al.*, (2006)
Scenedesmus obliquus CNW-N	821	Ho *et al.*, (2012)
Chlorella vulgaris	254	Liang *et al.*, (2009)
Chlorella vulgaris FSP-E	1363	Ho *et al.*, (2013)

2.2 Microalgal Cultivation

2.2.1 Autotrophic cultivation macro nutrient requirements

Shurin *et al.*, (2013) described the main chemical composition of Microalgae as $C_{106}H_{263}O_{110}N_{16}P$ in accordance to the Redfield ratio (Shurin *et al.*, 2013, Redfield, 1958). Given this chemical composition, the cultivation of microalgae can be seen as a chemical reaction with a balanced stoichiometric relationship as displayed in Figure 8.

$$106\ CO_2 + 263\ H_2O + 16\ NO_3^{-1} + PO_4^{-1} \longrightarrow C_{106}H_{263}O_{110}N_{16}P + 417\ O_2$$

Figure 8: Balanced chemical reaction for the generation of microalgal biomass.

In microalgal cultivation, there are three essential nutrient sources required for generation of biomass and for normal cell function. These nutrient sources include nitrogen, phosphorous and carbon sources. Monod (1941) demonstrated how the decrease of an essential macronutrient can negatively affect the growth rate of a microbial organism. Monod (1941) demonstrated that a hyperbolic curve can be used to explain the relation between substrate concentration at low levels and the growth rate of an organism (Figure 9).

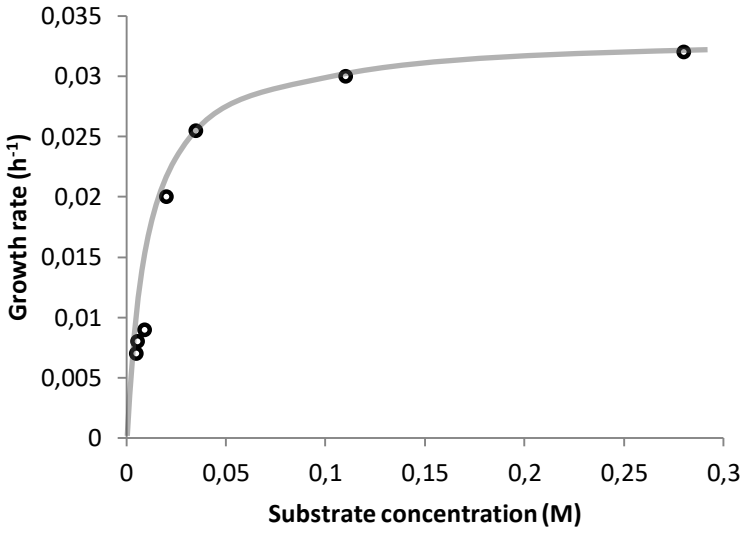


Figure 9: Growth rate of *Mycobacterium tuberculosis* in Dubos' medium as a function of glucose concentration (Monod, 1949).

Using the hyperbolic relationship between substrate and growth rate, Monod (1949) was able to create a mathematical model, which can be seen in Equation 6, for predicting the growth rate of an organism, given the concentration of a macro nutrient. In this equation the K_m is referred to as the Monod constant, which is an organism specific constant for the effect, depletion of a specific nutrient has on the growth rate of that organism (Monod, 1949). The K_m value can be derived by deriving the formula of a hyperbolic trend line (Figure 9).

$$\mu = \mu_{max}[\frac{C_s}{K_m + C_s}] \qquad 6$$

Where:

C_s = the substrate concentration
K_m = the Monod constant
μ_{max} = the maximum growth rate

Microbial growth rate is not only affected by substrate depletion but also substrate inhibition due to excess amounts of a substrate. Edwards (1970) explored the relationship between microbial growth rate and high substrate concentrations and compared it to models proposed by Uemura *et al*, (1969) and Grant (1969). One of the models was shown to have the most accurate predictions is that of the Monod-Haldane model (Edwards, 1970). The Monod-Haldane model predicts the effect of both low and high substrate concentration on the growth rate of an organism (Edwards, 1970). The Monod-Haldane equation can be seen in Equation 7 (Monod, 1949).

$$\mu = \mu_{\max}\left(\frac{C_s}{K_m + C_s + \frac{C_s^2}{K_I}}\right) \qquad 7$$

Where:

K_I = the inhibition constant

A typical Monod-Haldane curve generated by Equation 7 can be seen in Figure 10. Nur *et al.*, (2017), Vergara-Fernández *et al*., (2008) and Klecka *et al*., (1985), demonstrated that the Monod-Haldane curve can represent an array of microbe-substrate interactions for microbes including microalgae, fungi and bacteria (Nur *et al*., 2017, Vergara-Fernández *et al*., 2008, Klecka and Maier, 1985).

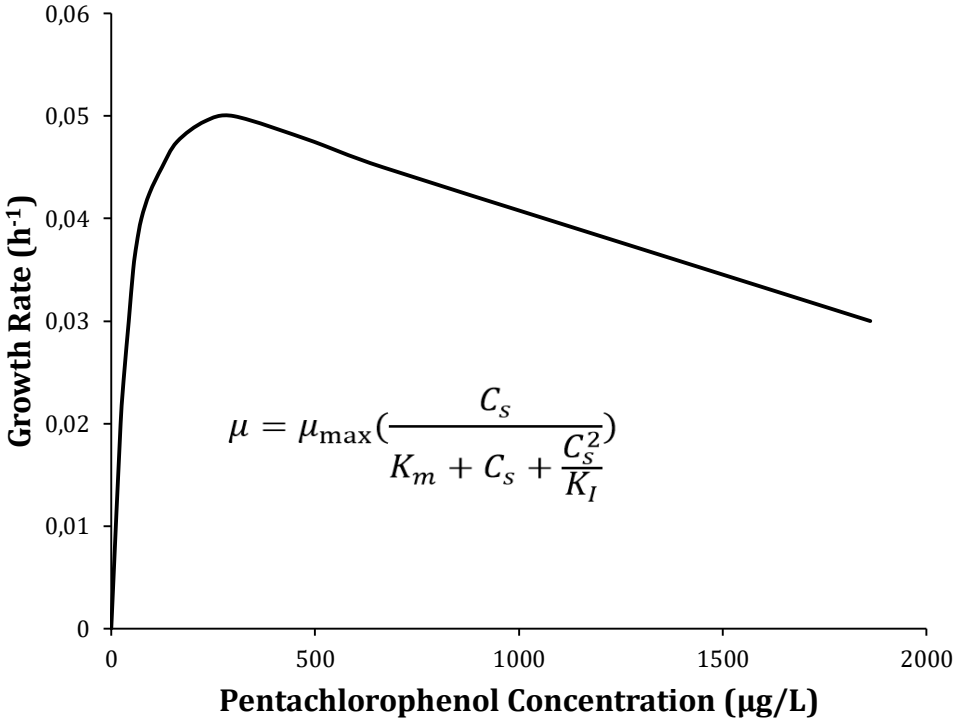


Figure 10: Relationship between pentachlorophenol concentration and microbial growth rate calculated using the Haldane modification of the Monod equation (Klecka *et al*., 1985).

Nitrogen

A source of nitrogen is required by microalgae to perform cellular functions such as amino acid synthesis. Nitrate ions (NO_3^{-1}), nitrite ions (NO_2^{-1}), ammonium ions and urea can act as nitrogen sources for microalgae. Urea and NO_3^{-1} have been shown to be good nitrogen sources for microalgal culturing with the aim of lipid production (Fidalgo *et al.*, 1998).

The abundance of nitrogen source in a microalgal culture media has a significant effect on the growth rate and also the lipid content (Li *et al.*, 2008a). There is a trade-off between growth rate and lipid content as high nitrogen allows fast growth rates, while nitrogen limitation stimulates lipid accumulation (Chisti, 2007). Griffiths and Harrison (2009) demonstrated the accumulation of lipids in different microalgal species due to nitrogen starvation as can be seen in Figure 11. Cobos *et al.*, (2017) displayed the balance between maintaining growth rate and lipid accumulation. In Figure 12, the distinct difference in biomass accumulation between nitrogen sufficient and deficient media can be seen (Cobos *et al.*, 2017). In Figure 13 however, it is clear that the nitrogen limited cultures provided higher cellular lipid contents.

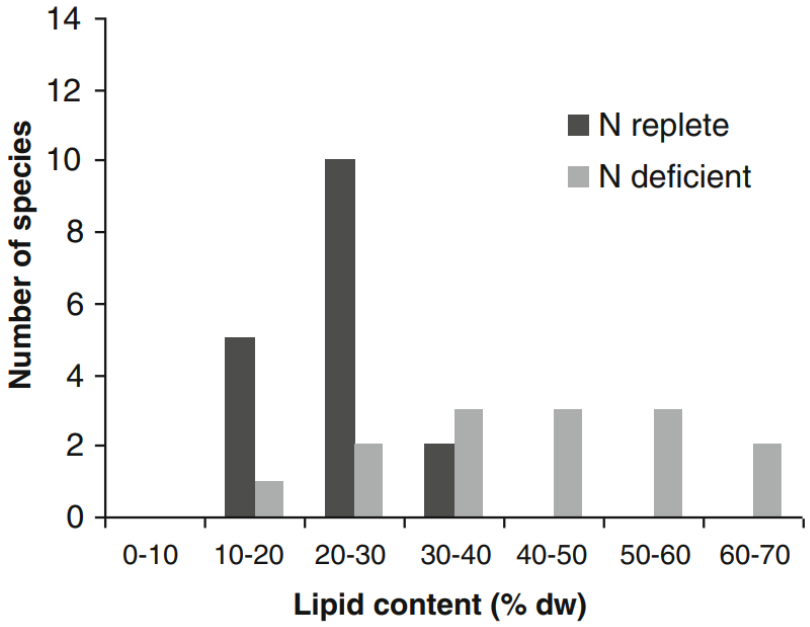


Figure 11: Number of algal species in each lipid content category under Nitrogen replete and deficient conditions (Griffiths and Harrison, 2009).

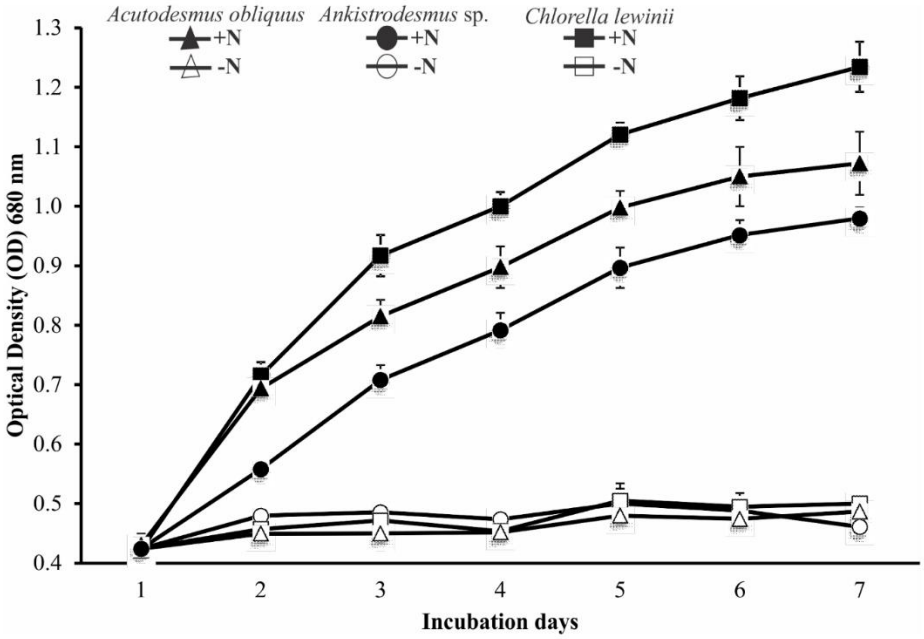


Figure 12: Growth profiles of three microalgal strains cultivated under increased nitrogen (+N) and reduced nitrogen (-N) Chu medium No. 10 (Cobos *et al.*, 2017).

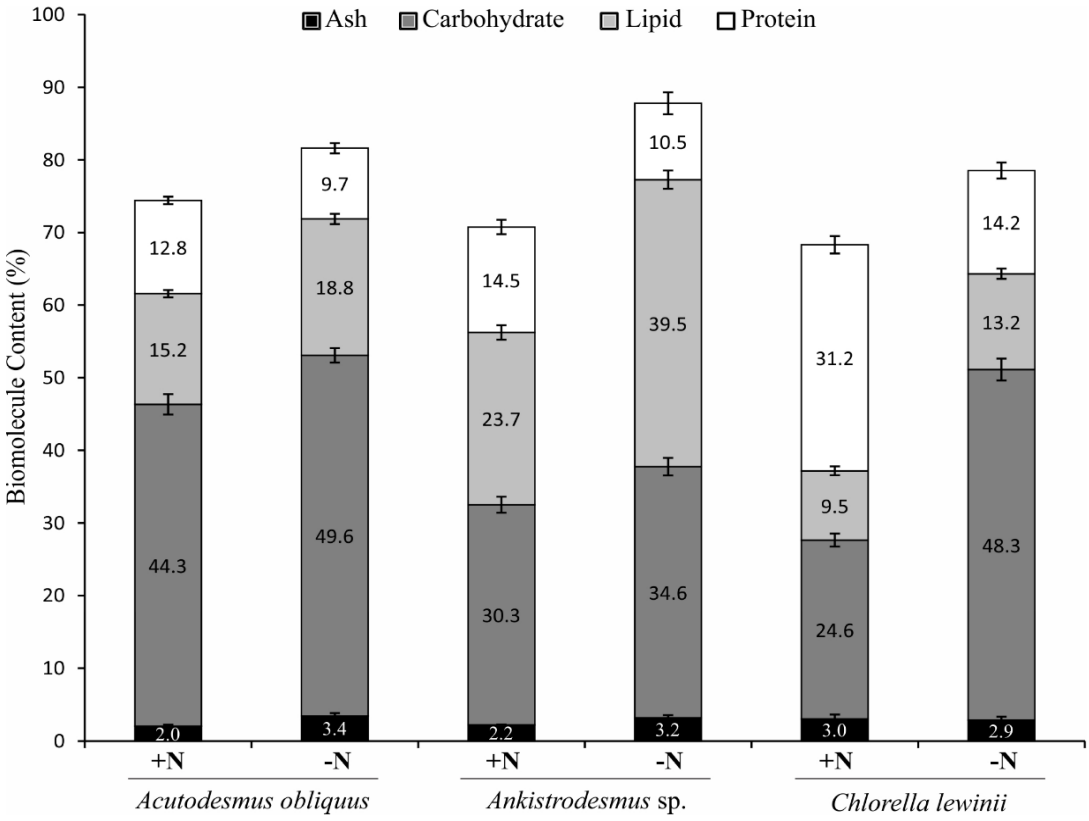


Figure 13: Biomolecule content (ash, carbohydrate, total lipid and protein) of three microalgal strains cultivated under +N and −N Chu medium No. 10 (Cobos *et al.*, 2017).

Phosphorus

Additionally, a source of phosphorus is required by microalgae to grow and replicate. Phosphorus is required for the generation of nucleic acids in microalgae. Nucleic acids form the building blocks of DNA and RNA required for replication and normal cellular function. Nucleic acids such as adenosine tri phosphate (ATP) are directly involved with cellular energy generation and glycogenesis. A utilisable source of phosphorus for microalgae is in the form of phosphate ions (PO_4^{-3}). PO_4^{-3} concentrations have been shown to affect the growth rate, cellular lipid content and cellular carbohydrate content of microalgae. Markou *et al*., (2012) showed that the dry mass carbohydrate percentage of filamentous cyanobacteria, *Arthrospira platensis*, could be increased from 10-20% to 60-65% by phosphorus limitation.

Carbon

Most biotic life, microalgae require a source of carbon. Autotrophic microalgae commonly utilise carbon dioxide as a carbon source similar to plants. Dissolved carbon dioxide can be supplied to a microalgal culture media by bubbling carbon dioxide through the culture or by adding a carbonate salt to the culture medium. A common form of carbonate added to microalgal culture mediums is sodium bicarbonate. Sodium bicarbonate has the added advantage of acting as a buffer in the culture media, with a buffer capacity of pH 8.5 to 9.5 (Hashemi and Rahmani, 2006). Sodium bicarbonate usage in commercial production has the disadvantages of not mitigating CO_2 and has an increased energy footprint, compared to CO_2 bubbling. Sodium bicarbonate has a solubility in water of 87- 100 g/L at 20°C and 30°C respectively (Ullmann *et al*., 1985). Sodium bicarbonate usage should be monitored as it can cause the media to become alkaline.

2.2.2 Environmental factors affecting microalgal growth

In addition to media composition, microalgal cultivation is also affected by environmental factors. Such factors include medium pH, environmental temperature, light irradiation and salinity.

Environmental pH

The environmental pH is a very important factor affecting microalgal growth rate and ultra-structure (Visviki and Santikul, 2000). The external pH is so essential due to the pH regulating membrane potential and transport across membranes, which in turn affects the internal pH of the organism. Maintenance of a stable internal pH of an organism is essential for normal enzyme, protein and metabolism functioning. Lane and Burris (1981) and Coleman and Colman (1981) demonstrated how changes in pH can affect growth rates and photosynthetic rate (Lane and Burris, 1981, Coleman and Colman, 1981). Fluctuations in pH affect the availability of dissolved carbon dioxide in water

which is an essential factor to consider during the cultivation of microalgae, as can be seen in Figure 14 (Wojtowicz, 2001).

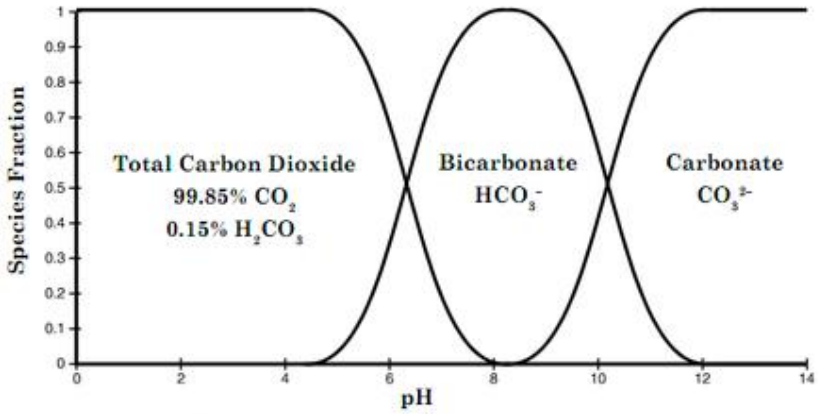


Figure 14: Fluctuation of CO_2, HCO_3^{-1} and CO_3^{-2} concentrations vs pH (Wojtowicz, 2001).

Temperature

Environmental temperature affects growth rate, biochemical composition, microalgal cell size and nutrient requirements (Juneja *et al.*, 2013).

Microalgae are often adapted to specific conditions due to evolution to fit their habitat. As temperatures increase, microalgae show increase in growth rate up to a certain point where the growth rate starts to decline again. This means that there is an optimal cultivation temperature for each microalgal culture, which can differ between strains (Renaud et al., 2002). The temperature has been shown to affect the photosynthetic rate of microalgae by gradually reducing photosynthetic rate at temperatures lower or higher than optimal temperature (Konopka and Brock, 1978). Decreased photosynthetic rate can result in a decreased growth rate. Temperatures exceeding the optimal temperature showed a reduction in protein synthesis and thus a reduction in growth rate (Rhee and Gotham, 1981). Similarly, an increase in protein content has been noticed with a decrease of temperature (Rhee and Gotham, 1981).

An increase in fatty acid un-saturation in microalgae has been linked with a decrease in temperature (Renaud et al., 2002). This could be the cell's mechanism to counteract the reduction of cell membrane fluidity due to decreased temperature. An increase in temperature led to an increase of carotenoids such as Beta-carotene and astaxanthin in selected organisms. The increase in carotenoids is most likely in response to an increase of photo and oxidative damage on the photosystem due to the increase of temperatures (Tjahjono *et al.*, 1994). Cultivation temperature has been explained to affect the accumulation of lipids. In a few cases, the increase of temperature from a low temperature up to optimal temperature leads to the increase of cellular lipid contents. Increasing the temperature over the optimal temperature has showed a decrease of lipid content (Converti *et al.*, 2009). An increase of cellular phosphorus (P), nitrogen (N) and

carbon (C) content in some microalgal strains have been seen with a decrease in temperature (Rhee and Gotham, 1981). Cells from some microalgal strains showed cell size increase with a decrease in temperature but this is not always directly correlated with the higher cellular P, N and C content (Rhee, 1982).

Nutrient utilisation has been shown to decrease at non-optimal temperatures (Rhee and Gotham, 1981). Decrease in nutrient uptake is most likely due to the reduction in growth rate and cytoplasmic viscosity (Raven and Geider, 1988).

Light irradiation

For autotrophic microalgae light acts as the main energy source. Light energy is converted to chemical energy through photosynthesis. Light intensity is an important factor in microalgal cultivation. The optimal light intensity for microalgae can be referred to as the saturation intensity. Light intensities higher or lower than the saturation intensity can lead to a reduction in growth rate (Sorokin and Krauss, 1958). If light intensity increases to levels higher than the saturation intensity, the photo complex starts experiencing photo inhibition and photo damage (Gordillo *et al*., 1998, You and Barnett, 2004). Photo damage can lead to a reduction in growth rate, cell bleaching and even cell death. Microalgae can undergo photo-adaptation and photo-acclimation, where changes in cell properties take place according to the availability of light to increase photosynthetic efficiency (Dubinsky *et al*., 1995). Photo-adaptation can take place by altering the type and quantity of pigments, growth rate, dark respiration rate or the availability of essential fatty acids (Juneja *et al*., 2013, Fábregas *et al*., 2004). Morphological photo acclimation can lead to a change in cell size and number and density of thylakoid membranes (Berner *et al*., 1989). Light intensity has been shown to affect the chemical composition of microalgae (Cuhel *et al*., 1984). Cuhel *et al*. (1984) showed that *Dunaliela tertiolecta* can exhibit an increase of lipid concentration and decrease in protein concentration with the increase of light intensities. Iqbal and Zafar (1993) showed that low light intensities can increase protein synthesis. Increase in light intensities has been linked to increased extracellular polysaccharide content (Iqbal and Zafar, 1993). High light intensities can lead to oxidative damage of poly unsaturated fatty acids (PUFA), resulting in a reduction of PUFA content (Renaud *et al*., 1991, Orcutt and Patterson, 1974).

Light cycles and light spectrum composition also affect microalgal growth. Similar to plants, microalgae have light and dark cycles. Constant light illumination can reduce microalgal growth rate by inhibiting the dark cycle. Light utilisation can be increased by prolonged dark cycles in systems with high light intensity. Prolonged dark cycle allows efficient utilisation of captured photons to be converted to chemical energy and allow the repair of photo damaged photo complexes (Long *et al*., 1994). Most microalgal chloroplasts, like plants, dominantly use the blue and red light spectrums for photosynthesis (You and Barnett, 2004, Emerson and Lewis, 1943). The ratio of blue and

red light has shown to also affect microalgal chemical composition (You and Barnett, 2004, Miyachi *et al*., 1978). UV light spectrums have shown to inhibit microalgal growth and cause cell damage (Pessoa, 2012).

Salinity

Medium salinity or salt concentration is a very important parameter for the growth of most unicellular organisms. The salinity is essential to organism health because it affects the osmotic pressures of the cell. High salinity can lead to the efflux of water from a cell into the environment from a low to high ion concentration due to osmotic pressure. High salinity can lead to hypertonic cells which can lead to dehydration. Low salinity can lead to the influx of water into a cell due to the osmotic pressure. Low salinities can lead to hypotonic cells, which in severe cases can rupture due to the internal osmotic pressure (Ginzburg, 1981).

The environmental salinity above or below a microalgal organism's optimal salinity can alter its biochemical composition and reduce growth rate (Zhila *et al*., 2011). In a cultivation study of a *Dunaliella* strain, an increase of saturated and monounsaturated fatty acid contents was visualised with the increase of salinity (Xu and Beardall, 1997). A few other studies support this data by indicating higher cellular lipid contents for microalgae cultivated at higher salinities (Zhila *et al*., 2011, Renaud and Parry, 1994).

2.2.3 Cultivation systems

Cultivation systems can be classified as open, semi-closed and closed systems (Pulz, 2001). Open cultivation systems are systems like growth ponds and raceway ponds (Pulz, 2001). Open raceway ponds have long been the benchmark for microalgal culturing, some experts however believes that other cultivation systems can provide better biomass yields per hectare (Jorquera *et al*., 2010). Closed systems are commonly referred to photo bioreactors (PBR) (Pulz, 2001). There are multiple PBR designs, each with its own benefits, as can be seen in Table 4, and often designed to accommodate the properties of the strain cultured in it (Jorquera *et al*., 2010). Semi-closed cultivation systems can be described as insulated open cultivation systems, such as greenhouse or covered raceway ponds. One remarkable semi-closed cultivation system, which has recently seen much development, is the development of biofilm reactors. A biofilm reactor is a reactor where microalgae are cultured out of suspension as biofilm on a solid surface in a greenhouse (Ozkan *et al*., 2012). Such a cultivation system has the advantage of cutting costs associated with the harvest of microalgal biomass drastically (Ozkan *et al*., 2012). Examples of different cultivation systems are shown in Figure 15.

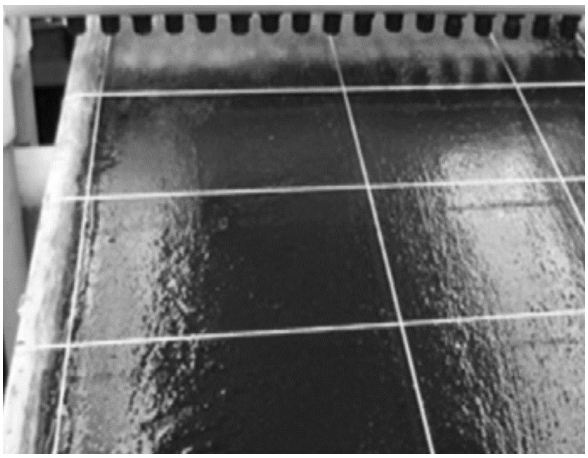
Table 4: The benefits and limitations of a few different cultivation systems (Brennan and Owende, 2010).

Cultivation system	Benefits	Limitations
Raceway pond	- Relatively cheap - Easy to clean - Low energy inputs - Easy maintenance	- Poor biomass productivity - Cultures are easily contaminated - Large area of land required - Limited to a few strains of algae - Poor mixing, light and CO_2 utilisation - Cultures are easily contaminated
Tubular photobioreactor	- Large illumination surface area - Suitable for outdoor cultures - Relatively cheap - Good biomass productivities	- Some degree of wall growth - Fouling - Requires large land space - Gradients of pH, dissolved oxygen and CO_2 along the tubes
Flat plate photobioreactor	- High biomass productivities - Easy to sterilise - Low oxygen build-up - Readily tempered - Good light path - Large illumination surface area - Suitable for outdoor cultures	- Difficult scale-up - Difficult temperature control - Small degree of hydrodynamic stress - Some degree of wall growth
Column photobioreactor	- Compact - High mass transfer - Low energy consumption - Good mixing with low shear stress - Easy to sterilise - Reduced photoinhibition and photo-oxidation	- Small illumination area - Shear stress - Sophisticated construction - Expensive compared to open ponds

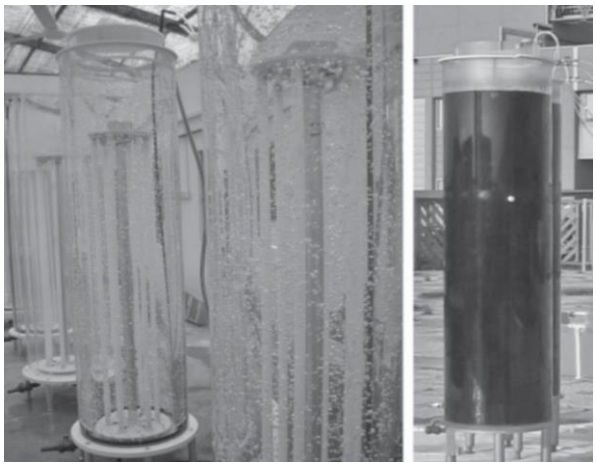
Phyto bag system



Biofilm reactor



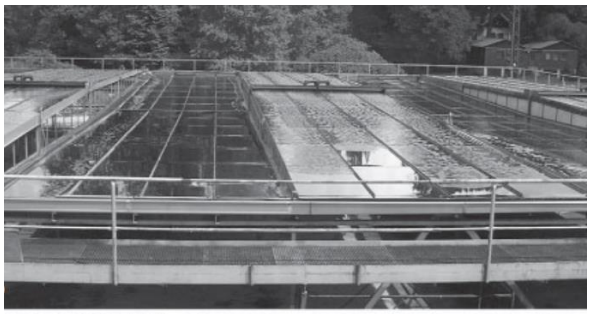
Vertical coloumn system



Horizontal tubular system



Outdoor cascade system







Flat plate panel system



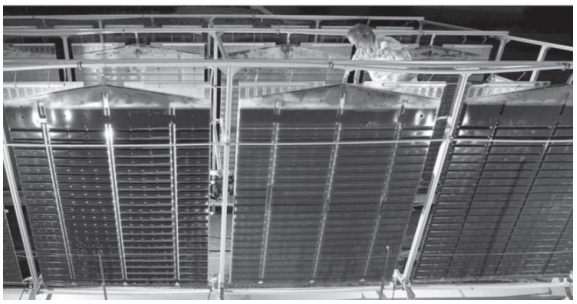


Figure 15: Representation of different types of cultivation systems and photobioreactors (Zittelli et al., 2013, Ozkan et al., 2012).

2.3 Biomass harvesting

In microalgal cultivation, most cultivation methods take place as liquid cultures; and the recovery of microalgal biomass from liquid cultures is one of the most challenging and costly process steps (Brennan and Owende, 2010). The recovery of microalgal biomass is challenging due to the low microalgal cell densities (0.3 – 5 $g.L^{-1}$) and small cell sizes (2 – 40 µm) (Brennan and Owende, 2010, Li *et al*., 2008b). According to Gudin and Thepenier (1986) microalgal biomass harvesting accounts for 20% to 30% of the total processing cost. Due to the costs and challenges of harvesting, multiple harvesting techniques have been developed. These harvesting techniques include:

- flocculation;
- flotation;
- sedimentation; and
- filtration.

2.3.1 Flocculation

Flocculation is used in combination with another harvesting technique to increase the effectiveness of the other technique (Grima *et al*., 2003). The aim of flocculation is to increase the particle size by aggregating cells to each other to help in solid-liquid separation. Microalgal cell usually carry a negative charge to avoid natural cell aggregation in suspension (Grima *et al*., 2003). The addition of a positive charge can facilitate the aggregation of microalgal cells. Metal salts like ferric chloride ($FeCl_3$), aluminium sulphate ($Al_2(SO_4)_3$) and ferric sulphate ($Fe_2(SO_4)_3$) can provide positive charges in the form of iron (+3) and aluminium (+3) cations to facilitate flocculation (Brennan and Owende, 2010). In addition to metal ion-based flocculation, other flocculation techniques are available:

- Divakaran and Pillai (2002) demonstrated the use of Chitosan as a bio-flocculent at pH 7 to facilitate the flocculation of fresh water microalgal species (Divakaran and Pillai, 2002);
- Flocculation by addition of NaOH and a non-ionic polymer Magnafloc LT-25 has been demonstrated (Knuckey *et al*., 2006); and
- Bosma *et al*. (2003) demonstrated the use of ultra-sonic waves to improve aggregation efficiency of microalgal cultures (Bosma *et al*., 2003).

2.3.2 Flotation

Flotation has been investigated as a possible option for microalgal biomass harvesting. Flotation methods using dispersed micro-air bubbles to stimulate microalgal flotation has been investigated. The advantage of such a process is that it can take place without the addition of chemicals (Wang *et al*., 2008). Natural flotation has been documented in some microalgal strains with the increase of cellular lipid content (Burton *et al*., 2009). There is however not much evidence regarding the technical and financial viability of using flotation as a microalgal biomass harvesting method (Brennan and Owende, 2010).

2.3.3 Sedimentation

Sedimentation techniques include gravitational and centrifugal sedimentation. Sedimentation occurs due to directional acceleration of solids within a suspension. The sedimentation rate increases as the size and mass of the solids increase (Schenk et al., 2008). Naturally sedimentation occurs due to gravitational force causing downward acceleration. Gravitational sedimentation tends to be time consuming and is mainly suitable for large microalgae (Munoz and Guieysse, 2006). Flocculation can increase gravitational sedimentation rate (Grima *et al*., 2003). Centrifugal sedimentation is a rapid sedimentation method. Sedimentation by centrifugation is energy intensive, require specialised equipment and have more maintenance requirements (Bosma *et al*., 2003). Centrifugal sedimentation is suitable for cultures containing high value compounds (Heasman *et al*., 2000).

2.3.4 Filtration

Filtration requires a solid phase which can allow the medium to pass without allowing microalgal biomass to pass. Conventional filtration techniques are most efficient when working with large cell sizes. As the cell sizes decrease, more specialised filters are required. As the filter pore size decreases, the filtration rate decreases. Increasing suction or pressure can increase filtration rate but increases energy cost and can lead to cell damage (Mohn, 1980). Diatomaceous earth or cellulose filtration aids can be added to conventional filtration techniques to improve efficiency (Grima *et al*., 2003). Micro- and ultra-filtration is a form of membrane filtration which uses hydrostatic pressure. Micro and ultra-filtration can be used to filter smaller cells without cell rupturing and can be more cost effective than centrifugation at small scale (Petrusevski *et al*., 1995, Doucha *et al*., 2005). Micro- and ultra-filtration is however not ideal for large scale filtration due to the membrane replacement costs and pumping energy intensity (MacKay and Salusbury, 1988, Brennan and Owende, 2010).

2.4 Commercial purposes for microalgal cultivation

Microalgal cultivation can be a costly and complex venture. The cultivation of microalgae can be justified by the range of services and products it can provide.

2.4.1 Services

Microalgal cultivation can provide services including CO_2 mitigation and waste water bioremediation.

CO_2 mitigation

Microalgae can efficiently mitigate CO_2. Studies showed that 10 – 50% of CO_2 from a flue gas containing 6 – 8% CO_2 by volume can be mitigated using a *Chlorella sp*. (Doucha *et al*., 2005). Microalgae have been shown to be able to tolerate high CO_2 contents in feeding air

streams allowing the use of flue gases of 5 – 15% CO_2 volume content for microalgal cultivation (Chang and Yang, 2003, Hsueh *et al*., 2007). Microalgae have potential to be used as a form of CO_2 mitigation, which can be combined with CO_2 emitting industries (Li *et al*., 2008b). In addition to mitigating CO_2, the addition of CO_2 also increases microalgal growth rate and reduces costs related to CO_2 supply.

Waste water treatment

Microalgae have the ability to utilise inorganic nitrogen and phosphate (Chisti, 2007). This shows great potential for microalgae to be used to bioremediate waste water, which can contain high concentrations of waste nitrogen and phosphorus (Pittman *et al*., 2011). Extensive work has been performed to study the ability of microalgae to remove waste nitrogen and phosphorus from effluents (Mallick, 2002, Aslan and Kapdan, 2006, Hameed, 2007). Munoz and Guieysse (2006) demonstrated the reduction of several heavy metals by microalgal culturing. This demonstrates the potential of microalgal cultivation for waste water treatment. In addition to bioremediating waste water, the use of waste water reduces fresh water usage during microalgal cultivation (Li *et al*., 2008b). One of the main concerns regarding the use of waste water in microalgal cultivation is the risk of contamination by other algae, bacteria and rotifers (Munoz and Guieysse, 2006). This risk can be reduced by water pre-treatment or by using mixed cultures for the cultivation (Tamer *et al*., 2006).

2.4.2 Products

Microalgal biomass can generate an array of valuable products (Griffiths *et al.*, 2016). In addition to lipids and carbohydrates, which can be used for bio-energy purposes, multiple high value co-products including pharmaceutical, nutritional and cosmetic products can be produced by microalgae (Li *et al*., 2008b).

High value co-products

There are multiple high value products, which can be produced by microalgae. Some of these include β-carotene, B-vitamins (such as *Spirulina* supplements), astaxanthin, polyunsaturated fatty acids and lutein (Huang *et al*., 2006, Del Campo *et al*., 2007, He *et al*., 2005, Ip and Chen, 2005, Wen and Chen, 2003, Jiang *et al*., 2004, Blanco *et al*., 2007, Shi and Chen, 2002, Li *et al*., 2008b). The high-value co-product approach can improve the economic feasibility of microalgal bio-fuel by providing additional products, which can operate independent of the energy industry (Li *et al*., 2008b, Griffiths *et al*., 2016). Microalgal bio-energy indicators

To be able to screen microalgae for bio-fuel production purposes a few characteristics can be indicators of a suitable strain. Microalgal bio-energy is commonly derived from the lipid or carbohydrate fractions contained in the microalgal biomass. Accumulation of carbohydrates and lipids in microalgae is an indicator bio-energy potential. This potential

can be measured percentage accumulation per dry weight of biomass or even in the form of lipid or carbohydrate yield rate. The ability of microalgae to grow rapidly is an indirect bio-energy indicator as a culture with a fast growth rate can provide higher yields and be harvested more regularly. There are a few other characteristics which can be favourable in a strain for bio-energy production purposes. Favourable characteristics include characteristics which improves robustness, resistance to stress factors, ease of harvesting and easy cultivation.

Microalgal bio-diesel

Microalgae can have high lipid contents depending on the microalgal strain and environmental conditions. Some strains have been documented to have lipid contents of up to 77% per dry weight of biomass (Chisti, 2007). The lipids produced by microalgae can be used to produce fatty acid methyl esters (FAMEs) for use as bio-diesel (Demirbas, 2010).

Microalgal lipid yield rates have been reported to range from close to zero up to 204 mg/L/day (Rodolfi *et al*., 2009, Nascimento *et al*., 2013). Lipid yield rates can vary between strains and cultivation conditions greatly. Nascimento *et al*. (2013) displayed the variations in lipid yield rates of various algal species as can be seen in Table 5. Nascimento *et al*., (2013) demonstrated the importance of the biomass yield rate and cellular lipid content in determining the lipid yield rate. The lipid yield rate is thus a function of biomass yield rate and cellular lipid content.

Table 5: Biomass and lipid yield rates with accompanying cellular lipid contents for different microalgal species (Nascimento *et al*., 2013)

Species	Biomass yield rate ($mg.L^{-1}.d^{-1}$)	Lipid yield rate ($mg.L^{-1}.d^{-1}$)	Cellular lipid content %
Ankistrodesmus falcatus	340	56.07 ± 1.75	16.49 ± 0.44
Ankistrodesmus fusiformis	240	49.58 ± 5.74	20.66 ± 2.07
Kirchneriella lunaris	140	24.22 ± 1.81	17.30 ± 1.12
Chlamydomonas sp.	240	36.17 ± 2.61	15.07 ± 0.95
Chlamydocapsa bacillus	320	43.26 ± 2.40	13.52 ± 0.65
Coelastrum microporum	110	22.61 ± 1.26	20.55 ± 0.99
Desmodesmus brasiliensis	130	23.39 ± 0.63	17.99 ± 0.42
Scenedesmus obliquus	160	26.77 ± 2.53	16.73 ± 1.37
Pseudokirchneriella subcapitata	80	22.74 ± 4.97	28.43 ± 5.40
Chlorella vulgaris	730	204.91 ± 6.37	28.07 ± 4.31
Botryococcus braunii	250	112.43 ± 11.52	44.97 ± 4.00
Botryococcus terribilis	200	98.00 ± 3.42	49.00 ± 1.48

Ahmad *et al.*, (2011) compared predicted lipid and subsequent bio-diesel yields of microalgae with that of conventional food oil crops. Ahmad *et al.*, (2011) showed that microalgae can provide bio-diesel yields superior to that of conventional food oil crops (Table 6). This demonstrates the potential of microalgal biomass as a biomass source for bio-diesel production.

Table 6: Comparison of different oil sources for bio-diesel productivity (Ahmad *et al.*, 2011).

Plant source	Seed oil content (% oil by wt. in biomass)	Oil yield ($L.ha^{-1}.year^{-1}$)	Land use ($m^2.year.kg^{-1}$ bio-diesel)	Bio-diesel yield rate ($kg.ha^{-1}.year^{-1}$)
Corn/Maize	44	172	66	152
Hemp	33	363	31	321
Soybean	18	636	18	562
Jatropha	28	741	15	656
Camelina	42	915	12	809
Canola/rapeseed	41	974	12	862
Sunflower	40	1070	11	946
Castor	48	1307	9	1156
Palm oil	36	5366	2	4747
Microalgae (low oil content)	30	58 700	0.2	51 927
Microalgae (medium oil content)	50	97 800	0.1	86 515
Microalgae (high oil content)	70	136 900	0.1	121 104

Microalgal oil contains phospholipids, glycolipids, mono-, di- and triacyl glycerides in ratios varying between species and metabolic state. Only the triacyl glycerides are easily converted to bio-diesel by fatty acid methyl transesterification (Nascimento *et al.*, 2013).

The fatty acid methyl ester profile of bio-diesel is very important in determining the properties of the bio-diesel (Nascimento *et al.*, 2013). Lipid content characteristics that affect the properties of the bio-diesel product includes the number of saturated and unsaturated fatty acids, and carbon chain lengths of the fatty acids. The correct balance in saturation and carbon chain lengths should be achieved to produce a well performing bio-diesel. Bio-diesel viscosity, density, ignition time delay, oxidative stability and cold flow performance are properties which determine the performance of the bio-diesel (Nascimento *et al.*, 2013), and are listed below:

- Viscosity and density should be at the right balance as an increase in viscosity improves the lubrication ability of the fuel but increases the chance of fuel line and

filter blockages. The viscosity increases as the carbon chain lengths increase or the amount of saturated fatty acids increase.

- Ignition time delay should preferably be as little as possible. The ignition time delay decreases as the carbon lengths increase.

- Oxidative stability is an indicator of the fuel's stability over time. As the oxidative stability increases the chance of oxidation, deterioration of fuel lubricity and formation of deposits decrease. Oxidative stability decreases as fatty acid double bonds increase and is also affected by the double bond position.

- Bio-diesel often has the disadvantage of becoming more viscous and crystallising when the temperature is low, which can block fuel lines and filters. The cold flow performance of bio-diesel decreases as the saturation of the bio-diesel increases (Nascimento *et al*., 2013).

A high level of unsaturated fatty acids results in the polymerisation of glycerides, which leads to the formation of deposits. Considering the triacyl glycerides, some fatty acids are more suitable than others for bio-diesel purposes. Palmitic (C16:0) and stearic acid (C18:0) methyl esters have a tendency to precipitate as soon as the bio-diesel temperature cools. The viscosity increases as the fatty acid length increases. The ideal predicted lipid composition for bio-diesel use is a 5:4:1 ratio of C16:1, C18:1 and C14:0 to provide a fuel with low oxidative potential, good cold flow characteristics and a high cetane number (Schenk *et al*., 2008).

Due to the variation that can occur in bio-diesel properties, international fuel standards essential for market acceptance have been established. ASTM D 6751 and EN 14214 from North America and Europe respectively are two of the main fuel standards used in the market (Table 7) (Knothe, 2006).

Four measures for the properties of a bio-diesel are the cetane number (CN), cloud point (CP), cold filter plugging point (CFPP) and iodine value (IV) (Nascimento *et al*., 2013).

Fuel CN is a measure of the ignition time delay of fuel ignition. A high CN is indicative of a shorter ignition time and *vice versa* with hexadecane set to a default value of 100. The CN range required for bio-diesel is 40-50.

The IV refers to the ability of fuel to react with oxygen. The IV is affected by the number and position of double bonds in the carbon chains. As the IV increases the possibility of oxidation, formation of deposits and deterioration of the bio-diesel lubricity increases.

The CP of a fuel is defined as the temperature where the first methyl esters start to crystallise (Lopes *et al*., 2007). The CP is indicative of the temperature where the bio-diesel would start blocking filters.

Table 7: European bio-diesel standards EN 14214 for vehicle use and EN 14213 for heating oil use (Knothe, 2006).

		Limits		
Property	**Test method**	**EN 14214**	**EN 14213**	**Unit**
Ester content	EN 14103	≥ 96.5	≥ 96.5	$mol.mol^{-1}$
Density; 15°C	EN ISO 3675, EN ISO 12185	860 – 900	860 – 900	$kg.m^{-3}$
Viscosity; 40°C	EN ISO 3104, ISO 3105	3.5 – 5.0	3.5 – 5.0	$mm^2.s^{-1}$
Flash point	EN ISO 3679	≥ 120	≥ 120	°C
Sulfur content	EN ISO 20846; EN ISO 20884	≤ 10.0	≤ 10.0	$mg.kg^{-1}$
Carbon residue (10% distillation residue)	EN ISO 10370	≤ 0.30	≤ 0.30	% ($mol.mol^{-1}$)
Cetane number	EN ISO 5165	≥ 51	—	
Sulfated ash	ISO 3987	≤ 0.02	≤ 0.02	% ($mol.mol^{-1}$)
Water content	EN ISO 12937	≤ 500	≤ 500	$mg.kg^{-1}$
Total contamination	EN 12662	≤ 24	≤ 24	$mg.kg^{-1}$
Oxidative stability, 110°C	EN 14112	6.0 min	4.0 h	h
Acid value	EN 14104	≤ 0.50	≤ 0.50	mg $KOH.g^{-1}$
Oxidative stability, 110°C	EN 14112	≥ 6.0	4.0 h	h
Acid value	EN 14104	≤ 0.50	≤ 0.50	mg $KOH.g^{-1}$
Iodine value	EN 14111	≤ 120	≤ 130	g $I2.100\ g^{-1}$
Linolenic acid content	EN 14103	≤ 12.0	—	% ($mol.mol^{-1}$)
Content of FAME with ^{3}4 double bonds		≤ 1	≤ 1	% ($mol.mol^{-1}$)
Methanol content	EN 14110	≤ 0.20	—	% ($mol.mol^{-1}$)
MAG content	EN 14105	≤ 0.80	≤ 0.80	% ($mol.mol^{-1}$)
DAG content	EN 14105	≤ 0.20	≤ 0.20	% ($mol.mol^{-1}$)
TAG content	EN 14105	≤ 0.20	≤ 0.20	% ($mol.mol^{-1}$)
Free glycerine	EN 14105, EN 14106	≤ 0.020	≤ 0.02	% ($mol.mol^{-1}$)
Total glycerine	EN 14105	≤ 0.25	—	% ($mol.mol^{-1}$)
Group I metals (Na + K)	EN 14108, EN 14109	≤ 5.0	—	$mg.kg^{-1}$
Group II (Ca + Mg)	prEN 14538	≤ 5.0	—	$mg.kg^{-1}$
Phosphorus content	EN 14107	≤ 10.0	—	$mg.kg^{-1}$
Cold filter plugging point	EN 116	—	—	°C
Pour point	ISO 3016	—	≤ 0	°C

The CFPP value is a prediction of the flow performance of the fuel at low temperature. At low temperatures FAME molecules start to crystallise and clump to block filters and fuel lines. As the carbon chain length increases, the viscosity and density increases. The viscosity and density decrease with increase of double bonds. As the carbon chain length and saturation increases, the CFPP increases and the fuel cold temperature performance decreases.

Formulas have been developed to predict the CN, IV and CFPP values of a bio-diesel according to its fatty acid profile.

The CN can be calculated from a combination of formulas from Lapuerta *et al.,* (2009) and Tong *et al.,* (2011) as combined by Stansell *et al.,* (2012). The CN of individual methyl esters can be calculated using the formulas (equation 8 – 10) below. Equation 8 is used to calculate the CN for saturated methyl esters, for mono unsaturated methyl esters Equation 9 is used and for poly unsaturated methyl esters one should use Equation 10. (Stansell *et al*., 2012).

$$CN = -107.71 + 31.126n - 2.042n^2 + 0.0499n^3 \quad (8)$$

$$CN = 109 - 9.292n + 0.354n^2 \quad (9)$$

$$CN = -21.157 + (7.965 - 1.785db + 0.235db^2)n - 0.099n^2 \quad (10)$$

Where:

CN = cetane number
n = the carbon number of fatty acid chain
db = the number of double bonds

The CN for a specific fatty acid mixture can then be calculated using Equation 11, (Stansell *et al*., 2012).

$$CN = 1.068 \sum (CNimi) - 6.747 \quad (11)$$

Where:

CNi = the CN for a specific methyl ester
mi = is the mass faction of that methyl ester

. The CP of a methyl ester is the only cold-flow property which can be predicted. Prediction of the CP value is required to allow the prediction of the CFPP value. Equation 12 derived from Imahara *et al*., (2006) can be used to predict the CP (Stansell *et al*., 2012, Imahara *et al*., 2006). The "Tmi" and "ΔHmi" values were sourced from Dunn (2008) or predicted according to Lopes *et al*., (2007) (Table 8).

$$\ln(xi) = \frac{\Delta Hmi}{R}\left(\frac{1}{Tmi} - \frac{1}{CP}\right) \quad 12$$

Where:

CP = the cloud point
R = the universal gas constant,
Tmi = the melting points of individual methyl esters
ΔHmi = the enthalphy of melting of individual methyl esters
xi = the mass fraction of individual methyl esters.

The "Tmi" and "ΔHmi" values can be sourced from Dunn (2008) or predicted according to Lopes *et al*., (2007) (Table 8).

Table 8: Tmi and ΔHmi values derived from Dunn (2008) or Lopes (2007).

Saturated fatty acid	Tmi	Source	ΔHmi	Source
C8:0	-37.43	Dunn (2008)	20.48	Lopes *et al*., (2007)
C10:0	-13.48		28.34	
C11:0	-12.17		34.68	
C12:0	4.3		36.20	
C16:0	28.48		49.9	Dunn (2008)
C17:0	28.58		57.65	Lopes *et al*., (2007)
C18:0	37.66		57.04	Dunn (2008)
C20:0	46.43		67.66	Lopes *et al*., (2007)

According to thermodynamic prediction of CP, the individual methyl esters are assumed to precipitate out independently (Imahara *et al*., 2006). This means the highest CP value for an individual methyl ester will be the CP of the mixture. The CFPP value can then be calculated according to Equation 13 presented by Dunn and Bagby (1995):

$$CFPP = 1.0191 \times CP - 2.9 \quad 13$$

Nascimento *et al*., (2013) predicted bio-diesel properties of microalgal bio-diesel produced from an array of microalgal species. The predicted CN and CFPP values can be seen in Table 9 (Nascimento *et al*., 2013). To adhere to South African biodiesel standards a bio-diesel should have a CN value above 51 and a CFPP value below 3°C. The data from Nascimento *et al*., (2013) (Table 9) demonstrates that not any bio-diesel adheres to bio-diesel standards, which highlights the importance of bio-diesel property predictions.

Table 9: CN and CFPP values predicted for bio-diesel generated from an array of microalgal species as determined by Nascimento *et al.*, (2013).

Specie	CN	CFPP
Ankistrodesmus falcatus	50.5	−10.4
Ankistrodesmus fusiformis	48.0	−10.1
Kirchneriella lunaris	42.5	−9.6
Chlamydomonas sp	64.9	−12.2
Chlamydocapsa bacillus	48.4	−10.2
Coelastrum microporum	53.0	−9.5
Desmodesmus brasiliensis	53.3	−0.6
Scenedesmus obliquus	63.6	−11.9
Pseudokirchneriella subcapitata	53.9	−9.6
Chlorella vulgaris	61.8	−10.8
Botryococcus braunii	52.7	−8.0
Botryococcus terribilis	59.5	−10.3

Microalgal bioethanol

Microalgae have been documented to have carbohydrate contents up to 60% of biomass dry weight (Table 10) (Chena *et al*., 2013). The carbohydrate content is dependent on the strain, media composition and environmental factors. The carbohydrates produced by algae can be used for bio-ethanol yeast fermentation (Li *et al*., 2008b)

Table 10: Carbohydrate content as percentage of dry biomass of microalgal strains (Chena *et al*., 2013) .

Microalgal species	Carbohydrate or starch content (%)
Chlorella vulgaris **IAM C-534**	37.0
C. vulgaris **CCAP 211/11B**	55.0
C. vulgaris **P12**	41.0
C. vulgaris	55.0
Chlamydomonas reinhardtii **UTEX 90**	60.0
C. reinhardtii **IAM C-238**	55.0
Chlorococum sp**.**	32.5
Chlorococcum sp**. TISTR8583**	26.0
S. acutiformis **TISTR 8495**	16.4
S. obliquus **CNW-N**	51.8
Tetraselmis sp**.CS-362**	26.0

Chena *et al*., (2013) demonstrated the interspecific variation in microalgae carbohydrate yield rates, showing microalgal carbohydrate yield rates ranging between 21- and 687 $mg.L^{-1}.d^{-1}$. Biomass and carbohydrate yield rates for different microalgal strains as reported by Chena *et al*., (2013) can be seen in Table 11.

Table 11: Biomass and carbohydrate yield rates of different microalgal strains (Chena *et al.*, 2013).

Specie	Biomass yield rate ($mg.L^{-1}.d^{-1}$)	Carbohydrate yield rate ($mg.L^{-1}.d^{-1}$)	Source
C. vulgaris (CCAP 211/11B)	37	21	Illman *et al.*, (2000)
C. vulgaris (P12)	485	199	Dragone *et al.*, (2011)
C. reinhardtii UTEX 90	507	304	Nguyen *et al.*, (2009)
C. reinhardtii	484	257	Kim *et al.*, (2006)
S. obliquus CNW-N	821	383	Ho *et al.*, (2012)
C. vulgaris	254	112	Liang *et al.*, (2009)
C. vulgaris FSP-E	1363	687	Ho *et al.*, (2013)

Chaudhary *et al.,* (2014) predicted that microalgae cultivated at commercial scale can surpass bio-ethanol yield rates of other carbon sources per hectare such as switch grass and sugar beet (Table 12).

Table 12: Bio-ethanol yield from different carbon sources (Chaudhary et al., 2014b).

Sources	Ethanol yield ($L.ha^{-1}.year^{-1}$)
Corn stover	1050-1400
Wheat	2590
Cassava	3310
Sweet sorghum	3050-4070
Corn	3460-4020
Sugar beet	5010-6680
Switch grass	10760
Microalgae	46760-140290

The yeast strains typically used for ethanol fermentation can only use simple carbohydrates, such as monomeric glucose and fructose, as energy source. This means microalgal carbohydrates should be hydrolysed before they can be used in an anaerobic fermentation (Talebnia *et al*., 2010). Common hydrolysis methods include enzyme hydrolysis and acid hydrolysis (Tasić *et al*., 2009). Markou *et al*. (2013) showed that acid hydrolysis can be performed using 5 N HNO_3 or H_2SO_4.

2.4.3 Bio-energy bio-refinery

The term bio-refinery was coined to describe a system by which multiple products and chemicals can be generated from a single biomass source by integrating multiple extraction and processing techniques (Chisti, 2007).

The costs related to the cultivation and processing of microalgae for bio-energy purposes is one of the greatest challenges in this field of research. Integrated systems and bio-

refineries to provide multiple products from microalgal cultivation are possible options for reducing costs and maximising profits from such a system. Microalgal cultivation can be integrated to provide several of the services and products mentioned in this Chapter.

The dual extraction of microalgal lipid and carbohydrate contents can result in the generation of both bio-diesel and bio-ethanol, respectively, from a single biomass source (Chisti, 2007). Although some work has been performed on co-extraction of carbohydrates and lipids from microalgal biomass, most sources tend to focus on producing a single product from microalgal cultivation. Extracting multiple compounds require different equipment and a more diverse facility. Production of both bio-diesel and bio-ethanol could increase microalgal bio-energy outputs, but the additional costs and facilities required to generate both might become a challenge. An additional advantage of such an integrated energy system is that heat, waste water and waste CO_2 generated by a bio-ethanol facility can be returned to the microalgal cultivation facility for temperature regulation, feeding and carbon source respectively (Doucha *et al*., 2005, Li *et al*., 2008b, Pittman *et al*., 2011). Some additional co-products can be generated from microalgal bio-energy industry depending on the methods used. HVO bio-diesel production can lead to the production of propane bio-gas along with high quality bio-diesel (Aatola *et al*., 2009). Production of FAME bio-diesel leads to the co-production of glycerol. Glycerol can be sold or used as an additional carbon source in mixotrophic microalgal cultivation (Liang *et al*., 2009). With the production of bio-ethanol, yeast waste biomass is generated which can be used for animal nutrition or as bacterial growth medium component.

Considering these integration possibilities, it is possible to design a multi facet integrated system. Such a system would be able to provide CO_2 mitigation and water treatment services while providing multiple products to the market. System integration might be the future of microalgal biotechnology and bio-energy (Griffiths *et al.*, 2016, Griffiths *et al*., 2011). In this study we will explore the integration of microalgal bio-diesel and bio-ethanol production.

Chapter 3: Characterisation of isolates for bio-energy production potential and selection

3.1 Introduction

Microalgal bio-energy has been identified as a potential bio-energy source which does not compete with the food or agriculture industry. With that being said, South Africa is home to many algal species, of which very little is known. This provides a treasure trove of strains which can be explored for commercial value for bio-energy production purposes. This provides the need to explore indigenous microalgal strains to identify ones which can be used for the production of microalgal bio-fuel (Smit *et al*., 2017a). The biomass, lipid and carbohydrate productivities of South African indigenous microalgae would need to be characterised to investigate their bio-fuel production potential. This will help to contribute a microalgal strain, which may be used for the production of bio-fuel and future research for cleaner bio-energy in South Africa.

3.2 Methods

There were three main objectives in this section.

- Have fifteen microalgal isolates genetically identified;
- To characterize bio-fuel production potential of the isolates; and
- To select an isolate for further use in the current study.

The methods used to achieve each objective of this section is presented below.

3.2.1 Isolate identification

The Microalgal Culture Collection of South Africa (MiCCSA) is maintained in duplicate at the Council for Scientific and Industrial Research (CSIR), Pretoria, and the University of Witwatersrand, Johannesburg, South Africa (Smit *et al*., 2017b). The culture collection consists of uncharacterised South African indigenous microalgae isolated from eutrophic zones country wide. The culture collection is maintained on AF6 agarose medium (Smit *et al*., 2017a, Watanabe *et al*., 2000).

Fifteen isolates from this culture collection were selected at random from cultures isolated from the Free State (FSA/B), Limpopo (LPB), North West (NWA) and Western Cape (WCA/B/C) provinces, to be characterised for bio-energy production potential.

Microscopic imaging

The fifteen selected isolates were imaged by bright field microscopy. Using a sterile loop, microalgal cells were transferred from an agarose slant culture to a glass slide containing sterile water. The slide was imaged using a bright field microscope (Olympus BX40)

equipped with a camera (CC12 Soft Imaging System) and imaging software (Analysis LS Research). Images were captured using the 100X objective and immersion oil.

These organisms were presumptively identified with the aid of a phycological dichotomous key and training provided by Professor Stuart Sym (University of Witwatersrand).

Genetic sequencing

Genetic sequencing of the isolates entrusted to Doctor Pierre Durand and his team at the Evolution of Complexity Laboratory, University of Witwatersrand, Johannesburg. Durand and his team performed genetic sequencing on all fifteen isolates and were able to identify these isolates. Any genetic data provided in this chapter were supplied by Durand and his team. The methods below describe the methodology performed by Doctor Durand and his team at the Evolution of Complexity Laboratory.

Cultures were maintained in a Labotec growth chamber at 21.5°C with a 12-hour day-night cycle and maximum light intensity of 1000 Lux. Genotyping was performed on clonal samples by either capturing a single cell with a micropipette or picking a small single colony from agar plates and growing the colony or cell in medium until the culture density was sufficient for DNA extraction.

A Qiagen Plant DNA minikit was used to extract total DNA from cell culture and stored at -20°C. Target regions were amplified using a standard PCR amplification protocol comprising 10 ng of total DNA extract, 0.1 U PFu polymerase, 0.4 mM dNTPs and 0.2 mM of each primer in a 25 µL total volume of PFu x1 buffer.

The PCR cycling conditions were as follows: denaturation at 95°C for 5 minutes, 35 amplification cycles (95°C for 1 minutes, 55°C for 30 seconds and 72°C for 1 minutes 30 seconds) and a final extension step at 72°C for 10 minutes. PCR products were electrophoresed for 1 hour at 80 V in 1 % (w/v) agarose gel, the band excised and purified with a PCR clean-up gel extraction kit (Sigma).

The genetic regions to be amplified comprised standard barcoding markers and included conserved regions of genes 18S, tuf, cox1 and rbcL. For 18S, a home-made primer design algorithm (PisCator) developed by Prof Scott Hazelhurst and Andrew Ndhlovu at University of Witwatersrand, Johannesburg, identified 5 forward and reverse primer pairs (De Wever *et al*., 2009, Medlin *et al*., 1988, Nakayama *et al*., 1998). The remaining primer pairs for tuf, cox and rbcL were obtained from Fuωíková *et al*. (2010). PCR amplicons were sequenced with an ABIsystems Sanger sequencer at Inqaba Biotec and the raw sequence data imported manually into the BLASTn algorithm in "GenBank" for organism identification (Altschul *et al*., 1990).

Sequence data were available for the 18S region for all the organisms genotyped. The sequences were included with a set of previously published reference sequences of 18S data for chlorophytes and downloaded from "GenBank" (https://www.ncbi.nlm.nih.gov/genbank) (Leliaert *et al.*, 2012).

3.2.2 Isolate characterisation

Cultivation

All fifteen isolates were cultured in 2 L AF6 media as described by Watanabe *et al*,. (2000) in 4000 mL SIMAX round bottom flasks for fifteen days each in triplicate. The cultures were agitated on Heidolph MR Hei-Mix D magnetic stirrers at 400 RPM under ~7000 Lux Sylvania GRO-LUX F18W/GRO-78 neon light illumination (Figure 16). Samples of 20 mL volume were taken daily, using TPP 25 mL sterile pipettes.

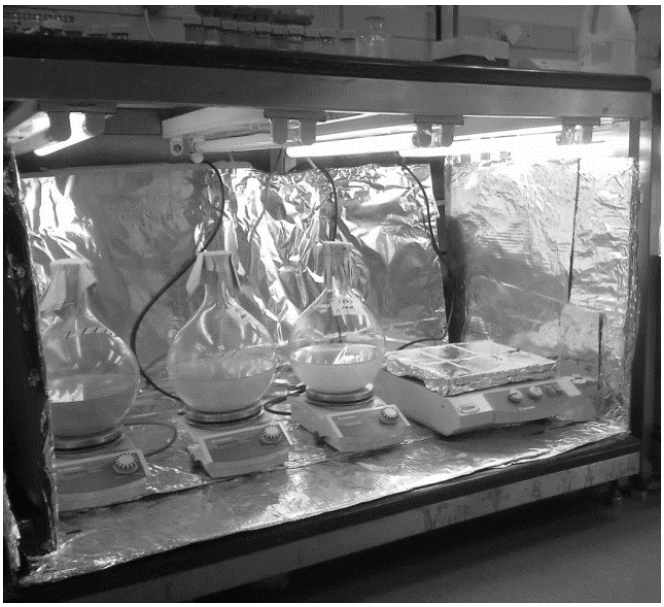


Figure 16: Neon light and magnetic stirrer setup for the flask study, under the work benches.

Characterisation of biomass productivity

To characterise biomass yield rate, a measure of biomass was required. For microalgal cultures, biomass measures include: Optical density (OD) readings, dry cell weight (DCW) determination by evaporation, DCW determination by filtering and drying, DCW determination by centrifugation and drying, microscopic cell counting and flow cytometric cell counting. Advantages and disadvantages of each method is displayed in Table 13. Biomass yield rate is displayed as a unit of mass/volume/duration.

Table 13: Summary of some advantages and disadvantages related to different biomass measures.

Method	Advantages	Disadvantages
DCW by drying	Data in mass units, which can be used for productivity calculations.	• Most energy intensive and time-consuming method. • Requires large sample volumes.
DCW by filtration	Data in mass units, which can be used for productivity calculations.	• Third most energy intensive and time-consuming method. • Requires large sample volumes. • Can have high standard error due to losses through the filter.
DCW by centrifugation	Data in mass units, which can be used for productivity calculations.	• Second most energy intensive and time-consuming method. • Requires large sample volumes. • Can have high standard error due to losses during supernatant decanting.
OD readings	• Can be performed on small sample sizes. • Fastest method.	• Value needs a DCW correlation before it can be used for productivity calculations.
Microscopic cytometric cell counting	• Can be performed on small sample sizes. • Simultaneous culture microscopic health and contamination status analysis may be performed.	• Value needs a DCW correlation before it can be used for productivity calculations • Can be time consuming if multiple samples should be analysed. • Labour intensive.
Flow cytometric cell counting	• Can be performed on small to medium sample sizes depending on the flow cytometer. • Relatively fast method.	• Value needs a DCW correlation before it can be used for productivity calculations. • Requires specialised equipment.

OD readings combined with DCW by filtration OD/DCW correlation were selected as the biomass measure of choice for this study. OD reading is an indirect method of biomass content determination. OD readings combined with a good DCW correlation can however be more effective than doing a DCW analysis with each sample. OD readings performed on a 96 well plate can be performed using 100-300 µL sample per replicate, this reduces the sample volume required for the biomass measure. OD readings are also suitable for high throughput studies because of its low labour and time requirements. The OD/DCW correlation by filtration was selected due to this method being the fastest and least energy intensive DCW method.

200 µL from each culture were transferred to 96-well microtiter plates in triplicate. OD 675 readings were performed on the loaded 96-well plates using a BioTek PowerWave HT spectrometer with the aid of Gen5 (v1.06) software.

At the end of each study an OD 675/dry cell weight (DCW) correlation was performed for each isolate. Culture/water (v/v) 16 mL dilutions of 100%, 80%, 60%, 40%, 20% and 0% were made for each culture. From each of the above-mentioned dilutions 200 µL were transferred to 96-well microtiter plates in triplicate. OD 675 readings were performed on the loaded 96-well plates using a BioTek PowerWave HT spectrometer with the aid of Gen5 (v1.06) software. Volumes of 5 mL from the above-mentioned dilutions were filtered in triplicate on a XX2702550 Millipore Model 1225 Sampling Manifold Vacuum Filtration Cell Harvester using pre-weighed 25 mm Macherey-Nagel GF2 glass fibre micro filters (~0.4 µm pore size). The filter papers were dried in a Mettler Toledo HS153 moisture analyser and weighed to determine the biomass DCW present on each filter.

Lipid content analysis

Three main methods of lipid content analysis; Fatty acid methyl ester gas chromatography (FAME-GC), Nile red fluorescent spectroscopy and Nile red fluorescent microscopy, were considered in this study. Advantages and disadvantages of each method is displayed in Table 14.

Table 14: Summary of some advantages and disadvantages related to different lipid content measures

Method	Advantages	Disadvantages
FAME-GC	• Quantitative measure. • High sensitivity. • Provides data on lipid profiles.	• High running cost. • Labour intensive. • Time consuming. • Requires specialised equipment. • Requires large sample volumes.
Nile red fluorescent spectroscopy	• Quantitative measure. • Low cost. • Fast method.	• Limited sensitivity. • Requires specialised equipment.
Nile red fluorescent microscopy	• Low cost. • Allow the visualisation of cellular lipid store locations.	• Time consuming. • Labour intensive. • Semi-quantitative method • Requires specialised equipment and software to estimate the lipid contents. • Very low sensitivity.

In this study FAME-GC was selected as the method of choice. FAME-GC was selected because it can provide lipid profile data, which can be used to predict biodiesel properties. The equipment needed for FAME-GC was made available for this study by CSIR, Biosciences. Griffiths *et al*., (2010) demonstrated that direct transesterification is ideal for obtaining higher lipid concentration extractions from microalgal biomass, indicating higher accuracy (Griffiths et al., 2010).

15 mL was centrifuged on a Beckman Coulter Allegra X-22R swinging bucket centrifuge at 3901 xg for 15 minutes. The supernatants were decanted without dislodging the pellets. The pellets were re-suspended in 800 µL Milli-Q Millipore water and transferred to 2 mL screw cap centrifuge tubes. The centrifuged tubes were centrifuged on an Eppendorf MiniSpin plus centrifuge at 10481 xg for 2 minutes. The supernatants were decanted without dislodging the pellets. To the pellets, 250 µL toluene was added, followed by 500 µL 0.5 N NaOH in methanol. The mixtures were vortex vigorously to re-suspend the pellets. The mixtures were incubated for 20 minutes at 80°C, agitating at 950 RPM, on an Eppendorf Thermomixer comfort. The reaction mixtures were cooled down to ambient temperature in a -20°C freezer for 5 minutes. To the reaction mixtures 500 µL 5% HCl in methanol was added. The reaction mixtures were incubated at 80°C with 950 RPM agitation for 20 minutes of Eppendorf Thermomixer comfort. The reaction mixtures were cooled down to ambient temperature in a -20°C freezer for 5 minutes. To the mixtures 200 µL Milli-Q water was added to stop the reactions, followed by 300 µL hexane. The mixtures were vigorously vortexed and centrifuged on an Eppendorf MiniSpin plus centrifuge at 10481 xg for 2 minutes. The hexane phases were transferred to 1.5 mL Eppendorf tubes containing ~2 µg anhydrous $MgSO_4$. The 1.5 mL Eppendorf tubes were centrifuged on an Eppendorf MiniSpin plus centrifuge at 10481 xg for 2 minutes. The hexane phase was transferred to inserts in appropriately labelled GC crimp cap vials and capped.

The GC was performed using a Supelco Omega Wax 320 column (30 m x 0.32 mm x 0.25 µm film thickness, cat # 24152) on an Agilent Technologies 7890A GC system equipped with an Agilent Technologies 7693 Auto sampler.

A FAME standard (Supelco 37 Component FAME Mix, 1 x 1 mL, varied concentration in dichloromethane Part Number: CRM47885) was run on the GC system to obtain area under the peak and substance concentration standard curves for 37 FAMEs (Appendix A, Figure A46 – A61). Linear trend lines were used to obtain straight line formulas for each correlation. These formulas were used to convert chromatogram peak areas to lipid concentrations per volume sample taken ($g.L^{-1}$). FAME-GC chromatograms can thus be converted back determine the lipid content of microalgal cell culture volumes. This technique was used to determine the lipid content in each volume unit of analysed microalgal culture.

The FAME-GC data for the fifteen isolates was collected over fifteen days. The lipid contents of all fifteen isolates were plotted over time (Appendix A, Figure A62 – A76). Linear trend lines were used to allow the determination of the average lipid yield rate over 15 days. The slopes of these trend lines were indicative of the average lipid yield rate of an isolate.

Carbohydrate content analysis:

Two carbohydrate content analysis methods, high performance anion exchange chromatography (HPAEC) and the Dubois phenol-sulphuric spectroscopy, were considered for this study (DuBois *et al*., 1956). Advantages and disadvantages of each method is displayed in Table 15.

Table 15: Summary of some advantages and disadvantages related to different carbohydrate content measures.

Method	Advantages	Disadvantages
HPAEC	• High sensitivity. • Provides data on carbohydrate profiles.	• Requires specialised equipment. • Time consuming. • Labour intensive. • High costs.
Dubois	• Low costs. • Fast method.	• Requires hazardous chemicals. • Medium sensitivity.

The Dubois spectroscopic method was selected for this study. The Dubois method can supply data with sufficient sensitivity to characterise the carbohydrate content. The Dubois method also has the advantage of being a relatively fast and inexpensive method.

565 µL of sample was transferred to a 2 mL Eppendorf tube. Under the fume hood 15 µL 80% (w/v) phenol (in water) was added to the 565 µL sample. To the reaction mixture, 1.45 mL 99.9% (v/v) sulfuric acid was slowly added under the fume hood. The mixture was incubated at 25°C for 10 minutes. From the reaction mixture 200 µL reaction mixture was transferred to a 96-well plate in triplicate under the fume hood. OD 490 readings were performed on the loaded 96-well plates using a BioTek PowerWave HT spectrometer with the aid of Gen5 (v1.06) software.

The above-mentioned method was performed with on glucose stock standards of 0-, 5.650-, 8.475-, 11.300-, 14.125- and 16.950 $mg.L^{-1}$. The stock standard samples were used to setup the glucose standard to convert OD 490 values to mg/L values.

Samples with OD 490 values higher than 1 were diluted and the DuBois reaction repeated on those samples. OD 490 values of some strains at specific time points seemed to be uncomfortably high. At closer investigation the cause for this was found to be over

dilution of samples, which lead to overestimation of the carbohydrate content. The Dubois method seems to have a lower detection limit of 0.2. Any sample diluted to such an extent where the OD value would be at 0.2 or lower would lead to an overestimation of the carbohydrate content. Overestimated data points were identified and not used for the productivity determination. The resulting effect however was the reduction of sample time points.

This method was used to generate an OD 490 nm glucose content correlation curve (Appendix A, Figure A77). Equation 14 generated from the linear trend line of the correlation curve, was used to covert OD 490 values to carbohydrate mg/L values.

$$y = 20.72x - 3.6108 \qquad 14$$

Where:

x = the OD value at 490 nm
y = the concentration of glucose ($mg.L^{-1}$)

The carbohydrate contents of all fifteen isolates were plotted over time (Appendix A, Figure A78 - A98). Linear trend lines were used to allow the determination of the average specific carbohydrate productivity over 15 days. The slopes of these trend lines were indicative of the average specific carbohydrate yield rate of an isolate.

3.2.3 Isolate selection

To select an isolate for use in further studies, a simple scoring matrix was generated from the biomass, lipid and carbohydrate productivity generated from the flask study. The weighting of biomass, lipid and carbohydrate productivity in the matrix was 30%, 50% and 20% respectively. The lipid yield rate was provided the highest priority and score due to bio-diesel production being the main aim. Biomass yield rate provided the second highest weighting due to the lipid and carbohydrate yield rates being directly influenced by the biomass yield rate. The carbohydrate yield rate provided the lowest weighting due to carbohydrates being a secondary product after bio-diesel production. The highest biomass, lipid and carbohydrate productivities generated in this study were used as the 100% productivity benchmarks.

3.3 Results and discussion

In this section, the results from the isolate identification, characterisation of the isolates are discussed in order to select the chosen isolate.

3.3.1 Isolate identification

All fifteen isolates were genetically sequenced and microscopically assessed to be able to identify gross morphological and genetic discrepancies. The presumptive morphological identification is listed alongside the genetic identification in Table 16. Micrograph for all fifteen isolates can be seen in Appendix A, Figure A1 – A15.

Table 16: Presumptive morphological presumptive ID and sequence data ID of fifteen isolates (Durand et al., 2016).

Isolate designation	Morphological presumptive ID	Sequence data ID
FSA 5.1	*Characiochloris*	*Raphidocelis contorta*
FSB 11.1	*Chlorococcum*	*Graesiella emersonii*
FSB 41.1	*Chlorococcum*	*Chlorella sorokiniana*
FSB 51.2	*Chlorella*	Unknown *chlorophyte*
LPB 5.1	*Chlorococcum*	*Heterochlorella luteoviridis* or *Chlorella variabilis*
LPB 12.1	*Scenedesmus*	*Lobochlamys segnis* or *Chlamydomonas*
LPB 15.1	*Chlamydomonas*	*Lobochlamys segnis*
NWA 1.1	*Selenastrum*	*Chlorella sorokiniana*
NWA 9.1	*Chlorella*	*Lobochlamys segnis* or *Chlorella pyrenoidosa*
NWA 11.1	*Scenedesmus*	*Lobochlamys segnis*
WCA 4.1	*Chlorella*	*Chlorella sorokiniana*
WCA 10.1	*Chlorella*	*Parachlorella kessleri*
WCB 4.1	*Chlorella*	*Tetradesmus acuminatus*
WCB 7.3	*Chlorella*	*Parachlorella kessleri*
WCC 2.1	*Chlorella*	*Chlorella sorokiniana*

Morphologically and genetically, all the organisms are *Chlorophytes*. This is most probably due to the culture collection being maintained on artificial fresh water 6 (AF6) media, a medium adapted for *Chlorophytes* (Smit et al., 2017a, Watanabe et al., 2000). The morphological identifications correspond to the genetic identification and no gross discrepancies can be seen.

3.3.2 Isolate characterisation

Cell density analysis

OD675 and DCW correlation data was generated for all fifteen isolates using the method described in Section 3.2.2. The correlation data was used to create DCW/OD correlation curves for each isolate (Appendix A, Figure A16 - A30). From each curve, a linear trend line equation was generated. The equations from these trend lines can be used to convert OD values from the study to estimated biomass (g/L) values as can be seen in Appendix A, Table A2.

The estimated biomass values were plotted over time (Appendix A, Figure A31 - A45). To calculate the average biomass yield rate of each isolate over 15 days, linear trend lines were plotted for each curve. The slope of such a trend line is indicative of the average specific biomass yield rate ($g.L^{-1}.d^{-1}$) for the duration of the study as explained in Chapter 2, Section 2.1.1. The yield rates were calculated and can be seen in Figure 17.

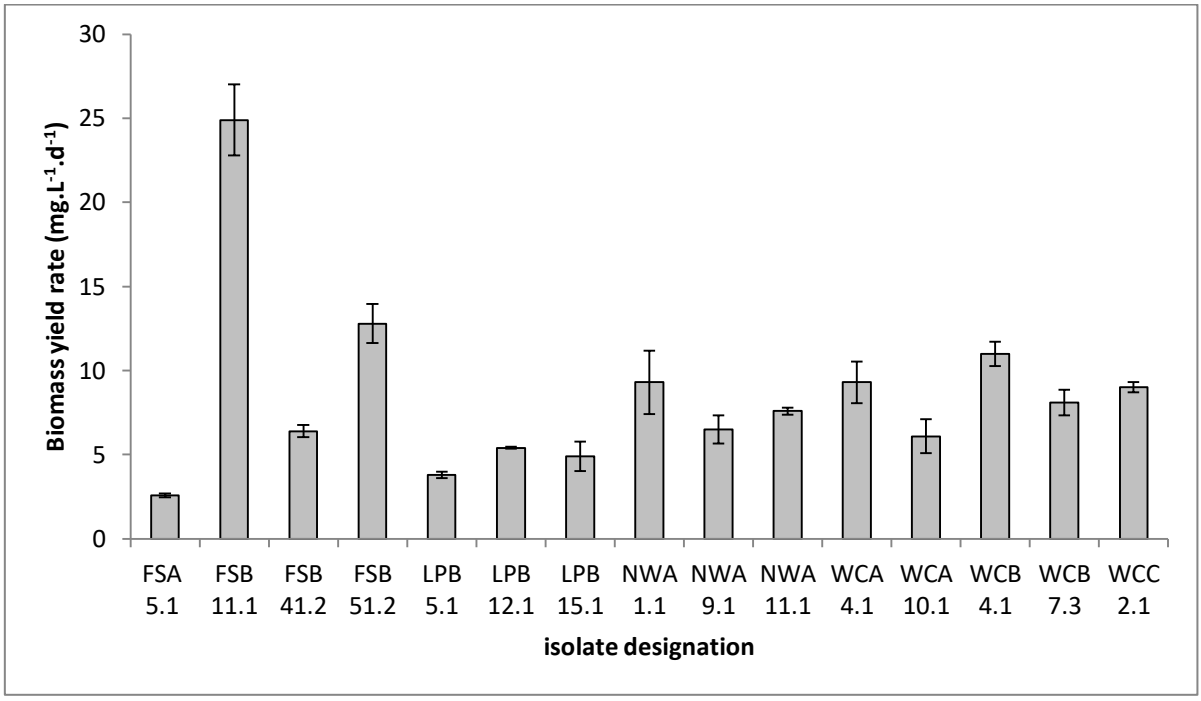


Figure 17: Biomass yield rate per culture volume of the fifteen isolates. The error bars indicate the standard deviation.

From the yield rates generated from trend lines, isolate FSB 11.1 had the highest biomass yield rate of 24.9 $mg.L^{-1}.d^{-1}$ followed by FSB 51.2 and WCB 4.1 with 12.8 $mg.L^{-1}.d^{-1}$ and 11 $mg.L^{-1}.d^{-1}$ respectively. Isolate FSA 5.1 and LPB 5.1 showed the lowest biomass yield rates at 2.6 $mg.L^{-1}.d^{-1}$ and 3.8 $mg.L^{-1}.d^{-1}$.

Compared to works by other authors, yield rates such as 0.783 and 0.120 $g.L^{-1}.d^{-1}$, as described by Sandnes *et al.*, (2005) and Gouveia and Oliveira (2009), the yield rates obtained in this study are very low. It should however be taken to mind that in the studies by Sandnes *et al.*, (2005) and Gouveia and Oliveira (2009) known species have been cultivated in optimised conditions to obtain such high yield rates. Although the fifteen isolates are showing low yield rates, these yield rates can be increased in future work by optimising the medium composition, growth conditions and harvesting time. This indicates great room for cultivation method improvement of these isolates.

Lipid content analysis

The determined lipid yield rates of all fifteen isolates can be seen in Figure 18. Microalgal lipid yield rates ranged from 0.1 to 4.1 $mg.L^{-1}.d^{-1}$. Three of the fifteen isolates showed lipid yield rates lower than 1 $mg.L^{-1}.d^{-1}$. Ten of the fifteen isolates had lipid yield rates above 2 $mg.L^{-1}.d^{-1}$. Seven of the fifteen isolates showed lipid yield rates above 3 $mg.L^{-1}.d^{-1}$. Only three of the isolates showed lipid yield rates above 4 $mg.L^{-1}.d^{-1}$.

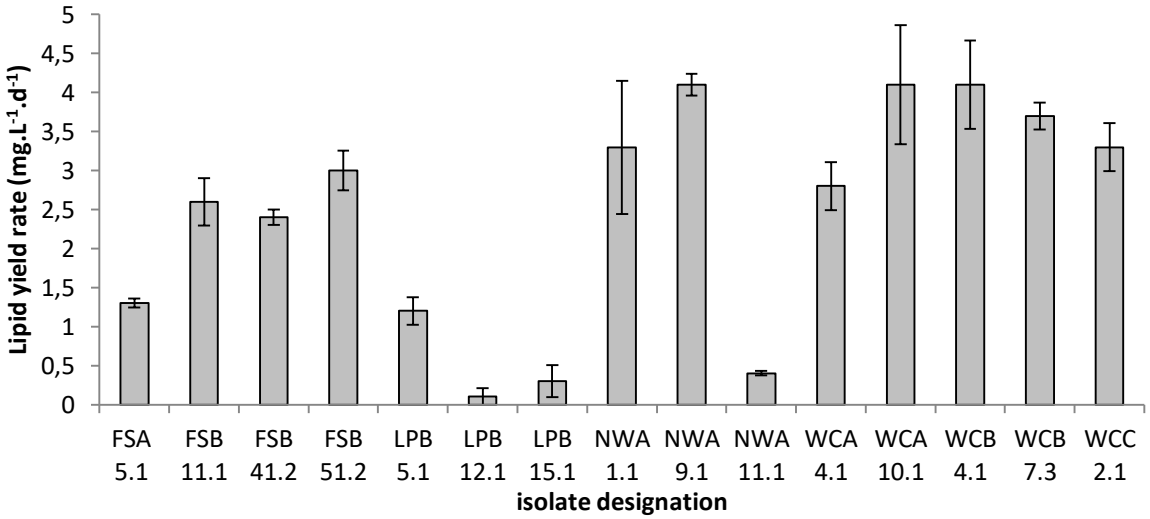


Figure 18: Lipid yield rate per culture volume of the fifteen isolates. The error bars indicate the standard deviation.

Isolates NWA 9.1, WCA 10.1 and WCB 4.1 have the highest lipid yield rates of 4.1 $mg.L^{-1}.d^{-1}$ each. Compared to microalgal lipid yield rates from other literature sources such as Nascimento *et al.*, (2013), displaying lipid yield rates ranging from 22.6- to 204.9 $mg.L^{-1}.d^{-1}$, indicates that the lipid yield rates measured in this study are very low compared to other sources such as the sources listed in table 5 from Chapter 2 Section 2.4.2 (Figure 19).

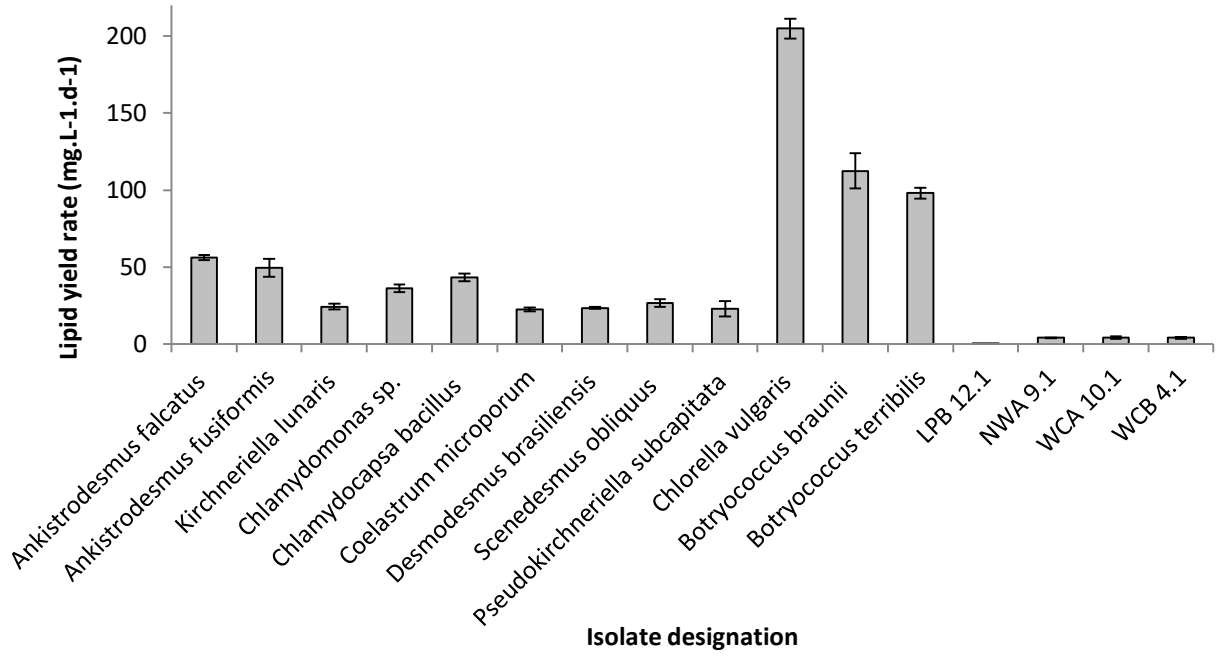


Figure 19: Comparison between literature lipid yield rates of microalgal strains according to Nascimento *et al.*, (2013) and lipid yield rates measured in this study. The error bars indicate the standard deviation.

Isolates NWA 9.1, WCA 10.1 and WCB 4.1 were able to have cellular lipid contents ranging from 25% to 50% nearing the end of the study, indicating that the low biomass productivities of these isolates were the main cause of low lipid yield rate. By increasing the biomass yield rate of these isolates, the lipid yield rate would subsequently be increased.

Carbohydrate content analysis

Calculated carbohydrate yield rates of each of the fifteen isolates can be seen in Figure 20. The minimum measured carbohydrate yield rate is that of LPB 15.1 at 0.6 $mg.L^{-1}.d^{-1}$. The maximum measured carbohydrate yield rate is that of WCB 4.1 at 3.2 $mg.L^{-1}.d^{-1}$. Of the fifteen isolates ~93% of the carbohydrate yield rates fall into the range of 0.5 – 2.0 $mg.L^{-1}.d^{-1}$.

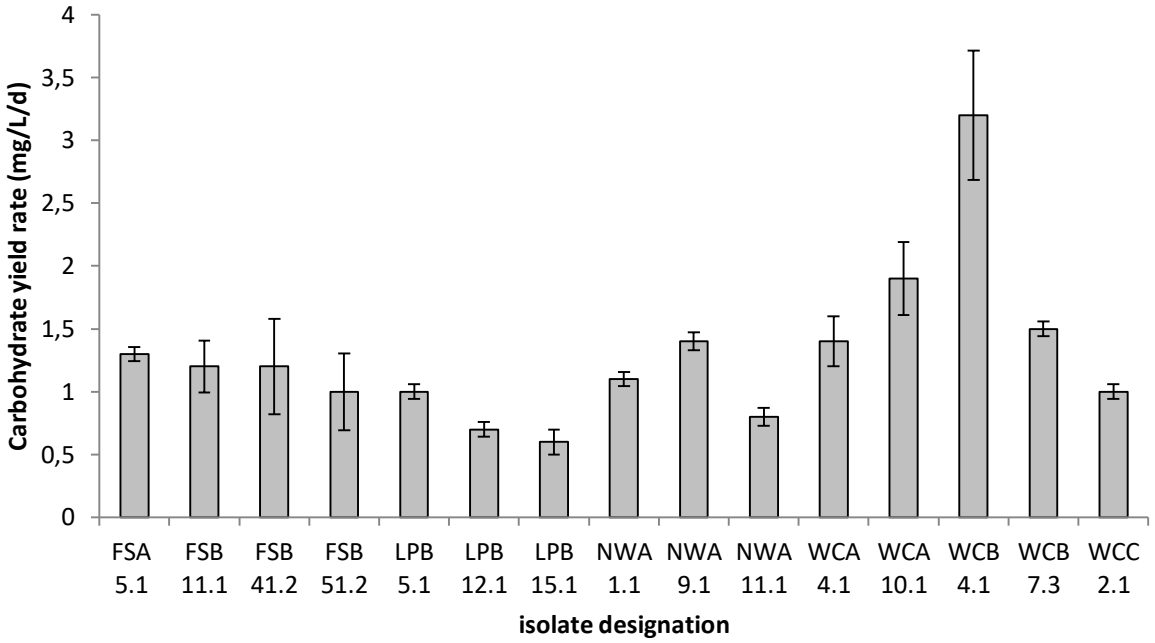


Figure 20: Carbohydrate yield rate of the fifteen isolates. The error bars indicate the standard deviation.

The carbohydrate yield rates are low compared to other literature yield rates from Chena *et al.*, (2013). Chena *et al.*, (2013) demonstrates carbohydrate yield rates ranging from 21 to 687 $mg.L^{-1}.d^{-1}$, which is substantially higher than the measured maximum of 3.2 $mg.L^{-1}.d^{-1}$. As seen with the lipid yield rate, the main limitation to the carbohydrate yield rate is the low biomass yield rate. The main tactic to increase the carbohydrate yield rate would be to increase the biomass yield rate. Due to yield rate being a function of time, one of the simplest methods to increase yield rate would be to identify the ideal harvest time or keeping the cultivation in exponential phase as long as possible by nitrogen, carbon or phosphor feeding.

3.3.3. Isolate selection

The biomass, lipid and carbohydrate average specific yield rates in $mg.L^{-1}.d^{-1}$ have been successfully estimated for all 15 isolates as can be seen in and Figure 21. Considering FSB 11.1 having the highest biomass yield rate but not the highest lipid or carbohydrate yield rates, demonstrates that an isolate cannot be selected based on its biomass productivity alone. In most of the isolates the lipid yield rate is higher than the carbohydrate yield rate.

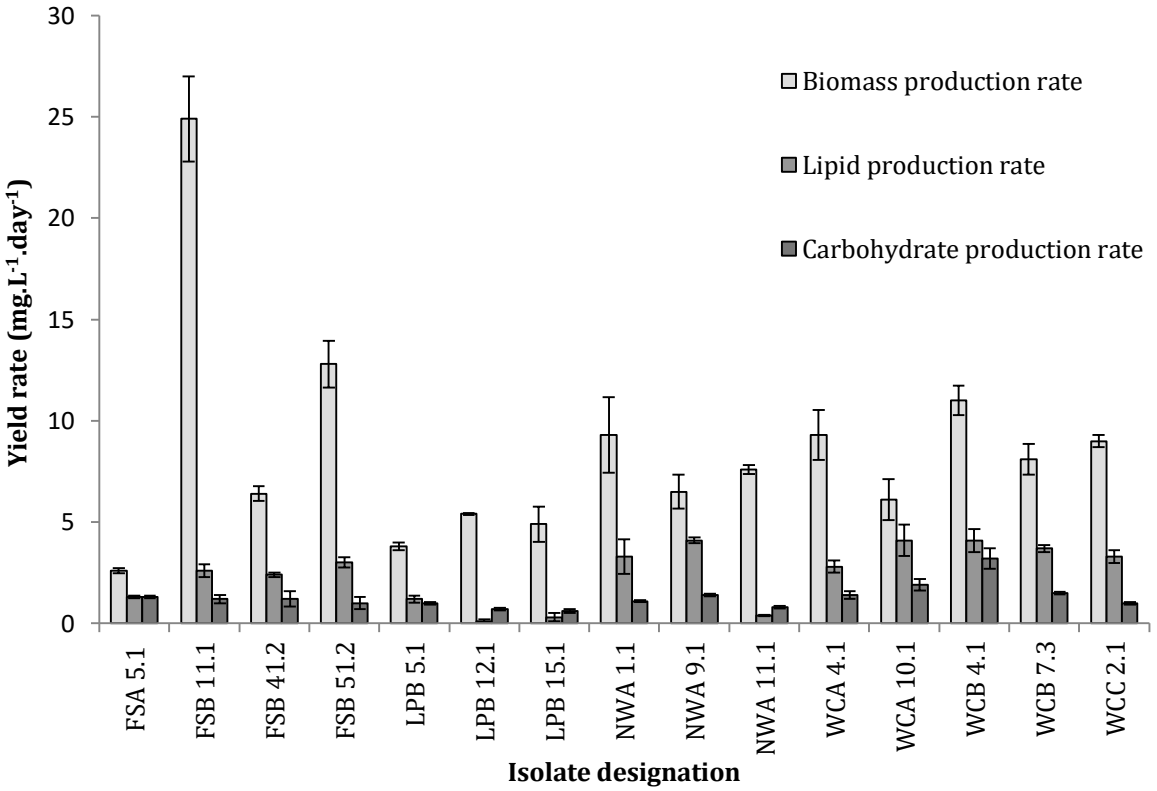


Figure 21: Average specific biomass, lipid and carbohydrate yield rates for the fifteen microalgal isolates. The error bars indicate the standard deviation.

Selecting an isolate can be a complicated process due to multiple parameters being measured. Be that as it may, to be able to select an isolate for further studies in this work, a scoring matrix was used where the biomass, lipid and carbohydrate yield rates were given weightings of 30%, 50% and 20% respectively. Individual parameter scores and final scores can be seen in Table 17. As a result, isolate WCB 4.1 received the highest score followed by WCA 10.1and then FSB 11.1. The scores can be visually compared in Figure 22. According to the scoring matrix WCB 4.1 is the highest scoring candidate and thus the best candidate isolate for further studies, which is shown in subsequent chapters.

Table 17: Scoring matrix of the specific isolate yield rates.

Organism ID	Biomass yield rate ($mg.L^{-1}.d^{-1}$)	Biomass score	Lipid yield rate ($mg.L^{-1}.d^{-1}$)	Lipid score	Carbohydrate yield rate ($mg.L^{-1}.d^{-1}$)	Carbohydrate score	Total average score
FSA 5.1	2.6	10.4	1.3	31.7	1.3	40.6	27.1
FSB 11.1	24.9	100.0	2.6	63.4	1.2	37.5	69.2
FSB 41.2	6.4	25.7	2.4	58.5	1.2	37.5	44.5
FSB 51.2	12.8	51.4	3	73.2	1.0	31.3	58.3
LPB 5.1	3.8	15.3	1.2	29.3	1.0	31.3	25.5
LPB 12.1	5.4	21.7	0.1	2.4	0.7	21.9	12.1
LPB 15.1	4.9	19.7	0.3	7.3	0.6	18.8	13.3
NWA 1.1	9.3	37.3	3.3	80.5	1.1	34.4	58.3
NWA 9.1	6.5	26.1	4.1	100.0	1.4	43.8	66.6
NWA 11.1	7.6	30.5	0.4	9.8	0.8	25.0	19.0
WCA 4.1	9.3	37.3	2.8	68.3	1.4	43.8	54.1
WCA 10.1	6.1	24.5	4.1	100.0	1.9	59.4	69.2
WCB 4.1	11.0	44.2	4.1	100.0	3.2	100.0	83.3
WCB 7.3	8.1	32.5	3.7	90.2	1.5	46.9	64.3
WCC 2.1	9.0	36.1	3.3	80.5	1.0	31.3	57.3

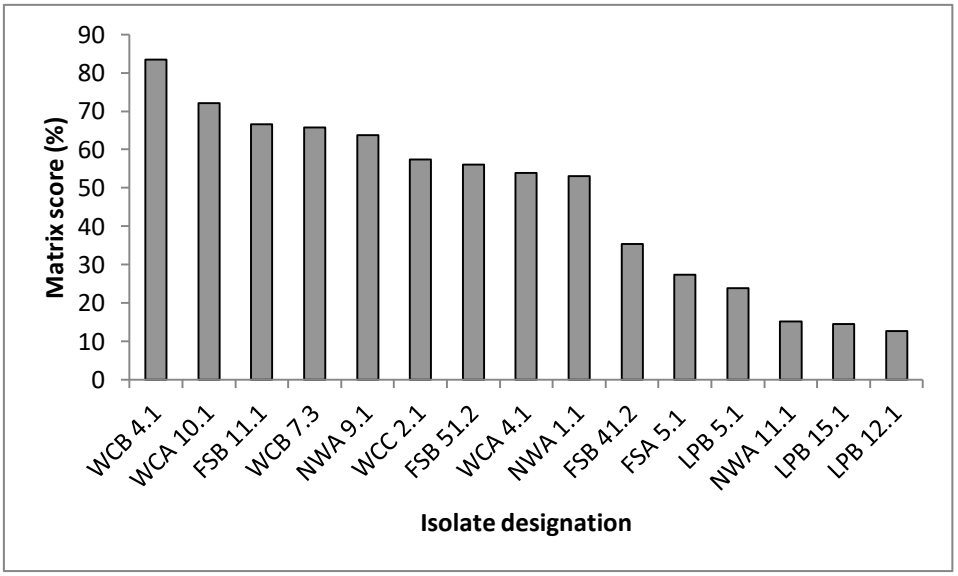


Figure 22: Bar graph indicating the matrix score of each respective studied isolate from the highest to the lowest from left to right.

3.4 Conclusion

Fifteen isolates were successfully characterised with the aid of this flask study. Data on all isolates regarding growth rate, biomass yield rate, lipid yield rate, lipid profile and carbohydrate yield rate were generated.

WCB 4.1isolate were identified as the strongest candidate with the highest score of 83.3. The closest competitors were WCA 10.1 and FSB 11.1 with scores of 72.2 and 66.6 respectively. With WCB 4.1 being the organism with the highest carbohydrate and lipid yield rate and third highest biomass yield rate, it is not surprising that it is the highest scoring organism. WCB 4.1 is the organism of choice for use in the rest of the studies shown in the following chapters, in order to fulfil the objectives of this work.

Chapter 4: Pre-cultivation and medium study of selected isolate WCB 4.1

4.1 Introduction

WCB 4.1 has been selected as the organism of choice to continue the study with. WCB 4.1 has been identified, in Chapter 3, according to BLAST sequence similarity as a *Tetradesmus acuminatus*. The organism is dominantly a large (8 - 15 µm diameter) spherical shaped green algae. In a healthy culture, the organism is "grass" green.

In Chapter 3, WCB 4.1 showed bio-fuel production potential. The main restriction in performance of WCB 4.1 was its low biomass yield rate. Medium composition is one of the main contributing factors affecting the biomass productivity of microalgae. By improving the medium composition used for the cultivation of WCB 4.1, the biomass productivity and subsequent biofuel productivity can be increased. This chapter will aim to identify potential cultivation mediums for WCB 4.1 and characterise the biomass productivity of WCB 4.1 in these mediums.

4.2 Methods

In this section, three main experiments were carried out. That was to perform:

1. Single cell isolation and pre-cultivation.
2. Genetic sequencing.
3. Cultivation experiments in different mediums.

4.2.1 Single cell isolation and pre-cultivation

A disposable glass Pasteur pipette was used to create a glass microtube. Using tweezers to grip the tip, a section of the end of the glass pipette, 3 cm behind the tip, was heated until the glass started to become malleable. In a swift motion the glass pipette was taken away from the flame and the tip stretched away from the rest of the pipette. The malleable section of the glass elongated to form a glass microfibre which solidified within seconds. The microfibre was divided in the centre of its length using the tweezers and placed in a sterile petri dish. This was repeated re-using the same glass pipette until six glass microfibres were created. Each microfibre had a microfibre and thick end.

A silicon tube (0.5 mm inner 1 mm outer) 30 cm in length was placed over the thick end of a glass micro tube. With the aid of the silicone tubing, the micro tube was operated by mouth pipetting. From the culture of WCB 4.1, from day 15 in Chapter 2, a 1 mL sample was taken. A ~50 µL drop of the sample culture was placed on a glass slide and placed under an invert microscope. Five drops of ~20 µL sterile AF6 was placed on the same slide with enough space between the drops to avoid mergence. While viewing the culture

drop through the microscope, the micro tube was used to suck up a few cells. Viewing one of the sterile AF6 drops, a few cells (ideally 1 - 5 cells) were transferred to the drop. The micro tube was rinsed before each transfer with water by mouth pipetting to remove any cells in the tube. Viewing the transferred cells in the first AF6 drop under the microscope, a cell was sucked up using the micro pipette and transferred to a new sterile drop. These steps were repeated until a drop contained only a single cell. The single cell was then be transferred to a well on a 96-well plate containing 100 µL sterile AF6 using the micro tube. Using this approach, 24 single cell isolations were performed. The 96 well plate was sealed with film and placed under Sylvania GRO-LUX F18W/GRO-78 neon lighting for seven days. After seven days, the wells were visualised on an invert microscope and the mono-septic status noted. On day seven, additional 100 µL sterile AF6 were slowly added to all cell containing wells. The 96-well plate was film sealed and placed under Sylvania GRO-LUX F18W/GRO-78 neon lighting for four more days.

On day eleven, the twenty-four 200 µL micro-cultures from the 96 well plate was suspended by pipetting and transferred to wells on a 24-well plate. To each culture on the 24-well plate, 500 µL sterile AF6 were added. The 24-well plate was film sealed and placed on a shaker under Sylvania GRO-LUX F18W/GRO-78 neon lighting for five days. On day five 1 mL sterile AF6 was added to each well and the cultures suspended by pipetting. The 24-well plate was film sealed and placed on a shaker under Sylvania GRO-LUX F18W/GRO-78 neon lighting for five days. On day ten, six of the healthy ~1.7 mL cultures, with mono-septic status, were transferred to sterile 20 mL McCartney bottles containing 10 mL sterile AF6. The McCartney bottles were secured on a shaker under Sylvania GRO-LUX F18W/GRO-78 neon lighting and incubated for nine days. After nine days the cultures were transferred to 250 mL Erlenmeyer flasks containing 100 mL sterile AF6 each. The cultures were placed on a Sylvania GRO-LUX F18W/GRO-78 neon light illuminated orbital shaker and incubated for seven days at 120 RPM.

4.2.2 Sequencing

Drops from the 100 mL cultures were visualised on an Olympus BX40 microscope to ensure monoseptic status. The healthiest mono-septic culture was selected. From the selected culture 50 mL was transferred to a 50 mL falcon tube. The 50 mL falcon tube culture was centrifuged on a Beckman Coulter Allegra X-22R swinging bucket centrifuge at 3901 xg for 15 minutes and the supernatant discarded.

The DNA extraction and sequencing explained below is as performed by Inqaba Biotec:

DNA was obtained from the pellet using a ZR Fungal/Bacterial DNA Kit™ (Zymo Research). Primers 18S-AB1 and 18S-TW4 were used to amplify the 18S target region (Appendix B, Table B1) (Lin et al., 2012).

The 18S target region was amplified using OneTaq™ DNA polymerase (NEB) and the above-mentioned primers. PCR products were gel extracted (Zymo Research, Zymoclean™ Gel DNA Recovery Kit), and sequenced in the forward and reverse directions on the ABI PRISM™ 3500xl Genetic Analyser by Inqaba biotech. Sequencing data was analyzed using CLC Main Workbench 7 followed by a BLAST search (NCBI).

4.2.3 WCB 4.1 medium study

Medium identification

For medium identification for WCB 4.1, preference was given to mediums adapted for *Chlorophytes*, *Scenedesmus* and *Tetradesmus.* Seven mediums were identified, which can be used for cultivation of *Scenedesmus* and *Tetradesmus,* from Andersen Algal Culturing Techniques (Andersen, 2005). The mediums identified were the AF6 medium, Bold Basal medium (BBM), C Medium, Chu #10 medium, DY-V Medium, Franquil medium and WC medium (Andersen, 2005). An additional three mediums were identified, the Zarrouk (1966), Lu (2015) and Hase (2000) mediums, which have been used for the cultivation of chlorophytes in open pond systems (Lu et al., 2015, Hase et al., 2000, Zarrouk, 1966). The medium compositions can be seen in Appendix B, Table B2.

The JG medium was derived from the Hase medium where the sodium and potassium molar ratio was set to a 4:1 ratio and nitrate and phosphate molar ratio to 16:1 (Redfield, 1958). The medium composition can be seen in Table 18.

Table 18: Medium composition of the JG medium.

Media Component	Component Concentration (mM)
NO_3	3
Na	7.635
Mg	0.15
SO_4	0.150
K	2.188
PO_4	0.188
Ca	0.2
Cl	0.409
CO_3	6.625
Fe	21×10^{-3}
Mn	200×10^{-6}
EDTA	5×10^{-3}
Zn	70×10^{-6}
Co	15×10^{-6}
Cu	4×10^{-6}
Mo	52×10^{-6}

Medium sterilisation

An autoclavable Schott bottle head plate mounted 45 µm filter sterilisation rig was prepared as depicted in Figure 23. The rig was used multiple times for different mediums by rinsing the rig with water, replacing the filter and re-autoclaving the rig.

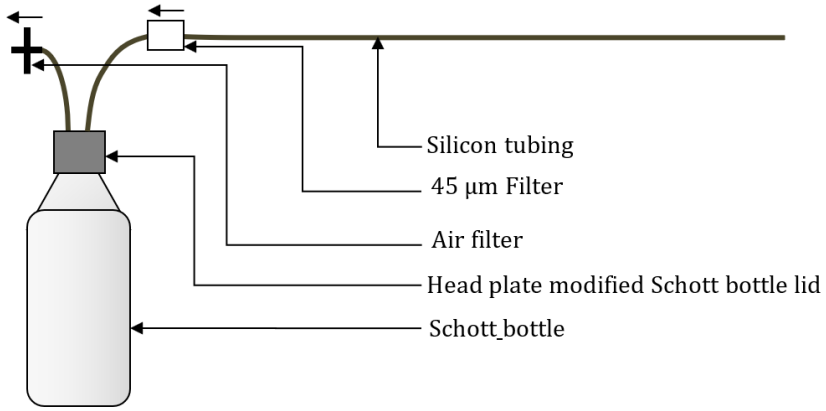


Figure 23: Diagrammatic depiction of the autoclavable filtration rig.

Half a litre media of each medium namely the AF6 medium, BBM medium, C-Medium, Chu#10 medium, DY-V medium, Franquil medium, WC medium, Hase medium, JG medium, Lu medium and Zarrouk medium was prepared. All mediums were adjusted to pH 7 using 1 N HCl and 1 N NaOH. All pH adjusted mediums were filter sterilised into sterile Schott bottles. The mediums were filter sterilised using the rig depicted in Figure 23 fitted with 0.45 µm sterile filters. Filter sterilisation was chosen over autoclaving to prevent autoclave induced pH fluctuations, $NaHCO_3$ heat degeneration and vitamin heat degeneration.

pH control sterilisation

A 1 L empty bottle, 2 L distilled water and 1 L 1 N NaOH was autoclaved. To an empty 1 L autoclaved bottle, 886 mL autoclaved water was transferred with the aid of an autoclaved measuring cylinder under aseptic conditions. Using an autoclaved funnel and measuring cylinder, 114 mL 32% (v/v) HCl was added to the water under aseptic conditions to obtain a final concentration of 1 N HCl. The 1 N HCl and autoclaved 1 N NaOH were used for the pH adjustment of media and cultures.

Incubation setup

The surface of an Innova 2000 orbital shaker has been covered with foil to allow the upwards reflection of light. Thirty-three orbital shaker clamps for 250 mL Erlenmeyer flasks have been secured on the orbital shaker platform. A four-leg lighting platform, fitted with four two bulb Sylvania GRO-LUX F18W/GRO-78 neon lights, was placed over the orbital shaker as depicted in Figure 24. The power supply of the lights was controlled

with a time switch to allow a 12-hour day-night cycle. The incubator was surrounded at all four corners with reflective sheets and also covered with a reflective sheet to reflect escaping light back towards the centre of the incubator.

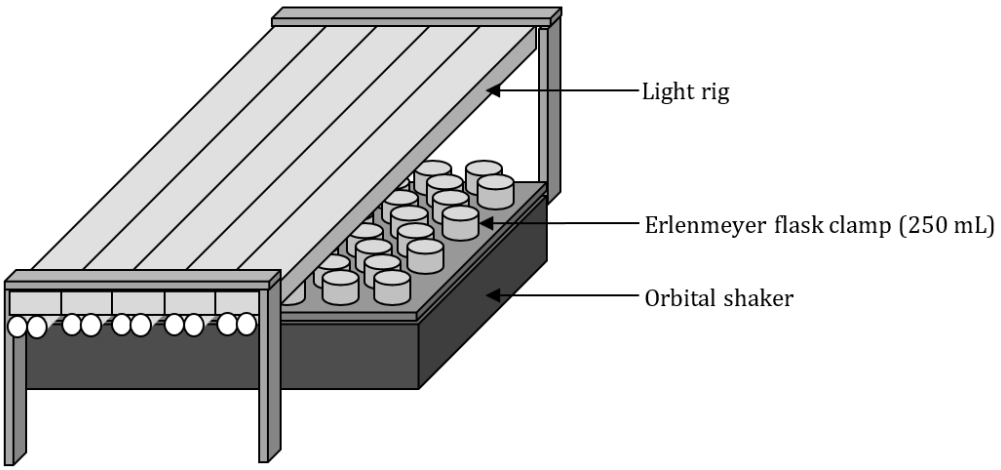


Figure 24: Diagrammatic depiction of the incubation setup including the light rigs and orbital shaker.

Inoculation and cultivation

Volumes of 135 mL from each filter sterilised media were transferred to 250 mL autoclaved Erlenmeyer flasks in triplicate. Each flask was inoculated with 15 mL monoseptic inoculum culture from Section 4.2.1., with a 675 nm optical density (OD675) of 0.2, measured using a BioTek PowerWave HT spectrometer. A volume of 100 µL of the inoculum was transferred to a 2 mL Eppendorf tube. A 10 time's dilution of the 100 µL inoculum was prepared by adding 900 µL water to the 2 mL Eppendorf tube. The dilution was transferred in 200 µL volumes to a 96-well plate in triplicate. The OD 675 was measured, on a BioTek PowerWave HT spectrometer, to be the universal time zero OD 675 reading.

The inoculated 250 mL flasks were placed on a Sylvania GRO-LUX F18W/GRO-78 neon light illuminated orbital shaker at 120 rpm and incubated at 25°C for 17 days. The pH was maintained at pH 7.5 with daily pH adjustment where required. For the duration of 17 days, daily 1 mL samples were taken using TPP 2 mL sterile pipettes. From each sample 200 µL were transferred to independent wells in a 96 well plate in triplicate. The OD 675 readings of the 96-well plate were taken on a BioTek PowerWave HT spectrometer. The OD 675 nm readings were used to determine the medium specific growth rates and the biomass yield rates. Ln (OD 675) functions were used to determine the specific growth

rates of WCB 4.1 in each medium. For all the Ln (OD) curves a straight trend line could be seen between the time points of day 1 and 4 indicating exponential growth.

The OD 675 nm values were converted to biomass ($g.L^{-1}$) values using the OD/DCW correlation curve generated for WCB 4.1 in Chapter 3. The estimated biomass values were plotted over time (Appendix B, Figure B1 – B11). To calculate the average biomass productivity of WCB 4.1 in each medium over 17 days, linear trend lines were plotted for each curve (Appendix B, Figure B1 – B11). The slopes of these trend lines were indicative of the average specific biomass yield rate ($mg.L^{-1}.d^{-1}$) for the duration of the study as explained in Chapter 2, Section 2.1.1. The biomass yield rate of WCB 4.1 in each medium over seventeen days was determined.

On the 17th day, 16 mL samples were taken, using TPP 25 mL sterile pipettes. A volume of 1 mL from the 16 mL samples were centrifuged in 2 mL eppendorf tubes, using and Eppendorf MiniSpin plus centrifuge at 10481 xg for 2 minutes, the supernatants were discarded and the pellets placed in the freezer. The remaining 15 mL of the samples were centrifuged using 15 mL falcon tubes on a Beckman Coulter Allegra X 22R swinging bucket centrifuge at 3901 xg for 15 minutes. The supernatants were discarded and the pellets placed in the freezer.

4.3 Results and discussion

4.3.1 Single cell isolation and pre-cultivation

Single cell isolations were performed successfully on WCB 4.1 to provide multiple healthy mono-septic cultures, which were up-scaled to be used for genetic sequencing and further studies. Monoseptic status can be seen in Figure 25.

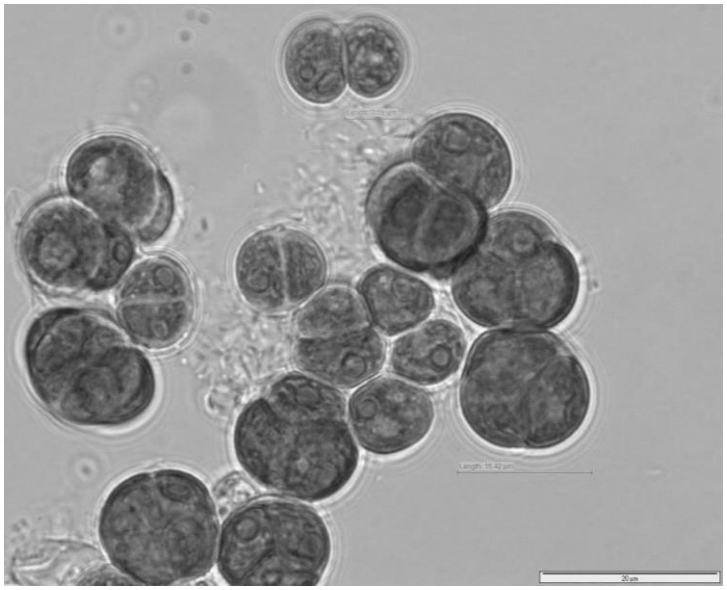


Figure 25: Mono septic culture of WCB 4.1 resulting from microscope assisted micro tube single cell isolation.

4.3.2 Sequencing

The DNA extraction, amplification and sequencing were performed successfully by Inqaba Biotec. In Figure 26 the amplification of the 18S target region can be seen as in an agarose gel electrophoresis as performed by Inqaba Biotec.

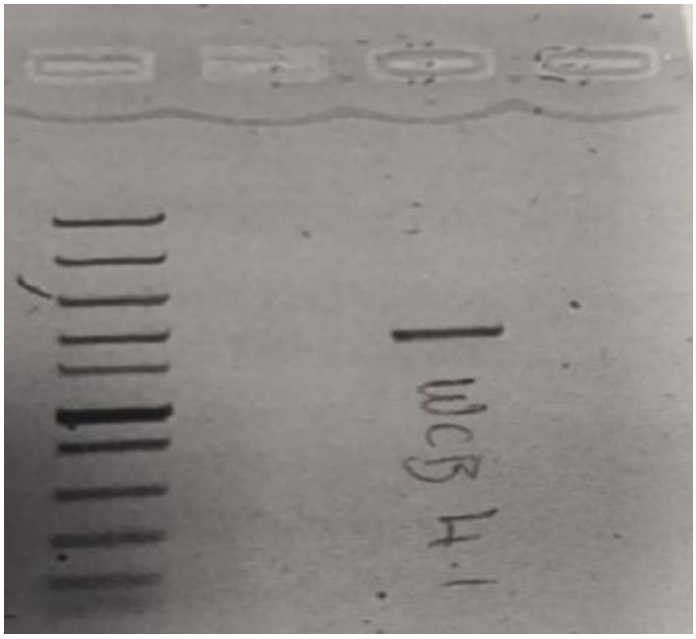


Figure 26: A photographic image of an agarose gel indicating the amplification of the 18S target region.

BLAST: The BLAST results correspond to the similarity between the sequence queried and the biological sequences within the NCBI database. The alignment with the highest similarity was with *Acutodesmus bajacalifornicus.* In the sequencing performed by Durand *et al.* (2016), WCB 4.1 was identified as *Tetradesmus acuminatus*. In the most recent sequencing event, a larger section of the 18S ribosomal gene was sequenced encompassing the 18S regions sequenced by Durand *et al.* (2016) to provide a bigger picture of the 18S region. The Genetic ID of *Acutodesmus bajacalifornicus* will thus be accepted as the most recent and accurate ID.

Therefore, this confirms the species to be *Acutodesmus bajacalifornicus*. The *Acutodesmus* genus is in the *Scenedesmaceae* family in the *Chlorophyta* phylum. The *Acutodesmus* genus is very closely related to the *Scenedesmus* and *Tetradesmus* genera and have a lot of morphological and genetic similarity with strains from these genera. The high similarity between these genera is the reason for *Acutodesmus bajacalifornicus* being previously identified as a *Tetradesmus acuminatus*. Strains from the *Scenedesmus, Tetradesmus* and *Acutodesmus* genera regularly used and widely studied, with the *Scenedesmus* genus

being one of the most popular genera of the three. Multiple strains from these genera have received a lot of attention for a range of purposes including waste water bioremediation, carbon dioxide fixation, microalgal bioenergy and caretonoid production. Information of the specie *Acutodesmus bajacalifornicus* is very limited. Some of the closest related species to *Acutodesmus bajacalifornicus* according to the genetic analysis, include: *Scenedesmus bajacalifornicus, Tetradesmus obliquus, Acutodesmus obliquus, Scenedesmus obliquus, Scenedesmus incrassatulus, Scenedesmus deserticola, Tetradesmus acuminatus* and *Scenedesmus acuminatus*.

4.3.3. WCB 4.1 medium study

Figure 28 A and B contains the biomass over time curves for all eleven mediums (Appendix B, Figure B1 - B11). Figure 27 A and B may be compared with each other directly. For all eleven cultures an initial sigmoid growth occurred in the first seven days. This indicates that the exponential growth phase occurred in this time. In most cases the growth continued at a slower rate after day seven. The biomass content of the Zarrouk medium started to diminish after day seven. According to the growth in terms of biomass over 17 days, the Hase and JG mediums were the top performing mediums followed by the Lu medium, C-medium, AF6 medium, WC medium, DYV medium, Chu #10 medium, BBM, Franquil medium and Zarrouk medium in order of declination. The JG and Hase mediums can be seen to increase in biomass content much faster than any of the competing mediums.

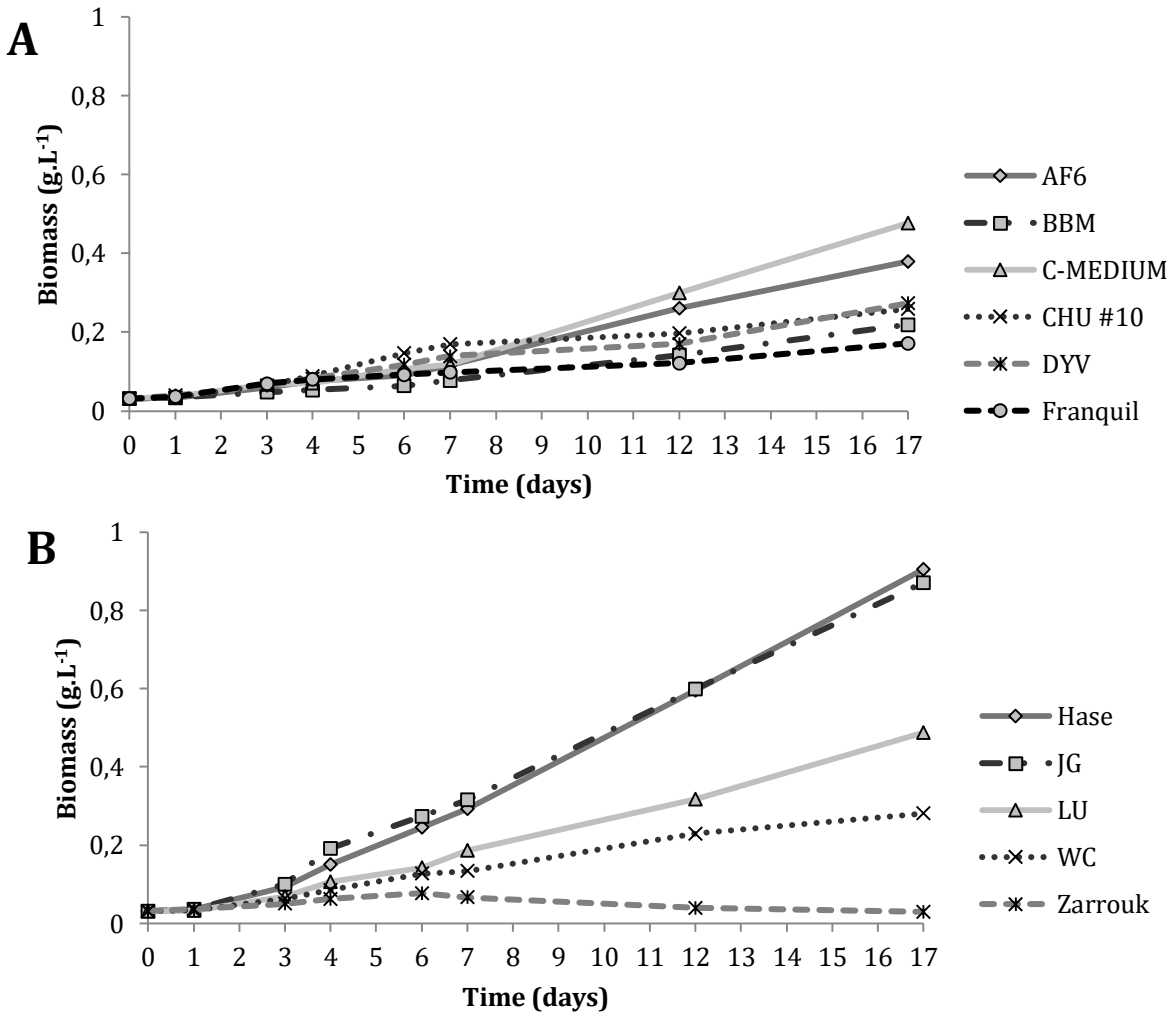


Figure 27: Biomass over time curves for the cultivation of WCB 4.1 in six different mediums (A) and five different mediums (B) over 17 days.

The calculated specific growth rate of WCB 4.1 in each medium is displayed in Figure 29 and Appendix B, Table B3. In Figure 28 it is clear that WCB 4.1 has the highest growth rate in the JG medium followed by the Hase and Lu mediums with growth rates of 0.47, 0.42 and 0.31 d^{-1} respectively. The growth rate of WCB 4.1 in the JG medium was 14.8% higher than in the Hase medium and 33.7% higher than in the Lu medium. WCB 4.1 had the lowest growth rate in the BBM and Zarrouk mediums with growth rates of 0.12 and 0.14 d^{-1} respectively. The growth rates of WCB 4.1 in the AF6, C-medium, Chu # 10, DYV, Franquil and WC mediums ranged from 0.18 up to 0.26 d^{-1}. According to the growth rates,

the JG and Hase mediums would be good mediums for cultivating WCB 4.1 for optimal biomass generation.

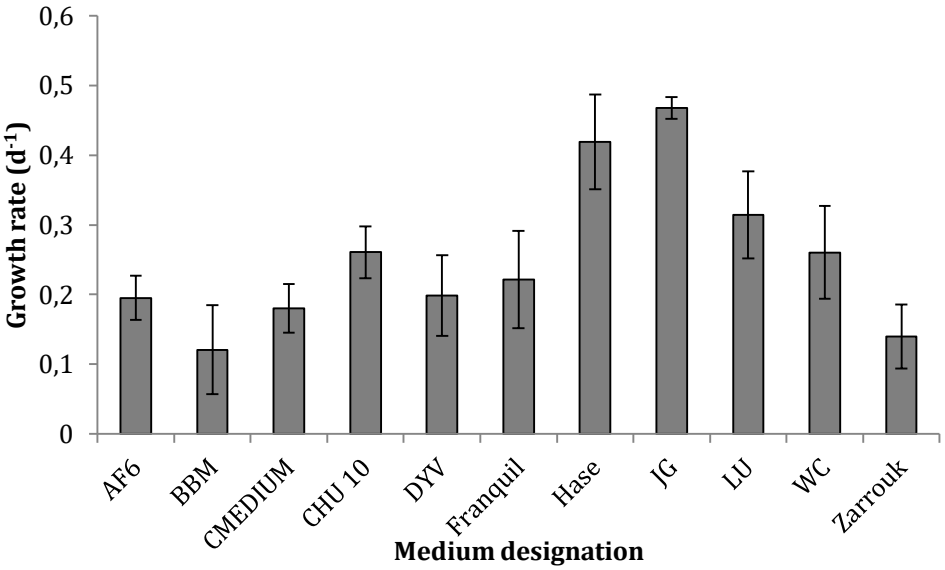


Figure 28: The specific maximum growth rate of WCB 4.1 in each medium with the error bars depicting the standard deviation.

The specific growth rate can be used to determine the doubling time of a culture using Equation 15. The daily and hourly doubling rates of WCB 4.1 in all eleven mediums can be seen in Table 19.

$$T2 = \frac{Ln(2)}{\mu} \qquad 15$$

Where:

T2 = the doubling time

μ = growth rate

Table 19: Doubling times of WCB 4.1 in 11 different mediums.

	Growth rate (d^{-1})	Doubling time (d^{-1})	Doubling time (h^{-1})
AF6	0.20	3.55	85.31
BBM	0.12	5.74	137.71
CMEDIUM	0.18	3.84	92.21
CHU 10	0.26	2.66	63.81
DYV	0.20	3.49	83.76
Franquil	0.22	3.13	75.00
Hase	0.42	1.65	39.70
JG	0.47	1.48	35.55
LU	0.31	2.21	52.93
WC	0.26	2.66	63.88
Zarrouk	0.14	4.97	119.17

JG has the fastest doubling time of 35h 6m, which is inversely proportional to the growth rate. The JG medium providing the fastest growth rate at 0.47 d^{-1} indicates faster growth rate than microalgal growth rates sourced from Choi and Lee, (2015), Cabanelas *et al*., (2013), Renaud *et al*., (2002) and Huerlimann *et al*., (2010) as can be seen in Figure 29. This demonstrates the potential of WCB 4.1 to be competing with other industrially significant microalgal strains. There are some microalgal growth rates such as that of *Chaetoceros sp*. (Renaud et al., 2002) *Isochrysis sp.* (Renaud et al., 2002) and *Scenedesmus sp.* (Rhee and Gotham, 1981) which show higher growth rates than WCB 4.1 in JG medium. Although this indicates that there are microalgae outcompeting WCB 4.1, it also indicates possible room for improvement of WCB 4.1 growth rates. With WCB 4.1 being an *Acutodesmus bajacalifornicus*, one of the most interesting growth rates to consider is that of *Scenedesmus* sp., as the *Scenedesmus* and *Acutodesmus* genera are closely related (Rhee and Gotham, 1981). This growth rate is 135% higher than that of WCB 4.1 cultivated JG medium. Growth rates can differ between strains and this does not indicate that WCB 4.1 can reach the growth rate of Scenedesmus sp. described by Rhee *et al*., (1981). This does however indicate that the growth rate of WCB 4.1 can potentially be increased even more by optimisation of cultivation conditions. A growth rate for a *Scenedesmus obliquus*, which is very closely related to WCB 4.1, has been determined by Nascimento *et al*., (2013) to be 0.21 d^{-1}. The growth rate of WCB 4.1 in the JG medium is 55.7% higher than that of *Scenedesmus obliquus* as mentioned by Nascimento *et al*., (2013).

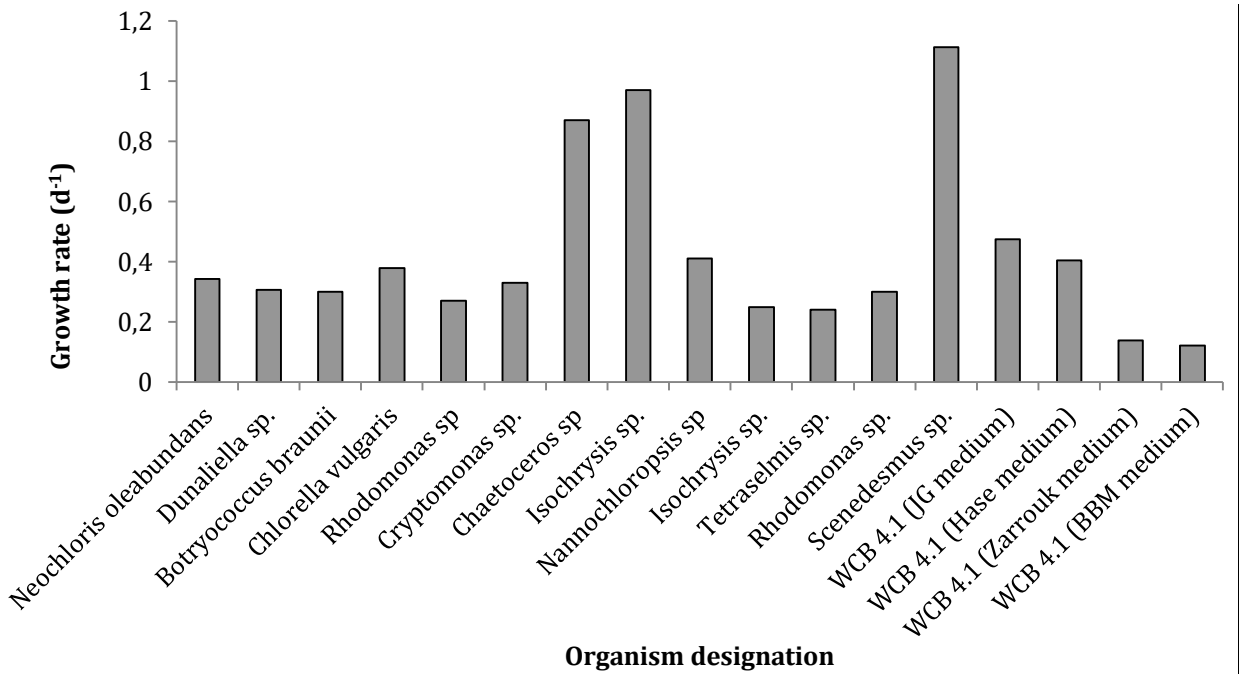


Figure 29: Comparison between microalgal growth rates from literature sources and the current study (Cabanelas et al., 2013, Choi and Lee, 2015, Huerlimann et al., 2010, Renaud et al., 2002, Rhee and Gotham, 1981).

The determined biomass yield rates for WCB 4.1 in eleven different mediums are displayed in Figure 30. The Hase and JG mediums had the highest biomass yield rates at 53.1 and 51.1 $mg.L^{-1}.d^{-1}$ respectively. The Franquil and Zarrouk mediums showed the lowest biomass yield rate at 7.8 $mg.L^{-1}.d^{-1}$ each. Microalgal biomass yield rates determined by other authors, as can be seen in Figure 31, ranges from 120 $mg.L^{-1}.d^{-1}$ up to 783 $mg.L^{-1}.d^{-1}$. Compared to these biomass yield rates, the biomass yield rate of WCB 4.1 is quite low.

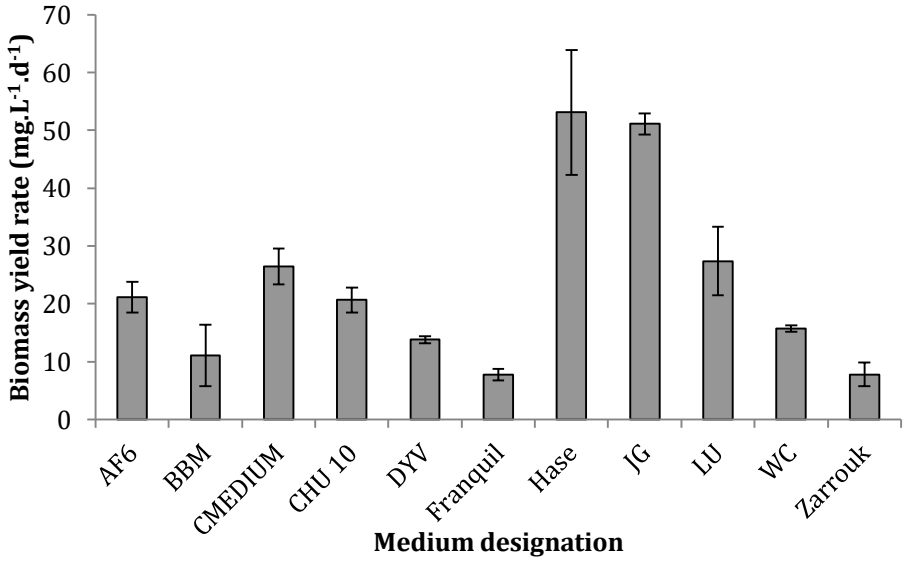


Figure 30: Bar graph depicting the biomass yield rate of WCB 4.1 in all eleven mediums, with error bars depicting the standard deviation.

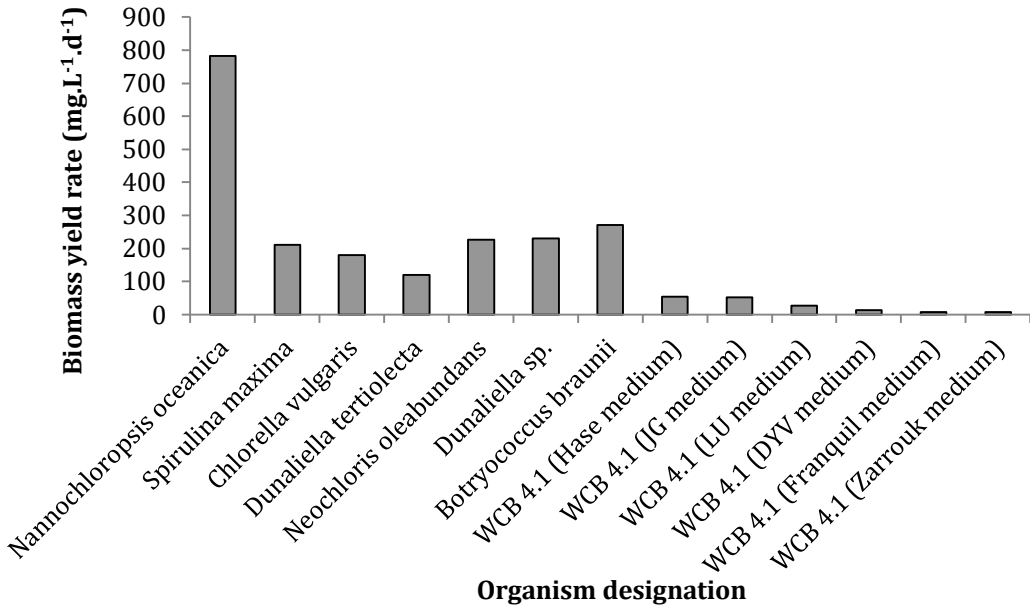


Figure 31: Biomass yield rates of different microalglal strains from literature in comparison with WCB 4.1 biomass yield rates (Sandnes *et al.*, 2005, Choi and Lee, 2015, Gouveia and Oliveira, 2009).

The *Neochloris oleabundans*, *Dunaliella* sp. and *Botryococcus braunii* growth rates and biomass yield rate in Figure 29 and Figure 31 are from the same study. This is interesting given that the top growth rates of WCB 4.1 is superior to that of *Neochloris oleabundans*, *Dunaliella* sp. and *Botryococcus braunii*, while the biomass yield rate of WCB 4.1 is inferior to the very same cultures. This indicates that the low biomass yield rate is not due to low growth rate. The biomass yield rate can thus be improved by improving the production process. Examples of improvements in process which can improve yield rates include:

- Implementation of fed batch systems.
- Implementation of continuous cultivation systems.
- Optimisation of harvesting time.
- Increasing light and CO_2 availability
- Optimising cultivation temperature and pH.

All cultures were subject to the same environmental conditions and were generated from the same inoculum culture. The fluctuation in performance can mainly be allocated to the medium compositions. The main medium components affecting the cultivation of microalgae are the nitrogen and phosphor source abundance.

To investigate the effect of the nitrogen and phosphor contents on growth rate, the growth rate of WCB 4.1 in each medium was plotted over the nitrogen and phosphor contents of each medium (Figure 32). Since there are multiple medium component

variables, Figure 32 cannot be used as a quantitative measure to indicate the optimal content of nitrogen or phosphor. Figure 33 can however serve as a tool to investigate possible relationships between growth rates and nitrogen/phosphor contents. In each curve a trend similar to the Monod-Haldane curve, as discussed in Chapter 2 section 2.2.1, can be seen. If we assume that WCB 4.1 has a Monod-Haldane relationship with nitrogen and phosphor medium contents, then the optimal nitrogen and phosphor levels can be expected to be in the range of 3 – 10 mM and 0.2 – 1 mM respectively. This can however only be proved by cultivating WCB 4.1 in varying concentrations of phosphor and nitrogen. The performance of such a study would allow the determination of the Monod-Haldane K_m (Monod constant) and K_I (Inhibition constant) values and would provide more insight regarding the relationship between WCB 4.1 and nitrogen/phosphor contents. The determination of the K_m and K_I will allow the use of models to predict the cultivation of WCB 4.1 at different scales and using different cultivation systems. This would allow the prediction of productivity of WCB 4.1 for continuous and fed batch cultivations to increase the chance of success of pilot scale studies and predict the optimal harvest times. This will allow improvement of WCB 4.1 biomass productivity by modelling and thus reducing costs involved with lab scale and pilot scale optimisation.

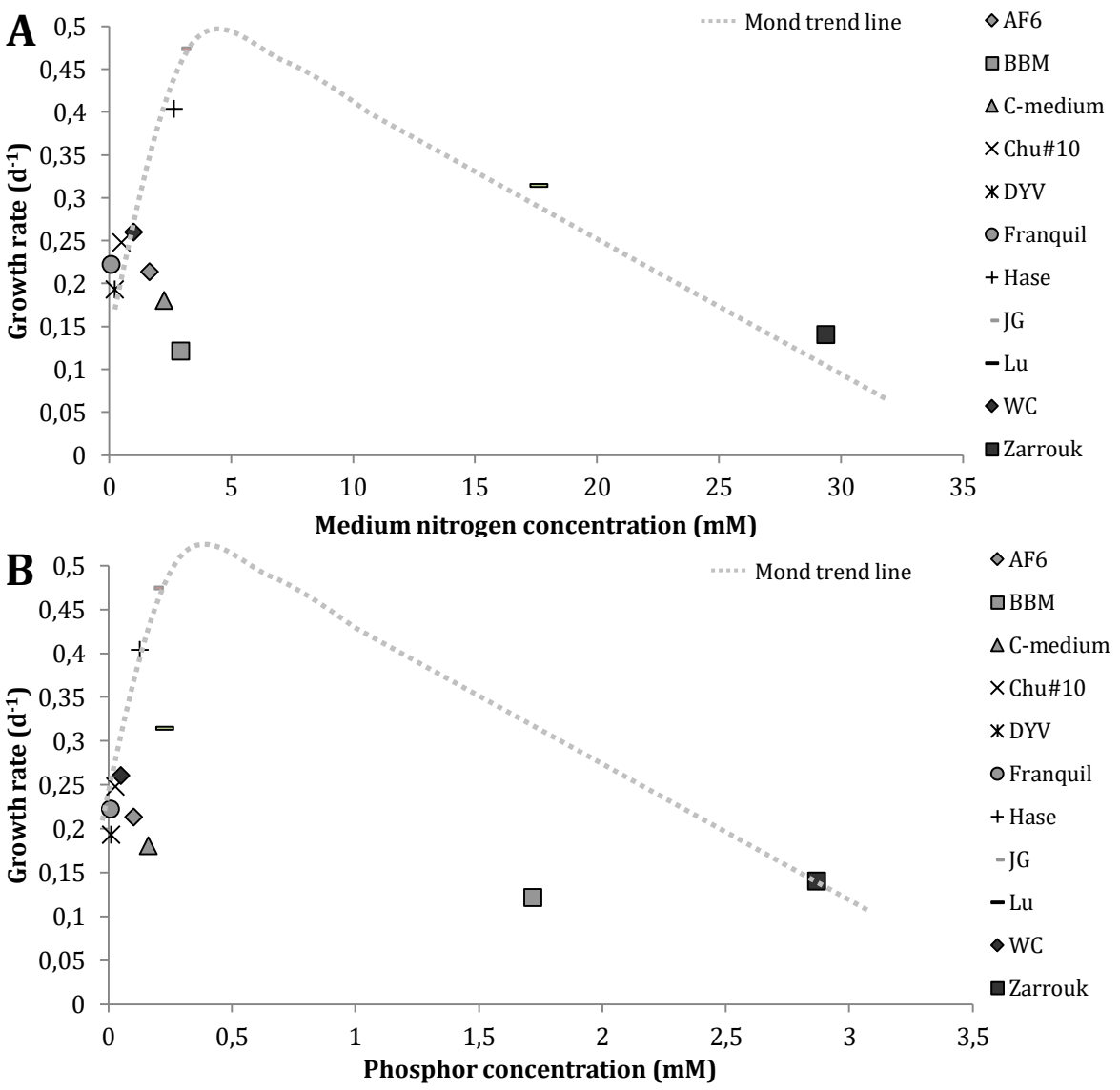


Figure 32: Respective medium growth rate over nitrogen (A) and phosphorus (B) concentration plots. The grey dotted line is a visual aid to recognise the potential Monod-Haldane trend.

An additional curve was included depicting the growth rate over the nitrogen to phosphor ratio (Figure 33). This curve shows two independent bell curve-like trends with the BBM, Franquil, Hase, JG and Lu mediums following the top bell curve trend and, the AF6, C-medium, Chu#10, DYV, WC and Zarrouk mediums following the bottom trend. The occurrence of two trends indicate that an additional factor other than nitrogen and phosphor ratio might be affecting the performance of these mediums. Due to more than one bell curve forming the optimum ratio cannot be accurately determined. Both trends however seem to form a bell curve peaking between a ratio (N:P) of 15:1 and 20:1. This corresponds to the Redfield (1958) ratio which specifies the optimum ratio (N:P) as 16:1. According to the Redfield ratio, a ratio higher than 16:1 indicates excess nitrogen or

phosphor limitation and *vice versa* for ratios lower than 16:1 (Falkowski, 1997, Tyrrell, 1999, Lenton and Watson, 2000).

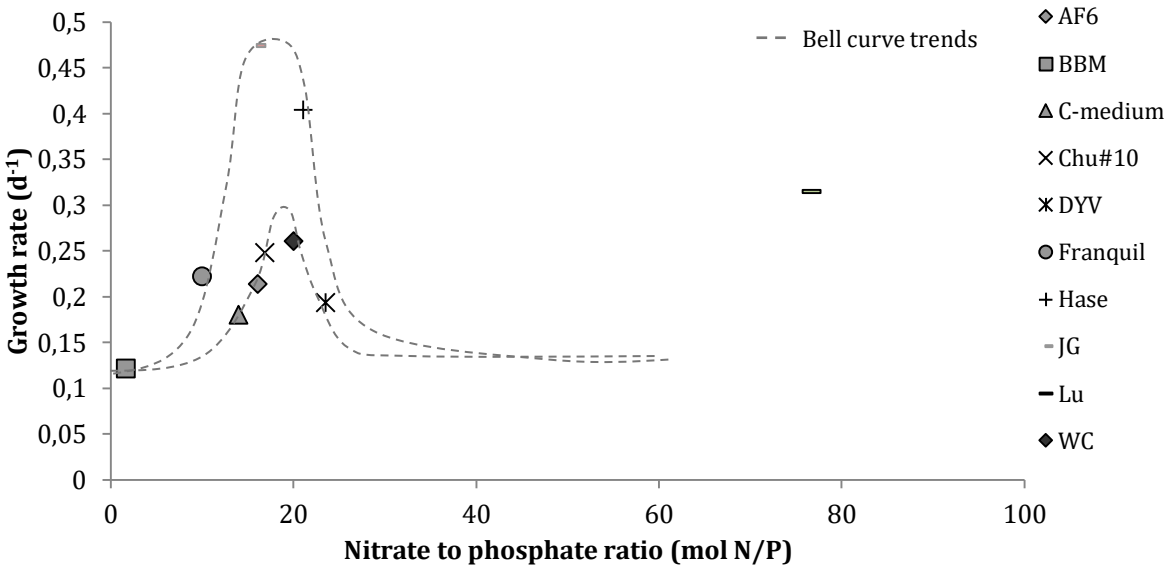


Figure 33: Growth rate over Nitrogen to phosphorous ratio plot for each medium.

If the trends generated in each curve (Figure 32 - 33) are considered as indications of the effect a component has on the medium performance, a few insights may be made for each medium:

1. The underperformance of the AF6 medium cannot be explained by the Nitrogen and phosphor trends alone.
2. The performance of the BBM medium was limited due to excess phosphor.
3. The underperformance of the C-medium cannot be explained by the nitrogen and phosphor trends alone.
4. The performance of the Chu#10 medium was limited due to phosphor and nitrogen limitation.
5. The performance of the DYV medium was limited due to phosphor and nitrogen limitation.
6. The performance of the Franquil medium was limited due to phosphor and nitrogen limitation.
7. The Hase medium was a good performer due to it having suitable nitrogen and phosphor levels in a suitable N:P ratio.
8. The JG medium was a good performer due to it having suitable nitrogen and phosphor levels in a suitable N:P ratio.
9. The performance of the Lu medium was limited due to excess nitrogen.
10. The performance of the WC medium was limited due to nitrogen and phosphor limitation.
11. The performance of the Zarrouk medium was stunted due to excess nitrogen and phosphor. The growth could also have been stunted due to salinity as this medium contains high dosages of sodium.

4.4 Conclusion

In this chapter we explored how medium composition affects the growth of WCB 4.1. We were able to genetically identify WCB 4.1 as *Acutodesmus bajacalifornicus*. Eleven mediums were identified which could be used for the cultivation of *Acutodesmus*. These elven mediums included: AF6, BBM (Bold Basal Medium), Chu #10, C-medium, DY-V medium, Franquil medium and the WC medium sourced from Andersen, the Hase, Lu and Zarrouk mediums and the newly formulated JG medium (Andersen, 2005, Hase *et al*., 2000, Lu *et al*., 2015, Zarrouk, 1966).

WCB 4.1 was cultivated in all eleven mediums and provided growth rates and biomass yield rates for WCB 4.1 in all of these mediums. WCB 4.1 showed the highest growth rate in the JG medium, with a competitive growth rate of 0.47 d^{-1}. WCB 4.1 showed the highest biomass yield rate in the Hase medium, with a yield rate of 53.1 $mg.L^{-1}.d^{-1}$, which is meagre to other literature biomass yield rates.

Correlating respective growth rates with nitrogen/phosphor medium contents allowed a better understanding for the growth rate over substrate relationship for the cultivation of WCB 4.1. This also provided some more understanding as to why certain mediums performed better than others.

WCB 4.1 shows potential for use in microalgal cultivation. The biomass yield rate alone does however not provide the full picture when it comes to cultivation for bioenergy production purposes. To be able to explore the bioenergy production potential of WCB 4.1, cultivated in these eleven mediums, lipid and carbohydrate content analysis would need to performed on the biomass generated in this study. This further work can be found in Chapter 5.

Chapter 5: Lipid and carbohydrate fractional extraction

5.1 Introduction

In the previous chapter WCB 4.1, an *Acutodesmus bajacalifornicus,* was cultivated in eleven different cultivation mediums to study its growth rate and biomass productivities in these mediums. Species from the *Acutodesmus* family have been studied for bio-energy production potential. They have been shown to be able to accumulate high cellular lipid and carbohydrate percentages (Chokshi *et al*., 2015). The cellular lipid and carbohydrate content have been shown to be affected by the cultivation conditions and the medium composition the organism is cultivated in.

To be able to relate the growth data of WCB 4.1 in each medium with the bio-energy potential of WCB 4.1 in each medium, the carbohydrate and lipid contents of the harvested biomass must be analysed. This will provide data on the lipid and carbohydrate yields, which can be expected from the cultivation of WCB 4.1 in each of these mediums. The lipid and carbohydrate productivities can be converted to biodiesel and bio-ethanol productivities and the lipid profile can be used to predict the bio-diesel properties.

The aim of this chapter would be to characterise the biodiesel and bio-ethanol production potential of WCB 4.1 in eleven different cultivation mediums. We will be evaluating the lipid and carbohydrate content from experimental analysis and translating that into theoretical predictions. This would allow better understanding of the feasibility of using WCB 4.1 for microalgal bio-energy production, which includes theoretical calculations of large-scale production.

5.2 Methods

The lipid and carbohydrate content analysis are shown in this section. Furthermore, the theoretical equations are shown which will be used for predications of bio-diesel property indicators, cetane number (CN) and cold filter plug point (CFPP), and large-scale yield rate predictions.

5.2.1 Lipid content analysis

To ensure uniformity FAME-GC, the same lipid measure used in Chapter 3, was used in this Chapter. The transesterification reaction used, had the advantage of separating the hydrophilic and hydrophobic phases of the microalgal biomass contents. The aqueous phase generated during the transesterification reaction, thus can be used for Dubois phenol sulphuric colorimetry.

From each day 17 sample from section 4.2.3, 15 mL was centrifuged on a Beckman Coulter Allegra X-22R swinging bucket centrifuge at 3901 xg for 15 minutes. The

supernatants were decanted without dislodging the pellets. The pellets were re-suspended in 800 µL Milli-Q Millipore water and transferred to 2 mL screw cap centrifuge tubes. The centrifuged tubes were centrifuged on an Eppendorf MiniSpin plus centrifuge at 10481 xg for two minutes. The supernatants were decanted without dislodging the pellets. To the pellets 250 µL toluene was added, followed by 500 µL 0.5 N NaOH in methanol. The mixtures were vortex vigorously to re-suspend the pellets. The mixtures were incubated for 20 minutes at 80°C, agitating at 950 rpm, on an Eppendorf Thermomixer comfort. The reaction mixtures were cooled down to ambient temperature in a -20°C freezer for five minutes. To the reaction mixtures 500 µL 5% HCl methanol was added. The reaction mixtures were incubated at 80°C with 950 rpm agitation for 20 minutes of Eppendorf Thermomixer comfort. The reaction mixtures were cooled down to ambient temperature in a -20°C freezer for five minutes. To the mixtures 200 µL Milli-Q water was added to stop the reactions, followed by 300 µL hexane. The mixtures were vigorously vortexed and centrifuged on an Eppendorf MiniSpin plus centrifuge at 10481 xg for two minutes. The hexane phases were transferred to 1.5 mL Eppendorf tubes containing ~2 µg anhydrous MgSO4. The aqueous phases, after hexane extraction, were stored in the fridge to be used in section 5.2.2. The 1.5 mL Eppendorf tubes were centrifuged on an Eppendorf MiniSpin plus centrifuge at 10481 xg for two minutes. The hexane phase was transferred to inserts in appropriately labelled GC crimp cap vials and capped.

The GC was performed using a Supelco Omega Wax 320 column (30 m x 0.32 mm x 0.25 µm film thickness, cat # 24152) on an Agilent Technologies 7890A GC system equipped with an Agilent Technologies 7693 Auto sampler.

A FAME standard (Supelco 37 Component FAME Mix, 1 × 1 ml, Varied concentration in dichloromethane Part Number: CRM47885) was run on the GC system to obtain area under the peak and substance concentration standard curves for 37 FAMEs. Linear trend line was used to obtain straight line formulas for each correlation (Appendix C, Figure C1 – C35). These formulas can be used to convert chromatogram peak areas to lipid concentration ($g.L^{-1}$) values. The correlation curves and trend line for each compound can be found in Appendix C, Figure C1 – C35.

The areas under the peaks were used to determine the lipid contents of WCB 4.1 at day 17 cultivated in eleven different mediums. The sum of the lipid contents provided the total lipid content of WCB 4.1 in each medium (Appendix C, Table A1).

The potential bio-diesel properties of the biodiesel, which can be generated from WCB 4.1 biomass cultivated in each media, was predicted using the generated FAME-GC lipid profiles.

The CN values were calculated from a combination of formulas from (Lapuerta *et al*., 2009) and (Tong *et al*., 2011) as combined by (Stansell *et al*., 2012) (Equation 16 – 19). The CN values of individual methyl esters were calculated using the formulas below (Stansell *et al*., 2012).

$$CN = -107.71 + 31.126n - 2.042n^2 + 0.0499n^3 \quad 16$$

$$CN = 109 - 9.292n + 0.354n^2 \quad 17$$

$$CN = -21.157 + (7.965 - 1.785db + 0.235db^2)n - 0.099n^2 \quad 18$$

Where:

n = the number of carbons in a fatty acid
db = the number of double bonds in a fatty acid

The CN for a specific fatty acid mixture were calculated using equation 20 (Stansell *et al*., 2012).

$$CN = 1.068 \sum (CNimi) - 6.747 \quad 19$$

Where:

CNi = the CN for a specific methyl ester
mi = the mass faction of a specific methyl ester

Prediction of the CP value is required to allow the prediction of the CFPP value. Equation 20 derived from Imahara *et al*. (2006) were used to predict the CP (Stansell *et al*., 2012, Imahara *et al*., 2006). The "Tmi" and "ΔHmi" values were sourced from Dunn (2008) or predicted according to Lopes *et al*. (2007) (Table 22).

Table 20: Tmi and ΔHmi values derived from Dunn (2008) or Lopes *et al*., (2007).

Saturated fatty acid	Tmi	Source	ΔHmi	Source
C8:0	-37.43	Dunn (2008)	20.48	Lopes *et al*., (2007)
C10:0	-13.48		28.34	
C11:0	-12.17		34.68	
C12:0	4.3		36.20	
C16:0	28.48		49.9	Dunn (2008)
C17:0	28.58		57.65	Lopes *et al*., (2007)
C18:0	37.66		57.04	Dunn (2008)
C20:0	46.43		67.66	Lopes *et al*., (2007)

$$\ln(xi) = \frac{\Delta Hmi}{R}\left(\frac{1}{Tmi} - \frac{1}{CP}\right) \quad 20$$

Where:

CP = the cloud point
R = the universal gas constant
Tmi = the melting points of individual methyl esters
ΔHmi = the enthalpy of melting of individual methyl esters
xi = the mass fraction of individual methyl esters

According to thermodynamic prediction of CP, the individual methyl esters are assumed to precipitate out independently (Imahara *et al.*, 2006). This means the highest CP value for an individual methyl ester is the CP of the mixture. The CFPP value were then calculated according to Equation 21 as presented by Dunn and Bagby (1995).

$$CFPP = 1.0191 \times CP - 2.9 \quad 21$$

Where:

CFPP = Cold filter plug point

5.2.2 Carbohydrate content analysis

To ensure uniformity Dubois phenol-sulphuric colorimetry, the same carbohydrate measure used in Chapter 3, was used in this Chapter. The aqueous phases from section 5.2.1 were vigorously vortexed. From each aqueous phase 100 µL was transferred to a 2 mL Eppendorf tube. To the 100 µL, 1400 µL dH_2O was added and the mixtures were vigorously vortexed. From each of these mixtures 565 µL was transferred to 2 mL Eppendorf tubes. Under the fume hood 15 µL 80% (w/v) phenol (in water) was added to each 565 µL sample. To the reaction mixture 1.45 mL 99.9% (v/v) sulphuric acid was slowly added under the fume hood. The mixtures were incubated at 25°C for 10 minutes. From each reaction mixture 200 µL was transferred to a 96-well plate in triplicate under the fume hood. OD 490 readings were performed on the loaded 96-well plates using a BioTek PowerWave HT spectrometer with the aid of Gen5 (v1.06) software.

The OD 490 values from each replicate of the 11 mediums after the lipid extraction was obtained and converted to carbohydrate mass per culture volume ($g.L^{-1}$) values. The correlation curve generated in Chapter 3 (Section 3.2.2) was used to convert OD 490 values to carbohydrate ($g.L^{-1}$) values.

5.3 Results and discussion

5.3.1 Lipid Fraction

Lipid content analysis

The lipid contents of WCB 4.1 biomass from all eleven different mediums can be seen in Figure 34. The JG, Chu#10, Hase and DYV mediums provided the highest lipid yields in descending order.

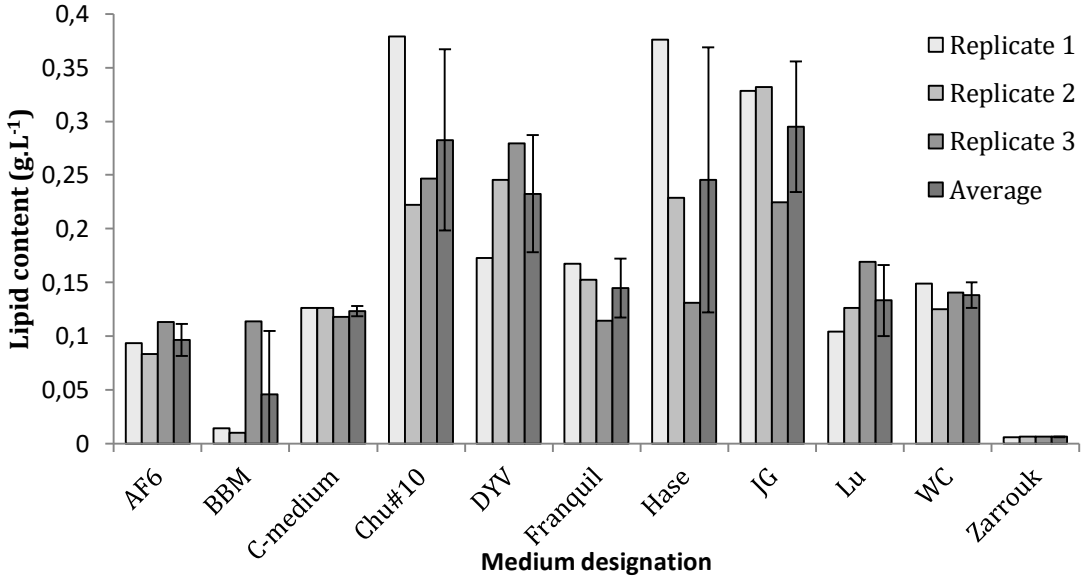


Figure 34: Medium specific lipid yield of WCB 4.1 biomass after 17 days cultivation.

From the biomass productivity data, from 4.3.3, the JG and Hase mediums are by far the highest biomass yielding mediums. The Chu#10 and DYV are not within the top five biomass producing mediums. This raises the question as to how such low biomass yielding mediums can be yielding such high lipid contents. This can be related to which life stages WCB 4.1 is in each medium at day 17 and the cellular lipid percentage. Considering lipid yield in relation to biomass yield shows that WCB 4.1 has very high cellular lipid contents (>80% w/w) in the Chu#10, DYV and Franquil mediums (Figure 35 and Appendix C, Table C2). In most of the other mediums WCB 4.1 has cellular lipid contents percentages ranging between 20% and 50%.

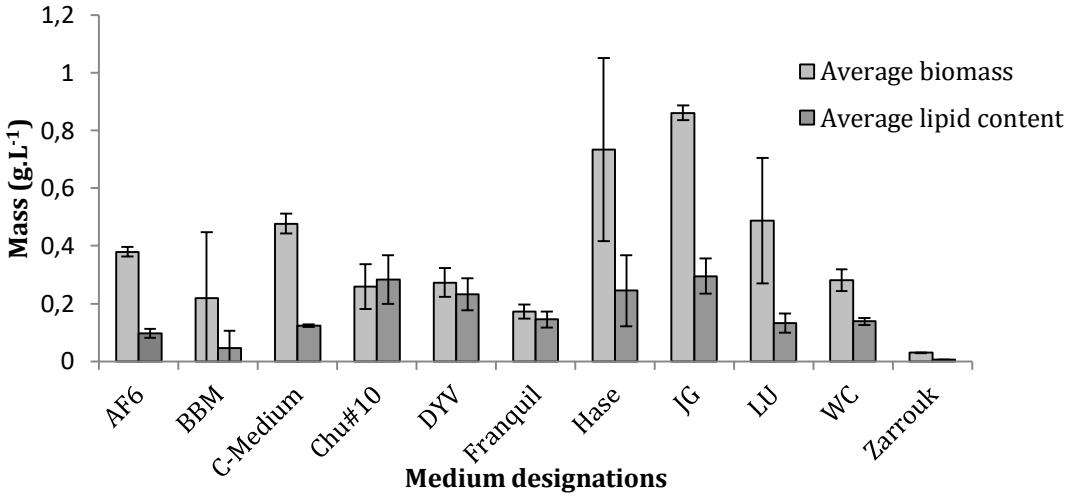


Figure 35: Medium specific lipid and biomass yield of WCB 4.1 after 17 days of cultivation.

Chokshi *et al*. (2017) and Cobos *et al*. (2017) demonstrated that nitrogen limitation can lead to lipid content increase in *Acutodesmus dimorphus*, close family to *Acutodesmus bajacalifornicus*. The high lipid content in Chu#10, DYV and Franquil can be accounted to nutrient stress. The most important nutrient stress resulting in increased lipid stores is nitrogen stress. Considering the 11 medium compositions (Appendix B Table B1), the Chu#10, DYV and Franquil mediums have the lowest nitrogen contents (Table 21). Having the lowest nitrogen contents will result in earliest nitrogen depletion in these mediums. The WC medium has the fourth highest cellular lipid percentage after the Chu#10, DYV and Franquil mediums. WC medium also has the fourth lowest nitrogen content at 1 mM. WCB 4.1 in the WC medium started to show lipid accumulation due to nitrogen depletion. The AF6 medium with a nitrogen content of 1.64 mM however did not show signs of increased lipid accumulation. Most healthy cultures in mediums, with nitrogen concentrations of 1.64 mM and higher, had higher growth rates compared to nitrogen limited mediums such as the Chu#10, DYV, Franquil and WC mediums.

Table 21: Nitrogen content of each respective medium.

Medium designation	Nitrogen concentration (mM)
AF6	1.64
BBM	2.94
C-medium	2.259
Chu#10	0.488
DYV	0.235
Franquil	0.1
Hase	2.647
JG	3
Lu	17.648
WC	1
Zarrouk	29.414

A trade-off in WCB 4.1 cultures can be seen between a fast growth rate and high cellular lipid content due to nitrogen abundance or limitation respectively. This corresponds with results from Cobos *et al*., (2017), where an *Acutodesmus obliquus* displayed a similar trade-off where high nitrogen content allowed fast growth rates, where nitrogen limitation led to slower growth rates but higher cellular lipid percentages. This displays why the balance of nitrogen is so important in microalgal culture.

Bio-diesel production potential

During FAME-GC the lipid contents are measured in the form of fatty acid methyl esters which is also referred to as bio-diesel. The FAME-GC results are thus indicative of the bio-diesel yield after 17 days. The yield after 17 days can be used to provide specific bio-diesel productivity for each. The determined bio-diesel yield and yield rate of WCB 4.1 in each medium can be seen in Table 22.

Table 22: Bio-diesel yield and productivity of WCB 4.1 biomass cultivated in eleven different mediums.

	Bio-diesel yield ($mg.L^{-1}.17days^{-1}$)	Bio-diesel yield rate ($mg.L^{-1}.day^{-1}$)
AF6	96.44	5.67
BBM	45.94	2.70
C-medium	123.20	7.25
Chu#10	282.70	16.63
DYV	232.56	13.68
Franquil	144.81	8.52
Hase	245.40	14.44
JG	294.97	17.35
Lu	133.19	7.83
WC	138.23	8.13
Zarrouk	6.11	0.36

Nascimento *et al*., (2013) demonstrated microalgal bio-diesel yield rates ranging from 22.61 up to 204.91 $mg.L^{-1}.d^{-1}$, as can be seen in Table 23. Comparing this data with the maximum yield rate of WCB 4.1 at 17.35 $mg.L^{-1}.d^{-1}$, shows that the bio-diesel yield rate of WCB 4.1 is low in comparison with other sources. Low lipid yield rates can be caused due to low biomass yield rates or low cellular lipid contents. WCB 4.1 cultivated in JG medium had a growth rate of 0.47 d^{-1}, which is higher than nine of the growth rates determined by Nascimento *et al*., (2013). WCB 4.1 cultivated in JG medium had a cellular lipid content of ~34.29 % at harvest, which is higher than 10 of the cellular lipid contents determined by Nascimento *et al*., (2013). If WCB 4.1 has a growth rate and cellular lipid percentage competitive with that of the strains mentioned by Nascimento *et al*., (2013), the main cause for low lipid yield rate is due to low biomass yield rate. The low biomass yield rate is also not due to low growth rate of WCB 4.1. This indicates that improvement in process design can play a huge role in improving biomass and lipid yield rates. Process optimisations, which might greatly increase yield rates, would include optimising the harvest time and keeping the culture in exponential growth for longer. Due to yield rates

being a function of time, reducing the harvesting time can often lead to an increase of yield rate. Keeping the culture growing exponentially for longer would allow the biomass to increase more rapidly and lead to increase of biomass yield rates. Fed batch and continuous cultivation can be used to keep a culture in exponential phase for longer.

Table 23: Specie specific lipid yield rates with accompanying growth rates, biomass yield rates and cellular lipid contents as determined by Nascimento *et al.*, (2013).

Species	Growth rate	Biomass yield rate ($mg.L^{-1}.d^{-1}$)	Lipid yield rate ($mg.L^{-1}.d^{-1}$)	Cellular lipid content (%)
Ankistrodesmus falcatus	0.57	340	56.07	16.49±0.44
Ankistrodesmus fusiformis	0.39	240	49.58	20.66±2.07
Kirchneriella lunaris	0.25	140	24.22	17.30±1.12
Chlamydomonas sp.	0.3	240	36.17	15.07±0.95
Chlamydocapsa bacillus	0.75	320	43.26	13.52±0.65
Coelastrum microporum	0.13	110	22.61	20.55±0.99
Desmodesmus brasiliensis	0.28	130	23.39	17.99±0.42
Scenedesmus obliquus	0.21	160	26.77	16.73±1.37
Pseudokirchneriella subcapitata	0.27	80	22.74	28.43±5.40
Chlorella vulgaris	0.53	730	204.91	28.07±4.31
Botryococcus braunii	0.14	250	112.43	44.97±4.00
Botryococcus terribilis	0.13	200	98.00	49.00±1.48
WCB 4.1 (JG medium)	0.47	51.1	17.35	34.29±6.53

The competitive growth rates and the cellular lipid contents of WCB 4.1 demonstrates its potential to be an industrially competitive isolate.

Bio-diesel Quality prediction

Using the FAME-GC lipid profiles generated for WCB 4.1 for each medium, the bio-diesel properties were predicted using Equations 16-21 in section 5.2.1. In Table 24 the predicted CN, CP and CFPP values for bio-diesel produced from each medium can be seen. For a bio-diesel to adhere to South African bio-diesel standards, the CN should be 51 or higher. The predicted bio-diesel CN generated from WCB 4.1 biomass cultivated in BBM, C-medium, DYV medium, Franquil medium, Hase medium, JG medium, Lu medium, WC medium and Zarrouk medium adheres to South African bio-diesel standards. The predicted bio-diesel CN generated from WCB 4.1 biomass cultivated in AF6 medium and Chu # 10 medium does however not adhere to South African bio-diesel standards. For the CFPP of bio-diesel to adhere to South African summer grade bio-diesel standards, the CFPP should be lower than 3˚C. WCB 4.1 cultivated in all mediums eleven mediums except for the Zarrouk medium is predicted to generate bio-diesel with CFPP values in adherence to South African summer grade standards. Bio-diesel predicted to be generated from WCB 4.1 biomass in the Zarrouk medium have been predicted to have a CFPP of 5.4 ˚C, which is too high to adhere to South African bio-diesel standards.

Table 24: Estimated CN and CFPP values for bio-diesel generated from WCB 4.1 biomass cultivated in eleven different mediums.

Medium designation	Cetane number	Cold Filter Plug Point
AF6	48.6	0.4
BBM	60.7	2.5
Chu #10	49.6	1.0
C-medium	54.5	1.6
DYV	54.5	1.6
Franquil	54.4	1.8
Hase	51.1	1.3
JG	53.5	1.9
Lu	51.6	1.5
WC	53.5	1.6
Zarrouk	73.8	5.4
SA Summer Grade	>51	<3

The predicted bio-diesel properties for WCB 4.1 mainly adheres to South African bio-diesel standards. This further demonstrates the feasibility of using WCB 4.1 for bio-diesel production.

5.3.2 Carbohydrate content analysis

WCB 4.1 had the highest carbohydrate yields in the JG, Hase, Chu#10 and DYV mediums in descending order as seen in Figure 36. Similar to the situation with the lipid contents, it is interesting that the Chu#10 and DYV mediums have such high carbohydrate yields in comparison with mediums which showed higher growth rates. The Chu#10, DYV and Franquil mediums show higher cellular carbohydrate percentages than most other cultures as displayed in Figure 37.

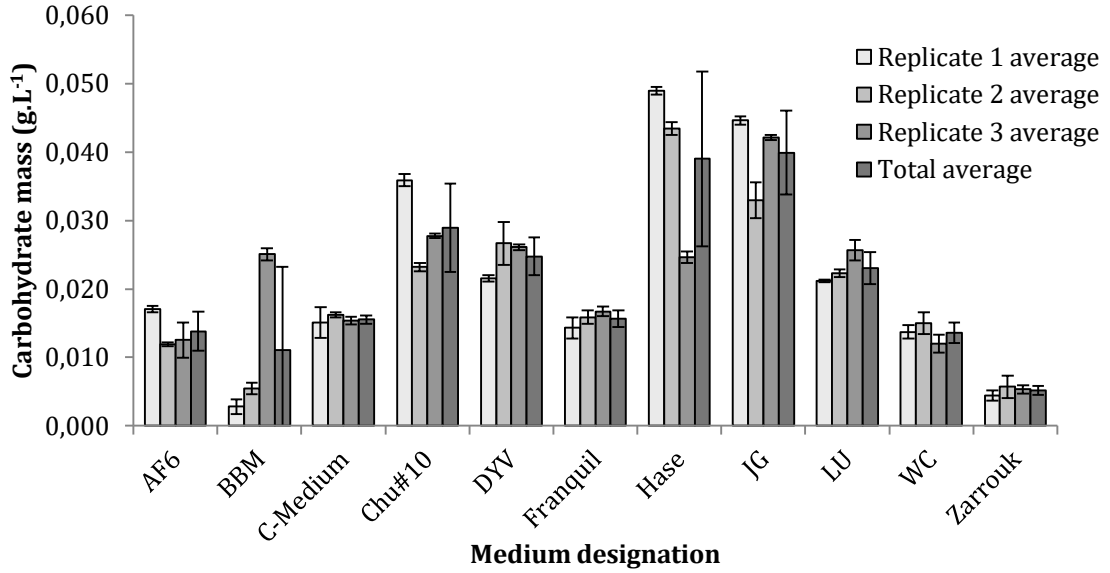


Figure 36: Medium specific carbohydrate yield of WCB 4.1 over 17 days including each replicate and the average yield. The error bars represent the standard deviation.

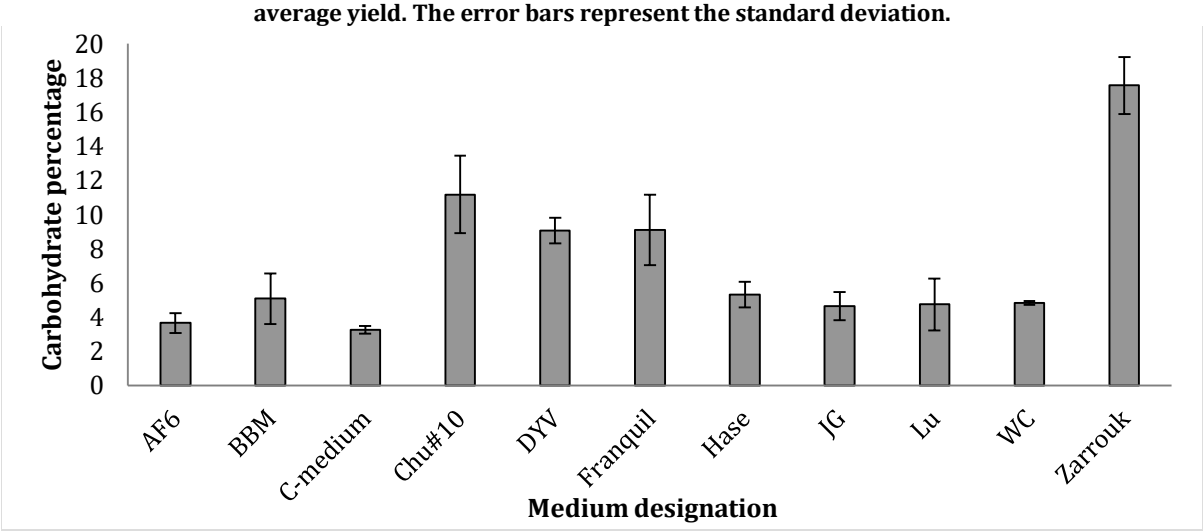


Figure 37: Medium specific carbohydrate percentage with the error bars representing the standard deviation.

Similar to the increase of lipid content in the Chu#10, DYV and Franquil mediums in section 5.3.1, the high carbohydrate percentage can most likely be contributed to nitrogen limitation.

The ethanol yield from fermentation can be predicted as a 90-93% (w/w) conversion of glucose to ethanol (Bai *et al.*, 2008). With ethanol tolerance of yeast going up to ~15% the ideal concentration of glucose to avoid residual sugar and low yield should be ~17% (w/v).

5.3.3 Large scale cultivation prediction:

The combined biomass, lipid and carbohydrate yields of WCB 4.1 in each respective medium can be seen in Figure 38.

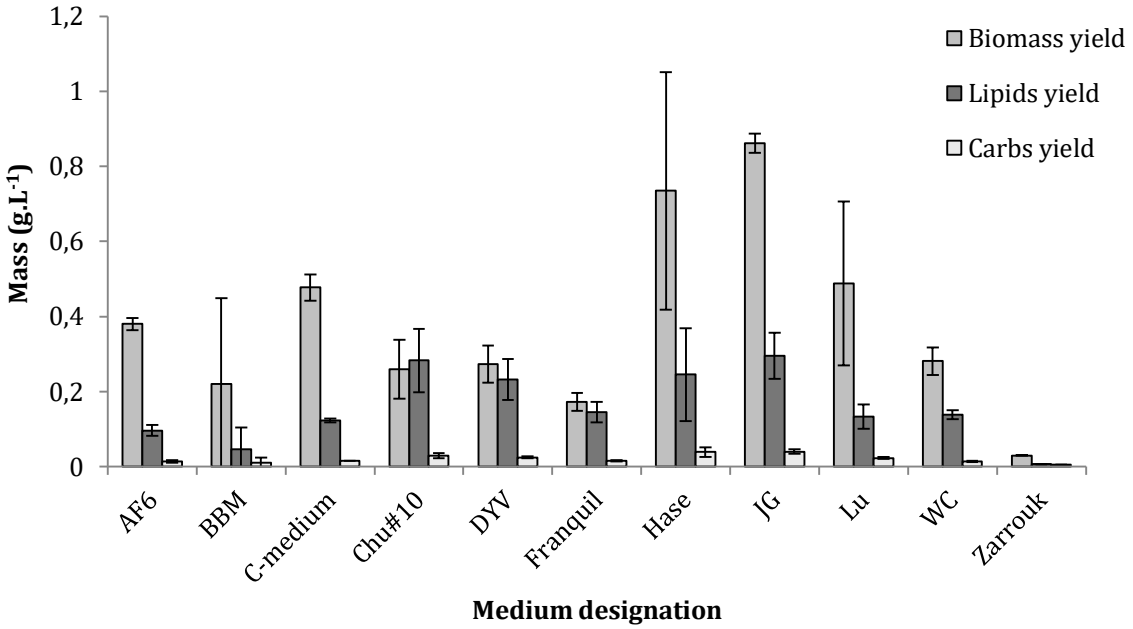


Figure 38: Combined medium respective biomass, lipid and carbohydrate yield at g/L scale.

There are a number of variables which can influence the estimation of large-scale productivity of WCB 4.1 in each medium. Variables which can influence the predictions include: temperature, light intensity, culture volume, photo bioreactor design and cultivation approach (batch / continuous / semi-continuous batch). To be able to simplify estimation we will make a few selections and assumptions:

- Assume a culture volume of 150 L per square meter irrespective of the reactor type.
- Assume constant temperature.
- Assume light intensity similar to the lab scale cultivation with no photo inhibition or light limitation taking place.
- Assume sufficient agitation and that every cell receives enough light.

The prediction was made assuming the theoretical system as described below:

For batch cultivation the first step would be preparing the inoculum. This would be in the form of a pond where the culture is transferred to the cultivation ponds when the inoculum pond reaches an OD of 0.2. The inoculum will be transferred to the ponds as a 10% inoculum. The batch cultivation will then take place for 17 days and be harvested. With this type of cultivation 10% of the cultivation area will go towards the inoculum cultivation and 90% can be harvested every 17 days. To predict the yield rate using this system the day 17 biomass, lipid and carbohydrate yields in Kg can be used with the volume per square meter as 150 L. Considering there are 10 000 square meter in a hectare (Ha), Equation 22 can be used to predict the yield rate per year.

$$P = (Y \div 17 \times 10000 \times 365.25) \times 0.9 \qquad 22$$

Where:

P = predicted yield rate

Y = yield

The predicted biomass, bio-diesel and bio-ethanol yield rates can be seen in Table 25.

Table 25: Estimated bio-diesel and bio-ethanol productivities from WCB 4.1 biomass cultivated in eleven different mediums.

Medium designation	Biomass yield rate ($kg.ha^{-1}.year^{-1}$)	Bio-diesel yield rate ($kg.ha^{-1}.year^{-1}$)	Carbohydrate yield rate ($kg.ha^{-1}.year^{-1}$)	Bio-ethanol yield rate ($kg.ha^{-1}.year^{-1}$)
AF6	11014.42	2797.35	401.12	361.01
BBM	6365.15	1332.44	322.19	289.97
C-medium	13832.23	3573.39	450.53	405.47
Chu#10	7512.84	8199.66	839.30	755.37
DYV	7928.35	6745.45	718.40	646.56
Franquil	4981.46	4200.37	453.55	408.19
Hase	21307.37	7117.85	1131.17	1018.05
JG	24990.49	8555.64	1156.96	1041.27
Lu	14138.81	3863.10	668.43	601.59
WC	8144.17	4009.30	393.43	354.09
Zarrouk	854.59	177.29	150.01	135.01

The bio-ethanol yield can be compared with bio-ethanol yields from other traditional bio-energy crops as can be seen in Figure 39. According to the comparison, the bio-ethanol yield of WCB 4.1 in any of the mediums cannot compete with the productivities of traditional bio-ethanol crops. Bio-ethanol from WCB 4.1 can thus not be used as a main energy product due to the low productivities.

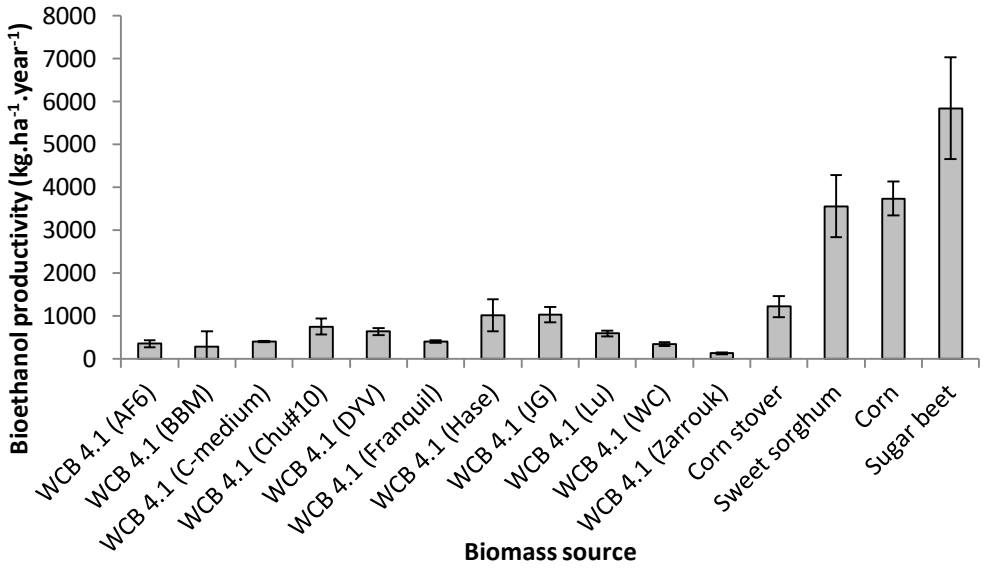


Figure 39: Comparison between bio-ethanol yields from different crop sources with that from WCB 4.1 cultivated in different mediums. The error bars represents the standard deviation (Chaudhary et al., 2014a).

The bio-diesel yield can be compared with bio-diesel yields from other traditional bio-energy crops as can be seen in Figure 40. The estimated bio-diesel yields of WCB 4.1 cultivated in the Chu#10, DYV, Hase and JG mediums are substantially higher than that of palm oil. This demonstrates the potential of WCB 4.1 to be used for the production of bio-diesel. At this point the bio-diesel properties of WCB 4.1 in the Chu#10, DYV, Hase and JG mediums can be considered. WCB 4.1 cultivated in the DYV, Hase and JG mediums can produce bio-diesel with properties accepted as summer grade bio-diesel according to South African bio-diesel standards. The Chu #10 medium is however predicted to not produce bio-diesel with a Cetane number above 51 and does not adhere to South African summer grade bio-diesel standards.

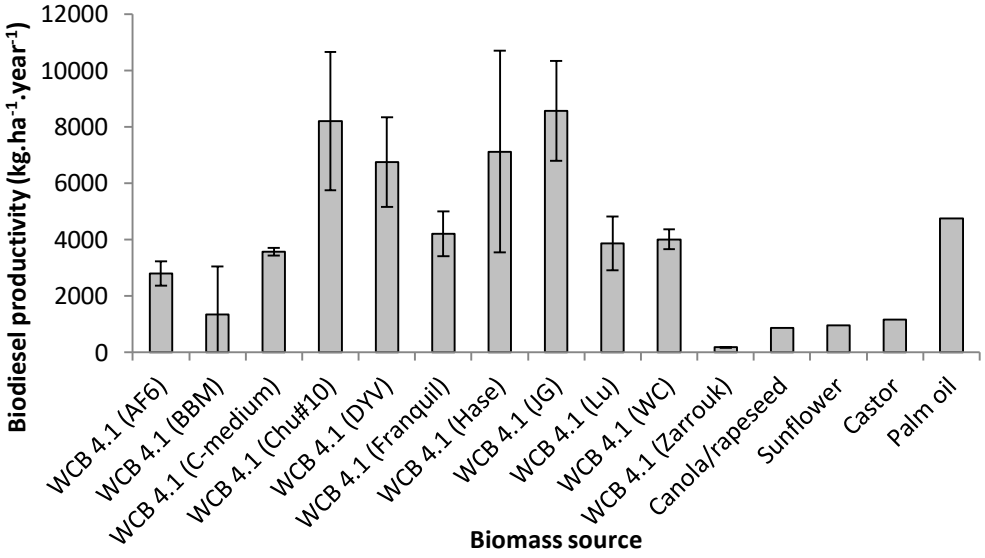


Figure 40: Comparison between bio-diesel yields from different crop sources with that from WCB 4.1 cultivated in different mediums. The error bars represents the standard deviation (Mata *et al.*, 2010).

The highest predicted bio-ethanol yield from WCB 4.1 is 1041 kg/ha/year. Sources such as Chaudhary *et al.* (2014) have estimated microalgal bio-ethanol productivities of 36893.6 – 110689 $kg.ha^{-1}.year^{-1}$. Such productivities are exponentially higher than the estimated productivities in our current estimation. This indicates that there is great room for improving the cultivation of WCB 4.1 for bio-ethanol production purposes.

The highest predicted bio-diesel yield from WCB 4.1 is 8556 $kg.ha^{-1}.year^{-1}$. Sources from Mata *et al.* (2014) have estimated microalgal bio-diesel productivities of 51927 – 121104 $kg.ha^{-1}.year^{-1}$. Such productivities are exponentially higher than the estimated productivities in our current estimation. This indicates that there is great room for improving the cultivation of WCB 4.1 for bio-ethanol production purposes.

WCB 4.1 shows great potential for use in bio-diesel production with bio-ethanol as a secondary product. The productivity of both bio-diesel and bio-ethanol would however need to be greatly increased to compete with productivities described by other sources.

Options to consider to improve productivity in future research includes:

- Further medium optimisation: Such as finding the ideal nitrogen and phosphor medium contents for the cultivation of WCB 4.1. This would require cultivating WCB 4.1 in varying conditions of nitrogen or phosphor with all other medium components kept constant.
- Fed batch cultivation: This would include fed batch process development for the cultivation of WCB 4.1, process optimisation and yield rate analysis of biomass, carbohydrates and lipids.
- Continuous cultivation: Similar to fed batch cultivation, exploring continuous cultivation of WCB 4.1 would require continuous cultivation process development, process optimisation and yield rate analysis of biomass, carbohydrates and lipids.
- Identifying the ideal harvest time: Harvesting time plays a huge role in increasing yield rate of a cultivation. The ideal harvesting time can increase the yield of batch, fed batch and continuous cultivations.
- Including carbon dioxide feed: Inclusion of carbon dioxide feed can increase the growth rate of a microalgal culture. The inclusion of carbon dioxide feed would open a new avenue for further process optimisation. Different carbon dioxide feeding regimes can be explored and different carbon sources such as gaseous carbon dioxide and carbonate salts can be explored.
- Optimising lighting: the optimisation of lighting not only includes finding the ideal lighting intensity and regime, but would also require identifying different reactor designs to optimise light utilisation and improving areal yield.

5.4 Conclusions

In this chapter we were able to investigate the lipid and carbohydrate productivities of WCB 4.1 cultivated in 11 different mediums. The Chu#10, DYV, Hase and JG mediums were identified as the mediums providing the highest lipid and carbohydrate productivities.

We were able to convert lipid and carbohydrate ($mg.L^{-1}.day^{-1}$) productivities to bio-diesel and bio-ethanol ($kg.ha^{-1}.year^{-1}$) productivities and compare these productivities to productivities of first-generation bio-energy crops and microalgae bio-energy productivities from other sources. The bio-diesel productivity of WCB 4.1 in the Chu#10, DYV, Hase and JG mediums were superior to that of first-generation bio-energy crops. The bio-ethanol productivity from WCB 4.1 was inferior to first generation bio-energy crops. When comparing the microalgal bio-energy productivities of WCB 4.1 with other sources, WCB 4.1 had a lower productivity than other literature microalgal strains. This indicates that a lot more optimisation would be required before the large-scale cultivation of WCB 4.1 can be performed.

Furthermore, we were able to predict the bio-diesel properties of bio-diesel generated from WCB 4.1 biomass cultivated in eleven different mediums. WCB 4.1 biomass from the BBM, C-medium, DYV, Franquil, Hase, JG, Lu and WC mediums adhered to South African summer grade bio-diesel standards.

Chapter 6: Conclusion and Recommendation

In this work, the aim was to evaluate the potential of indigenous microalgae for use in bio-diesel and bio-ethanol production. Additionally, the fractional extraction of lipids and carbohydrates from the same microalgal biomass was to be investigated in order to determine the bio-fuel potential.

Fifteen isolates were successfully characterised as per the first objective. Data on isolate growth rate, biomass productivity, lipid productivity, lipid profile and carbohydrate productivity were generated. The data generated contributes to the knowledge of the the MiCCSA culture collection. The collected data is included in the records of the culture collection, which will be made available as an online database. The generated data also provides information on the diversity of strains occurring in South Africa, and provides insight into the commercial potential of South African Indigenous microalgae.

WCB 4.1 was identified as the promising candidate with highest total investigated parameters score. WCB 4.1 has become the organism of choice for use in the rest of this study. As per the second objective, WCB 4.1 was genetically identified as *Acutodesmus bajacalifornicus*. Eleven mediums were used for the cultivation of WCB 4.1, which included AF6, BBM (Bold Basal Medium), Chu # 10, C-medium, DY-V medium, Franquil medium and the WC medium sourced from Andersen (2005), the Hase *et al*., (2005), Lu *et al*., (2015) and Zarrouk (1966) mediums, and the newly formulated JG medium. In all investigated mediums, WCB 4.1 showed highest growth rate in the JG medium, with a growth rate of 0.47 d^{-1}, and the highest biomass productivity in the Hase medium, with productivity of 53.1 $mg.L^{-1}.d^{-1}$, which is low compared to other literature biomass productivities.

Correlating respective growth rates with nitrogen/phosphor medium contents allowed a better understanding for the growth rate over substrate relationship for the cultivation of WCB 4.1. This provided understanding as to why certain mediums performed better than others. Potential optimal nitrogen and phosphor molar concentrations for the cultivation of WCB 4.1 can range from 4 mM to 6 mM and 0.3 to 0.7 mM respectively. WCB 4.1 demonstrated elevated growth rates for media with nitrogen to phosphor molar ratios between 15:1 and 20:1. The Hase and JG media fit in perfectly with the above-mentioned nitrogen and phosphor concentrations and ratios. Medium optimisation studies could verify the true ideal nitrogen and phosphor concentrations and ratios for WCB 4.1. Additional parameters, which may be explored for cultivation condition optimisation includes salinity, pH, temperature and lighting intensity.

WCB 4.1 shows potential for use in microalgal cultivation. To further explore the bio-energy production potential of WCB 4.1, as per the third and fourth objectives, the lipid

and carbohydrate productivities of WCB 4.1, cultivated in eleven different mediums, were investigated.

The Chu#10, DYV, Hase and JG mediums were identified as the mediums providing the highest lipid and carbohydrate productivities. The Hase and JG media showed elevated lipid and carbohydrate productivity due to these media having the highest biomass productivity. The Chu #10 and DY-V media demonstrated elevated lipid and carbohydrate productivity most likely due to nitrogen starvation. This demonstrates that WCB 4.1 could be put through a starvation regime to increase lipid and carbohydrate yield. This would be a matter of consideration for future process development.

Estimated bio-diesel yield rates of WCB 4.1 in the Hase, JG, DY-V and Chu #10 media demonstrates potential to be superior to that of first-generation bio-energy crops. The bio-ethanol yield rates are estimated to be inferior to that of first-generation bio-energy crops. Lipid and carbohydrate yield rates of WCB 4.1 is estimated to be inferior to literature microalgal yield rates. Performing a theoretical investigation of the economic and energetic feasibility, using the growth rates and yield rates described in this study, is recommended. This will provide more insight to the way forward and potential of WCB 4.1 for bio-energy generation, before any larger-scale cultivation takes place.

By utilising obtained lipid profiles, the bio-diesel properties of bio-diesel generated from WCB 4.1 biomass cultivated in eleven different mediums were predicted. Bio-diesel generated by cultivation in the BBM, C-medium, DY-V, Franquil, Hase, JG, Lu and WC media adhered to South African summer grade bio-diesel standards. This indicates that WCB 4.1 cultivated in the Hase and JG media is predicted to provide bio-diesel, which would be safe for commercial use in South Africa. The Chu #10 medium is predicted to generate bio-diesel not adhering to South African standards, indicating potential danger in including a starvation regime in the cultivation as it may adversely affect the bio-diesel properties. WCB 4.1 shows potential to become a commercially competitive strain for bio-energy production. The key to unlock the potential of WCB 4.1 would be in research, process development and optimisation. Characterisation of the MiCCSA culture collection is also of high importance to further broaden the knowledge of the collection and of South African indigenous microalgal strains. Characterisation of the culture collection could provide more candidate strains with potential commercial use for an array of purposes.

Recommendations for future work includes:

1. Ethier et al., (2011) demonstrated that yield rates of a microalgal product can be increased by utilising fed-batch and continuous cultivation systems. The cultures in the current study were cultivated in batch systems. Exploring the cultivation of these cultures in fed-batch and continuous systems can unlock potential for increasing biomass and product yield rates.
2. Fábregas et al., (2000) demonstrated the potential of increasing microalgal yield rates by optimising medium compositions. In addition to increasing microalgal yield rate, medium optimisation can also lead to reduced usage of non-essential components resulting in cost reduction (Fábregas et al., 2000). Further medium optimisation can thus lead to possible yield rate increases and cultivation cost reduction.
3. Multiple high value products can be produced by microalgae, including β-carotene, B-vitamins, astaxanthin, polyunsaturated fatty acids and lutein (Huang *et al*., 2006, Del Campo *et al*., 2007, He *et al*., 2005, Ip and Chen, 2005, Wen and Chen, 2003, Jiang *et al*., 2004, Blanco *et al*., 2007, Shi and Chen, 2002, Li *et al*., 2008b). The economic feasibility of microalgal bio-fuel can be increased by providing additional products, which can operate independent of the energy industry (Li *et al*., 2008b, Griffiths *et al*., 2016). WCB 4.1 shows the formation of red pigmentation in highly stressed cultures, which is indicative of a carotenoid such as β-carotene or astaxanthin. Screening WCB 4.1 for high value compounds can provide a new avenue for increasing industrial feasibility of the production of WCB 4.1 biomass.
4. Up-scale production to pilot scale and perform pilot scale bio-diesel and bio-ethanol production.
5. Investigate utilisation of WCB 4.1 characteristics to improve ease of harvesting.
6. Perform a theoretical investigation of the economic and energetic feasibility, using the growth rates and yield rates described in this study.
7. Further medium and cultivation condition optimisation including nitrogen, phosphor, carbon, pH, salinity and light intensity optimisation.

References

AATOLA, H., LARMI, M., SARJOVAARA, T. & MIKKONEN, S. 2009. Hydrotreated Vegetable Oil (HVO) as a Renewable Diesel Fuel: Trade-off between NO_x, Particulate Emission, and Fuel Consumption of a Heavy Duty Engine. SAE International Journal of Engines, 1, 1251-1262.

AHMAD, A. L., MAT YASIN, N. H., DEREK, C. J. C. & LIM, J. K. 2011. Microalgae as a sustainable energy source for biodiesel production: A review. Renewable and Sustainable Energy Reviews, 15, 584-93.

ALTSCHUL, S. F., GISH, W., MILLER, W., MYERS, E. W. & LIPMAN, D. J. 1990. Basic local alignment search tool. Journal of Molecular Biology, 215, 403-410.

ANDERSEN, R. A. 2005. Algal culturing techniques, Academic Press.

ARTHUR, C. 2003. Oil and gas running out much faster than expected, says study. The Independent.

ASIF, M. & MUNEER, T. 2007. Energy supply, its demand and security issues for developed and emerging economies. Renewable and Sustainable Energy Reviews, 11, 1388-1413.

ASLAN, S. & KAPDAN, I. K. 2006. Batch kinetics of nitrogen and phosphorus removal from synthetic wastewater by algae. Ecological engineering, 28, 64-70.

BAI, F. W., ANDERSON, W. A. & MOO-YOUNG, M. 2008. Ethanol fermentation technologies from sugar and starch feedstocks. Biotechnology Advances 26, 89-105.

BELLINGER, E. G. & SIGEE, D. C. 2015. Freshwater algae: identification and use as bioindicators, John Wiley & Sons.

BERNER, T., DUBINSKY, Z., WYMAN, K. & FALKOWSKI, P. G. 1989. Photoadaptation and the "package" effect in *Dunaliella tertiolecta* (*Chlorophyceae*) 1. Journal of Phycology, 25, 70-78.

BLANCO, A. M., MORENO, J., DEL CAMPO, J. A., RIVAS, J. & GUERRERO, M. G. 2007. Outdoor cultivation of lutein-rich cells of *Muriellopsis sp*. in open ponds. Applied Microbiology and Biotechnology, 73, 1259-1266.

BOROWITZKA, M. A. 1995. Microalgae as sources of pharmaceuticals and other biologically active compounds. Journal of Applied Phycology, 7, 3-15.

BOSMA, R., VAN SPRONSEN, W. A., TRAMPER, J. & WIJFFELS, R. H. 2003. Ultrasound, a new separation technique to harvest microalgae. Journal of Applied Phycology, 15, 143-153.

BRENNAN, L. & OWENDE, P. 2010. Biofuels from microalgae—A review of technologies for production, processing, and extractions of biofuels and co-products. Renewable and Sustainable Energy Reviews, 14, 10.

BURTON, T., LYONS, H., LERAT, Y., STANLEY, M. & RASMUSSEN, M. B. 2009. A review of the potential of marine algae as a source of biofuel in Ireland.

CABANELAS, I. T. D., RUIZ, J., ARBIB, Z., CHINALIA, F. A., GARRIDO-PÉREZ, C., ROGALLA, F., NASCIMENTO, I. A. & PERALES, J. A. 2013. Comparing the use of different domestic wastewaters for coupling microalgal production and nutrient removal. Bioresource Technology, 131, 429-436.

CHANG, E.-H. & YANG, S.-S. 2003. Some characteristics of microalgae isolated in Taiwan for biofixation of carbon dioxide. Botanical Bulletin of Academia Sinica, 44.

CHAUDHARY, L., PRADHAN, P., SONI, N., SINGH, P. & TIWARI, A. 2014a. Algae as a Feedstock for Bioethanol Production: New Entrance in Biofuel World. Chem. Tech., 6, 1381-89.

CHAUDHARY, L., PRADHAN, P., SONI, N., SINGH, P. & TIWARI, A. 2014b. Algae as a feedstock for bioethanol production: new entrance in biofuel world. International Journal Chemistry and Technology. Res, 6, 1381-1389.

CHAUTON, M. S., REITAN, K. I., NORSKER, N. H., TVETERÅS, R. & KLEIVDAL, H. T. 2015. A techno-economic analysis of industrial production of marine microalgae as a source of EPA and DHA-rich raw material for aquafeed: Research challenges and possibilities. Aquaculture, 436, 95-103.

CHENA, C., ZHAOB, X., YENC, H., HOD, S., CHENGD, C., LEE, D., BAIB, F. & CHANGA, J. 2013. Microalgae-based carbohydrates for biofuel production. Biochemical Engineering Journal, 78, 1-10.

CHISTI, Y. 2007. Biodiesel from microalgae. Biotechnology Advances, 25, 294-306.

CHOI, H.-J. & LEE, S.-M. 2015. Biomass and oil content of microalgae under mixotrophic conditions. Environmental Engineering Research, 20, 25-32.

CHOKSHI, K., PANCHA, I., TRIVEDI, K., GEORGE, B., MAURYA, R., GHOSH, A. & MISHRA, S. 2015. Biofuel potential of the newly isolated microalgae Acutodesmus dimorphus under temperature induced oxidative stress conditions. Bioresource Technology, 180, 162-171.

COBOS, M., PAREDES, J. D., MADDOX, J. D., VARGAS-ARANA, G., FLORES, L., AGUILAR, C. P., MARAPARA, J. L. & CASTRO, J. C. 2017. Isolation and Characterization of Native Microalgae from the Peruvian Amazon with Potential for Biodiesel Production. Energies, 10, 224.

COLEMAN, J. R. & COLMAN, B. 1981. Inorganic carbon accumulation and photosynthesis in a blue-green alga as a function of external pH. Plant Physiology, 67, 917-921.

COMMISSION, N. P. 2012. Executive Summary–NDP 2030–Our future–make it work. Pretoria, Department: The Presidency.

CONVERTI, A., CASAZZA, A. A., ORTIZ, E. Y., PEREGO, P. & DEL BORGHI, M. 2009. Effect of temperature and nitrogen concentration on the growth and lipid content of *Nannochloropsis oculata* and *Chlorella vulgaris* for biodiesel production. Chemical Engineering and Processing: Process Intensification, 48, 1146-1151.

CUHEL, R. L., ORTNER, P. B. & LEAN, D. R. 1984. Night synthesis of protein by algae. Limnology and Oceanography, 29, 731-744.

DE WEVER, A., LELIAERT, F., VERLEYEN, E., VANORMELINGEN, P., VAN DER GUCHT, K., HODGSON, D. A., SABBE, K. & VYVERMAN, W. 2009. Hidden levels of phylodiversity in Antarctic green algae: further evidence for the existence of glacial refugia. Proceedings of the Royal Society of London B: Biological Sciences, 276, 3591-3599.

DEL CAMPO, J. A., GARCÍA-GONZÁLEZ, M. & GUERRERO, M. G. 2007. Outdoor cultivation of microalgae for carotenoid production: current state and perspectives. Applied Microbiology and Biotechnology, 74, 1163-1174.

DEMIRBAS, A. 2010. Use of algae as biofuel sources. Energy Converse Management, 51, 2738-2749.

DINCER, I. & ROSEN, M. A. 1999. Energy, environment and sustainable development. Applied Energy, 64, 427-440.

DIVAKARAN, R. & PILLAI, V. S. 2002. Flocculation of algae using chitosan. Journal of Applied Phycology, 14, 419-422.

DOUCHA, J., STRAKA, F. & LÍVANSKÝ, K. 2005. Utilization of flue gas for cultivation of microalgae *Chlorella sp*.) in an outdoor open thin-layer photobioreactor. Journal of Applied Phycology, 17, 403-412.

DRAGONE, G., FERNANDES, B. D., ABREU, A. P., VICENTE, A. A. & TEIXEIRA, J. A. 2011. Nutrient limitation as a strategy for increasing starch accumulation in microalgae. Applied Energy, 88, 3331-3335.

DUBINSKY, Z., MATSUKAWA, R. & KARUBE, I. 1995. Photobiological aspects of algal mass culture. Journal of Marine Biotechnology, 2, 61-65.

DUBOIS, M., GILLES, K. A., HAMILTON, J. K., REBERS, P. T. & SMITH, F. 1956. Colorimetric method for determination of sugars and related substances. Analytical Chemistry, 28, 350-356.

DUNN, R. & BAGBY, M. 1995. Low-temperature properties of triglyceride-based diesel fuels: transesterified methyl esters and petroleum middle distillate/ester blends. Journal of the American Oil Chemists' Society, 72, 895-904.

DUNN, R. O. 2008. Crystallization behavior of fatty acid methyl esters. Journal of the American Oil Chemists' Society, 85, 961-972.

DURAND, P. M., RAOOF, I. & NDHLOVU, A. 2016. Genotypic analysis of 20 isolates in the microalgal culture collection of South Africa (MiCCSA). University of Witwatersrand.

EDWARDS, V. H. 1970. The influence of high substrate concentrations on microbial kinetics. Biotechnology and Bioengineering, 12, 679-712.

ETHIER, S., WOISARD, K., VAUGHAN, D. & WEN, Z. 2011. Continuous culture of the microalgae *Schizochytrium limacinum* on biodiesel-derived crude glycerol for producing docosahexaenoic acid. Bioresource Technology, 102, 88-93.

EMERSON, R. & LEWIS, C. M. 1943. The dependence of the quantum yield of *Chlorella* photosynthesis on wave lenghth of light. American Journal of Botany, 165-178.

FÁBREGAS, J., DOMÍNGUEZ, A., REGUEIRO, M., MASEDA, A. & OTERO, A. 2000. Optimization of culture medium for the continuous cultivation of the microalga *Haematococcus pluvialis*. Applied Microbiology and Biotechnology, 53, 530-535.

FÁBREGAS, J., MASEDA, A., DOMÍNGUEZ, A. & OTERO, A. 2004. The cell composition of *Nannochloropsis sp*. changes under different irradiances in semicontinuous culture. World Journal of Microbiology and Biotechnology, 20, 31-35.

FALKOWSKI, P. G. 1997. Evolution of the nitrogen cycle and its influence on the biological sequestration of CO_2 in the ocean. Nature, 387, 272.

FIDALGO, J., CID, A., TORRES, E., SUKENIK, A. & HERRERO, C. 1998. Effects of nitrogen source and growth phase on proximate biochemical composition, lipid classes and fatty acid profile of the marine microalga *Isochrysis galbana*. Aquaculture, 166, 105-116.

FUΩÍKOVÁ, K., CHIEN, L., LEWIS, L. A. & KAROL, K. G. 2010. An assessment of proposed DNA barcodes in freshwater green algae. Cryptogamie, Algologie, 31, 529-555.

GINZBURG, M. 1981. Measurements of ion concentrations in *Dunaliella parva* subjected to hypertonic shock. Journal of Experimental Botany, 32, 333-340.

GORDILLO, F. J., GOUTX, M., FIGUEROA, F. L. & NIELL, F. X. 1998. Effects of light intensity, CO_2 and nitrogen supply on lipid class composition of *Dunaliella viridis*. Journal of Applied Phycology, 10, 135-144.

GOUVEIA, L. & OLIVEIRA, A. C. 2009. Microalgae as a raw material for biofuels production. Journal of Industrial Microbiology & Biotechnology, 36, 269-274.

GRANT, D. 1967. Kinetic aspects of the growth of *Klebsiella aerogenes* with some benzenoid carbon sources. Microbiology, 46, 213-224.

GRIFFITHS, M., HARRISON, S. T., SMIT, M. & MAHARAJH, D. 2016. Major commercial products from micro-and macroalgae. Algae Biotechnology. Springer.

GRIFFITHS, M., VAN HILLE, R. & HARRISON, S. 2010. Selection of direct transesterification as the preferred method for assay of fatty acid content of microalgae. Lipids, 45, 1053-1060.

GRIFFITHS, M. J., DICKS, R. G., RICHARDSON, C. & HARRISON, S. T. 2011. Advantages and challenges of microalgae as a source of oil for biodiesel. Biodiesel-feedstocks and processing technologies. InTech.

GRIFFITHS, M. J. & HARRISON, S. T. 2009. Lipid productivity as a key characteristic for choosing algal species for biodiesel production. Journal of Applied Phycology, 21, 493-507.

GRIMA, E. M., BELARBI, E.-H., FERNÁNDEZ, F. A., MEDINA, A. R. & CHISTI, Y. 2003. Recovery of microalgal biomass and metabolites: process options and economics. Biotechnology Advances, 20, 491-515.

GUDIN, C. & THEPENIER, C. 1986. Bioconversion of solar energy into organic chemicals by microalgae. Advances in Biotechnological Processes (USA).

HAMEED, M. A. 2007. Effect of algal density in bead, bead size and bead concentrations on wastewater nutrient removal. African Journal of Biotechnology, 6.

HASE, R., OIKAWA, H., SASAO, C., MORITA, M. & WATANABE, Y. 2000. Photosynthetic production of microalgal biomass in a raceway system under greenhouse conditions in Sendai city. Journal of Bioscience and Bioengineering, 89, 157-163.

HASHEMI, P. & RAHMANI, Z. 2006. A novel homocystine–agarose adsorbent for separation and preconcentration of nickel in table salt and baking soda using factorial design optimization of the experimental conditions. Talanta, 68, 1677-1682.

HE, H.-Z., LI, H.-B. & CHEN, F. 2005. Determination of vitamin B1 in seawater and microalgal fermentation media by high-performance liquid chromatography with fluorescence detection. Analytical and Bioanalytical Chemistry, 383, 875-879.

HEASMAN, M., DIEMAR, J., O'CONNOR, W., SUSHAMES, T. & FOULKES, L. 2000. Development of extended shelf-life microalgae concentrate diets harvested by centrifugation for bivalve molluscs–a summary. Aquaculture Research, 31, 637-659.

HO, S.-H., CHEN, C.-Y. & CHANG, J.-S. 2012. Effect of light intensity and nitrogen starvation on CO2 fixation and lipid/carbohydrate production of an indigenous microalga *Scenedesmus obliquus* CNW-N. Bioresource Technology, 113, 244-252.

HO, S.-H., HUANG, S.-W., CHEN, C.-Y., HASUNUMA, T., KONDO, A. & CHANG, J.-S. 2013. Characterization and optimization of carbohydrate production from an indigenous microalga *Chlorella vulgaris* FSP-E. Bioresource Technology, 135, 157-165.

HOEL, M. & KVERNDOKK, S. 1996. Depletion of fossil fuels and the impacts of global warming. Resource and Energy Economics, 18, 115-136.

HSUEH, H., CHU, H. & YU, S.-T. 2007. A batch study on the bio-fixation of carbon dioxide in the absorbed solution from a chemical wet scrubber by hot spring and marine algae. Chemosphere, 66, 878-886.

HUANG, G., CHEN, F., WEI, D., ZHANG, X. & CHEN, G. 2010. Biodiesel production by microalgal biotechnology. Applied Energy, 87, 38-46.

HUANG, J.-C., CHEN, F. & SANDMANN, G. 2006. Stress-related differential expression of multiple β-carotene ketolase genes in the unicellular green alga *Haematococcus pluvialis*. Journal of Biotechnology, 122, 176-185.

HUERLIMANN, R., DE NYS, R. & HEIMANN, K. 2010. Growth, lipid content, productivity, and fatty acid composition of tropical microalgae for scale-up production. Biotechnology and Bioengineering, 107, 245-257.

IAGS. 2004. The Future of Oil [Online]. Available: http://www.iags.org/futureofoil.html [Accessed 2017/07/09 2017].

ILLMAN, A. M., SCRAGG, A. H. & SHALES, S. W. 2000. Increase in *Chlorella* strains calorific values when grown in low nitrogen medium. Enzyme Microbiology Technology, 27, 631-635.

IMAHARA, H., MINAMI, E. & SAKA, S. 2006. Thermodynamic study on cloud point of biodiesel with its fatty acid composition. Fuel, 85, 1666-1670.

IP, P.-F. & CHEN, F. 2005. Employment of reactive oxygen species to enhance astaxanthin formation in *Chlorella zofingiensis* in heterotrophic culture. Process Biochemistry, 40, 3491-3496.

IQBAL, M. & ZAFAR, S. 1993. Effects of photon flux density, CO 2, aeration rate, and inoculum density on growth and extracellular polysaccharide production by *Porphyridium cruentum*. Folia microbiologica, 38, 509-514.

JANAUN, J. & ELLIS, N. 2010. Perspectives on biodiesel as a sustainable fuel. Renewable and Sustainable Energy Reviews, 14, 1312-1320.

JANET, R., STEIN, E. & STEIN, J. R. 1973. Handbook of Phycological Methods: Culture Methods and Growth Measurements, Cambridge University Press.

JIANG, Y., FAN, K.-W., TSZ-YEUNG WONG, R. & CHEN, F. 2004. Fatty acid composition and squalene content of the marine microalga *Schizochytrium mangrovei*. Journal of Agricultural and Food Chemistry, 52, 1196-1200.

JORQUERA, O., KIPERSTOK, A., SALES, E. A., EMBIRUCU, M. & GHIRARDI, M. L. 2010. Comparative energy life-cycle analyses of microalgal biomass production in open ponds and photobioreactors. Bioresource Technology, 101, 1406-13.

JUNEJA, A., CEBALLOS, R. M. & MURTHY, G. S. 2013. Effects of environmental factors and nutrient availability on the biochemical composition of algae for biofuels production: a review. Energies, 6, 4607-4638.

KIM, M.-S., BAEK, J.-S., YUN, Y.-S., SIM, S. J., PARK, S. & KIM, S.-C. 2006. Hydrogen production from *Chlamydomonas reinhardtii* biomass using a two-step conversion process: anaerobic conversion and photosynthetic fermentation. International Journal of Hydrogen Energy, 31, 812-816.

KLECKA, G. & MAIER, W. 1985. Kinetics of microbial growth on pentachlorophenol. Applied and Environmental Microbiology, 49, 46-53.

KNOTHE, G. 2006. Analyzing biodiesel: standards and other methods. Journal of the American Oil Chemists' Society, 83, 823-833.

KNUCKEY, R. M., BROWN, M. R., ROBERT, R. & FRAMPTON, D. M. 2006. Production of microalgal concentrates by flocculation and their assessment as aquaculture feeds. Aquacultural Engineering, 35, 300-313.

KONOPKA, A. & BROCK, T. D. 1978. Effect of temperature on blue-green algae (cyanobacteria) in Lake Mendota. Applied and Environmental Microbiology, 36, 572-576.

LANE, A. E. & BURRIS, J. E. 1981. Effects of environmental pH on the internal pH of *Chlorella pyrenoidosa*, *Scenedesmus quadricauda*, and *Euglena mutabilis*. Plant Physiology, 68, 439-442.

LAPUERTA, M., RODRÍGUEZ-FERNÁNDEZ, J. & DE MORA, E. F. 2009. Correlation for the estimation of the cetane number of biodiesel fuels and implications on the iodine number. Energy Policy, 37, 4337-4344.

LEE, R. E. 2018. Phycology, Cambridge University Press.

LELIAERT, F., SMITH, D. R., MOREAU, H., HERRON, M. D., VERBRUGGEN, H., DELWICHE, C. F. & DE CLERCK, O. 2012. Phylogeny and molecular evolution of the green algae. Critical Reviews in Plant Sciences, 31, 1-46.

LENTON, T. M. & WATSON, A. J. 2000. Redfield revisited: 1. Regulation of nitrate, phosphate, and oxygen in the ocean. Global Biogeochemical Cycles, 14, 225-248.

LI, Y., HORSMAN, M., WANG, B., WU, N. & LAN, C. Q. 2008a. Effects of nitrogen sources on cell growth and lipid accumulation of green alga *Neochloris oleoabundans*. Applied Microbiology and Biotechnology, 81, 629-636.

LI, Y., HORSMAN, M., WU, N., LAN, C. Q. & DUBOIS-CALERO, N. 2008b. Biofuels from microalgae. Biotechnology Progress, 24, 815-820.

LIANG, Y., SARKANY, N. & CUI, Y. 2009. Biomass and lipid productivities of *Chlorella vulgaris* under autotrophic, heterotrophic and mixotrophic growth conditions. Biotechnology Letters, 31, 1043-1049.

LIN, Z., LIN, Z., LI, H. & SHEN, S. 2012. Sequences analysis of ITS region and 18S rDNA of Ulva. ISRN Botany, 2012.

LONG, S., HUMPHRIES, S. & FALKOWSKI, P. G. 1994. Photoinhibition of photosynthesis in nature. Annual Review of Plant Biology, 45, 633-662.

LOPES, J., BOROS, L., KRÄHENBÜHL, M., MEIRELLES, A., DARIDON, J.-L., PAULY, J., MARRUCHO, I. & COUTINHO, J. 2007. Prediction of cloud points of biodiesel. Energy & Fuels, 22, 747-752.

LU, W., WANG, Z. & YUAN, Z. 2015. Characteristics of lipid extraction from *Chlorella sp*. cultivated in outdoor raceway ponds with mixture of ethyl acetate and ethanol for biodiesel production. Bioresource Technology, 191, 433-437.

MACKAY, D. & SALUSBURY, T. 1988. Choosing between centrifugation and crossflow microfiltration. Chemical Engineer, 45-50.

MALLICK, N. 2002. Biotechnological potential of immobilized algae for wastewater N, P and metal removal: a review. Biometals, 15, 377-390.

MARKOU, G., ANGELIDAKI, I., NERANTZIS, E. & GEORGAKAKIS, D. 2013. Bioethanol production by carbohydrate-enriched biomass of *Arthrospira (Spirulina) platensis*. Energies, 6, 3937-3950.

MARKOU, G., CHATZIPAVLIDIS, I. & GEORGAKAKIS, D. 2012. Carbohydrates production and bio-flocculation characteristics in cultures of *Arthrospira (Spirulina) platensis*: improvements through phosphorus limitation process. BioEnergy Research, 5, 915-925.

MATA, T. M., MARTINS, A. A. & CAETANO, N. S. 2010. Microalgae for biodiesel production and other applications: a review. Renewable and Sustainable Energy Reviews, 14, 217-232.

MEDLIN, L., ELWOOD, H. J., STICKEL, S. & SOGIN, M. L. 1988. The characterization of enzymatically amplified eukaryotic 16S-like rRNA-coding regions. Gene, 71, 491-499.

MIYACHI, S., MIYACHI, S. & KAMIYA, A. 1978. Wavelength effects on photosynthetic carbon metabolism in *Chlorella*. Plant and Cell Physiology, 19, 277-288.

MOHN, F. 1980. Experiences and strategies in the recovery of biomass from mass cultures of microalgae. Algae biomass: production and use/[sponsored by the National Council for Research and Development, Israel and the Gesellschaft fur Strahlen-und Umweltforschung (GSF), Munich, Germany]; editors, Gedaliah Shelef, Carl J. Soeder.

MONOD, J. 1949. The growth of bacterial cultures. Annual Reviews in Microbiology, 3, 371-394.

MUNOZ, R. & GUIEYSSE, B. 2006. Algal–bacterial processes for the treatment of hazardous contaminants: a review. Water Research, 40, 2799-2815.

NAGARAJAN, D., LEE, D.-J. & CHANG, J.-S. 2018. Heterotrophic Microalgal Cultivation. Bioreactors for Microbial Biomass and Energy Conversion. Springer.

NAKAYAMA, T., MARIN, B., KRANZ, H. D., SUREK, B., HUSS, V. A., INOUYE, I. & MELKONIAN, M. 1998. The basal position of scaly green flagellates among the green algae (*Chlorophyta*) is revealed by analyses of nuclear-encoded SSU rRNA sequences. Protist, 149, 367-380.

NASCIMENTO, I. A., MARQUES, S. S. I., CABANELAS, I. T. D., PEREIRA, S. A., DRUZIAN, J. I., DE SOUZA, C. O., VICH, D. V., DE CARVALHO, G. C. & NASCIMENTO, M. A. 2013. Screening Microalgae Strains for Biodiesel Production: Lipid Productivity and Estimation of Fuel Quality Based on Fatty Acids Profiles as Selective Criteria. Bioenergy Research, 6, 1-13.

NGUYEN, M. T., CHOI, S. P., LEE, J., LEE, J. H. & SIM, S. J. 2009. Hydrothermal acid pretreatment of *Chlamydomonas reinhardtii* biomass for ethanol production. Journal of Microbiology and Biotechnology, 19, 161-166.

NIGAM, P. S. & SINGH, A. 2011. Production of liquid biofuels from renewable resources. Prog. Energy Combust. Sci., 37, 52-68.

NUR, M. M. A., SETYONINGRUM, T. M. & BUDIAMAN, I. G. S. 2017. Potency of *Botryococcus braunii* cultivated on palm oil mill effluent wastewater as a source of biofuel. Environmental Engineering Research, 22, 417-425.

ORCUTT, D. M. & PATTERSON, G. W. 1974. Effect of light intensity upon lipid composition of *Nitzschia closterium (Cylindrotheca fusiformis)*. Lipids, 9, 1000-1003.

OZKAN, A., KINNEY, K., KATZ, L. & BERBEROGLU, H. 2012. Reduction of water and energy requirement of algae cultivation using an algae biofilm photobioreactor. Bioresource Technology, 114, 542-8.

PESSOA, M. F. 2012. Harmful effects of UV radiation in algae and aquatic macrophytes-a review. Emirates Journal of Food and Agriculture, 24, 510.

PETRUSEVSKI, B., BOLIER, G., VAN BREEMEN, A. & ALAERTS, G. 1995. Tangential flow filtration: a method to concentrate freshwater algae. Water Research, 29, 1419-1424.

PITTMAN, J. K., DEAN, A. P. & OSUNDEKO, O. 2011. The potential of sustainable algal biofuel production using wastewater resources. Bioresource Technology, 102, 17-25.

PRICE, K. & FARAG, I. H. 2013. Resources Conservation in Microalgae Biodiesel Production. International Journal of Engineering and Technical Research, 49-56.

PULZ, O. 2001. Photobioreactors: production systems for phototrophic microorganisms. Applied Microbiology and Biotechnology, 57, 287-93.

RAVEN, J. A. & GEIDER, R. J. 1988. Temperature and algal growth. New Phytologist, 110, 441-461.

REDFIELD, A. C. 1958. The biological control of chemical factors in the environment. American Scientist, 46, 230A-221.

RENAUD, S. & PARRY, D. 1994. Microalgae for use in tropical aquaculture II: Effect of salinity on growth, gross chemical composition and fatty acid composition of three species of marine microalgae. Journal of Applied Phycology, 6, 347-356.

RENAUD, S., PARRY, D., THINH, L.-V., KUO, C., PADOVAN, A. & SAMMY, N. 1991. Effect of light intensity on the proximate biochemical and fatty acid composition of *Isochrysis sp*. and *Nannochloropsis oculata* for use in tropical aquaculture. Journal of Applied Phycology, 3, 43-53.

RENAUD, S. M., THINH, L.-V., LAMBRINIDIS, G. & PARRY, D. L. 2002. Effect of temperature on growth, chemical composition and fatty acid composition of tropical Australian microalgae grown in batch cultures. Aquaculture, 211, 195-214.

RHEE, G.-Y. 1982. Effects of environmental factors and their interactions on phytoplankton growth. Advances in microbial ecology. Springer.

RHEE, G. & GOTHAM, I. J. 1981. The effect of environmental factors on phytoplankton growth: temperature and the interactions of temperature with nutrient limitation. Limnology and Oceanography, 26, 635-648.

RODOLFI, L., CHINI ZITTELLI, G., BASSI, N., PADOVANI, G., BIONDI, N., BONINI, G. & TREDICI, M. R. 2009. Microalgae for oil: strain selection, induction of lipid synthesis and outdoor mass cultivation in a low-cost photobioreactor. Biotechnol Bioeng, 102, 100-12.

SACKETT, J. I. 2001. The future of nuclear energy. Fuel Processing Technology, 71, 197-204.

SALAMEH, M. G. 2004. Oil Crises, Historical Perspective☆.

SANDNES, J., KÄLLQVIST, T., WENNER, D. & GISLERØD, H. R. 2005. Combined influence of light and temperature on growth rates of *Nannochloropsis oceanica*: linking cellular responses to large-scale biomass production. Journal of Applied Phycology, 17, 515-525.

SATYARTHI, J., CHIRANJEEVI, T., GOKAK, D. & VISWANATHAN, P. 2013. An overview of catalytic conversion of vegetable oils/fats into middle distillates. Catalysis Science & Technology, 3, 70-80.

SCHENK, P. M., THOMAS-HALL, S. R., STEPHENS, E., MARX, U. C., MUSSGNUG, J. H., POSTEN, C., KRUSE, O. & HANKAMER, B. 2008. Second generation biofuels: high-efficiency microalgae for biodiesel production. Bioenergy Research, 1, 20-43.

SHAFIEE, S. & TOPAL, E. 2009. When will fossil fuel reserves be diminished? Energy Policy, 37, 181-189.

SHI, X. M. & CHEN, F. 2002. High-Yield Production of Lutein by the Green Microalga *Chlorella protothecoidesin* Heterotrophic Fed-Batch Culture. Biotechnology Progress, 18, 723-727.

SHURIN, J. B., ABBOTT, R. L., DEAL, M. S., KWAN, G. T., LITCHMAN, E., MCBRIDE, R. C., MANDAL, S. & SMITH, V. H. 2013. Industrial-strength ecology: trade-offs and opportunities in algal biofuel production. Ecology Letters, 16, 1393-1404.

SMIT, M., GROBLER, J., MALPERMAL, V. & MAHARAJH, D. 2017a. Sub-culture and Establishment of the Microalgae Culture Collection of South Africa, Pretoria, South Africa: CSIR Biosciences.

SMIT, M., MALPERMAL, V., GROBLER, J. & MAHARAJH, D. 2017b. Sub-culture and Consolidation of Indigenous Microalgae into the Microalgae Culture Collection of South Africa, Pretoria, South Africa: CSIR Biosciences.

SOROKIN, C. & KRAUSS, R. W. 1958. The Effects of Light Intensity on the Growth Rates of Green Algae. Plant Physiology, 33, 109.

STANSELL, G. R., GRAY, V. M. & SYM, S. D. 2012. Microalgal fatty acid composition: implications for biodiesel quality. Journal of Applied Phycology, 24, 791-801.

TALEBNIA, F., KARAKASHEV, D. & ANGELIDAKI, I. 2010. Production of bioethanol from wheat straw: an overview on pretreatment, hydrolysis and fermentation. Bioresource Technology, 101, 4744-4753.

TAMER, E., AMIN, M., OSSAMA, E., BO, M. & BENOIT, G. 2006. Biological treatment of industrial wastes in a photobioreactor. Water Science and Technology, 53, 117-125.

TASIĆ, M. B., KONSTANTINOVIĆ, B. V., LAZIĆ, M. L. & VELJKOVIĆ, V. B. 2009. The acid hydrolysis of potato tuber mash in bioethanol production. Biochemical Engineering Journal, 43, 208-211.

TJAHJONO, A. E., HAYAMA, Y., KAKIZONO, T., TERADA, Y., NISHIO, N. & NAGAI, S. 1994. Hyper-accumulation of astaxanthin in a green alga *Haematococcus pluvialis* at elevated temperatures. Biotechnology Letters, 16, 133-138.

TONG, D., HU, C., JIANG, K. & LI, Y. 2011. Cetane number prediction of biodiesel from the composition of the fatty acid methyl esters. Journal of the American Oil Chemists' Society, 88, 415-423.

TYRRELL, T. 1999. The relative influences of nitrogen and phosphorus on oceanic primary production. Nature, 400, 525.

UEMURA, N., TAKAHASHI, J. & UEDA, K. 1969. Fundamental studies on cultivation of hydrocarbon-utilizing microorganisms. 2. determination of transfer rate of n-pentane into culture medium. Journal of Fermentation Technology, 47, 220-+.

ULLMANN, F., GERHARTZ, W., YAMAMOTO, Y. S., CAMPBELL, F. T., PFEFFERKORN, R., ROUNSAVILLE, J. F. & ULLMANN, F. 1985. Ullmann's Encyclopedia of Industrial Chemistry, Weinheim, Federal Republic of Germany; Deerfield Beach, FL, USA, VCH.

VAN DER CRUYS, P. 2014. Consolidated bioprocessing – the future of second generation bioethanol production [Online]. Worpress. Available: https://paulvandecruys.wordpress.com/2014/03/19/consolidated-bioprocessing-the-future-of-second-generation-bioethanol-production/.

VAN GERPEN, J. 2009. Biodiesel: small scale production and quality requirements. Methods Mol Biol, 581, 281-90.

VERGARA-FERNÁNDEZ, A., HERNÁNDEZ, S. & REVAH, S. 2008. Phenomenological model of fungal biofilters for the abatement of hydrophobic VOCs. Biotechnology and Bioengineering, 101, 1182-1192.

VISVIKI, I. & SANTIKUL, D. 2000. The pH tolerance of Chlamydomonas applanata (*Volvocales, Chlorophyta*). Archives of Environmental Contamination and Toxicology, 38, 147-151.

WANG, B., LI, Y., WU, N. & LAN, C. Q. 2008. CO_2 bio-mitigation using microalgae. Applied Microbiology and Biotechnology, 79, 707-718.

WATANABE, M., KAWACHI, M., HIROKI, M. & KASAI, F. 2000. NIES-collection. list of strains. microalgae and protozoa. microbial culture collection. National Institute for Environmental Studies, Tsukuba, 159.

WEN, Z.-Y. & CHEN, F. 2003. Heterotrophic production of eicosapentaenoic acid by microalgae. Biotechnology Advances, 21, 273-294.

WOJTOWICZ, J. A. 2001. The carbonate system in swimming pool water. Journal of the Swimming Pool and Spa Industry, 3, 54-59.

XU, X.-Q. & BEARDALL, J. 1997. Effect of salinity on fatty acid composition of a green microalga from an antarctic hypersaline lake. Phytochemistry, 45, 655-658.

YANG, C., HUA, Q. & SHIMIZU, K. 2000. Energetics and carbon metabolism during growth of microalgal cells under photoautotrophic, mixotrophic and cyclic light-autotrophic/dark-heterotrophic conditions. Biochemical Engineering Journal, 6, 87-102.

YOU, T. & BARNETT, S. M. 2004. Effect of light quality on production of extracellular polysaccharides and growth rate of *Porphyridium cruentum*. Biochemical Engineering Journal, 19, 251-258.

ZARROUK, C. 1966. Influence de divers facteuors physiques et chimiques sur lacroissance et la photosynthese de, Geitle, *Spirulina maxima*. Ph. D. thesis, University of Paris, France.

ZHILA, N. O., KALACHEVA, G. S. & VOLOVA, T. G. 2011. Effect of salinity on the biochemical composition of the alga *Botryococcus braunii* Kütz IPPAS H-252. Journal of Applied Phycology, 23, 47-52.

ZITTELLI, G. C., BIONDI, N., RODOLFI, L. & TREDICI, M. R. 2013. Photobioreactors for mass production of microalgae. Handbook of microalgal culture: Applied Phycology and Biotechnology, 2, 225-266.

Appendix A

Chapter 3 data

Isolate micrographs

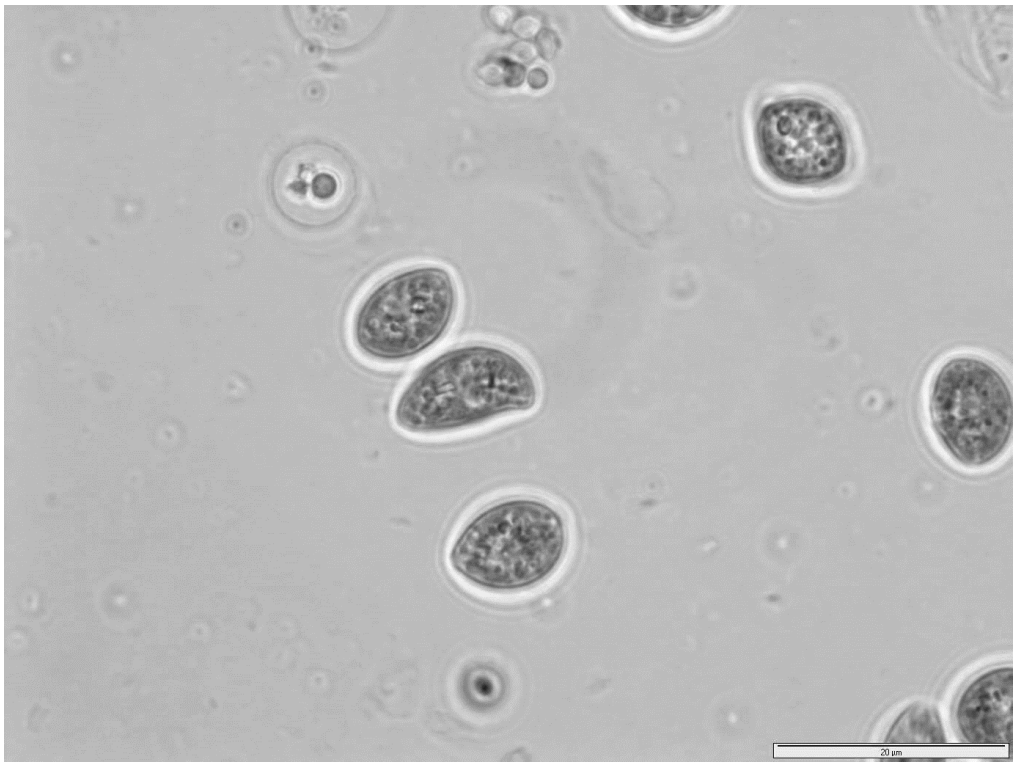


Figure A41: FSA 5.1 microscopic image at x100 magnification.

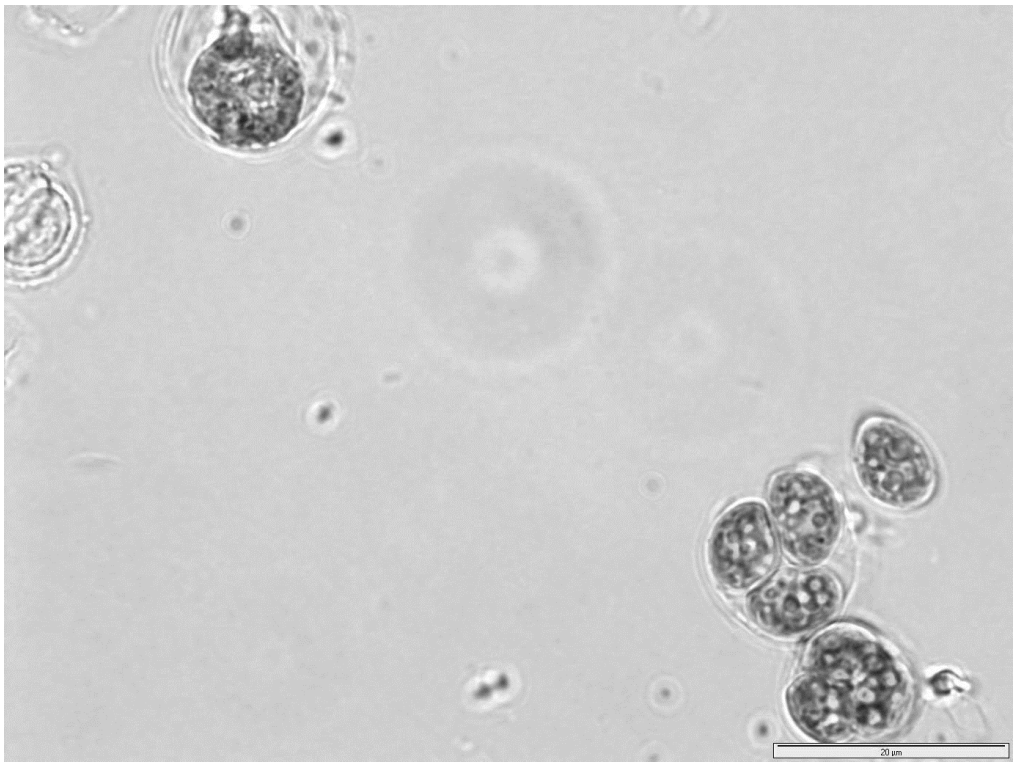


Figure A42: FSB 11.1 microscopic image at x100 magnification.

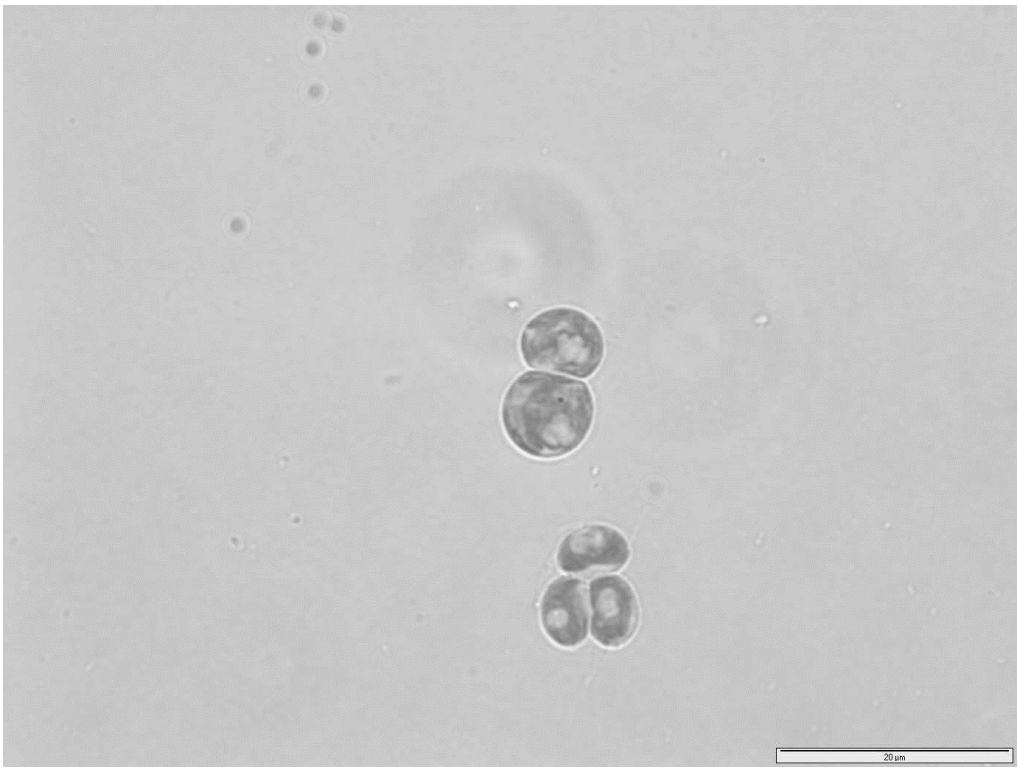


Figure A43: FSB 41.2 microscopic image at x100 magnification.

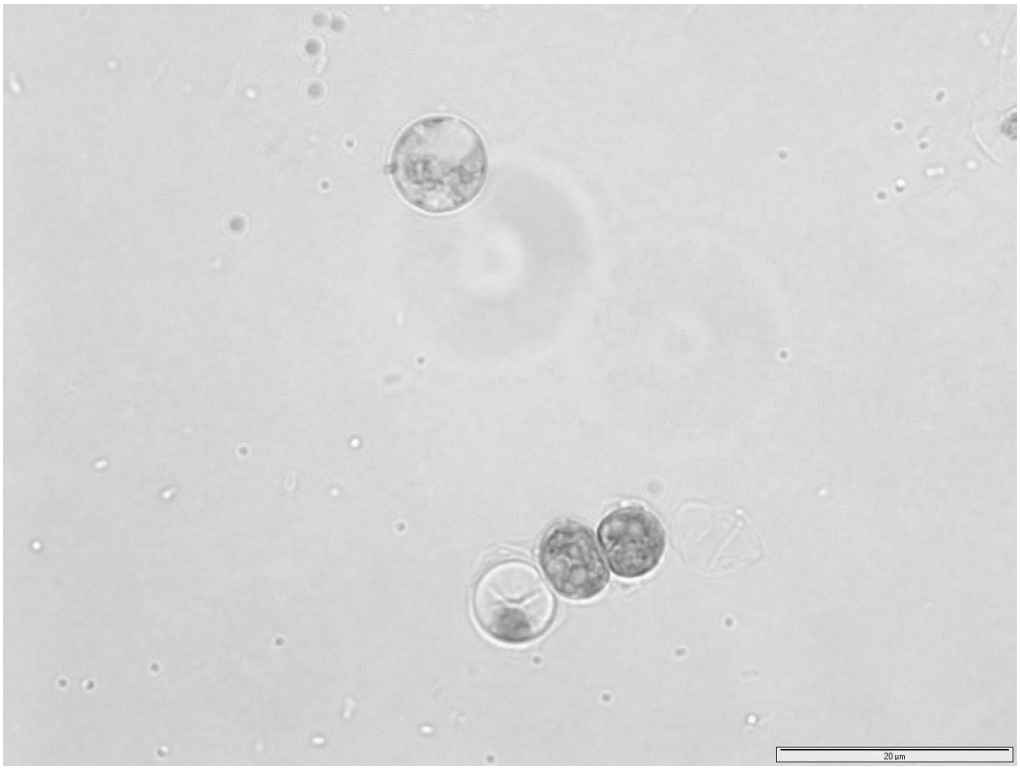


Figure A44: FSB 51.2 microscopic image at x100 magnification.

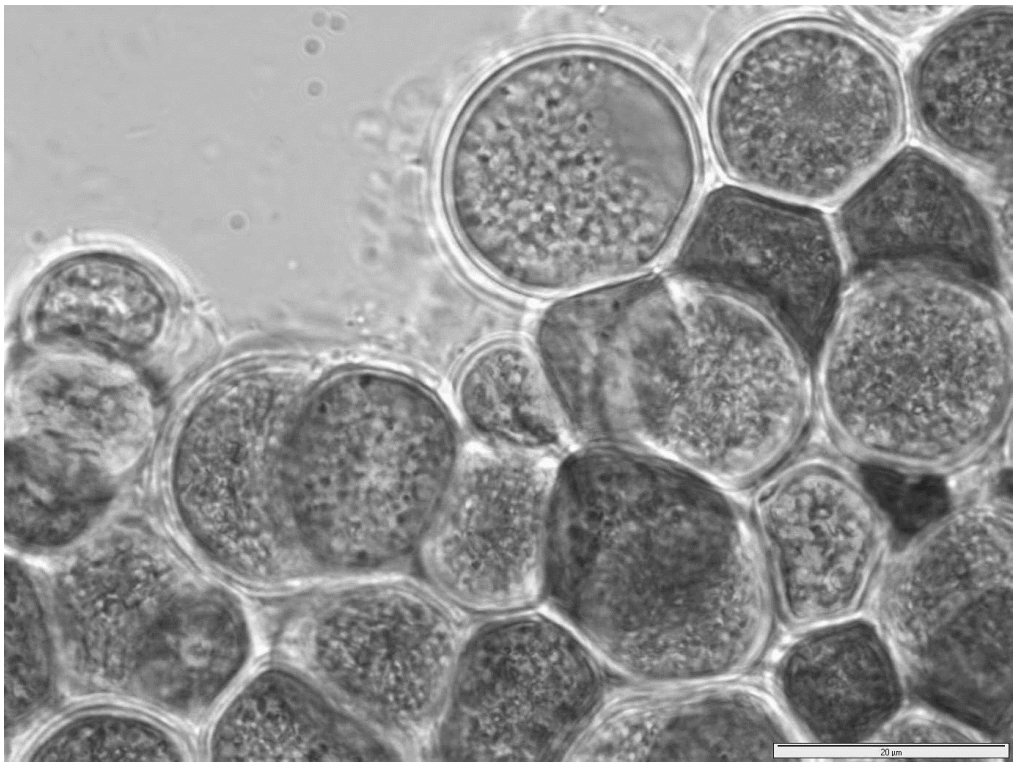


Figure A45: LPB 5.1 microscopic image at x100 magnification.

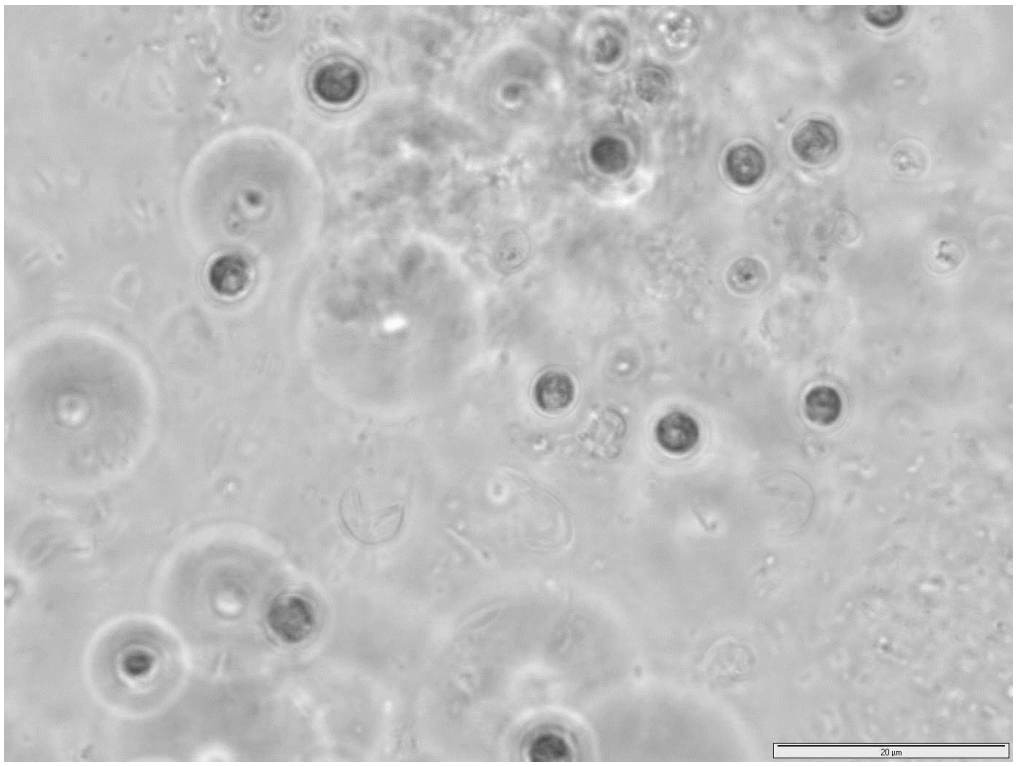


Figure A46: LPB 12.1 microscopic image at x100 magnification.



Figure A47: LPB 15.1 microscopic image at x100 magnification.

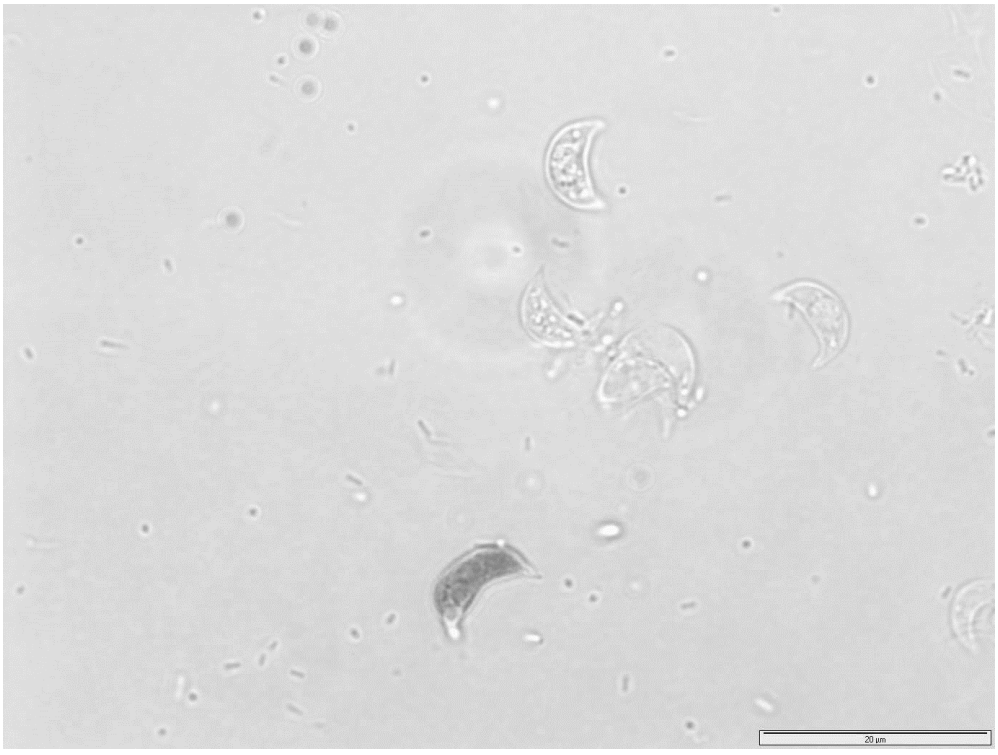


Figure A48: NWA 1.1 microscopic image at x100 magnification

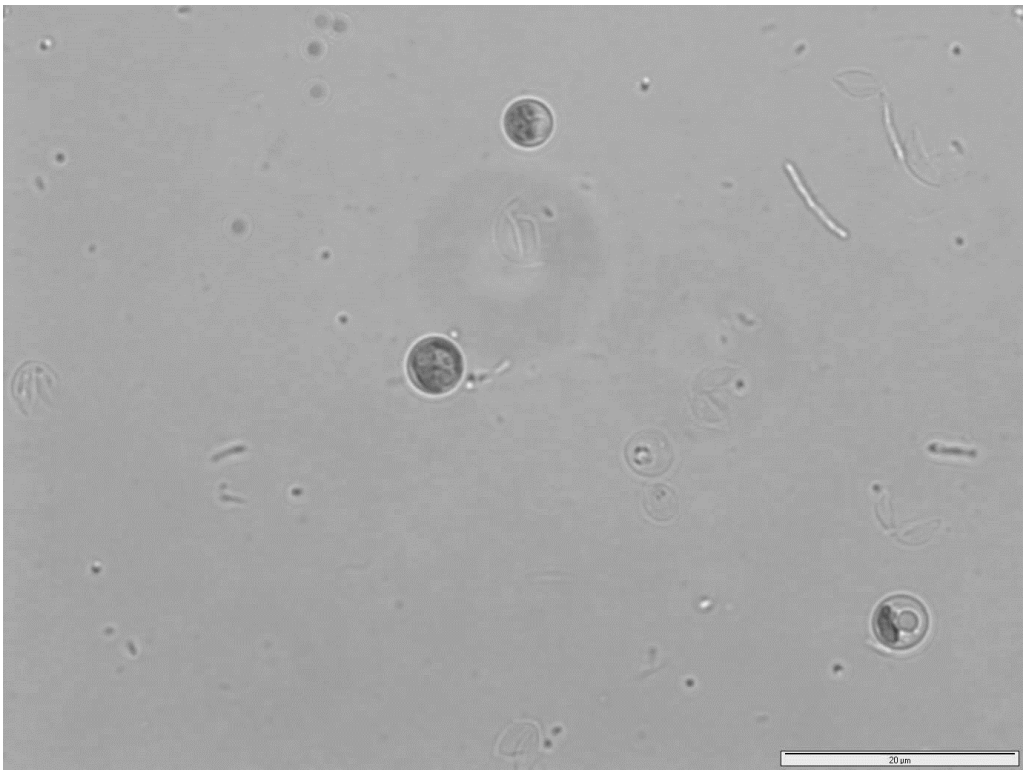


Figure A49: NWA 9.1 microscopic image at x100 magnification

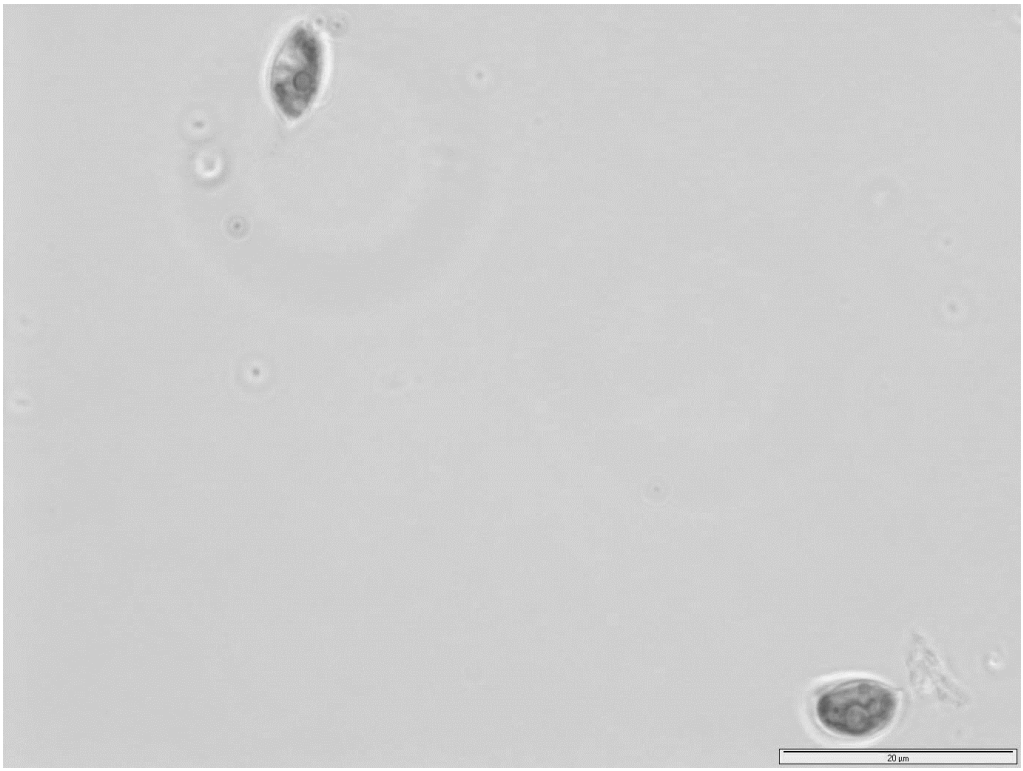


Figure A50: NWA 11.1 microscopic image at x100 magnification

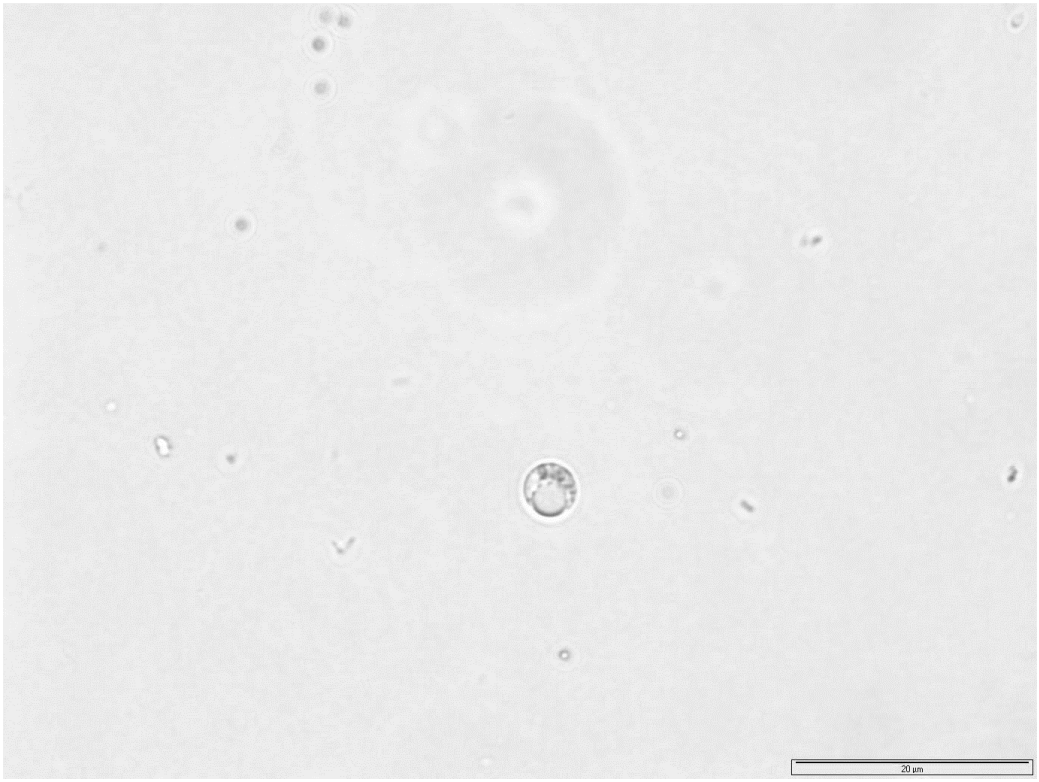


Figure A51: WCA 10.1 microscopic image at x100 magnification

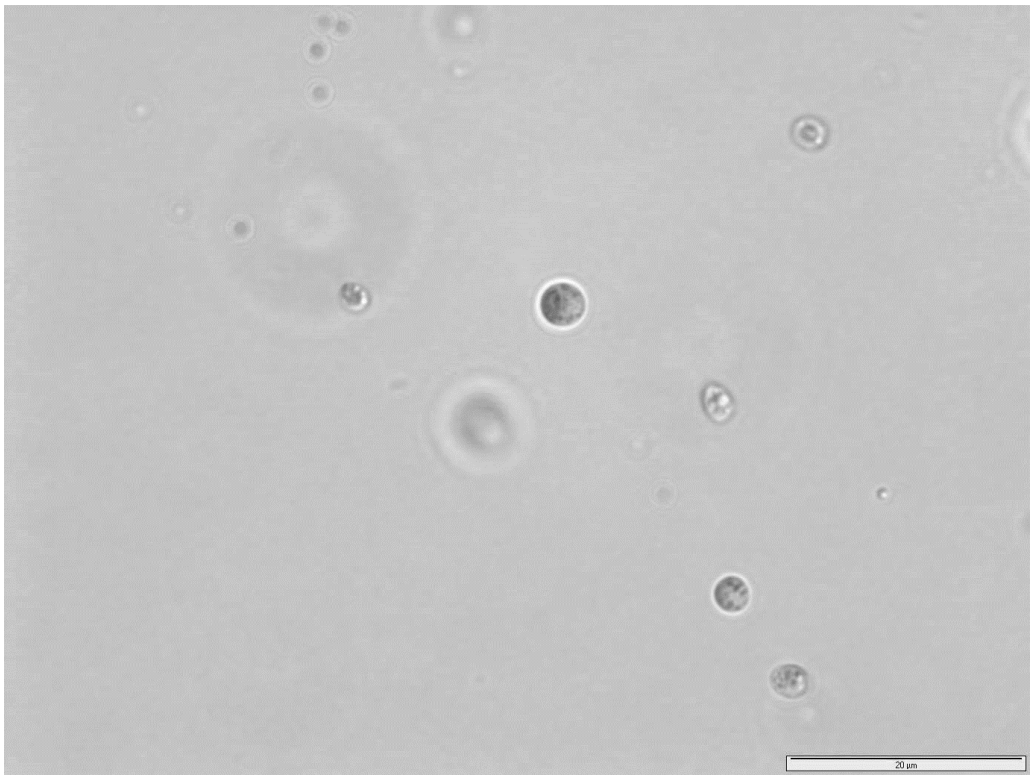


Figure A52: WCA 4.1 microscopic image at x100 magnification.

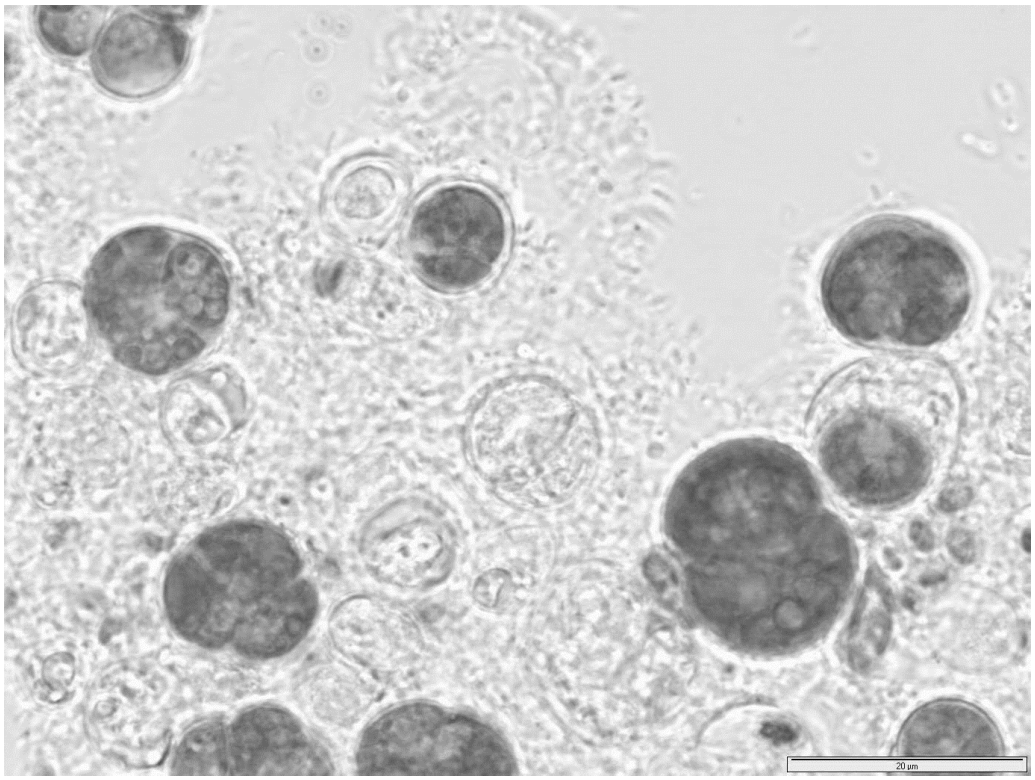


Figure A53: WCB 4.1 microscopic image at x100 magnification.

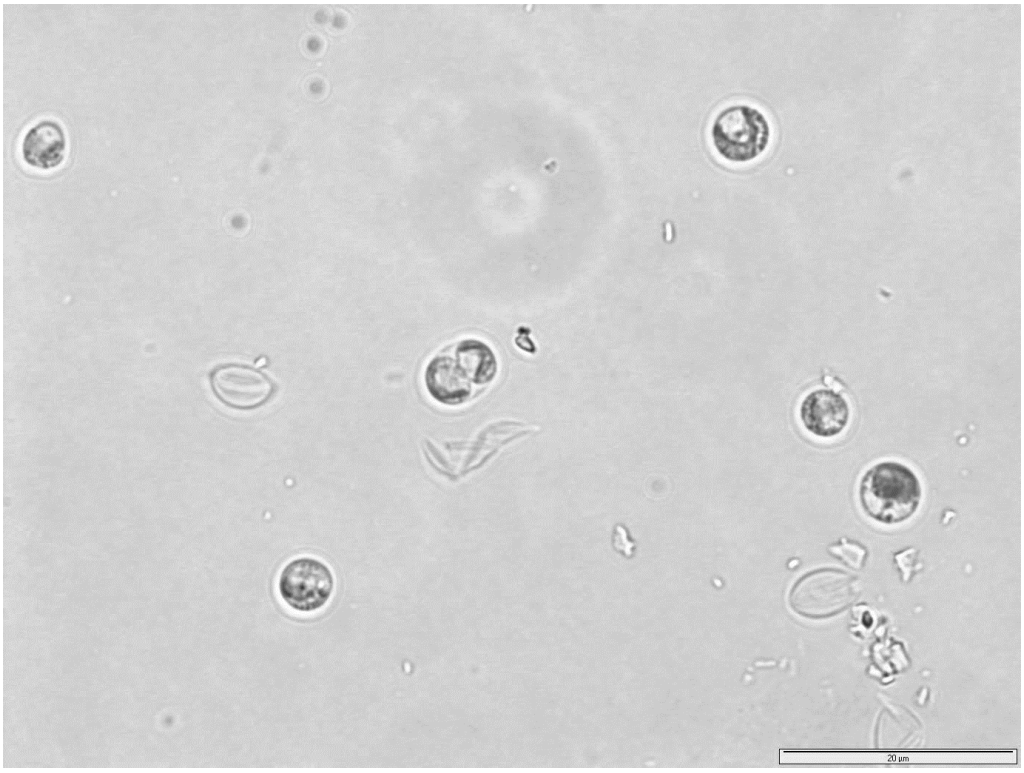


Figure A54: WCB 7.3 microscopic image at x100 magnification

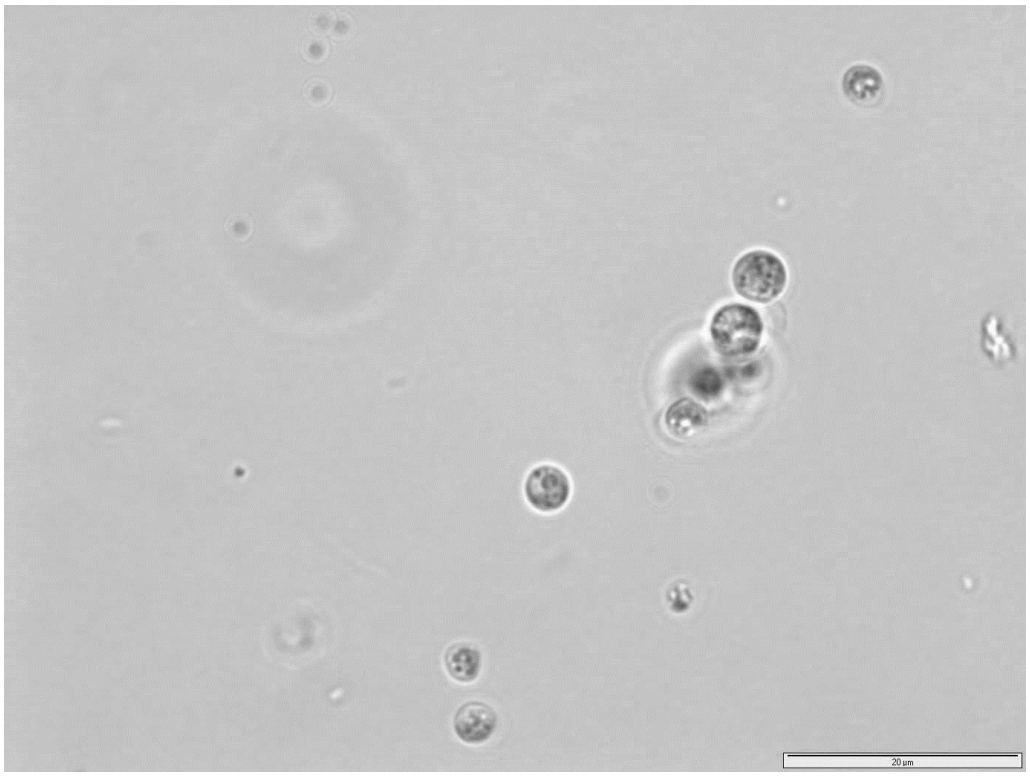


Figure A55: WCC 2.1 microscopic image at x100 magnification

Genetic sequencing

Table A1: Primer pairs for amplification protocols as used by Durand *et al.*, (2016).

Table 1: Primer pairs for amplification protocols. Genetic region	Forward primer (name and sequence)	Reverse primer (name and sequence)
18S (set 1)	P2-TGGTTGATTCTGCCAGT	P4-TGATCCTTCYGCAGGTTCAC
18S (set 2)	A-AACCTGGTTGATCCTGCCAGT	ITS055R-CTCCTTGGTCCGTGTTTCAAGACGGG
18S (set 3)	AB1-GAGGATTAGGGTCCGATTCC	TW4-CTTCCGTCAATTCCTTTAAG
18S (set 4)	18A-CTACTGGCAGGATCAACCA	18L-CACCTACGGAAACCTTGTTACGACTT
18S (set 5)	SR1-TACCTGGTTGATCCTGCCAG	SR12-CCTTCCGCAGGTTCACCTAC
tuf	TGAAACAGAAMAWCGTCATTATGC	CCTTCNCGAATMGCRAAWCGC
cox1	TGGTCTGGTGTWATWGCTAC	TCACCWCCACCWGCWGGC
rbcL	GCATATGTTGCTTATCCTCTT	ATCACCACCAGAAAGACGAAG

BLAST data as obtained by Doctor Durand and his team

Isolate FSA5.1 - gi|664686838|gb|KF673377.

Genbank description: Raphidocelis contorta strain SAG 11.81 18S ribosomal RNA gene, complete sequence. Sequence length 730; sequence identity 704; E value 0.0.

Isolate FSB11.1 - gi|359385272|emb|FR865687.1

Genbank description: Graesiella emersonii genomic DNA containing 18S rRNA gene, ITS1, 5.8S rRNA gene, ITS2, 28S rRNA gene, culture collection CCAP 211/8P. Sequence length 733; sequence identity 717; E value 0.0.

Isolate FSB41.2 - gi|1111664109|gb|KY303731.1

Genbank description: Chlorella sorokiniana voucher BR001 small subunit ribosomal RNA gene, partial sequence. Sequence length 736; sequence identity 729; E value 0.0.

Isolate FSB51.2 - gi|387912510|dbj|AB721066.1

Three different equally significant hits were obtained for the 18S data. There were organisms Raphidocelis rotunda strain SAG 31.88; Raphidocelis contorta strain SAG 11.81; Ourococcus multisporus strain LUCC 007. For each the alignment length was 420 with sequence identity of 372 and E value of -160. This organism is therefore listed as unknown chlorophyte.

Isolate LPB12.1 - gi|442571929|gb|JQ315506.1 and gi|359385151|emb|FR865562.1

Two equally likely hits were returned. The data for rbcL also provided equally likely hits.

1. Genbank description: Lobochlamys segnis strain KMMCC 1045 18S ribosomal RNA gene, partial sequence. Sequence length 1034; sequence identity 1017; E value 0.0.

2. Genbank description: Chlamydomonas sp. CCAP 11/168 genomic DNA containing 18S rRNA gene, ITS1, 5.8S rRNA gene, ITS2, 28S rRNA gene, culture collection CCAP 11/168. Sequence length 729; sequence identity 728; E value 0.0.

Isolate LPB5.1 - gi|844315789|gb|KM514870.1 and gi|760173399|gb|KP271969.1

Two equally likely hits were returned. The data for rbcL also provided equally likely hits.

1. Genbank description: Heterochlorella luteoviridis isolate 1_3 ribulose-1,5-bisphosphate carboxylase/oxygenase large subunit (rbcL) gene, partial cds; plastid. Sequence length 1040; sequence identity 959; E value 0.0.

2. Genbank description: Chlorella variabilis isolate NC64A chloroplast, complete genome. Sequence length 1000; sequence identity 934; E value 0.0.

Isolate NWA1.1* - gi|1111664109|gb|KY303731.1

Genbank description: Chlorella sorokiniana voucher BR001 small subunit ribosomal RNA gene, partial sequence. Sequence length 736; sequence identity 734; E value 0.0.

Isolate NWA11.1 - gi|442572188|gb|JQ315765.1

Genbank description: Lobochlamys segnis strain KMMCC 52 18S ribosomal RNA gene, internal transcribed spacer 1, 5.8S ribosomal RNA gene, internal transcribed spacer 2, and 28S ribosomal RNA gene, region. Sequence length 991; sequence identity 967; E value 0.0.

Isolate NWA4.1 - gi|442572006|gb|JQ315583.1 and gi|1049566973|gb|KU900221.1

Two equally likely hits were returned. The data for rbcL also provided equally likely hits.

1. Genbank description is listed as both (a) Scenedesmus sp. KMMCC 343 18S ribosomal RNA gene, partial sequence. Sequence length 370; sequence identity 339; E value -153 or (b) Tetradesmus obliquus strain CCAP 276/3A 18S ribosomal RNA gene, partial sequence. Sequence length 365; sequence identity 336, E value -153.

2. Genbank description: Parachlorella kessleri strain TY02 18S ribosomal RNA gene, partial sequence. Sequence length 734; sequence identity 607. E value 0.0.

Isolate NWA9.1 - gi|442572188|gb|JQ315765.1 and gi|844315849|gb|KM514900.1

Two equally likely hits were returned. The data for rbcL also provided equally likely hits.

1. Genbank description: Lobochlamys segnis strain KMMCC 52 18S ribosomal RNA gene, internal transcribed spacer 1, 5.8S ribosomal RNA gene, internal transcribed spacer 2, and 28S ribosomal RNA gene, region. Sequence length 731; sequence identity 729; E value 0.0.9

2. Chlorella pyrenoidosa isolate 5_5 ribulose-1,5-bisphosphate carboxylase/oxygenase large subunit (rbcL) gene, partial cds; plastid. Sequence length 1050; sequence identity 996. E value 0.0.

Isolate WCA4.1 - : gi|1111664109|gb|KY303731.1

Genbank description: Chlorella sorokiniana voucher BR001 small subunit ribosomal RNA gene, partial sequence. Sequence length 732; sequence identity 730; E value 0.0.

Isolate WCB4.1 - gi|338857494|gb|HQ246355.1 and gi|1092175645|dbj|LC192133.1

Two equally likely hits were returned. The data for rbcL also provided equally likely hits.

1. Genbank description: Scenedesmus bajacalifornicus strain ZA1-7 18S ribosomal RNA gene, partial sequence. Sequence length 1028; sequence identity 1003. E value 0.0.

2. Tetradesmus acuminatus gene for 18S ribosomal RNA, partial sequence, strain: NIES-92. Sequence length 1091; sequence identity 1052; E value 0.0.

Isolate WCC2.1 - gi|1111664109|gb|KY303731.1,

Genbank description: Chlorella sorokiniana voucher BR001 small subunit ribosomal RNA gene, partial sequence. Sequence length 721; sequence identity 720; E value 0.0.

Isolate WCA10.1 - gi|229915563|gb|FJ968741.1

Genbank decription: Parachlorella kessleri culture-collection SAG:211-11g chloroplast, complete genome. Sequence length 1052; sequence identity 1031; E value 0.0.

Isolate WCB7.3 - gi|229915563|gb|FJ968741.1

Organism identification is based solely on rbcL data. Sequence data for 18S are available; however, the region comprising an unambiguous clean read was only 34bp. Identification is therefore based on rbcL data.

Genbank description: Parachlorella kessleri culture-collection SAG:211-11g chloroplast, complete genome. Sequence length 1041; sequence identity 1026; E value 0.0.

Isolate LPB15.1 - gi|442572188|gb|JQ315765.1

Genbank description: Lobochlamys segnis strain KMMCC 52 18S ribosomal RNA gene, internal transcribed spacer 1, 5.8S ribosomal RNA gene, internal transcribed spacer 2,

and 28S ribosomal RNA gene, region. Sequence length 728; sequence identity 725. E value 0.0.10

Phylogenetic analyses

To examine the relationships between isolates and the results of the BLASTn queries more closely a combined phylogram was generated (Figure 1 – attached as a pdf image). The phylogram includes the culture isolates, the BLASTn query results and a previously published reference set of chlorophytes (Laeliart et al, 2012). The findings corroborate and support the combined morphological and BLASTn results described above, however, there are a few noteworthy points. Isolates NWA1.1 and NWA1.2 appear to be a Chlorella sorokiniana strain and a Lobochlamys segnis strain, respectively. This appears to be the case even if the morphology is not typical.

In some instances the BLASTn results resulted in two equally likely possibilities. The phylogenetic data suggested more definitive identities. For isolate LPB12.1 the identity is a Lobochlamy segnis strain. Isolate LPB5.1 is Chlorella variabilis, isolate NWA4.1 is Tetradesmus obliquus, isolate NWA9.1 is Chlorella pyrenoidosa, isolate WCB4.1 is Tetradesmus accuminata, and isolate LPA1.1 is Chlorella sorokiniana.

Isolate FSB51.2 remains problematic. The BLASTn results as well as the phylogenetic tree failed to suggest an identification with any certainty. This organism may be a genetically distant organism or an as yet uncharacterized chlorophyte.

Figure 1 (see attachment): Genetic distance phylogram of isolates.

The phylogram includes the 20 isolates described here and a reference set of chlorophytes obtained from (Leliaert et al, 2012). Isolates are entered as their unique identification numbers. Bootstrap values for nodes that lead to isolates are given in red.

OD/DCW correlation

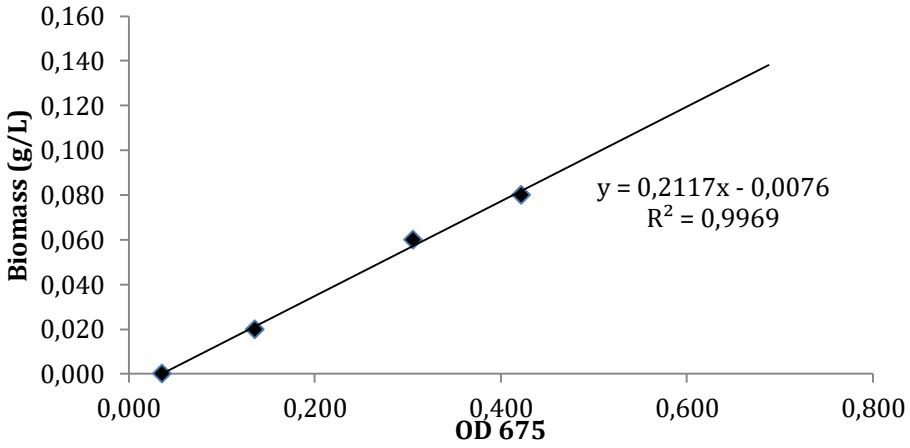


Figure A56: The DCW/OD correlation curve for microalgal isolate "FSA 5.1". The linear trend line of best fit is included. The formula of the trend line can be used to directly convert OD 675 values to biomass (g/L) values.

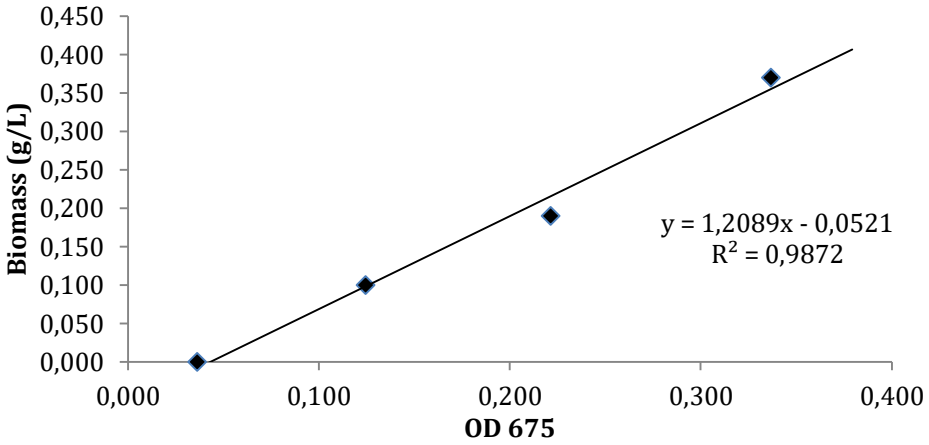


Figure A57: The DCW/OD correlation curve for microalgal isolate FSB 11.1. The linear trend line of best fit is included. The formula of the trend line can be used to directly convert OD 675 values to biomass (g/L) values.

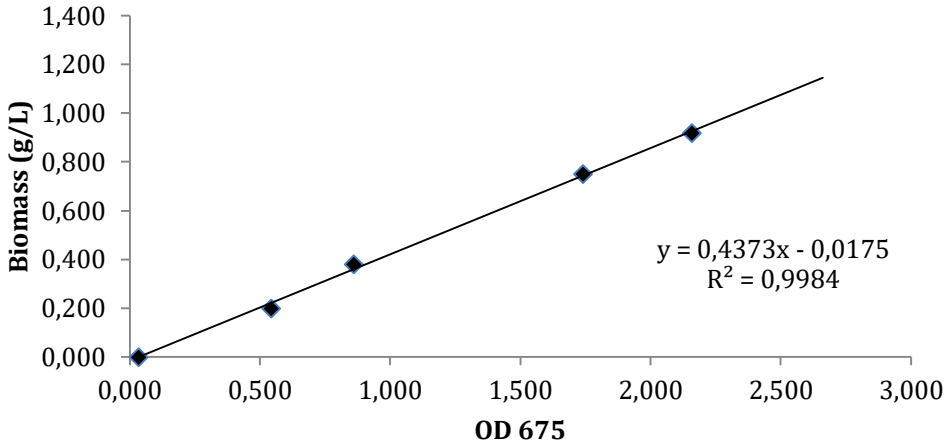


Figure A58: The DCW/OD correlation curve for microalgal isolate FSB 41.2. The linear trend line of best fit is included. The formula of the trend line can be used to directly convert OD 675 values to biomass (g/L) values.

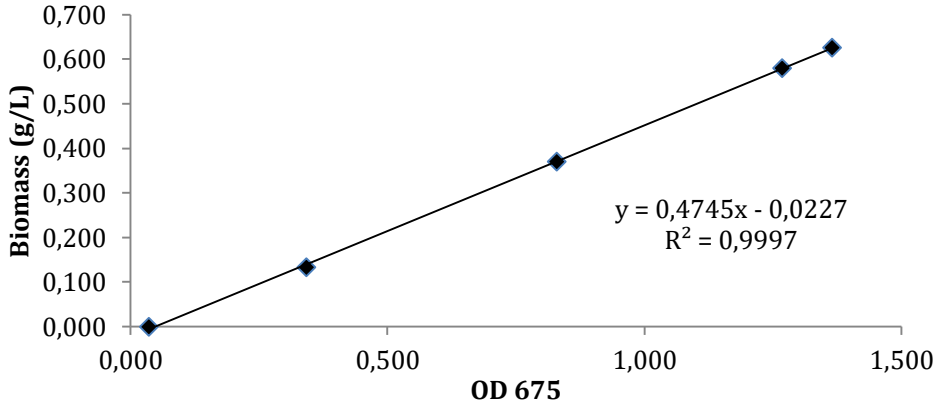


Figure A59: The DCW/OD correlation curve for microalgal isolate FSB 51.2. The linear trend line of best fit is included. The formula of the trend line can be used to directly convert OD 675 values to biomass (g/L) values.

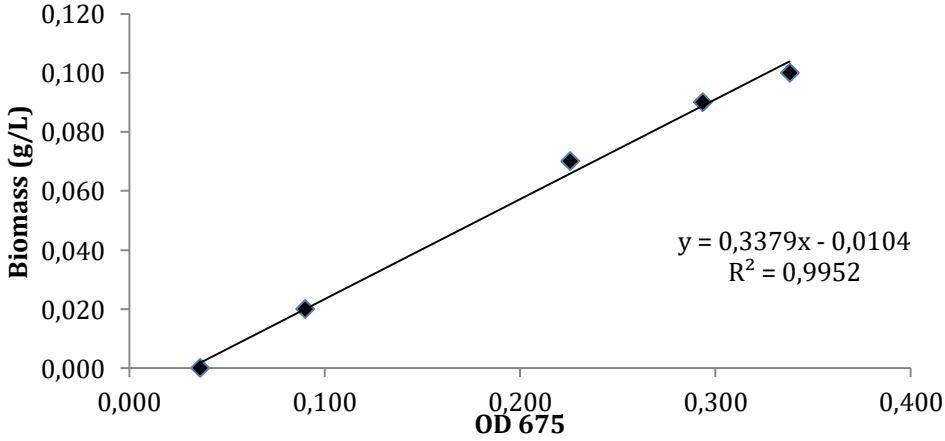


Figure A60: The DCW/OD correlation curve for microalgal isolate LPB 5.1. The linear trend line of best fit is included. The formula of the trend line can be used to directly convert OD 675 values to biomass (g/L) values.

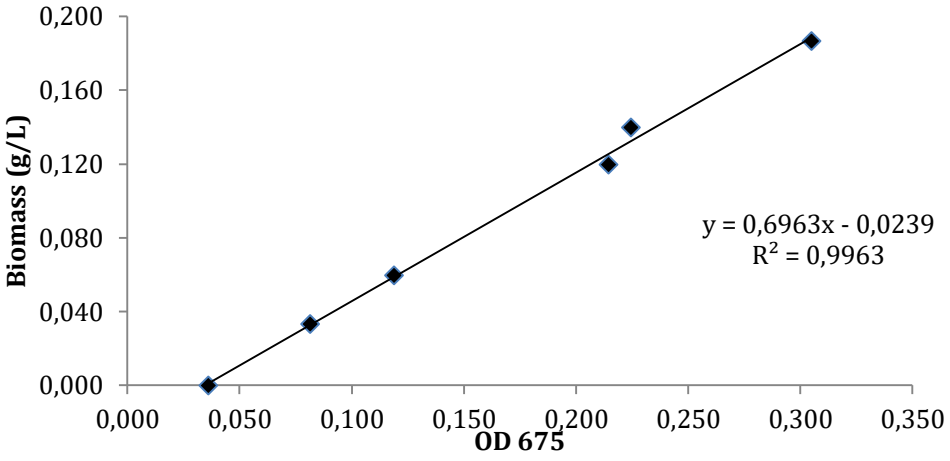


Figure A61: The DCW/OD correlation curve for microalgal isolate LPB 12.1. The linear trend line of best fit is included. The formula of the trend line can be used to directly convert OD 675 values to biomass (g/L) values.

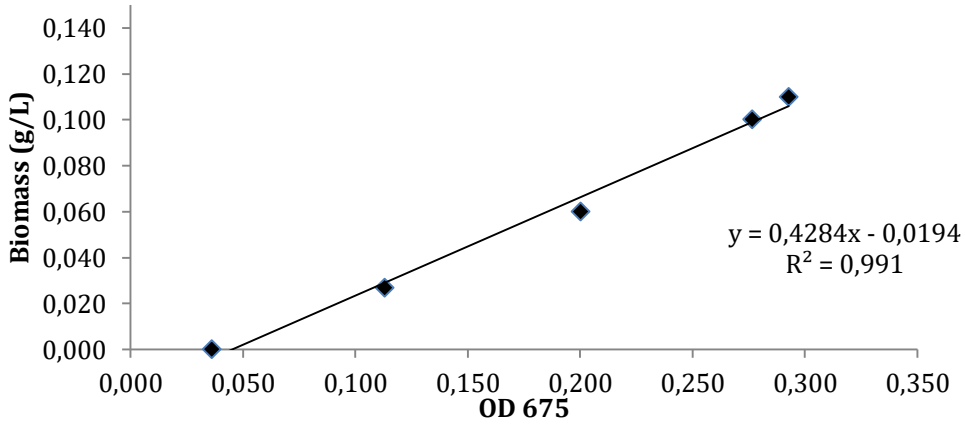


Figure A62: The DCW/OD correlation curve for microalgal isolate LPB 15.1. The linear trend line of best fit is included. The formula of the trend line can be used to directly convert OD 675 values to biomass (g/L) values.

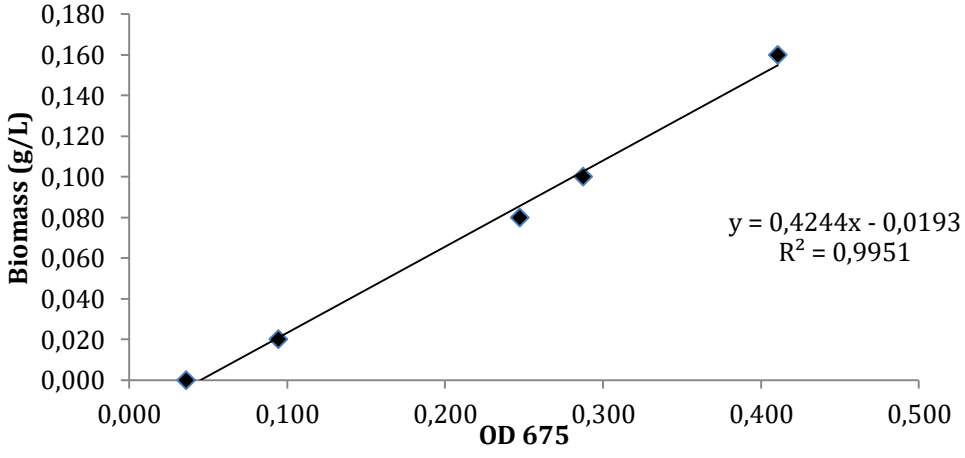


Figure A63: The DCW/OD correlation curve for microalgal isolate NWA 1.1. The linear trend line of best fit is included. The formula of the trend line can be used to directly convert OD 675 values to biomass (g/L) values.

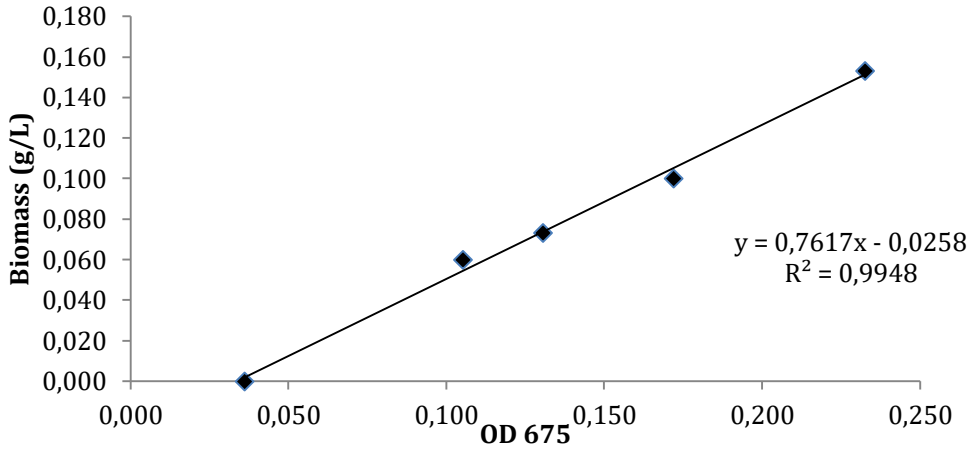


Figure A64: The DCW/OD correlation curve for microalgal isolate NWA 9.1. The linear trend line of best fit is included. The formula of the trend line can be used to directly convert OD 675 values to biomass (g/L) values.

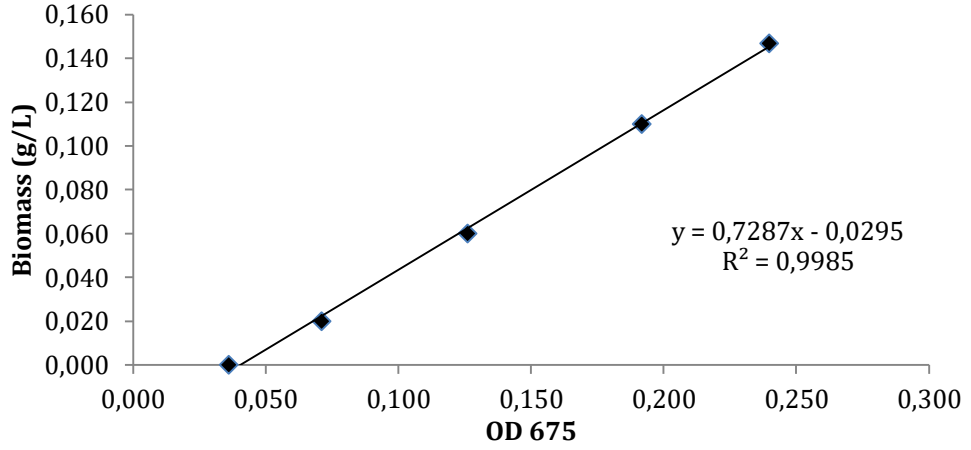


Figure A65: The DCW/OD correlation curve for microalgal isolate NWA 11.1. The linear trend line of best fit is included. The formula of the trend line can be used to directly convert OD 675 values to biomass (g/L) values.

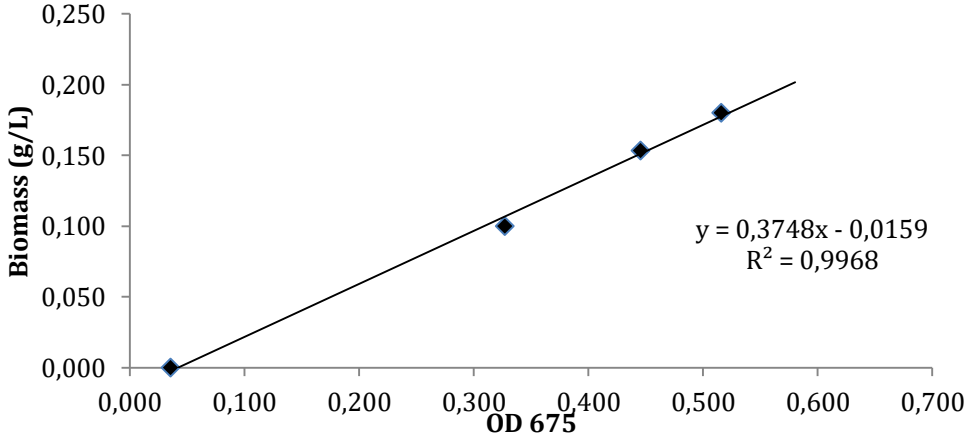


Figure A66: The DCW/OD correlation curve for microalgal isolate WCA 4.1. The linear trend line of best fit is included. The formula of the trend line can be used to directly convert OD 675 values to biomass (g/L) values.

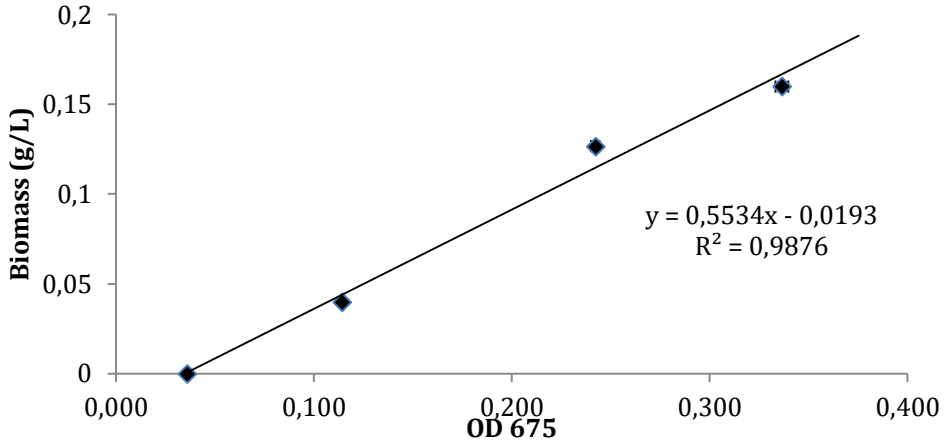


Figure A67: The DCW/OD correlation curve for microalgal isolate WCA 10.1. The linear trend line of best fit is included. The formula of the trend line can be used to directly convert OD 675 values to biomass (g/L) values.

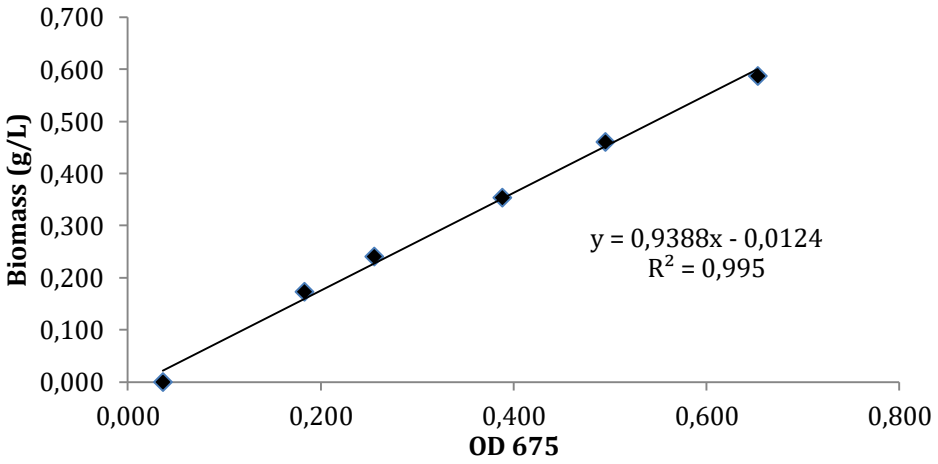


Figure A68: The DCW/OD correlation curve for microalgal isolate WCB 4.1. The linear trend line of best fit is included. The formula of the trend line can be used to directly convert OD 675 values to biomass (g/L) values.

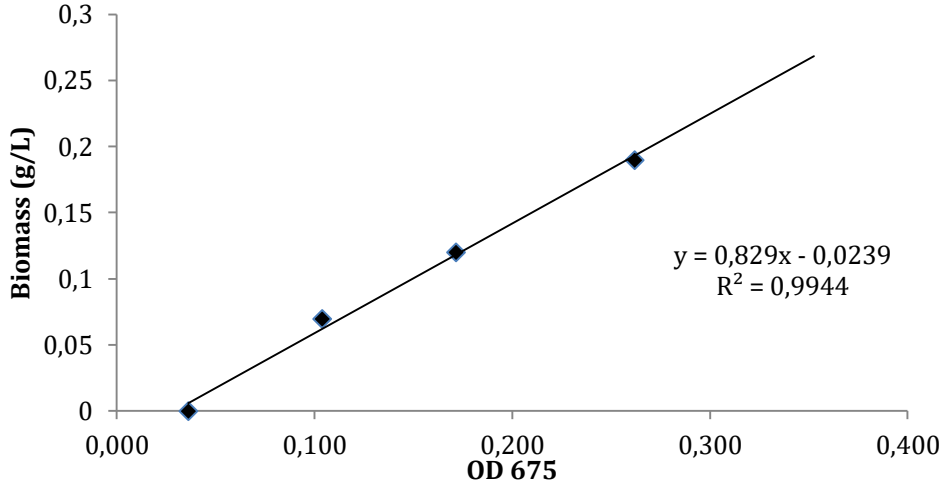


Figure A69: The DCW/OD correlation curve for microalgal isolate WCB 7.3. The linear trend line of best fit is included. The formula of the trend line can be used to directly convert OD 675 values to biomass (g/L) values.

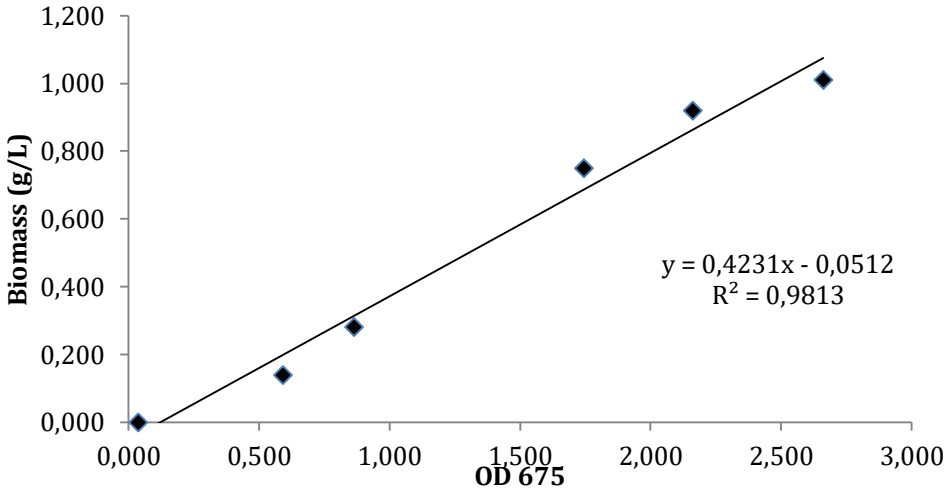


Figure A70: The DCW/OD correlation curve for microalgal isolate WCC 2.1. The linear trend line of best fit is included. The formula of the trend line can be used to directly convert OD 675 values to biomass (g/L) values.

Table A2: Formulas derived from the OD/DCW correlation curves for estimation of a biomass value (y) from an OD reading (x).

Organism designation	Linear trend line equation
FSA 5.1	y = 2.117x - 0.0076
FSB 11.1	y = 1.2089x - 0.0521
FSB 41.2	y = 0.4373x - 0.0175
FSB 51.2	y = 0.4745x - 0.0227
LPB 5.1	y = 0.3379x - 0.0104
LPB 12.1	y = 0.6963x - 0.0239
LPB 15.1	y = 0.4284x - 0.0194
NWA 1.1	y = 0.4244x - 0.0193
NWA 9.1	y = 0.7617x - 0.0258
NWA 11.1	y = 0.7287x - 0.0295
WCA 4.1	y = 0.3748x - 0.0159
WCA 10.1	y = 0.5534x - 0.0193
WCB 4.1	y = 0.9388x - 0.0124
WCB 7.3	y = 0.8290x - 0.0239
WCC 2.1	y = 0.4231x - 0.0512

Growth curves for fifteen isolates

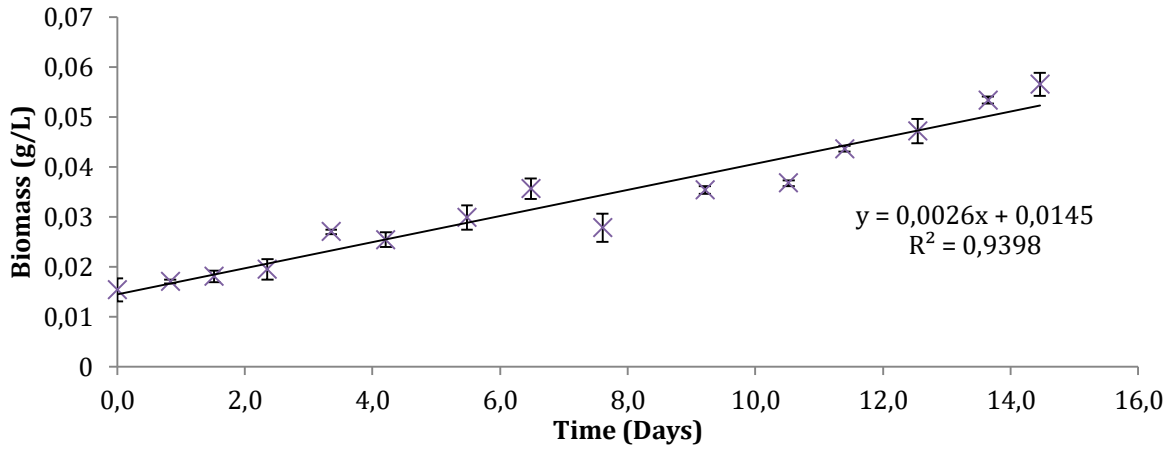


Figure A71: Biomass generation of FSA 5.1 over 15 days cultivated in AF6 media. The trend line indicates the average growth in biomass of FSA 5.1 over the 15 days. The slope of the trend line indicates the average specific biomass productivity of FSA 5.1 in units of g/L/day.

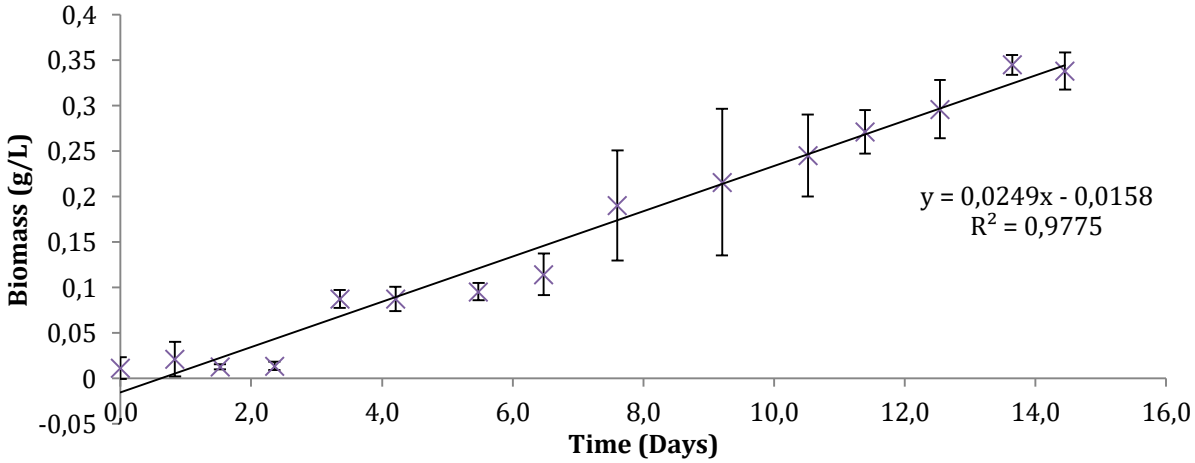


Figure A72: Biomass generation of FSB 11.1 over 15 days cultivated in AF6 media. The trend line indicates the average growth in biomass over the 15 days. The slope of the trend line indicates the average specific biomass productivity in units of g/L/day.

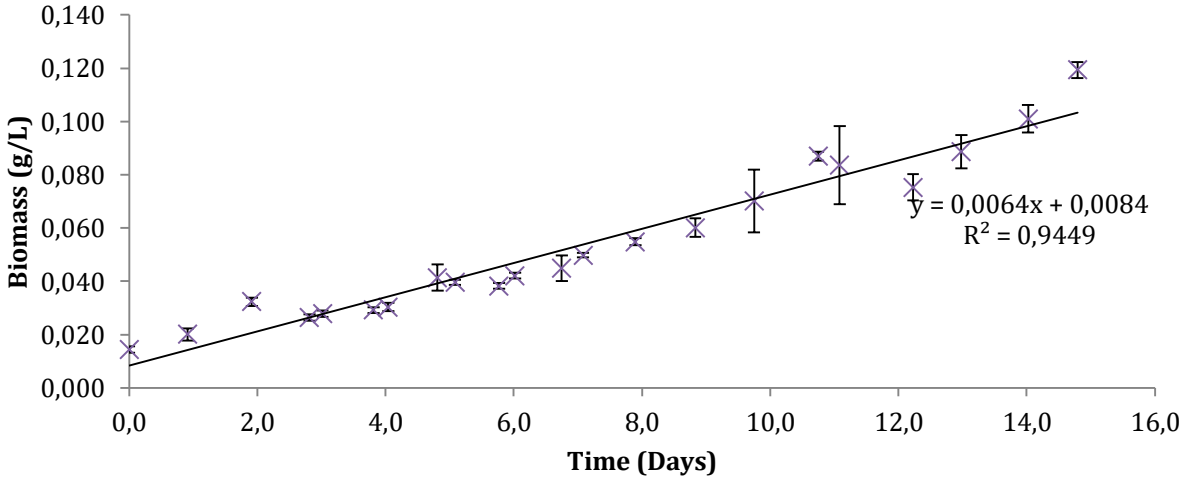


Figure A73: Biomass generation of FSB 41.2over 15 days, cultivated in AF6 media. The trend line indicates the average growth in biomass over the 15 days. The slope of the trend line indicates the average specific biomass productivity in units of g/L/day.

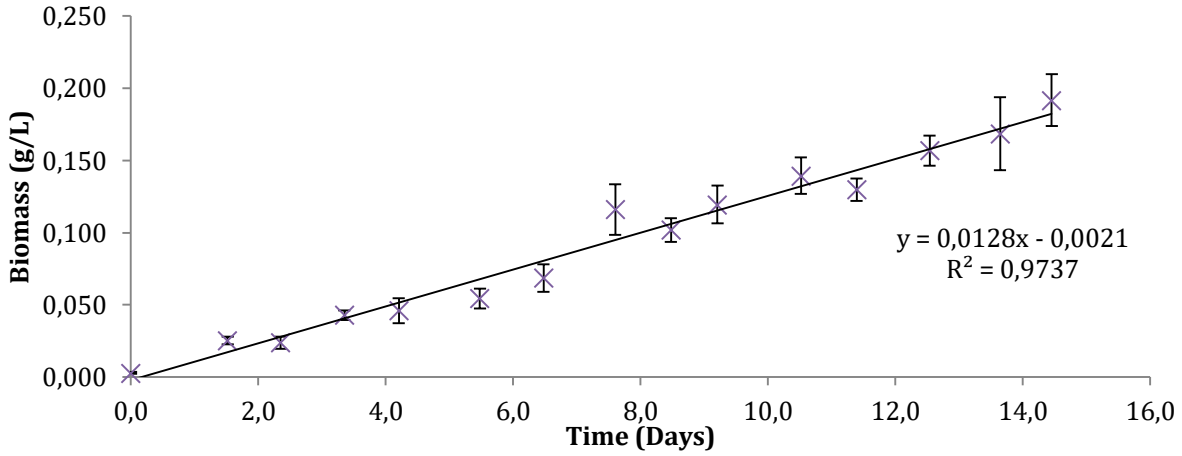


Figure A74: Biomass generation of FSB 51.2 over 15 days, cultivated in AF6 media. The trend line indicates the average growth in biomass over the 15 days. The slope of the trend line indicates the average specific biomass productivity in units of g/L/day.

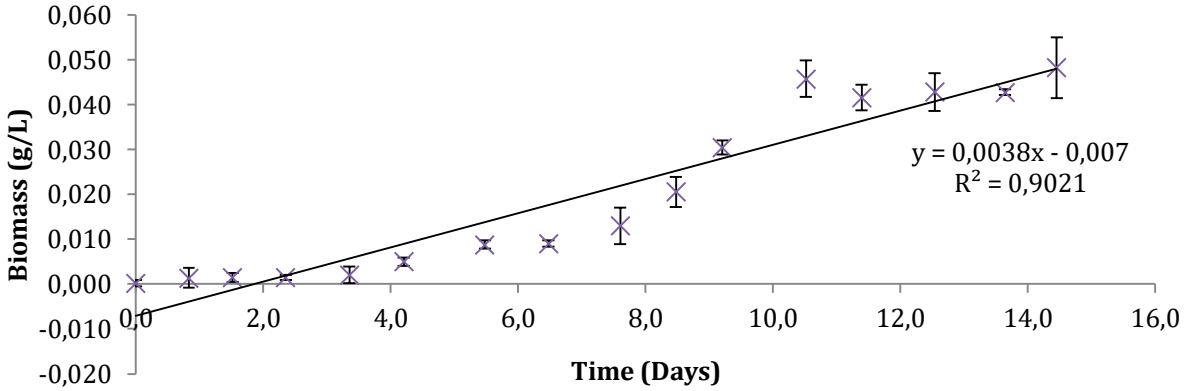


Figure A75: Biomass generation of LPB 5.1 over 15 days, cultivated in AF6 media. The trend line indicates the average growth in biomass over the 15 days. The slope of the trend line indicates the average specific biomass productivity in units of g/L/day.

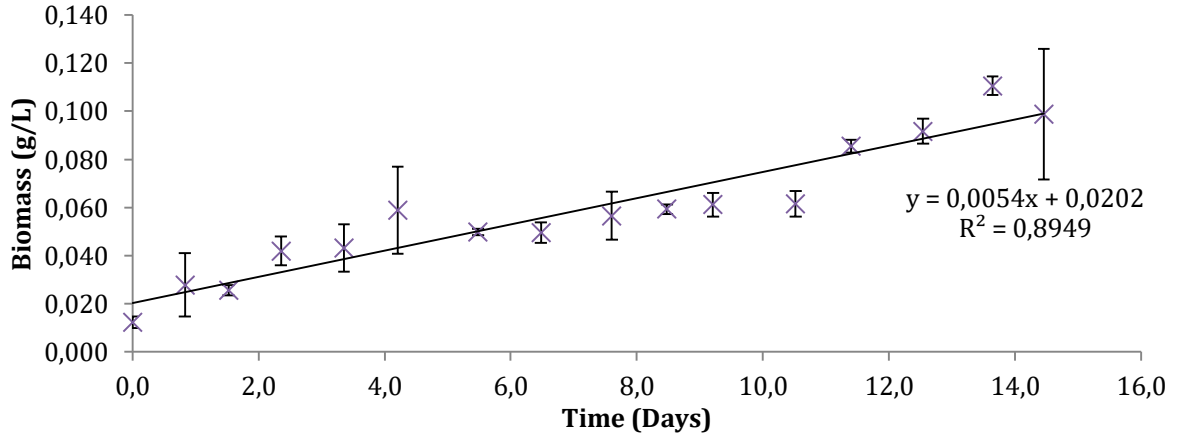


Figure A76: Biomass generation of LPB 12.1 over 15 days, cultivated in AF6 media. The trend line indicates the average growth in biomass over the 15 days. The slope of the trend line indicates the average specific biomass productivity in units of g/L/day.

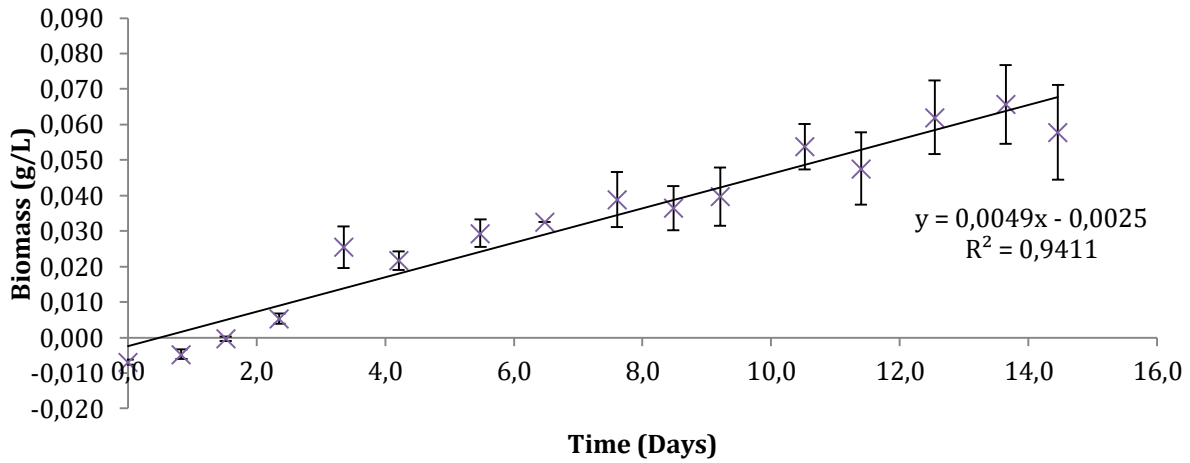


Figure A77: Biomass generation of LPB 15.1 over 15 days, cultivated in AF6 media. The trend line indicates the average growth in biomass over the 15 days. The slope of the trend line indicates the average specific biomass productivity in units of g/L/day.

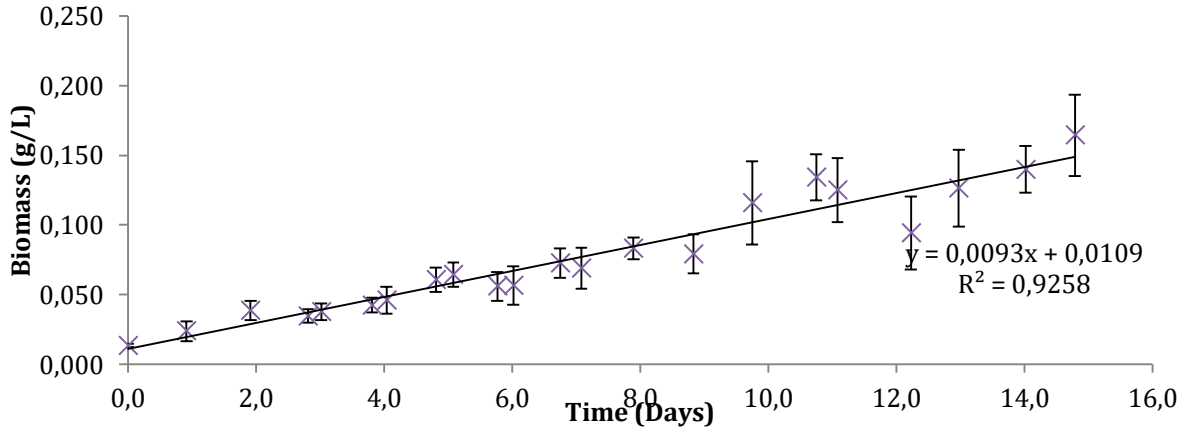


Figure A78: Biomass generation of NWA 1.1 over 15 days, cultivated in AF6 media. The trend line indicates the average growth in biomass over the 15 days. The slope of the trend line indicates the average specific biomass productivity in units of g/L/day.

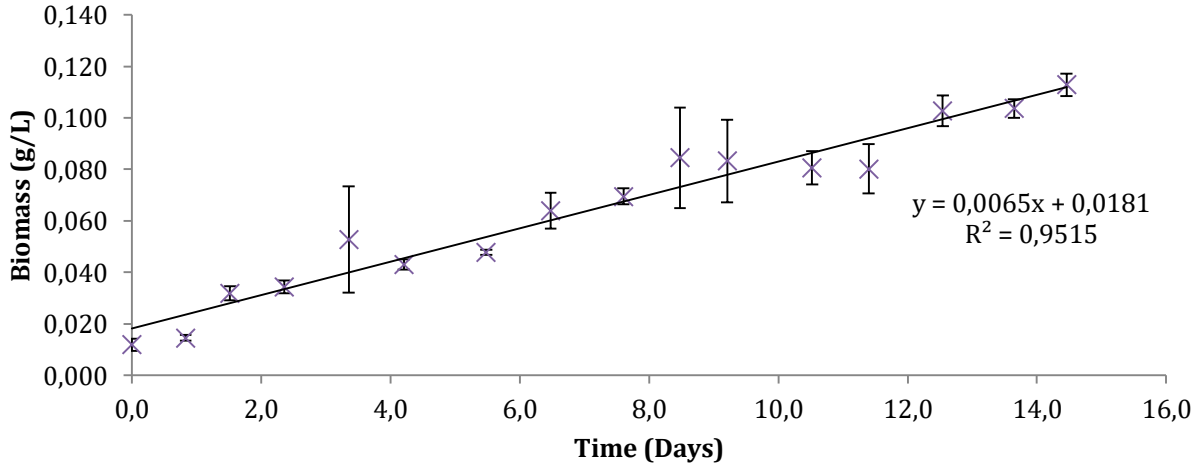


Figure A79: Biomass generation of NWA 9.1 over 15 days, cultivated in AF6 media. The trend line indicates the average growth in biomass over the 15 days. The slope of the trend line indicates the average specific biomass productivity in units of g/L/day.

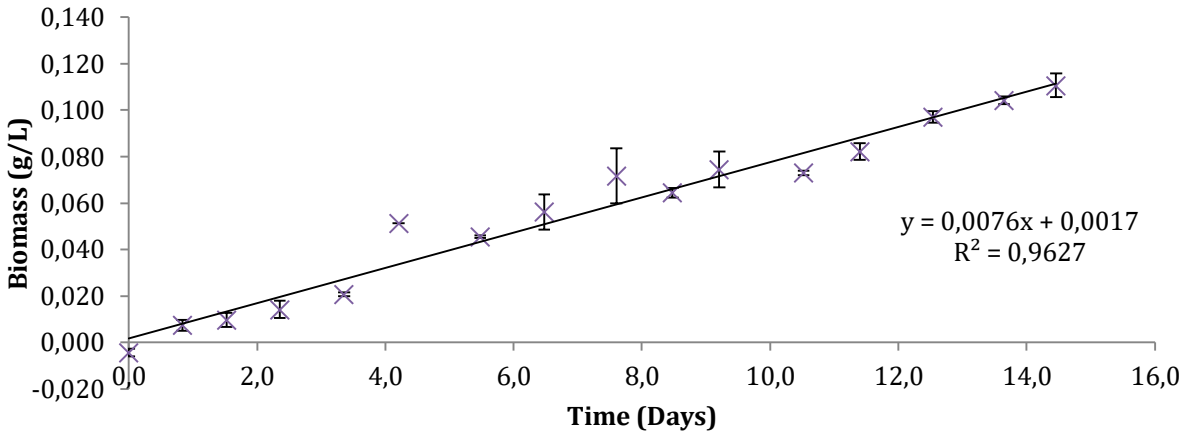


Figure A80: Biomass generation of NWA 11.1 over 15 days, cultivated in AF6 media. The trend line indicates the average growth in biomass over the 15 days. The slope of the trend line indicates the average specific biomass productivity in units of g/L/day.

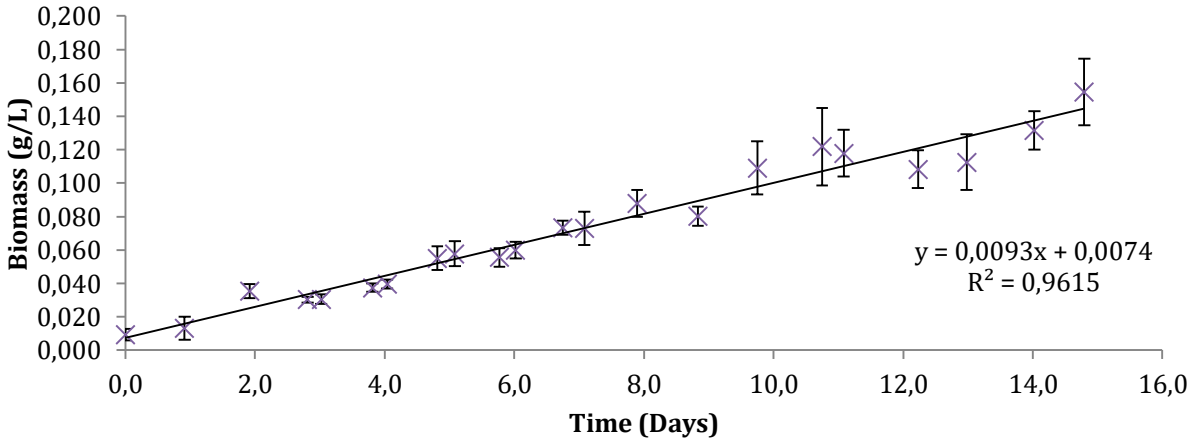


Figure A81: Biomass generation of WCA 4.1 over 15 days, cultivated in AF6 media. The trend line indicates the average growth in biomass over the 15 days. The slope of the trend line indicates the average specific biomass productivity in units of g/L/day.

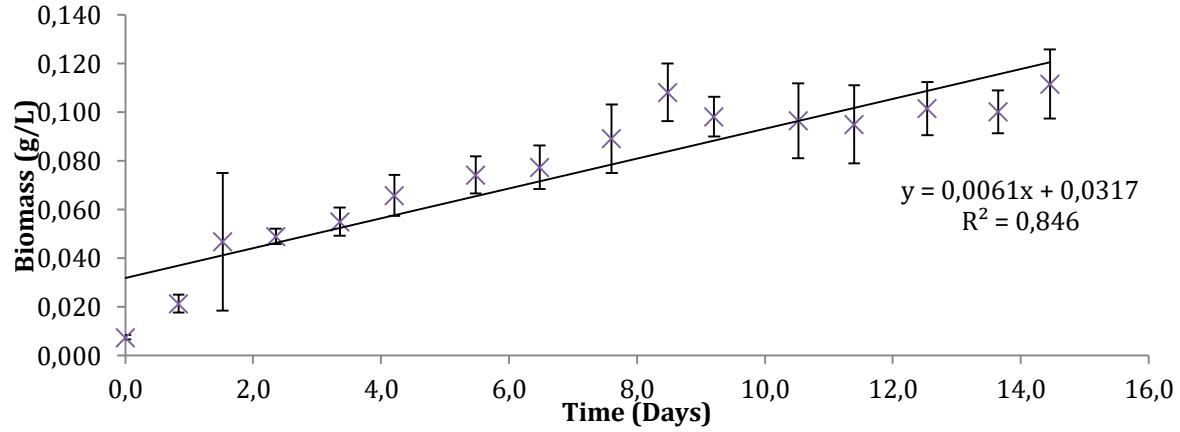


Figure A82: Biomass generation of WCA 10.1 over 15 days, cultivated in AF6 media. The trend line indicates the average growth in biomass over the 15 days. The slope of the trend line indicates the average specific biomass productivity in units of g/L/day.

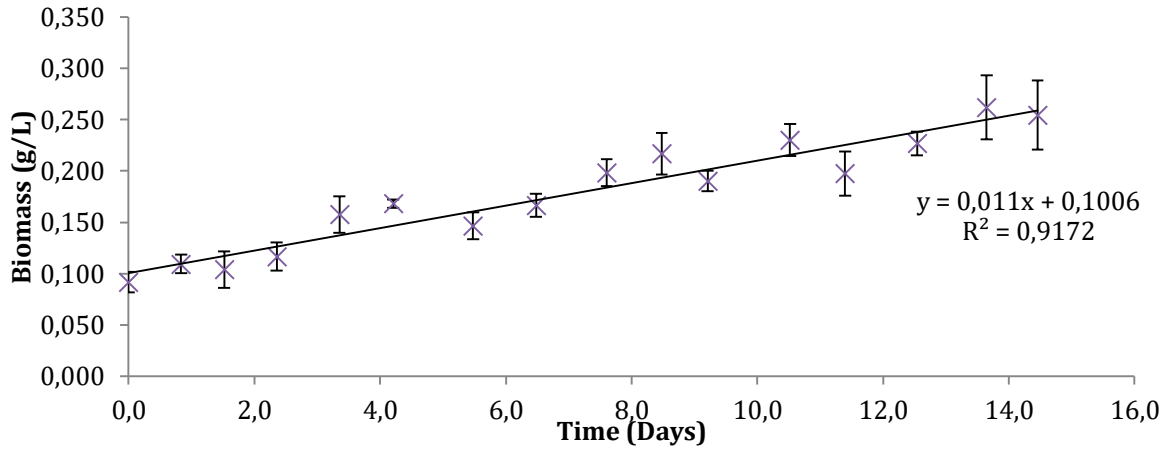


Figure A83: Biomass generation of WCB 4.1 over 15 days, cultivated in AF6 media. The trend line indicates the average growth in biomass over the 15 days. The slope of the trend line indicates the average specific biomass productivity in units of g/L/day.

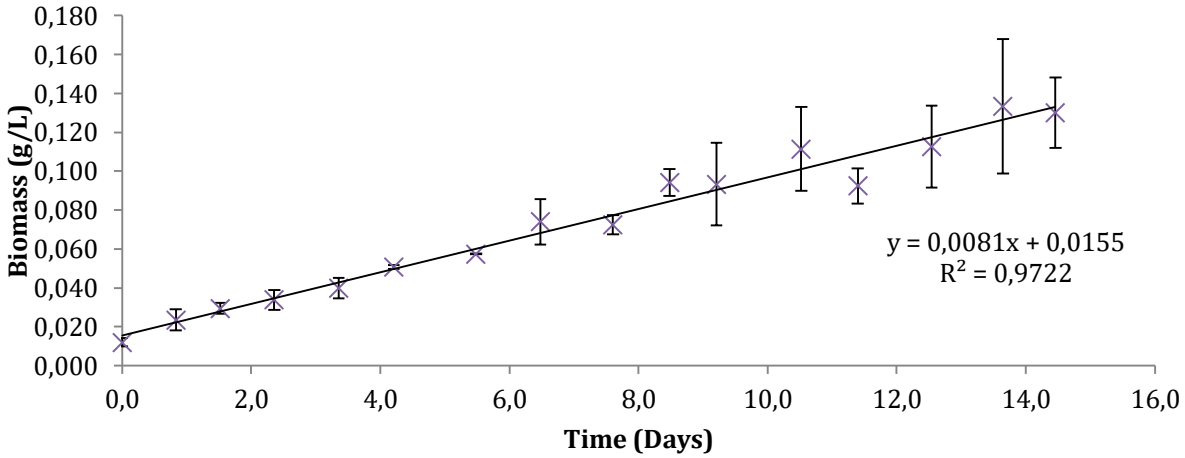


Figure A84: Biomass generation of WCB 7.3 over 15 days, cultivated in AF6 media. The trend line indicates the average growth in biomass over the 15 days. The slope of the trend line indicates the average specific biomass productivity in units of g/L/day.

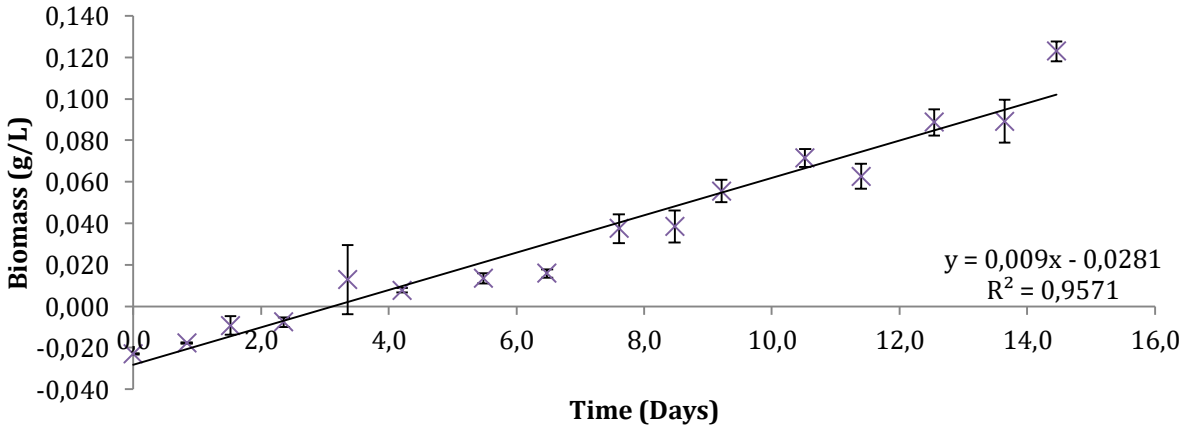


Figure A85: Biomass generation of WCC 2.1 over 15 days, cultivated in AF6 media. The trend line indicates the average growth in biomass over the 15 days. The slope of the trend line indicates the average specific biomass productivity in units of g/L/day.

Table A3: Biomass productivities derived from the linear trend lines from each culture.

Organism designation	Linear trend line equation	R^2 value for trend line	Average specific biomass productivity g/L/d
FSA 5.1	y=0.0026x+0.0145	0.9398	0.0026
FSB 11.1	y=0.0249x-0.0158	0.9775	0.0249
FSB 41.2	y=0.0064x-0.0084	0.9449	0.0064
FSB 51.2	y=0.0128x-0.0021	0.9737	0.0128
LPB 5.1	y=0.0038x-0.0070	0.9021	0.0038
LPB 12.1	y=0.0054x-0.0202	0.8949	0.0054
LPB 15.1	y=0.0049x-0.0025	0.9411	0.0049
NWA 1.1	y=0.0093x-0.0109	0.9258	0.0093
NWA 9.1	y=0.0065x-0.0181	0.9515	0.0065
NWA 11.1	y=0.0076x+0.0017	0.9627	0.0076
WCA 4.1	y=0.0093x+0.0074	0.9615	0.0093
WCA 10.1	y=0.0061x+0.0317	0.8460	0.0061
WCB 4.1	y=0.0110x+0.1006	0.9172	0.0110
WCB 7.3	y=0.0081x+0.0155	0.9722	0.0081
WCC 2.1	y=0.0090x-0.0281	0.9571	0.0090

FAMEs standard correlation curves

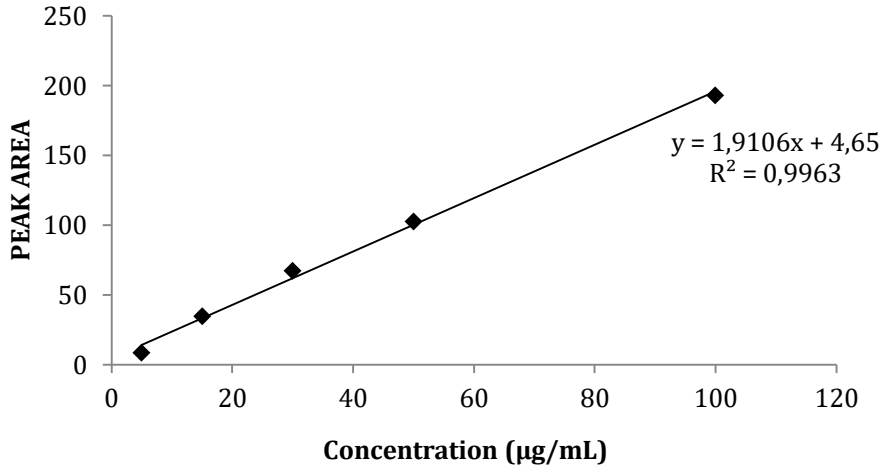


Figure A46: C6:0 FAME-GC standard curve.

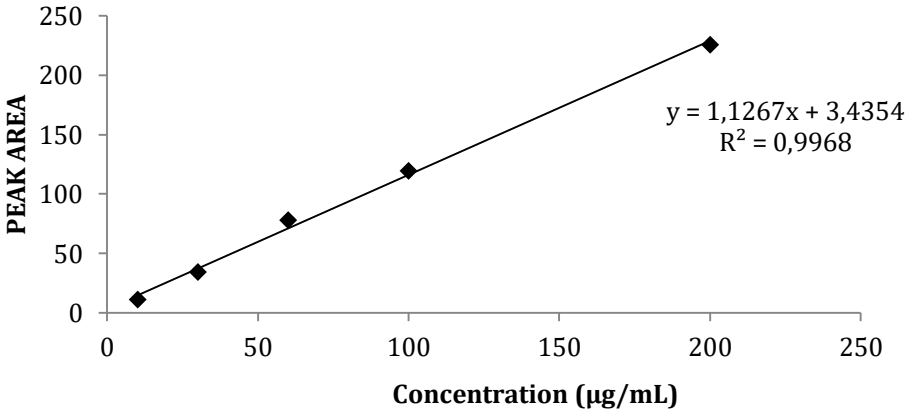


Figure A47: C8:0 FAME-GC standard curve.

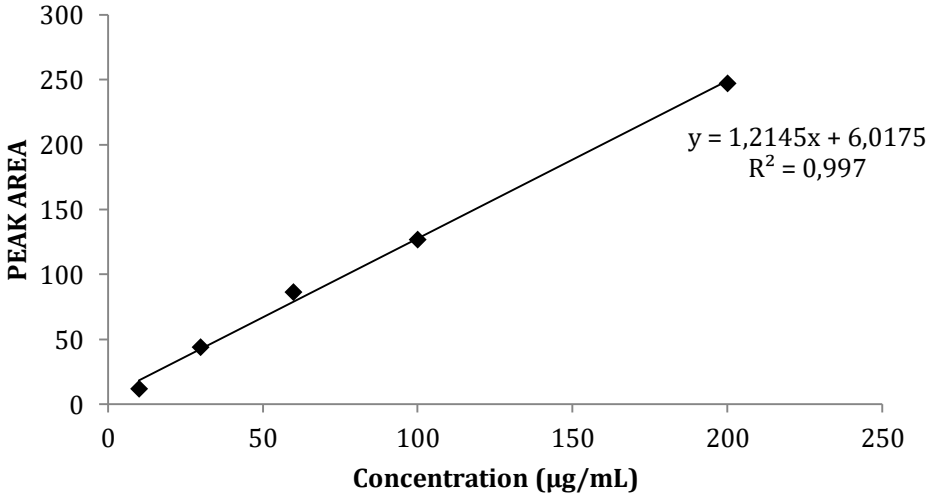


Figure A48: C10:0 FAME-GC standard curve.

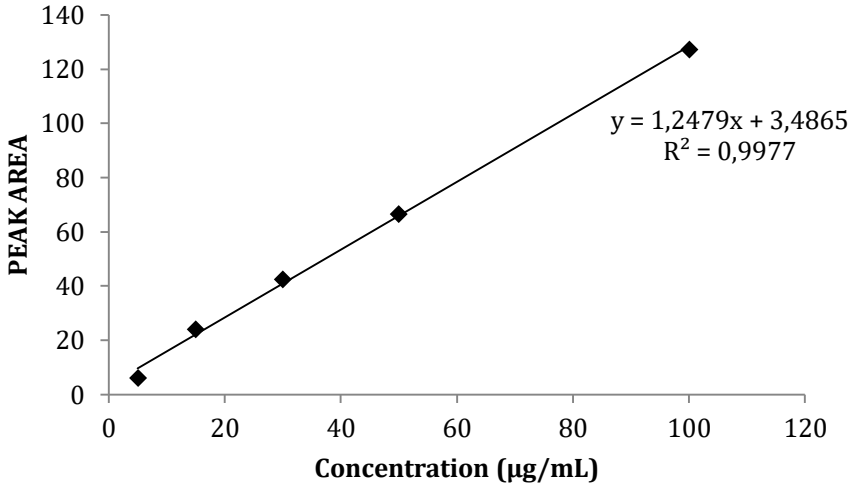


Figure A49: C11:0 FAME-GC standard curve.

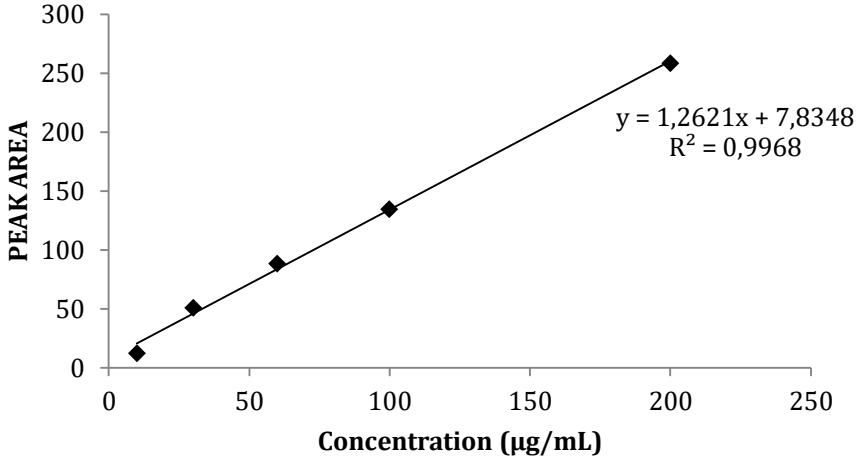


Figure A50: C12:0 FAME-GC standard curve.

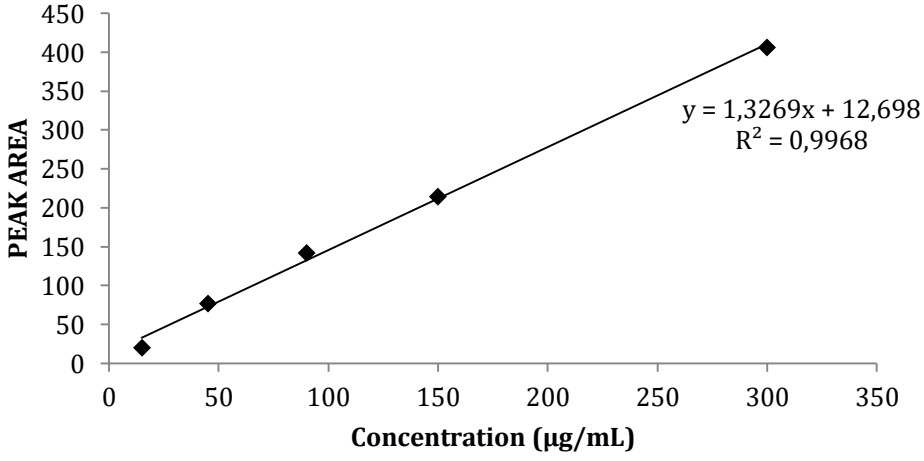


Figure A51: C16:0 FAME-GC standard curve.

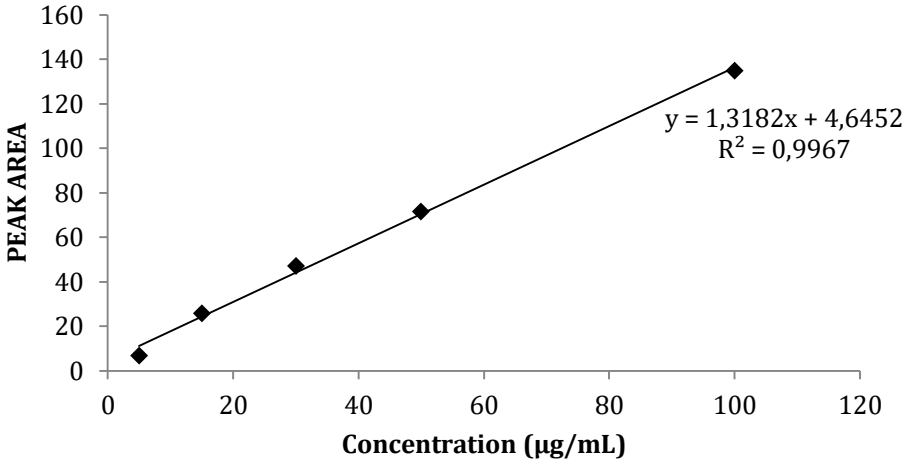


Figure A52: C16:1 FAME-GC standard curve.

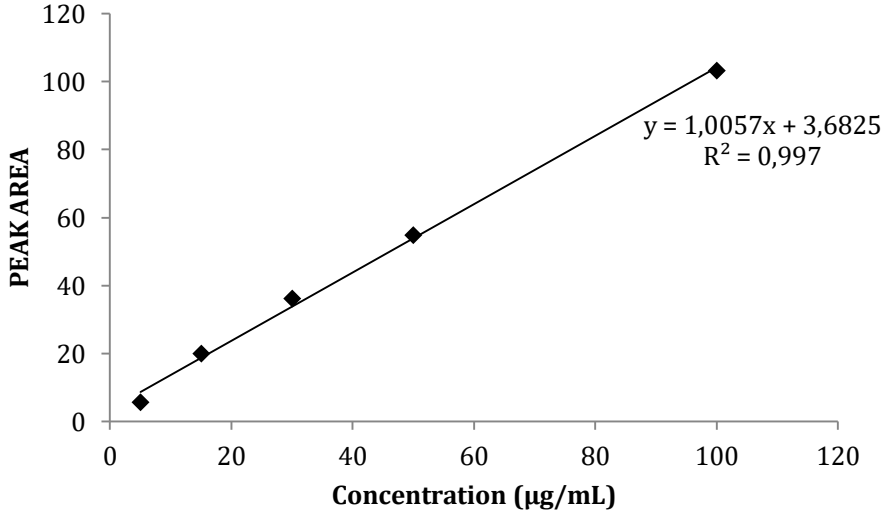


Figure A53: C17:0 FAME-GC standard curve.

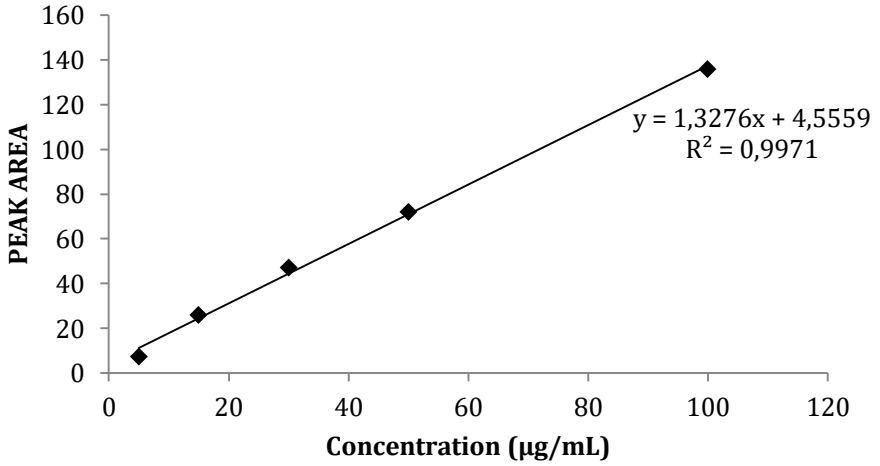


Figure A54: C17:1 FAME-GC standard curve.

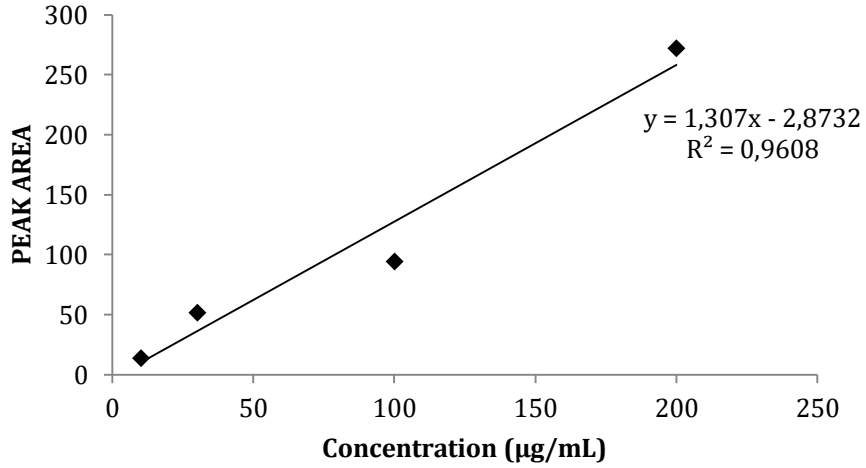


Figure A55: C18:0 FAME-GC standard curve.

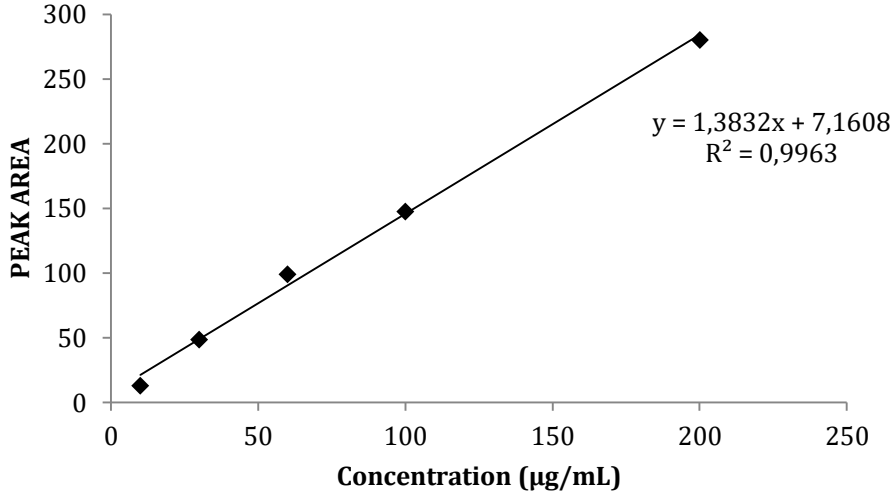


Figure A56: C18:1n9c FAME-GC standard curve.

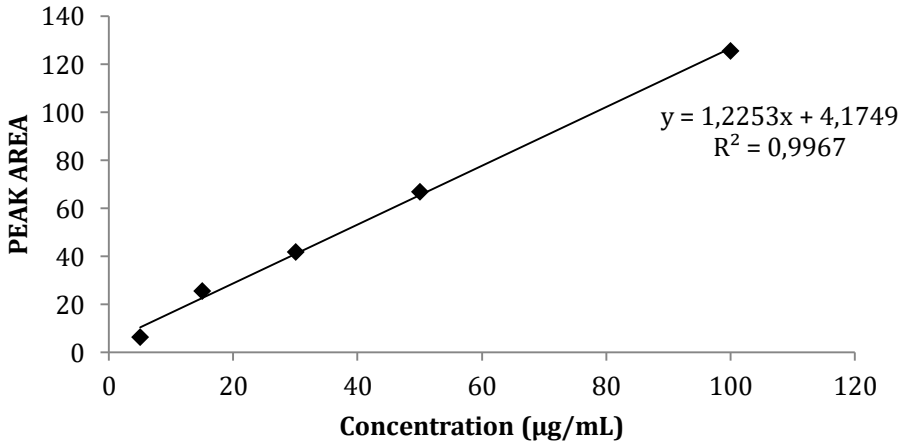


Figure A57: C18:1n9t FAME-GC standard curve.

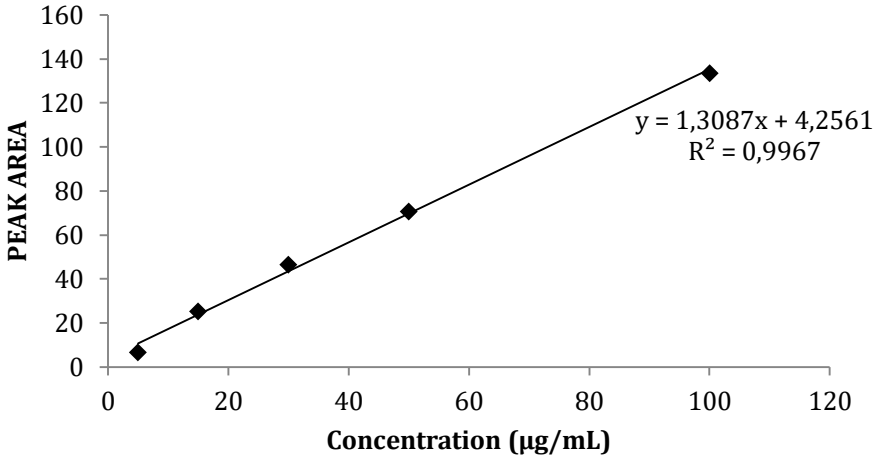


Figure A58: C18:2n6c FAME-GC standard curve.

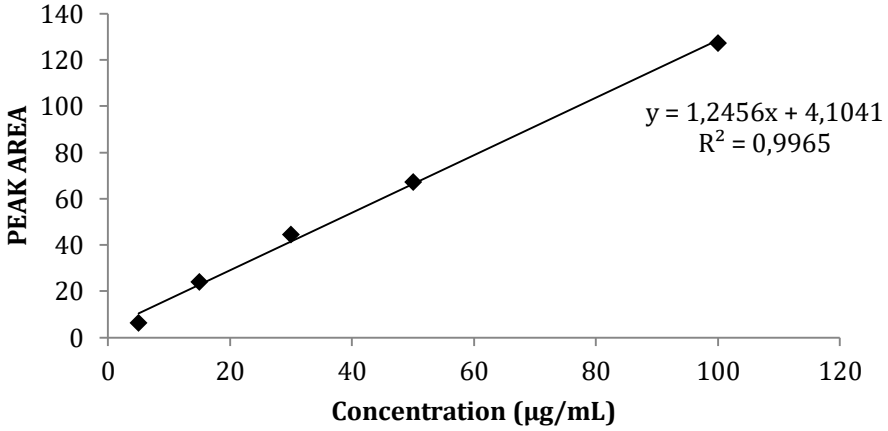


Figure A59: C18:2n6t FAME-GC standard curve.

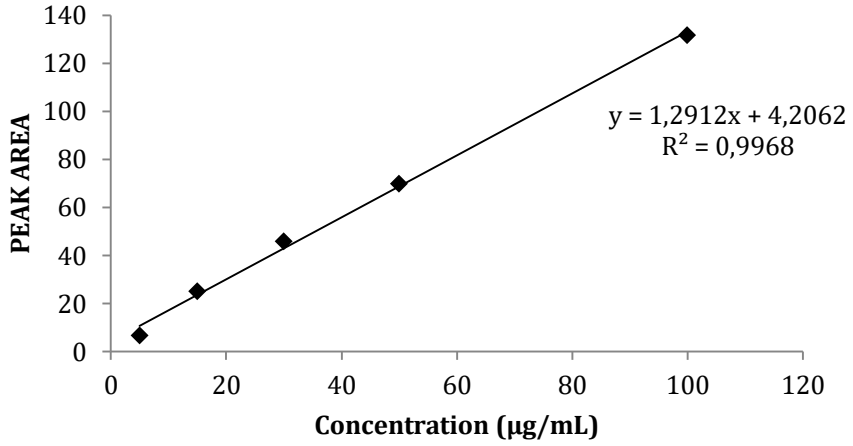


Figure A60: C18:3n6 FAME-GC standard curve.

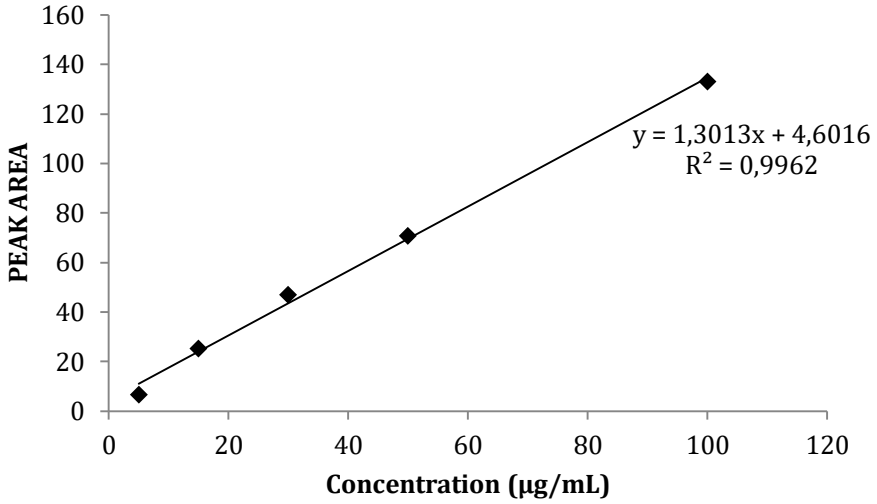


Figure A61: C18:3n3 FAME-GC standard curve.

Lipid content over time

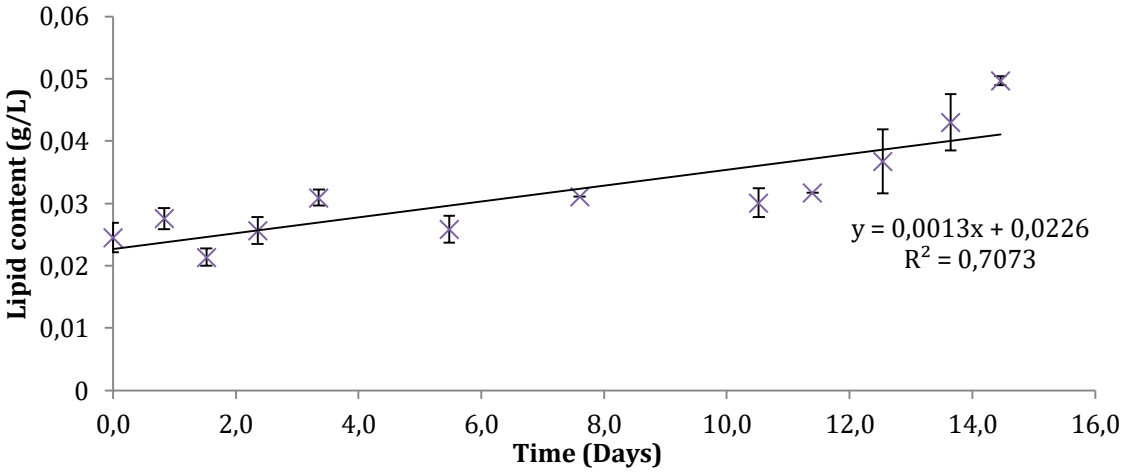


Figure A62: Lipid content over time scatter plot of FSA 5.1. The trend line predicts the average lipid contents of FSA 5.1 over the 15 days. The slope of the trend line indicates the average specific lipid productivity of FSA 5.1 in units of g/L/day.

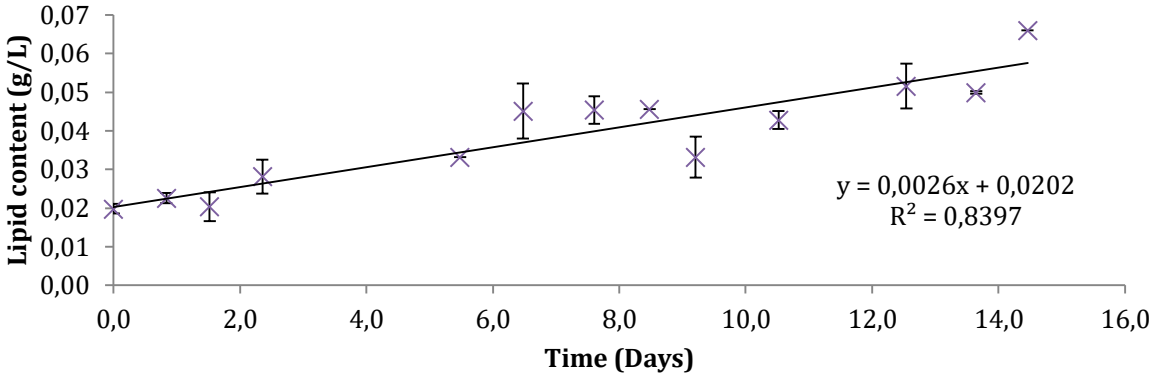


Figure A63: Lipid content over time scatter plot of FSB 11.1. The trend line predicts the average lipid contents of over the 15 days. The slope of the trend line indicates the average specific lipid productivity in units of g/L/day.

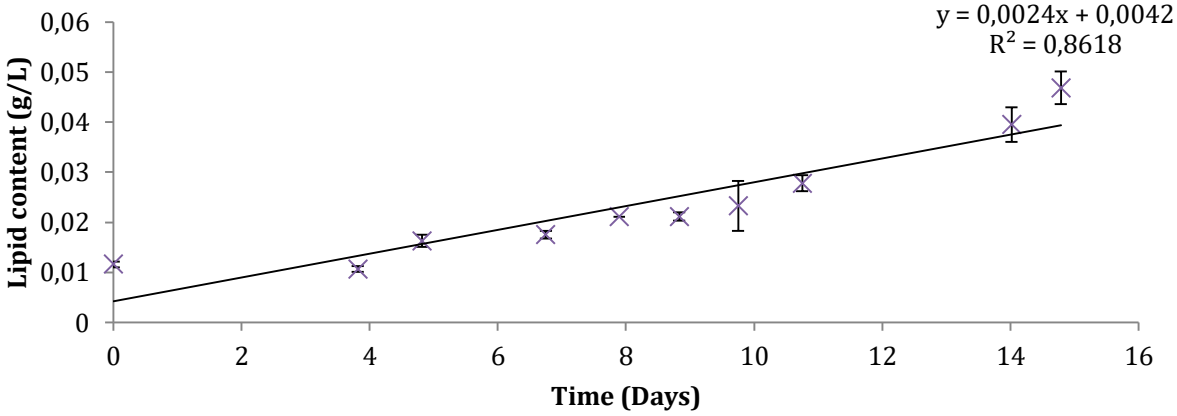


Figure A64: Lipid content over time scatter plot of FSB 41.2. The trend line predicts the average lipid contents of over the 15 days. The slope of the trend line indicates the average specific lipid productivity in units of g/L/day.

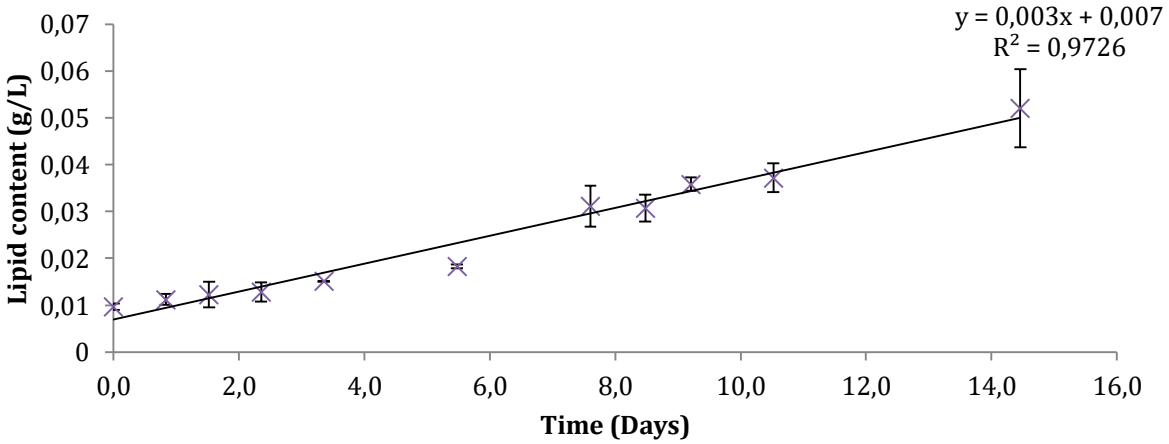


Figure A65: Lipid content over time scatter plot of FSB 51.2. The trend line predicts the average lipid contents of over the 15 days. The slope of the trend line indicates the average specific lipid productivity in units of g/L/day.

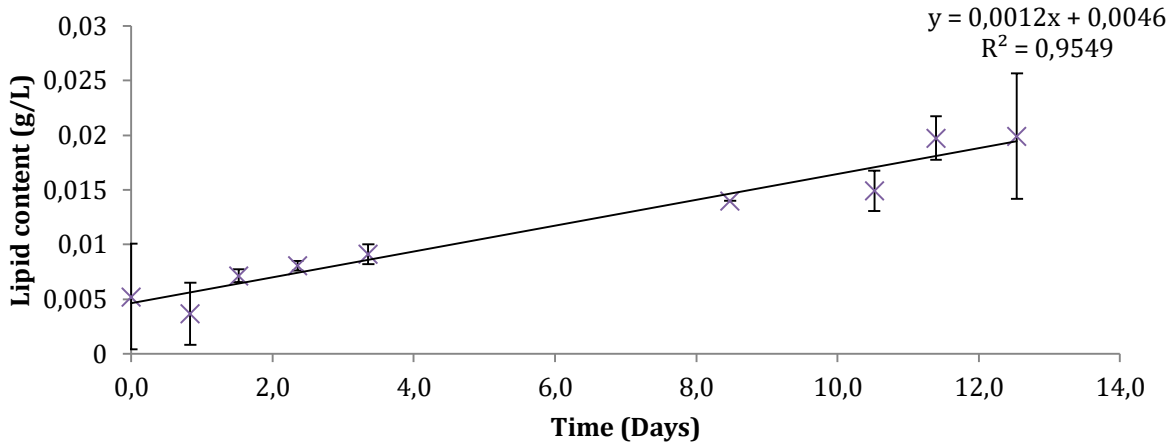


Figure A66: Lipid content over time scatter plot of LPB 5.1. The trend line predicts the average lipid contents of over the 15 days. The slope of the trend line indicates the average specific lipid productivity in units of g/L/day.

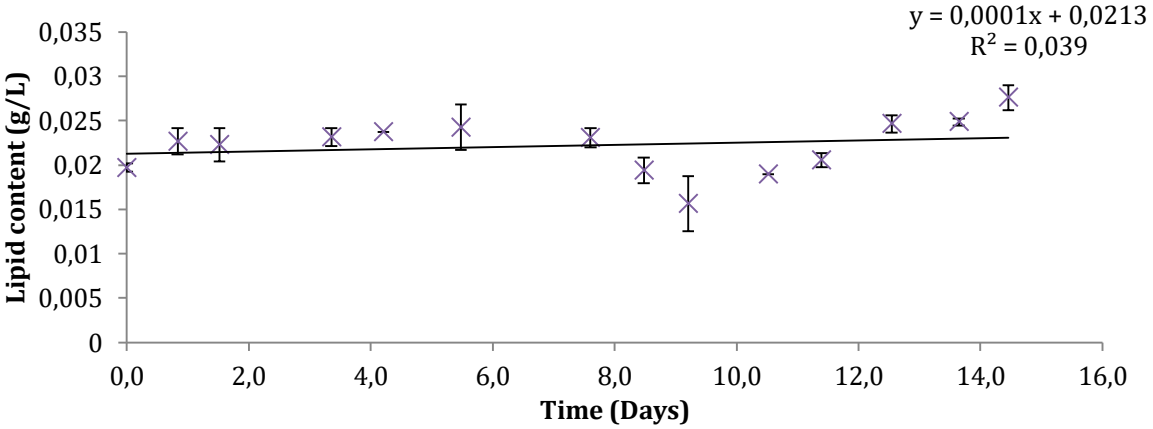


Figure A67: Lipid content over time scatter plot of LPB 12.1. The trend line predicts the average lipid contents of over the 15 days. The slope of the trend line indicates the average specific lipid productivity in units of g/L/day.

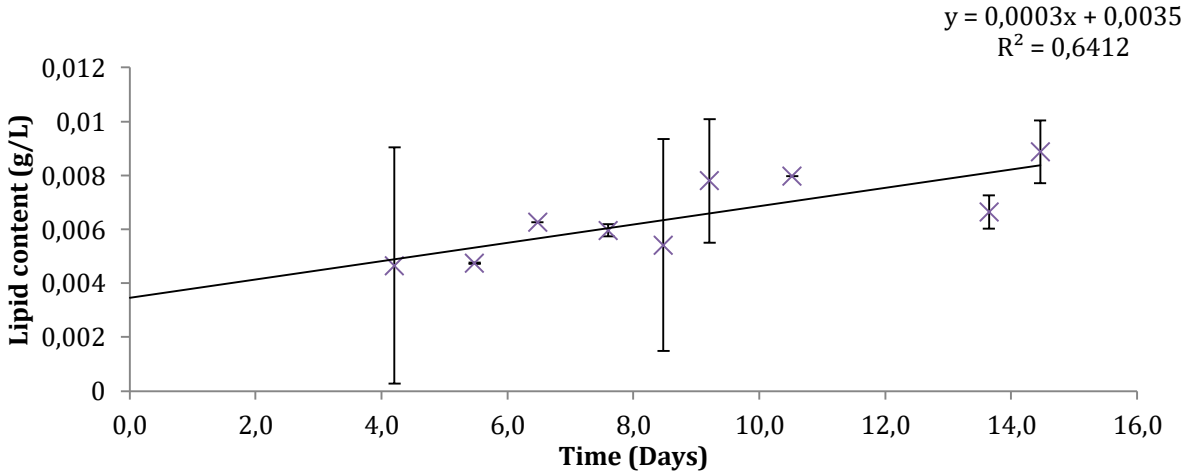


Figure A68: Lipid content over time scatter plot of LPB 15.1. The trend line predicts the average lipid contents of over the 15 days. The slope of the trend line indicates the average specific lipid productivity in units of g/L/day.

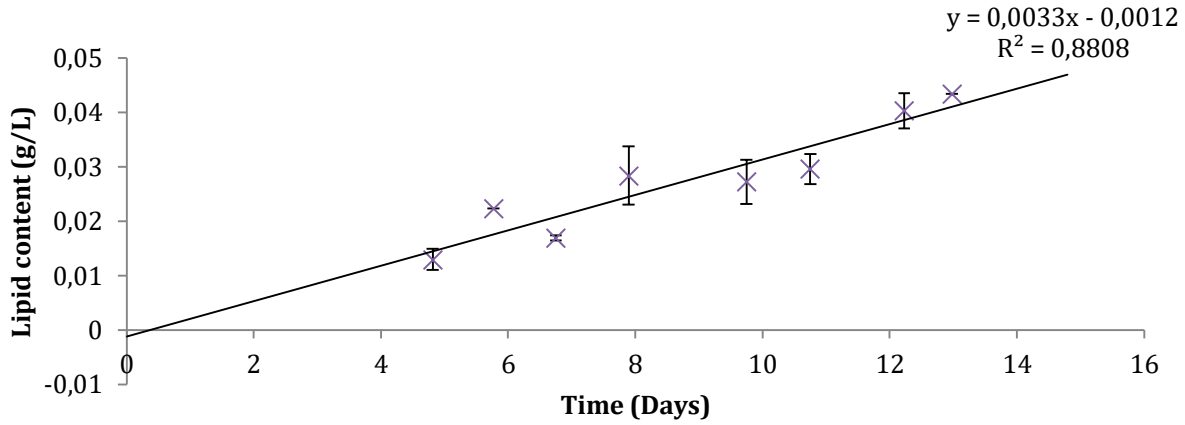


Figure A69: Lipid content over time scatter plot of NWA 1.1. The trend line predicts the average lipid contents of over the 15 days. The slope of the trend line indicates the average specific lipid productivity in units of g/L/day.

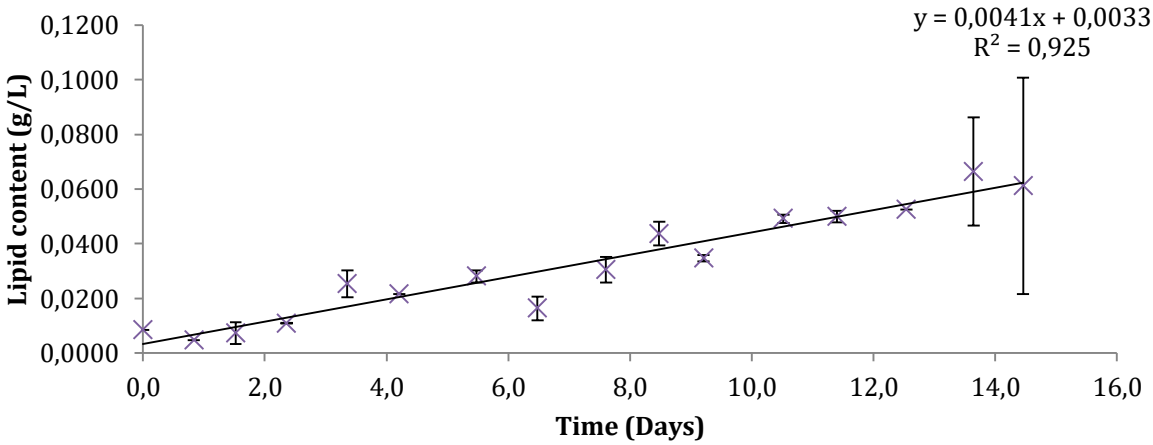


Figure A70: Lipid content over time scatter plot of NWA 9.1. The trend line predicts the average lipid contents of over the 15 days. The slope of the trend line indicates the average specific lipid productivity in units of g/L/day.

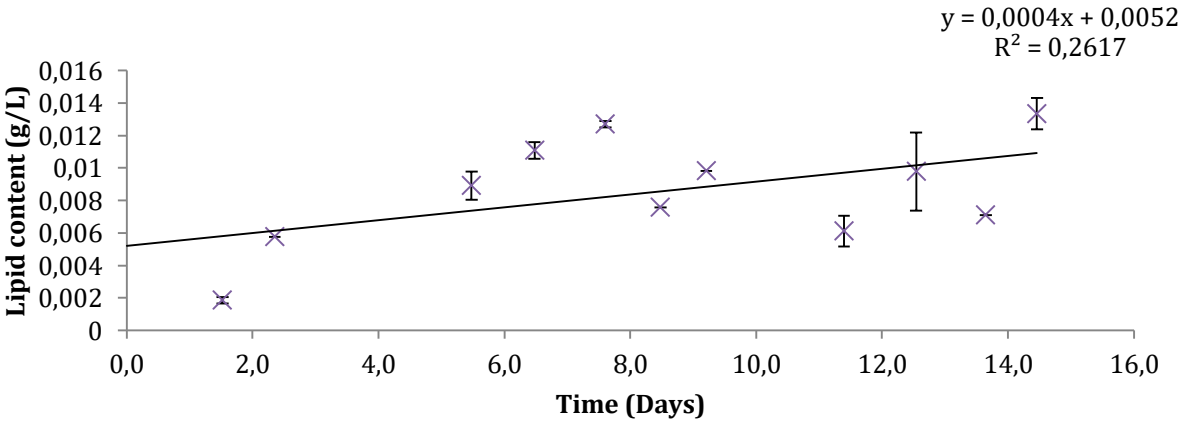


Figure A71: Lipid content over time scatter plot of NWA 11.1. The trend line predicts the average lipid contents of over the 15 days. The slope of the trend line indicates the average specific lipid productivity in units of g/L/day.

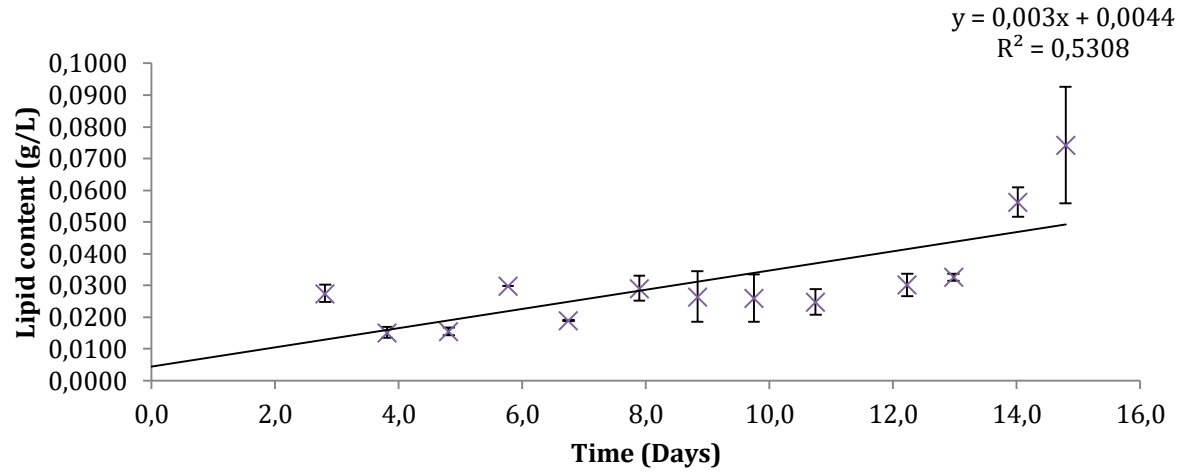


Figure A72: Lipid content over time scatter plot of WCA 4.1. The trend line predicts the average lipid contents of over the 15 days. The slope of the trend line indicates the average specific lipid productivity in units of g/L/day.

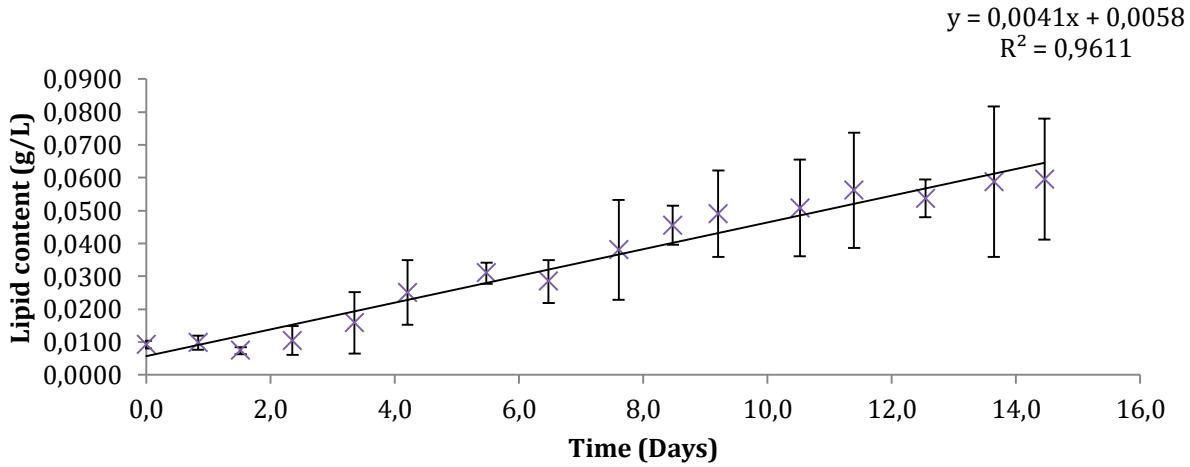


Figure A73: Lipid content over time scatter plot of WCA 10.1. The trend line predicts the average lipid contents of over the 15 days. The slope of the trend line indicates the average specific lipid productivity in units of g/L/day.

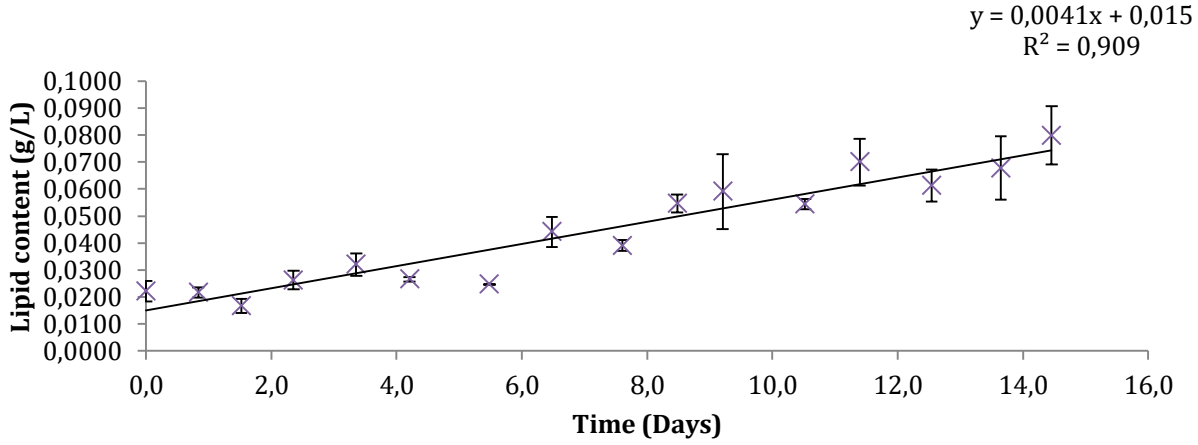


Figure A74: Lipid content over time scatter plot of WCB 4.1. The trend line predicts the average lipid contents of over the 15 days. The slope of the trend line indicates the average specific lipid productivity in units of g/L/day.

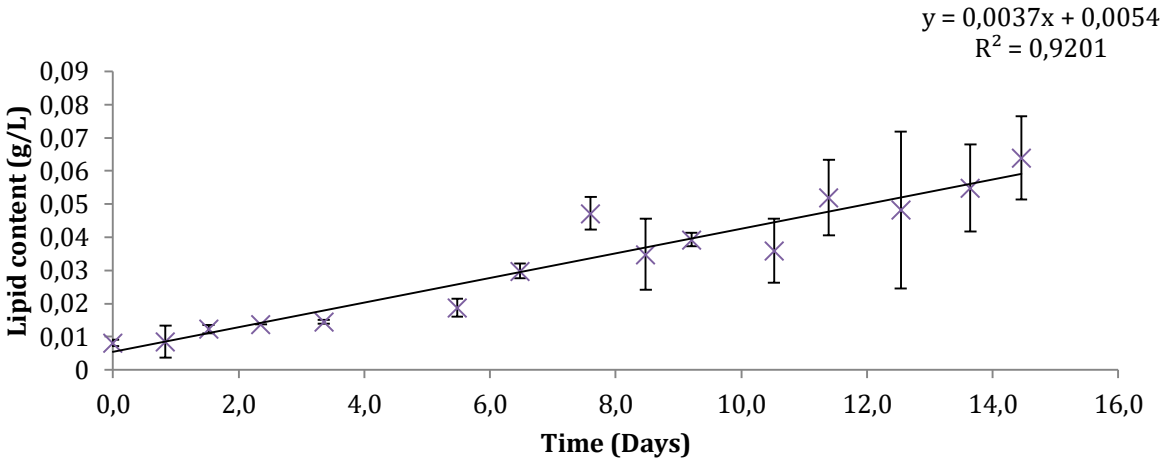


Figure A75: Lipid content over time scatter plot of WCB 7.3. The trend line predicts the average lipid contents of over the 15 days. The slope of the trend line indicates the average specific lipid productivity in units of g/L/day.

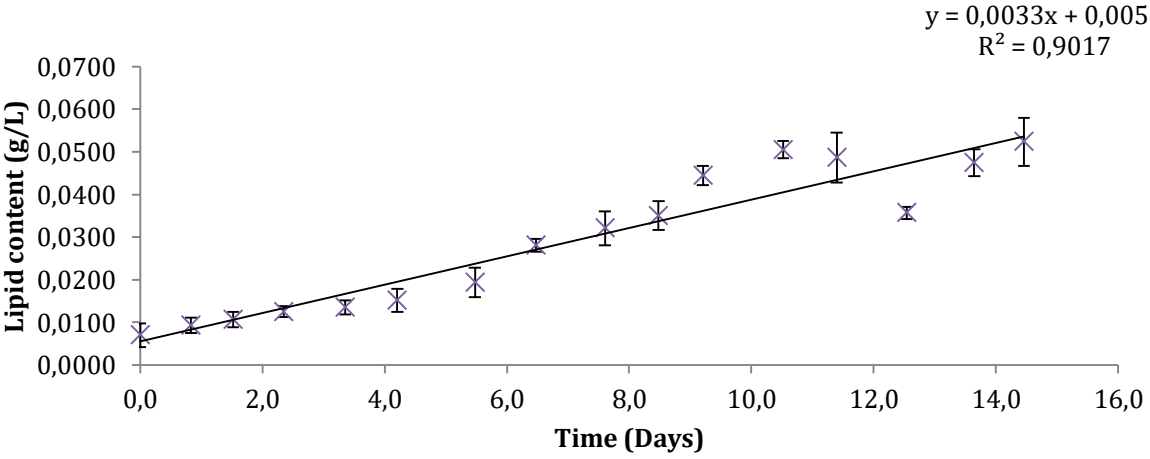


Figure A76: Lipid content over time scatter plot of WCC 2.1. The trend line predicts the average lipid contents of over the 15 days. The slope of the trend line indicates the average specific lipid productivity in units of g/L/day.

Carbohydrate correlation curve

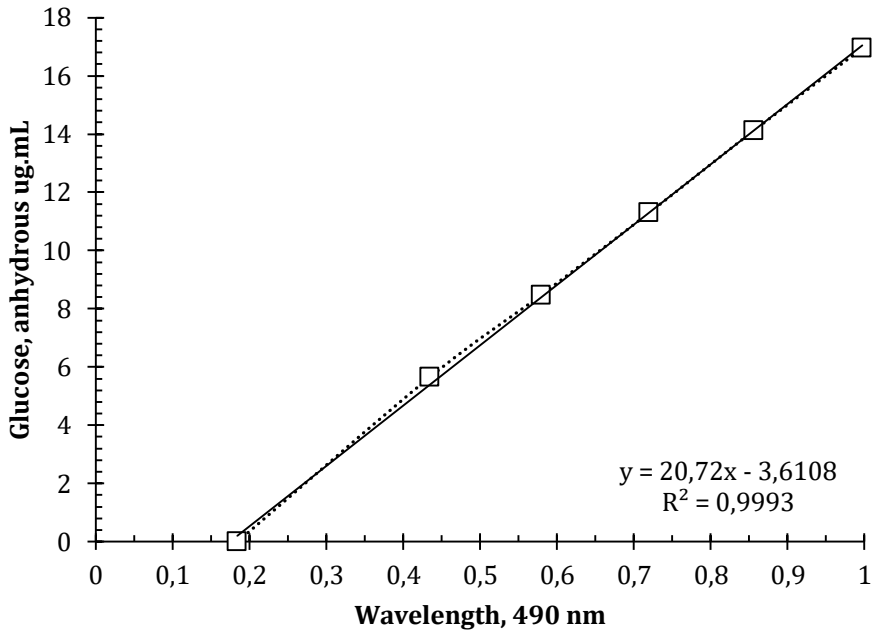


Figure A77: OD 490/Glucose correlation curve for estimating carbohydrate content.

Carbohydrate content over time

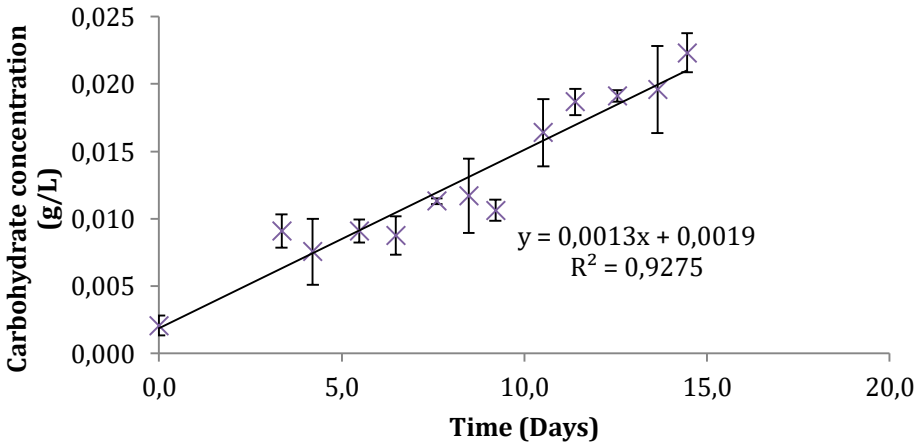


Figure A78: The carbohydrate content over time scatter plot of FSA 5.1. The slope of the linear trend line is indicative of the average specific carbohydrate productivity.

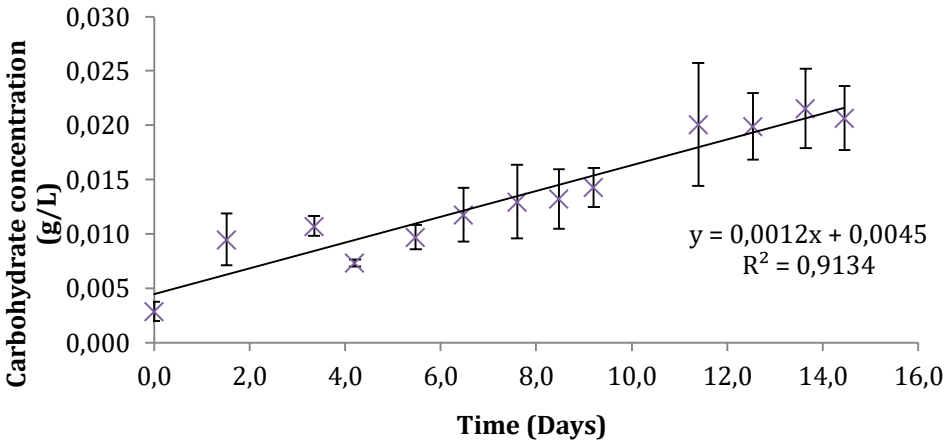


Figure A79: The carbohydrate content over time scatter plot of FSB 11.1. The slope of the linear trend line is indicative of the average specific carbohydrate productivity.

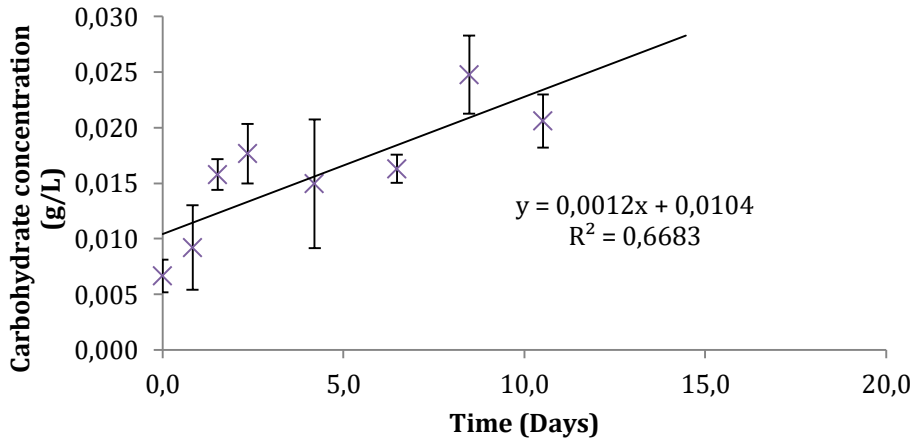


Figure A80: The carbohydrate content over time scatter plot of FSB 41.2. The slope of the linear trend line is indicative of the average specific carbohydrate productivity.

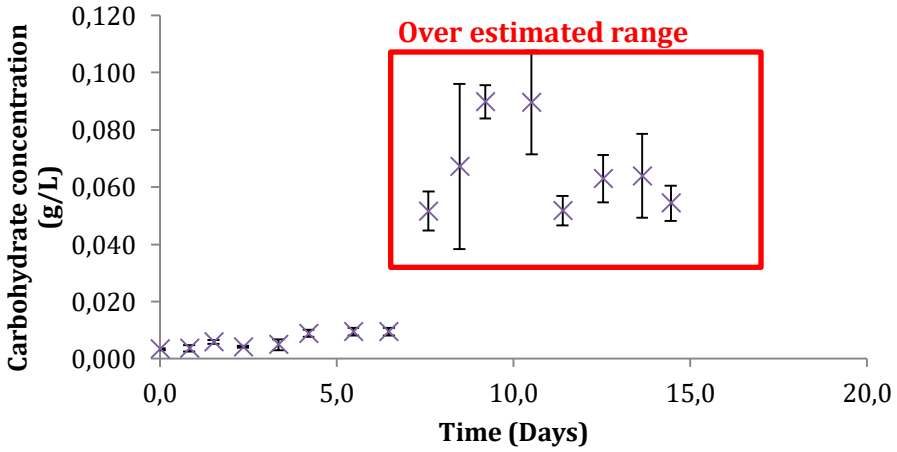


Figure A81: The carbohydrate content over 15 days scatter plot of FSB 51.2. The data in the red box are faulty due to experimental error. The data points in the red box should not be considered as it would lead to a gross overestimation of carbohydrate productivity.

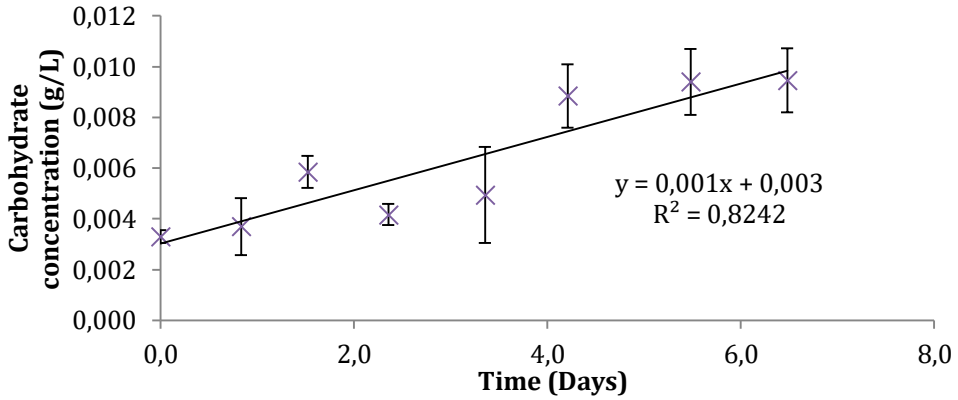


Figure A82: The carbohydrate content over time scatter plot of FSB 51.2. The slope of the linear trend line is indicative of the average specific carbohydrate productivity.

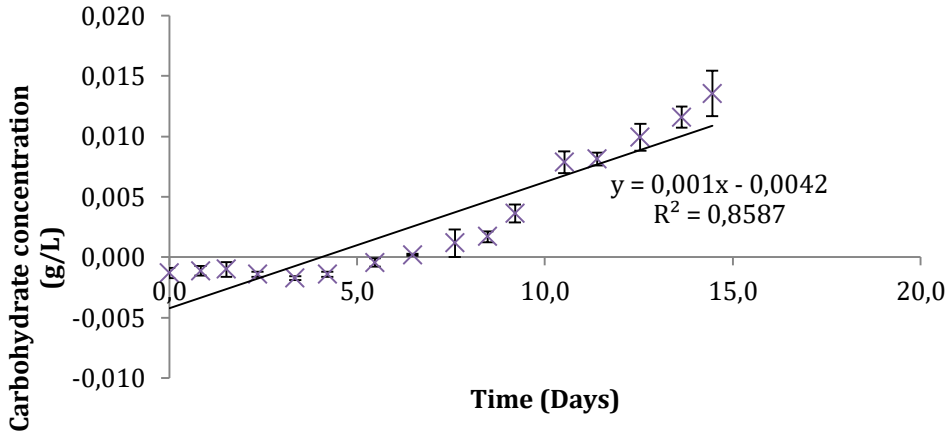


Figure A83: The carbohydrate content over time scatter plot of LPB 5.1. The slope of the linear trend line is indicative of the average specific carbohydrate productivity.

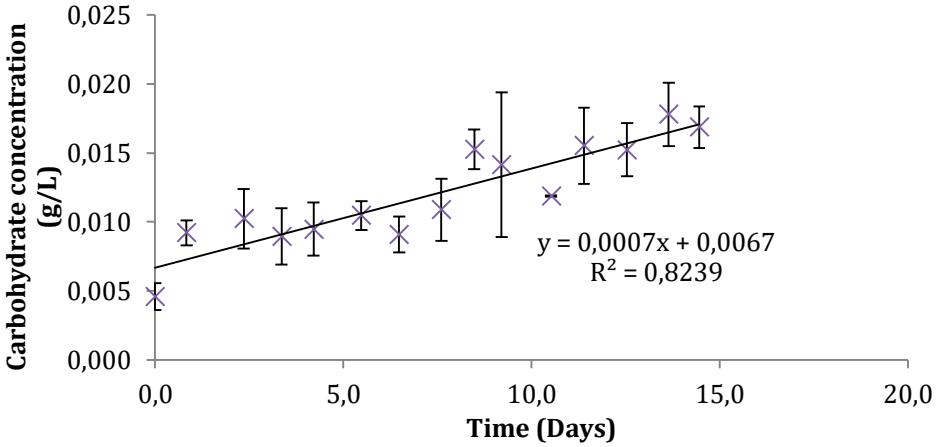


Figure A84: The carbohydrate content over time scatter plot of LPB 12.1. The slope of the linear trend line is indicative of the average specific carbohydrate productivity.

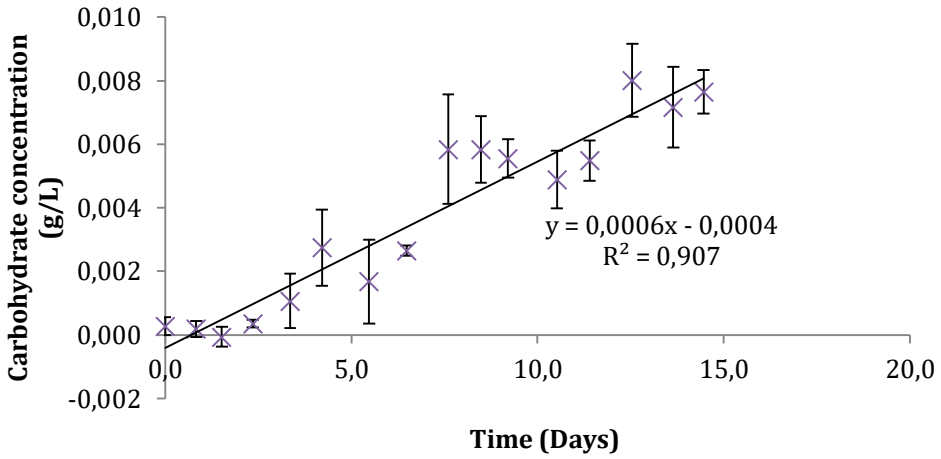


Figure A85: The carbohydrate content over time scatter plot of LPB 15.1. The slope of the linear trend line is indicative of the average specific carbohydrate productivity.

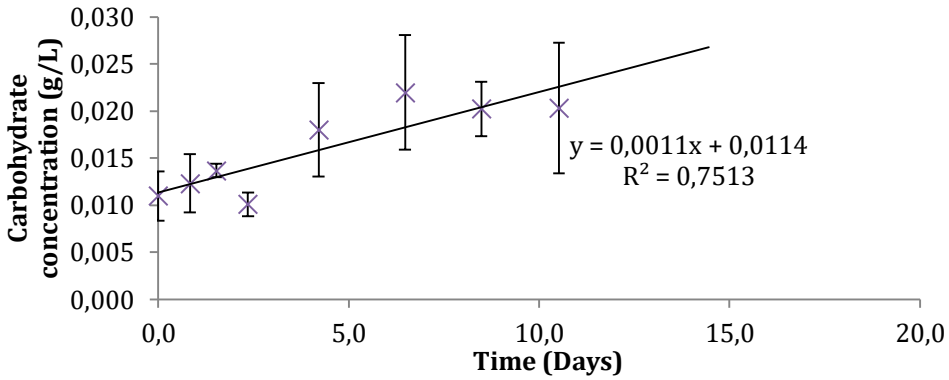


Figure A86: The carbohydrate content over time scatter plot of NWA 1.1. The slope of the linear trend line is indicative of the average specific carbohydrate productivity.

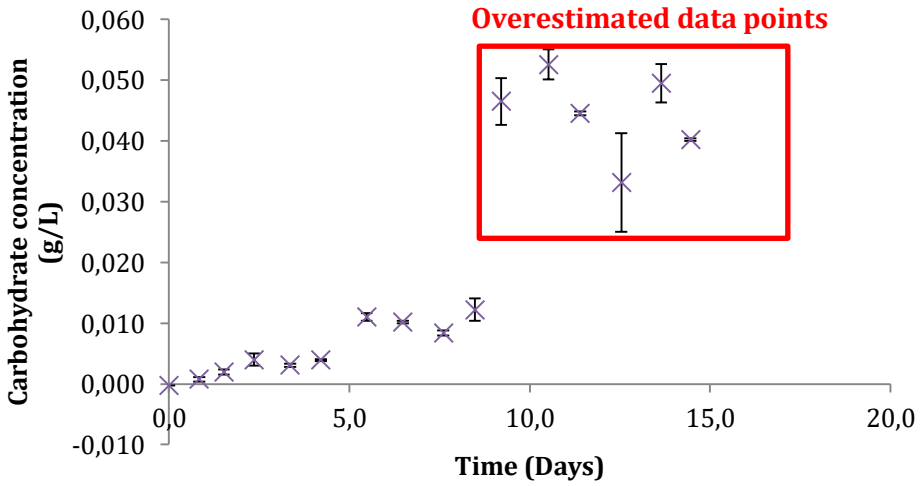


Figure A87: The carbohydrate content over 15 days scatter plot of NWA 9.1. The data in the red box are faulty due to experimental error. The data points in the red box should not be considered as it would lead to a gross overestimation of carbohydrate productivity.

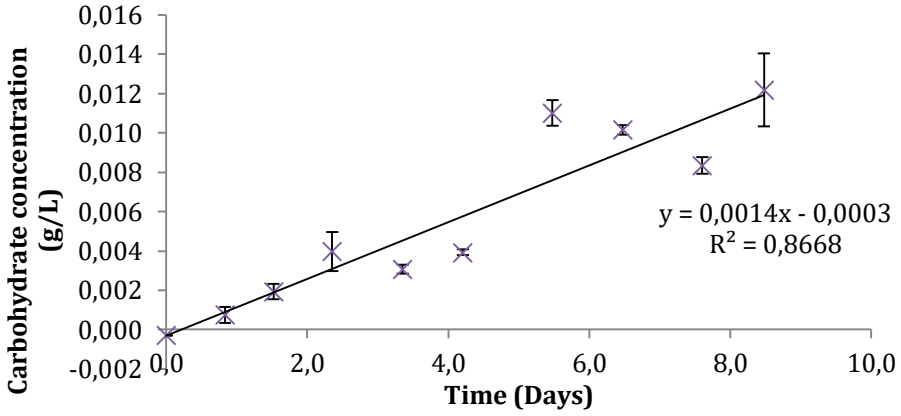


Figure A88: The carbohydrate content over 9 days scatter plot of NWA 9.1. The slope of the linear trend line is indicative of the average specific carbohydrate productivity.

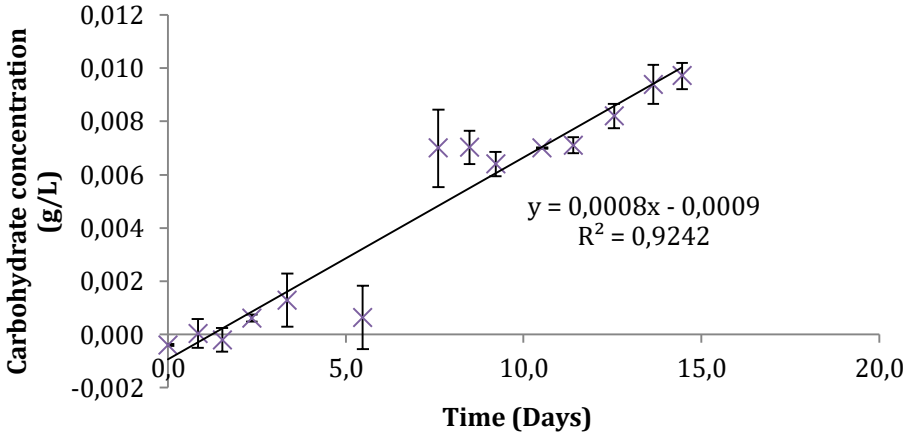


Figure A89: The carbohydrate content over time scatter plot of NWA 11.1. The slope of the linear trend line is indicative of the average specific carbohydrate productivity.

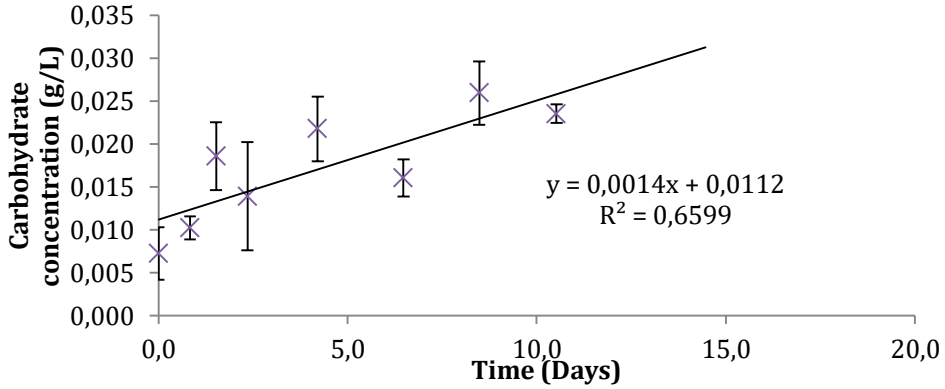


Figure A90: The carbohydrate content over time scatter plot of WCA 4.1. The slope of the linear trend line is indicative of the average specific carbohydrate productivity.

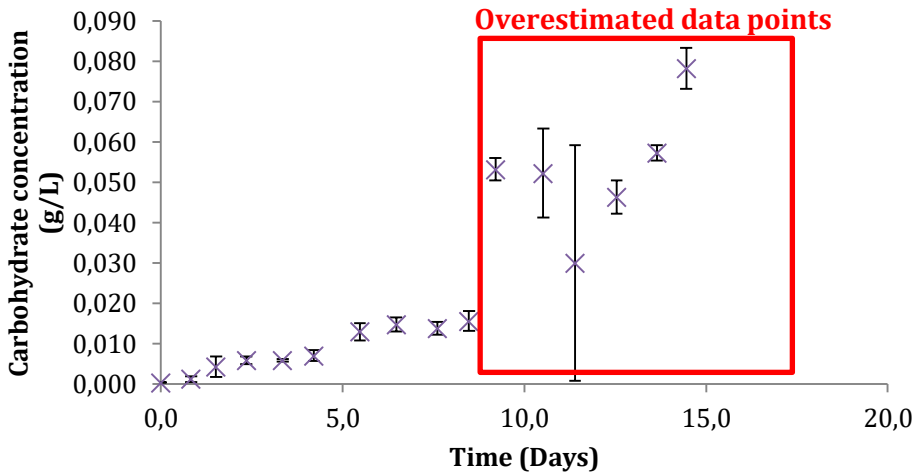


Figure A91: The carbohydrate content over 15 days scatter plot of WCA 10.1. The data in the red box are faulty due to experimental error. The data points in the red box should not be considered as it would lead to a gross overestimation of carbohydrate productivity.

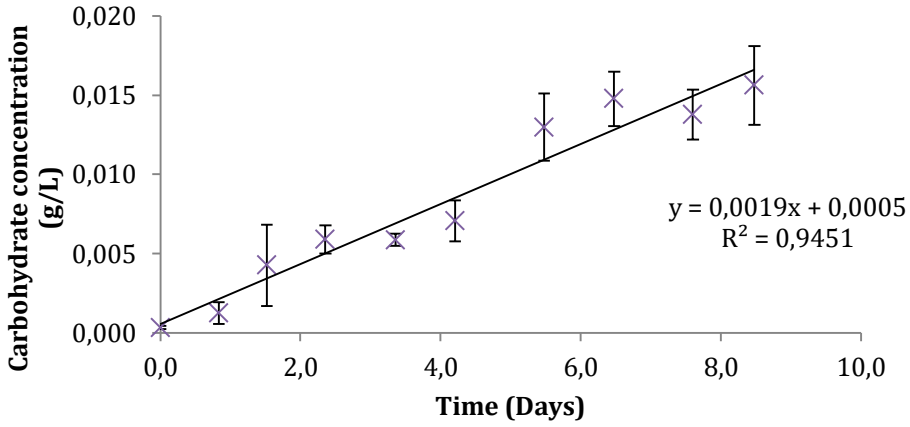


Figure A92: The carbohydrate content over 9 days scatter plot of WCA 10.1. The slope of the linear trend line is indicative of the average specific carbohydrate productivity.

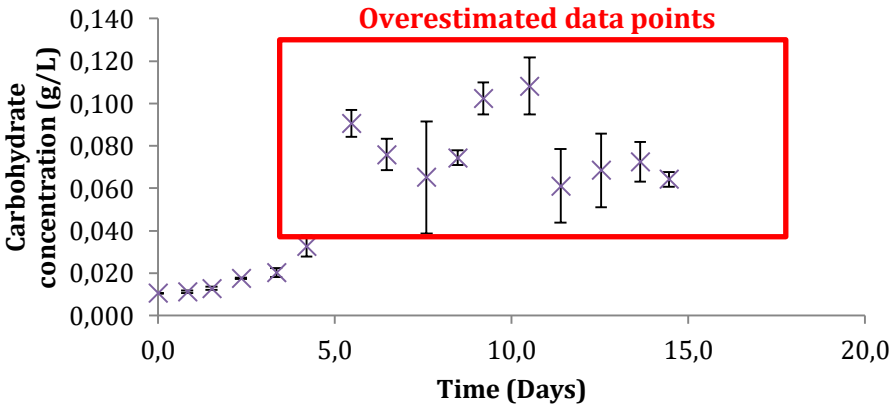


Figure A93: The carbohydrate content over 15 days scatter plot of WCB 4.1. The data in the red box are faulty due to experimental error. The data points in the red box should not be considered as it would lead to a gross overestimation of carbohydrate productivity.

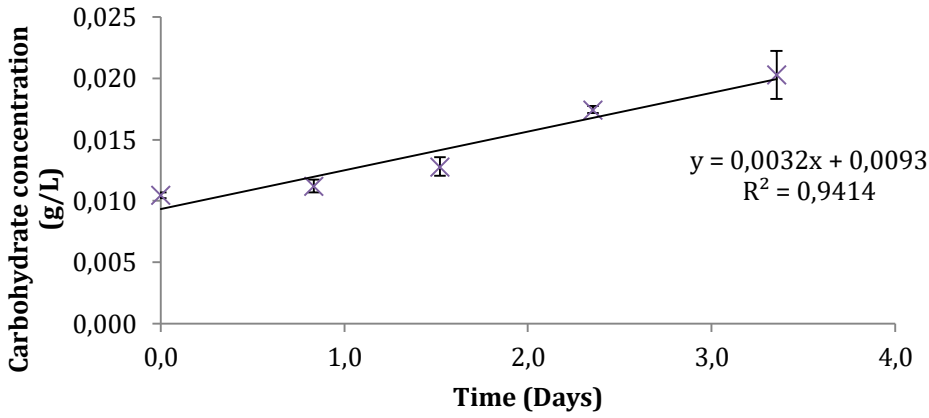


Figure A94: The carbohydrate content over 3.5 days scatter plot of WCB 4.1. The slope of the linear trend line is indicative of the average specific carbohydrate productivity.

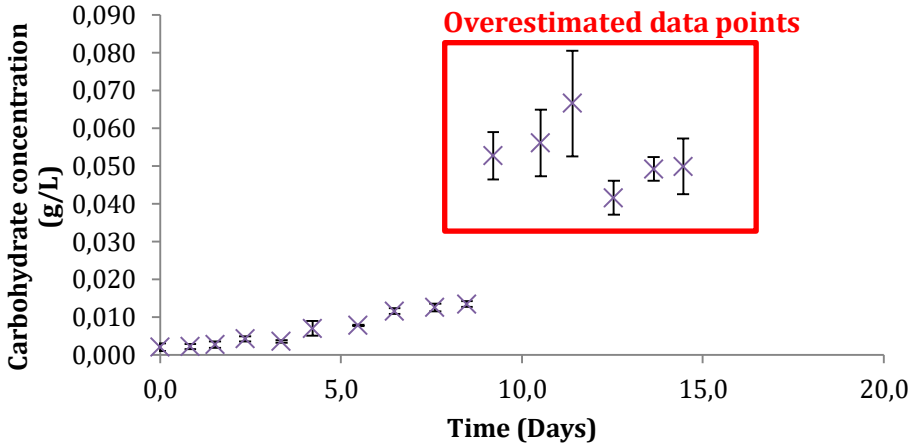


Figure A95: The carbohydrate content over 15 days scatter plot of WCB 7.3. The data in the red box are faulty due to experimental error. The data points in the red box should not be considered as it would lead to a gross overestimation of carbohydrate productivity.

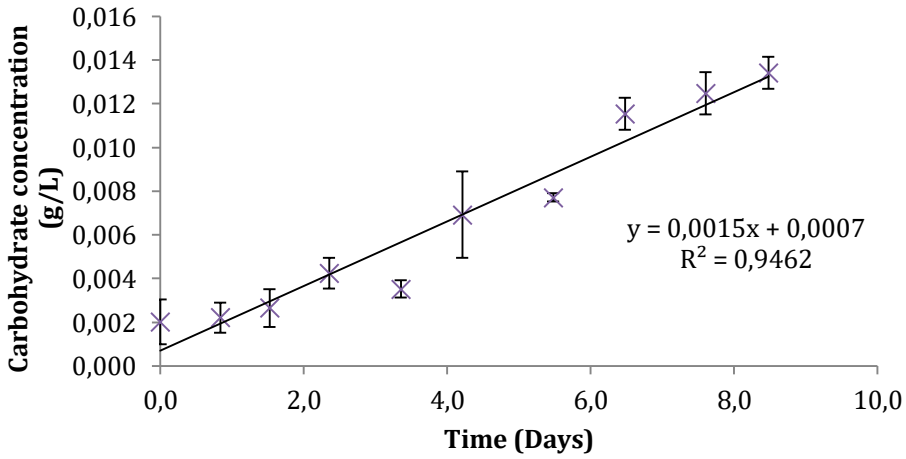


Figure A96: The carbohydrate content over 9 days scatter plot of WCB 7.3. The slope of the linear trend line is indicative of the average specific carbohydrate productivity.

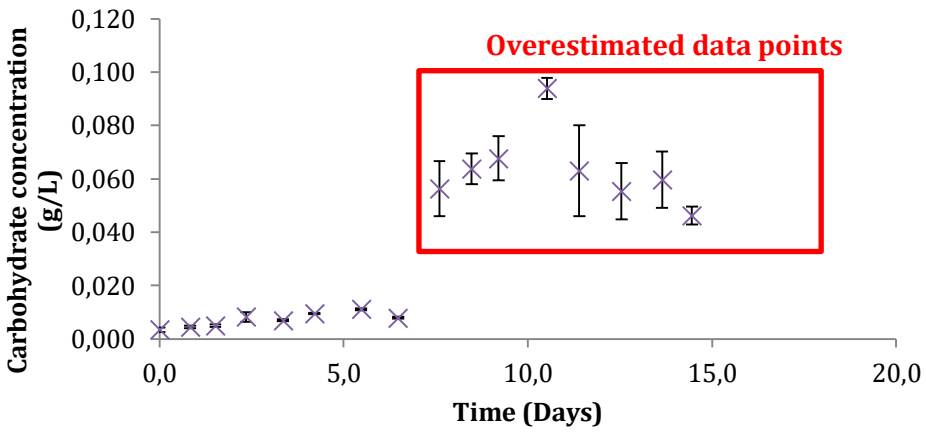


Figure A97: The carbohydrate content over 15 days scatter plot of WCC 2.1. The data in the red box are faulty due to experimental error. The data points in the red box should not be considered as it would lead to a gross overestimation of carbohydrate productivity.

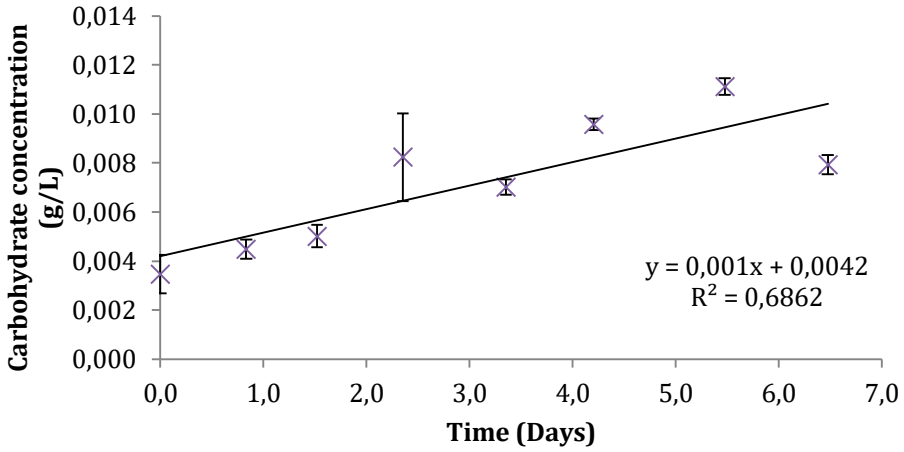


Figure A98: The carbohydrate content over 7 days scatter plot of WCC 2.1. The slope of the linear trend line is indicative of the average specific carbohydrate productivity.

Table A4: Carbohydrate productivities derived from the linear trend lines from each culture.

Organism designation	Linear trend line equation	R^2 value for trend line	Average specific carbohydrate productivity g/L/d
FSA 5.1	y=0.0013x+0.0019	0.9275	0.0013
FSB 11.1	y=0.0012x+0.0045	0.9134	0.0012
FSB 41.2	y=0.0012x+0.0104	0.6683	0.0012
FSB 51.2	y=0.0010x+0.003	0.8242	0.0010
LPB 5.1	y=0.0010x-0.0042	0.8587	0.0010
LPB 12.1	y=0.0007x+0.0067	0.8239	0.0007
LPB 15.1	y=0.0006x-0.0004	0.9070	0.0006
NWA 1.1	y=0.0011x+0.0114	0.7513	0.0011
NWA 9.1	y=0.0010x+0.003	0.8242	0.0014
NWA 11.1	y=0.0008x-0.0009	0.9242	0.0008
WCA 4.1	y=0.0014x-0.0112	0.6599	0.0014
WCA 10.1	y=0.0010x+0.003	0.8242	0.0019
WCB 4.1	y=0.0032x+0.0093	0.9414	0.0032
WCB 7.3	y=0.0015x+0.0007	0.9462	0.0015
WCC 2.1	y=0.0010x+0.0042	0.6862	0.0010

Comparison between isolates

Table A5: Average specific biomass, lipid and carbohydrate productivity of 15 microalgal isolates.

Organism designation	Average specific biomass productivity g/L/d	Average specific lipid productivity g/L/d	Average specific carbohydrate productivity g/L/d
FSA 5.1	0.0026	0.0013	0.0013
FSB 11.1	0.0249	0.0026	0.0012
FSB 41.2	0.0064	0.0024	0.0012
FSB 51.2	0.0128	0.003	0.0010
LPB 5.1	0.0038	0.0012	0.0010
LPB 12.1	0.0054	0.0001	0.0007
LPB 15.1	0.0049	0.0003	0.0006
NWA 1.1	0.0093	0.0033	0.0011
NWA 9.1	0.0065	0.0041	0.0014
NWA 11.1	0.0076	0.0004	0.0008
WCA 4.1	0.0093	0.0028	0.0014
WCA 10.1	0.0061	0.0041	0.0019
WCB 4.1	0.0110	0.0041	0.0032
WCB 7.3	0.0081	0.0037	0.0015
WCC 2.1	0.0090	0.0033	0.0010

Isolate selection

Table A6: Scoring matrix of the specific isolate productivities.

Organism ID	Average specific biomass productivity g/L/d	Score	Average specific lipid productivity g/L/d	Score	Average specific carbohydrate productivity g/L/d	Score	Score
FSA 5.1	0.0026	10.4	0.0013	31.7	0.0013	40.6	27.1
FSB 11.1	0.0249	100.0	0.0026	63.4	0.0012	37.5	69.2
FSB 41.2	0.0064	25.7	0.0024	58.5	0.0012	37.5	44.5
FSB 51.2	0.0128	51.4	0.003	73.2	0.0010	31.3	58.3
LPB 5.1	0.0038	15.3	0.0012	29.3	0.0010	31.3	25.5
LPB 12.1	0.0054	21.7	0.0001	2.4	0.0007	21.9	12.1
LPB 15.1	0.0049	19.7	0.0003	7.3	0.0006	18.8	13.3
NWA 1.1	0.0093	37.3	0.0033	80.5	0.0011	34.4	58.3
NWA 9.1	0.0065	26.1	0.0041	100.0	0.0014	43.8	66.6
NWA 11.1	0.0076	30.5	0.0004	9.8	0.0008	25.0	19.0
WCA 4.1	0.0093	37.3	0.0028	68.3	0.0014	43.8	54.1
WCA 10.1	0.0061	24.5	0.0041	100.0	0.0019	59.4	69.2
WCB 4.1	0.0110	44.2	0.0041	100.0	0.0032	100.0	83.3
WCB 7.3	0.0081	32.5	0.0037	90.2	0.0015	46.9	64.3
WCC 2.1	0.0090	36.1	0.0033	80.5	0.001	31.3	57.3

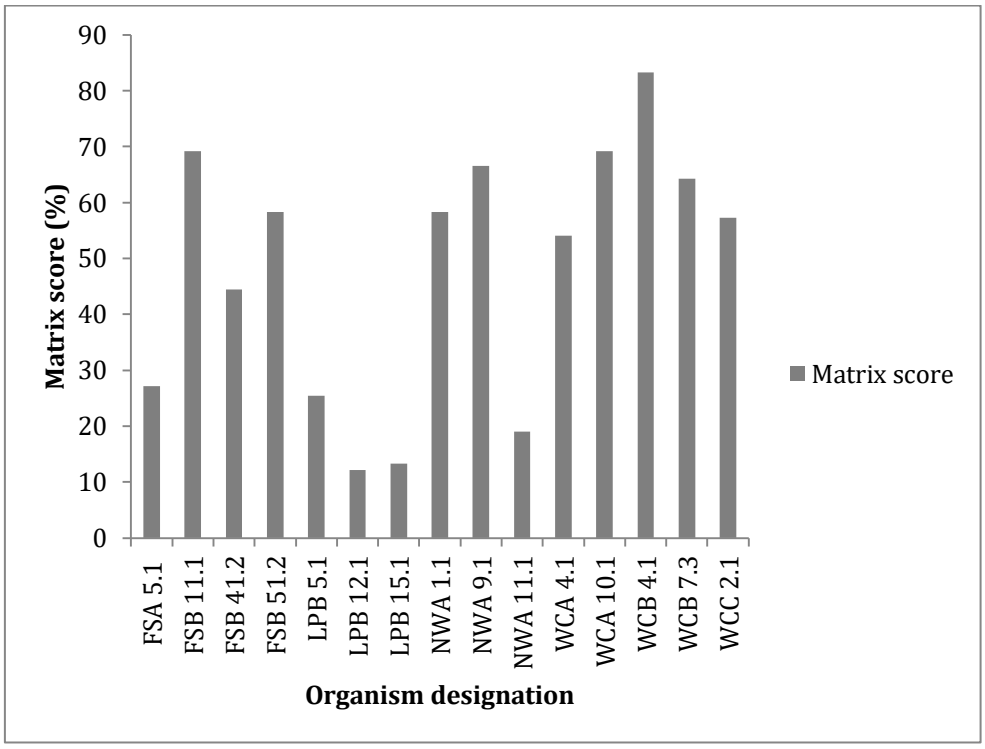


Figure A1: Bar graph indicating the matrix score of each respective studied isolate.

Appendix B

Chapter 4 data

Inqaba sequencing primers

Table B1: 18s primers used as described by Lin et al. 2012 (Lin et al., 2012).

Name of Primer	Target	Sequence (5' to 3')
18S-AB1	18S rDNA sequence	GGAGGATTAGGGTCCGATTCC
18S-TW4	18S rDNA sequence	CTTCCGTCAATTCCTTTAAG

Medium compositions

Table B2: Eleven identified medium compositions.

Media Component	Unit	AF6	BBM	C Medium	Chu #10	DY-V Medium	Franquil
MES buffer	mM	2.05				1.02	
Fe-citrate	mM	0.008					
Citric acid	mM	0.010					
NaNO3	mM	1.64	2.94			0.235	0.1
NH4NO3	mM	0.275					
$MgSO_4.7H_2O$	mM	0.122	0.304		0.101	0.203	0.15
KH2PO4	mM	0.074	1.29				
K2HPO4	mM	0.029	0.431		0.0287		0.01
CaCl2.2H2O	mM	0.068	0.17			0.676	0.25
KNO3	mM			0.989			
KOH	mM		0.553				
TRIS	mM			4.13			
Ca(NO3)2. 4H2O	mM			0.635	0.244		
Na2glycerophosphate	mM			0.162		0.01	
Na2CO3	mM				0.189		
NaSiO3	mM				0.205	0.0493	0.0355
FeCl3	mM	0.004		2.15 E-03	4.93 E-03	3.7 E-03	0.451 E-03
KCl	mM					0.04	
NH4Cl	mM					0.05	
NaHCO3	mM						0.15
Na2EDTA	mM	0.013	0.171	0.008		0.022	0.005
MnCl2	mM	0.001	0.728 E-03	0.546 E-03		0.001	0.02 E-03
ZnSO4	mM	0.38 E-03	0.031		0.8 E-06	0.14 E-03	0.4 E-05
CoCl2	mM	0.08 E-03		0.509 E-04		0.03 E-03	0.3 E-05
Na2MoO4	mM	0.05 E-03		0.156 E-03		0.083 E-03	
FeSO4	mM		0.018				
H3BO4	mM		0.185		0.401 E-04		
MoO3	mM		0.005				
CuSO4	mM		0.006		0.4 E-06		0.1 E-05
Co(NO3)2	mM		0.002		0.5 E-06		
MnSO4	mM				0.9 E-05		
ZnCl2	mM			0.23 E-03			
Thiamine	nM	29.6	0.452	29.7	148	296	296
Biotin	nM	8.19	0.512	0.409	10.2	2.05	2.05
Peridoxine	nM	5.91					
Cyanocobalamin	nM	0.738	0.092	0.074	1.84	0.369	0.406

Media Component	Unit	WC	Hase	Lu	Zarrouk	JG
MES buffer	mM					1
Fe-citrate	mM					
Citric acid	mM					0.010
NaNO3	mM	1	2.65	17.648	29.414	1
NH4NO3	mM					
$MgSO_4.7H_2O$	mM	0.15	0	0.304	6.548	0.15
KH2PO4	mM					0.188
K2HPO4	mM	0.05	0.126	0.230	2.870	0
CaCl2.2H2O	mM	0.25	0	0.245	0.272	0.2
KNO3	mM					2
KOH	mM					
TRIS	mM	4.13				
Ca(NO3)2. 4H2O	mM					
Na2glycerophosphate	mM					
Na2CO3	mM		0	0.050	0	
NaSiO3	mM	0.1	0.115	0.012	0	
FeCl3	mM	0.0117	0.035	0	0	0.003
KCl	mM					
NH4Cl	mM					
NaHCO3	mM	0.15	0	0	199.983	6.625
Na2EDTA	mM	0.012	0.035	0	0.215	0.005
MnCl2	mM	0.001	0.004	0.1 E-03	0.14 E-03	0.2 E-03
ZnSO4	mM	0.08 E-03	0.2 E-03	7.65 E-06	7.72 E-06	0.7 E-04
CoCl2	mM	0.04 E-03				0.15 E-04
Na2MoO4	mM	0.02 E-03	8.68 E-05	1.61 E-05	0	0.517 E-04
FeSO4	mM		0	0	0.036	0.0179
H3BO4	mM	0.016	0	0.37 E-03	0.37 E-03	
MoO3	mM		0	0	1.04 E-06	
CuSO4	mM	0.04 E-03	8.41 E-05	3.20 E-06	2.96 E-06	0.4 E-05
Co(NO3)2	mM		0	1.72 E-06	0	
MnSO4	mM					
ZnCl2	mM					
Thiamine	nM	296	1.131	0	0	29.6
Biotin	nM	2.05	0.006	0	0	8.19
Peridoxine	nM		0	0	0	5.91
Cyanocobalamin	nM	0.369	0.001	0	0	0.738

Biomass over time

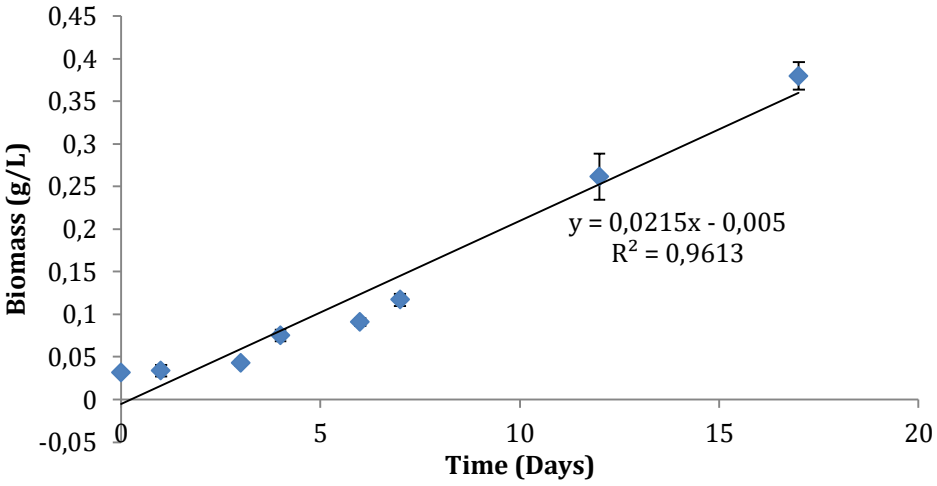


Figure B2: Biomass over time for WCB 4.1 cultured in AF6 medium. The trendline slope indicates biomass productivity and the error bars indicates standard deviation.

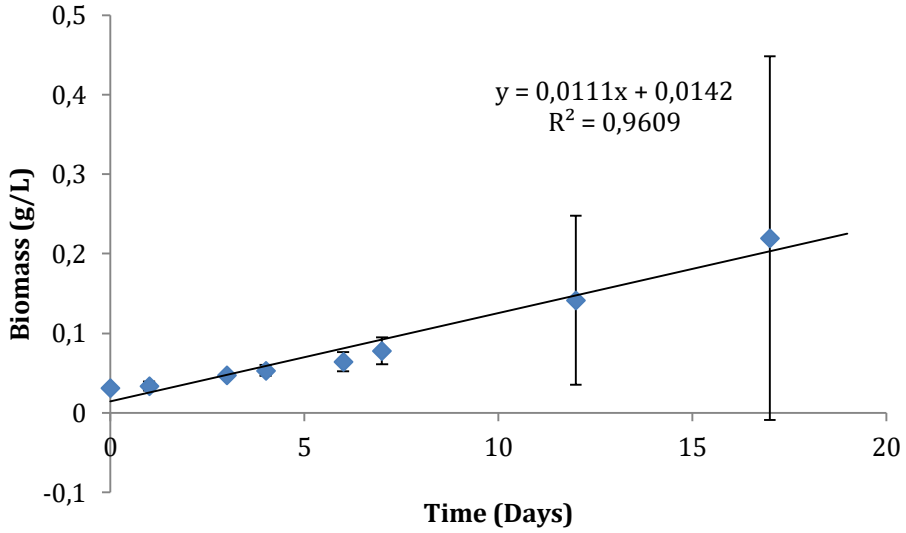


Figure B3: Biomass over time for WCB 4.1 cultured in BBM medium. The trendline slope indicates biomass productivity and the error bars indicates standard deviation.

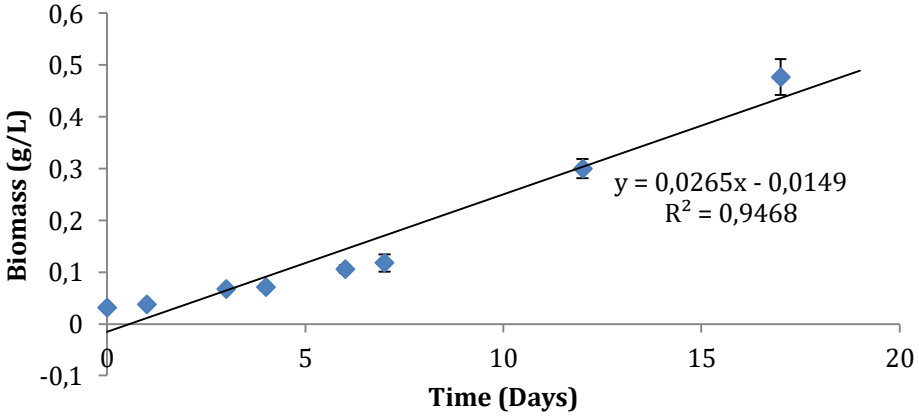


Figure B4: Biomass over time for WCB 4.1 cultured in C-medium. The trendline slope indicates biomass productivity and the error bars indicates standard deviation.

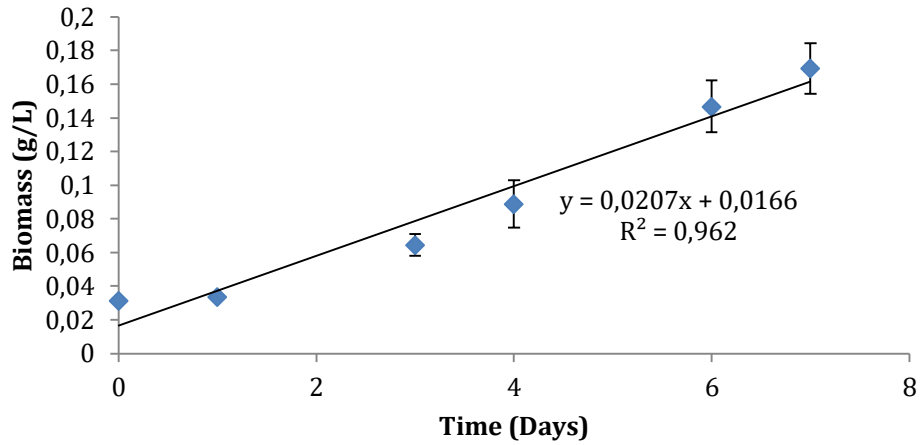


Figure B5: Biomass over time for WCB 4.1 cultured in Chu#10 medium. The trendline slope indicates biomass productivity and the error bars indicates standard deviation.

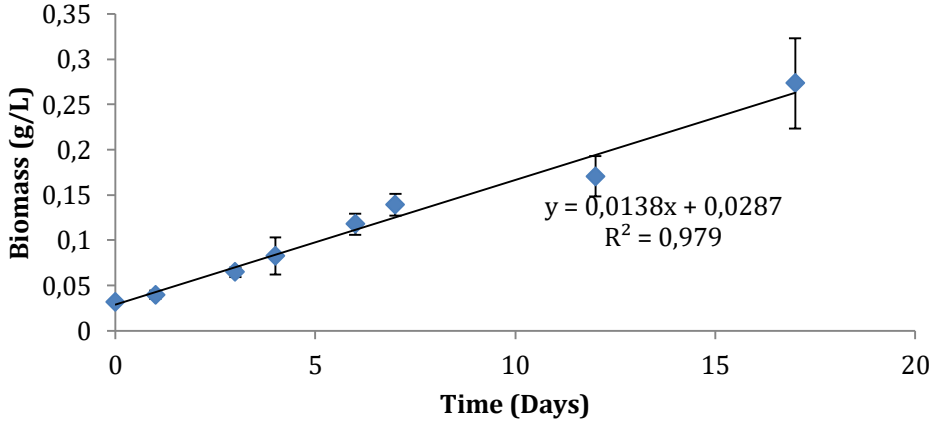


Figure B6: Biomass over time for WCB 4.1 cultured in DYV medium. The trendline slope indicates biomass productivity and the error bars indicates standard deviation.

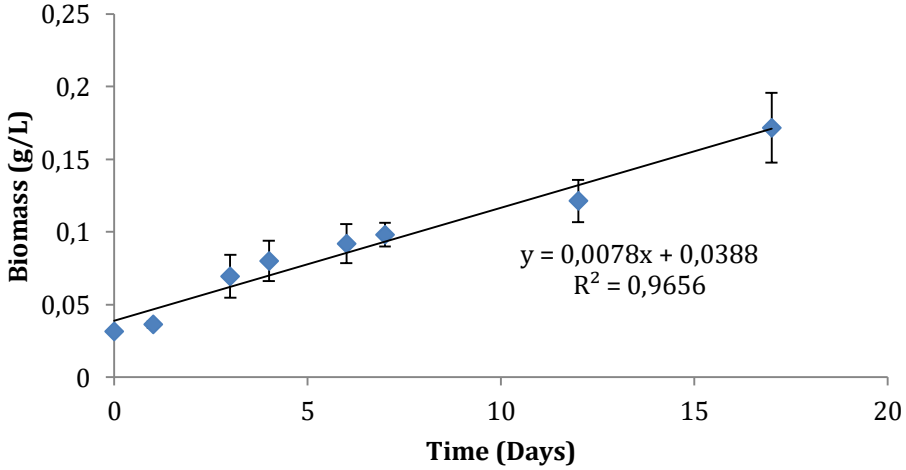


Figure B7: Biomass over time for WCB 4.1 cultured in Franquil medium. The trendline slope indicates biomass productivity and the error bars indicates standard deviation.

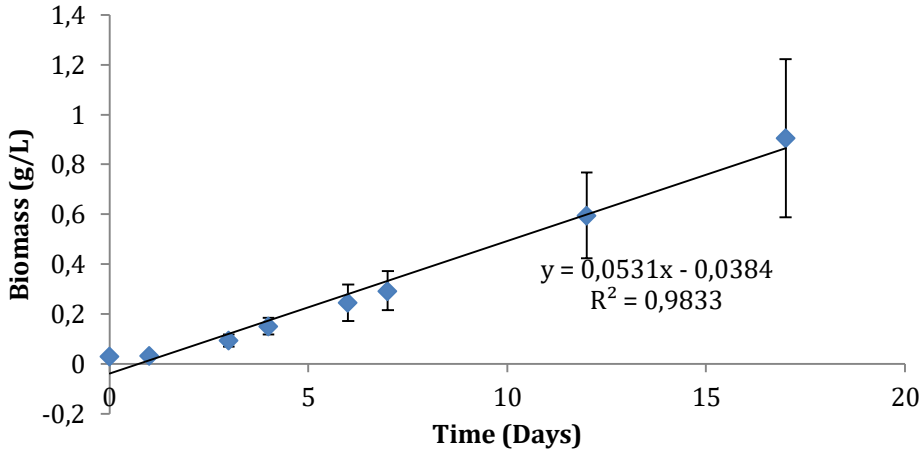


Figure B8: Biomass over time for WCB 4.1 cultured in Hase medium. The trendline slope indicates biomass productivity and the error bars indicates standard deviation.

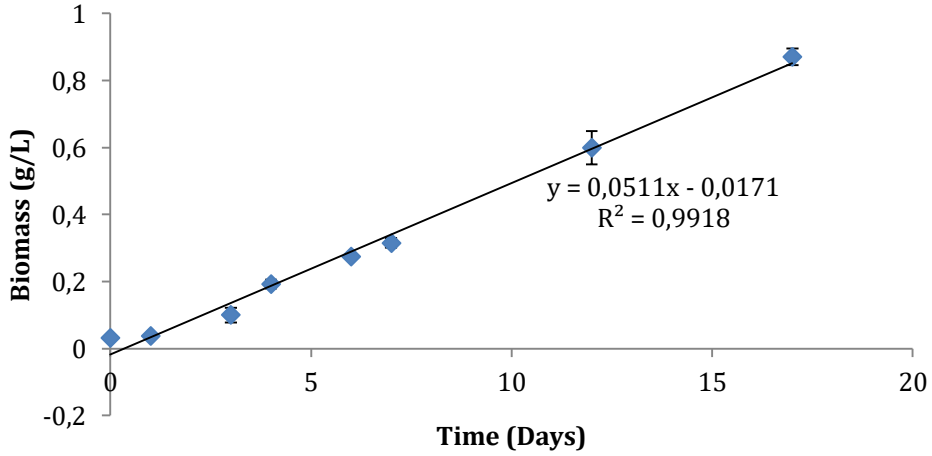


Figure B9: Biomass over time for WCB 4.1 cultured in JG medium. The trendline slope indicates biomass productivity and the error bars indicates standard deviation.

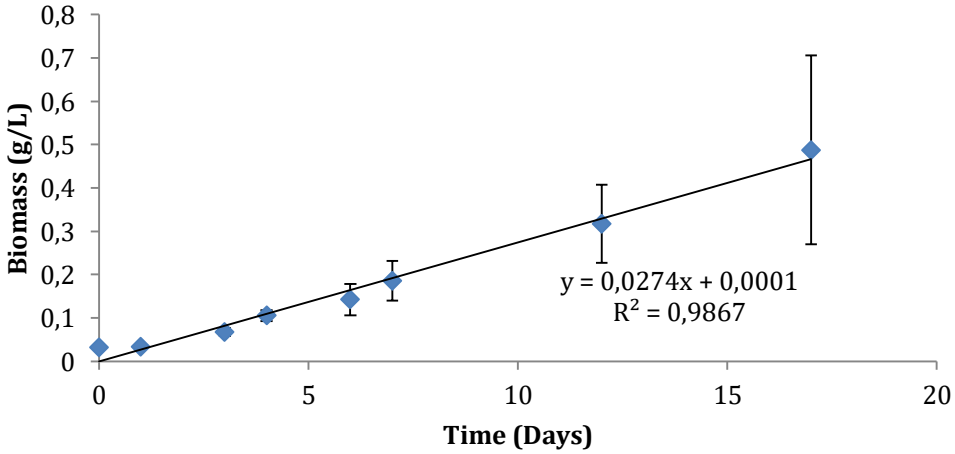


Figure B10: Biomass over time for WCB 4.1 cultured in Lu medium. The trendline slope indicates biomass productivity and the error bars indicates standard deviation.

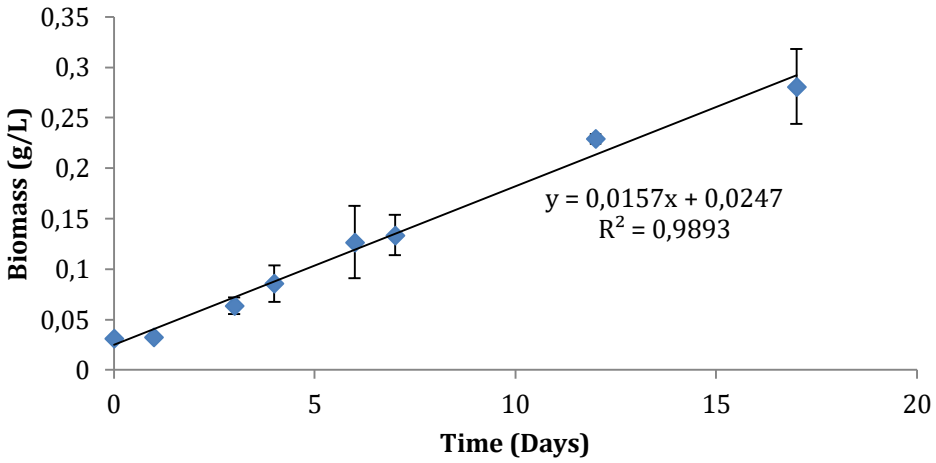


Figure B11: Biomass over time for WCB 4.1 cultured in WC medium. The trendline slope indicates biomass productivity and the error bars indicates standard deviation.

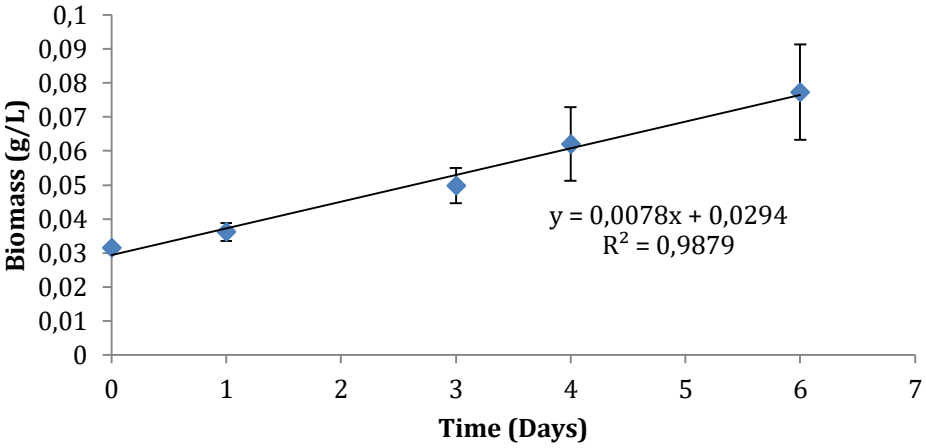


Figure B12: Biomass over time for WCB 4.1 cultured in Zarrouk medium. The trendline slope indicates biomass productivity and the error bars indicates standard deviation.

Growth rates

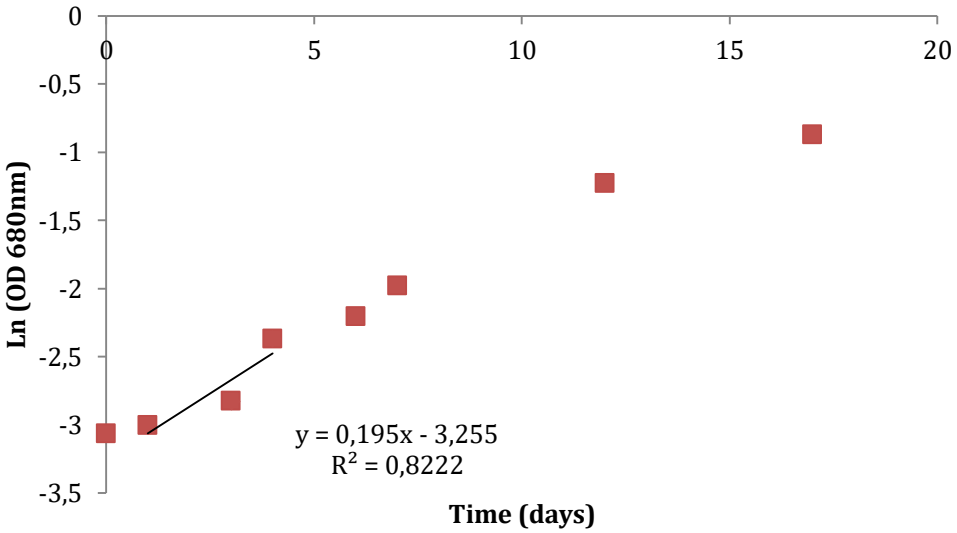


Figure B13: Ln (OD) curve of WCB 4.1 cultivated in AF6 medium. The slope of the trend line indicates the growth rate.

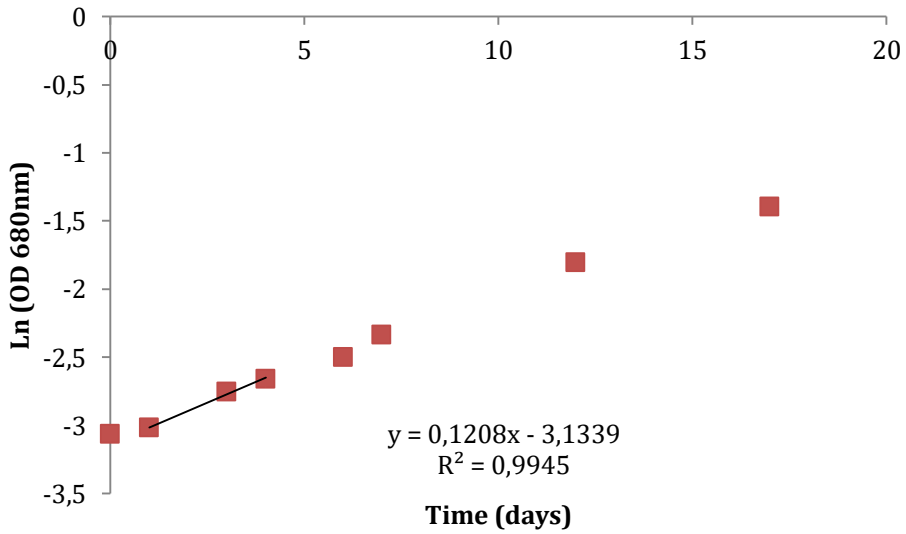


Figure B14: Ln (OD) curve of WCB 4.1 cultivated in BBM medium. The slope of the trend line indicates the growth rate.

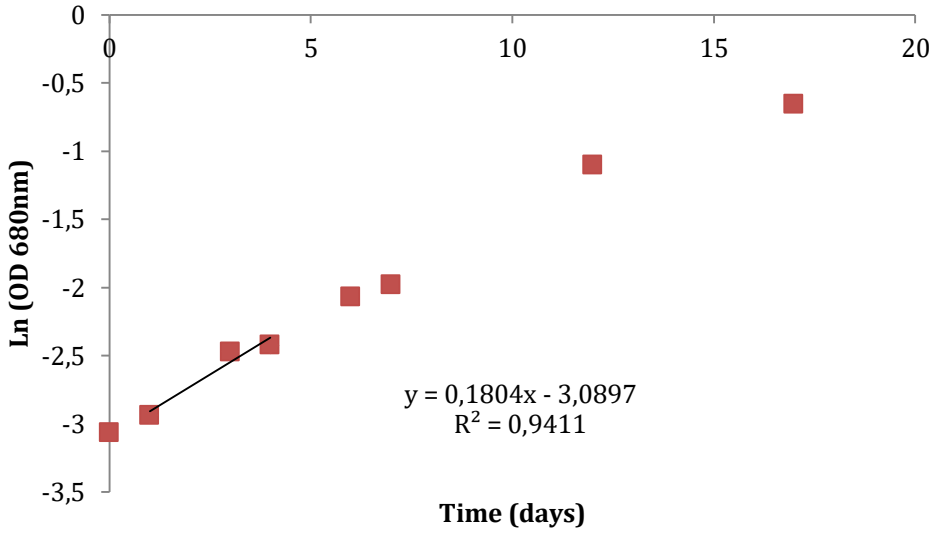


Figure B15: Ln (OD) curve of WCB 4.1 cultivated in C-medium. The slope of the trend line indicates the growth rate.

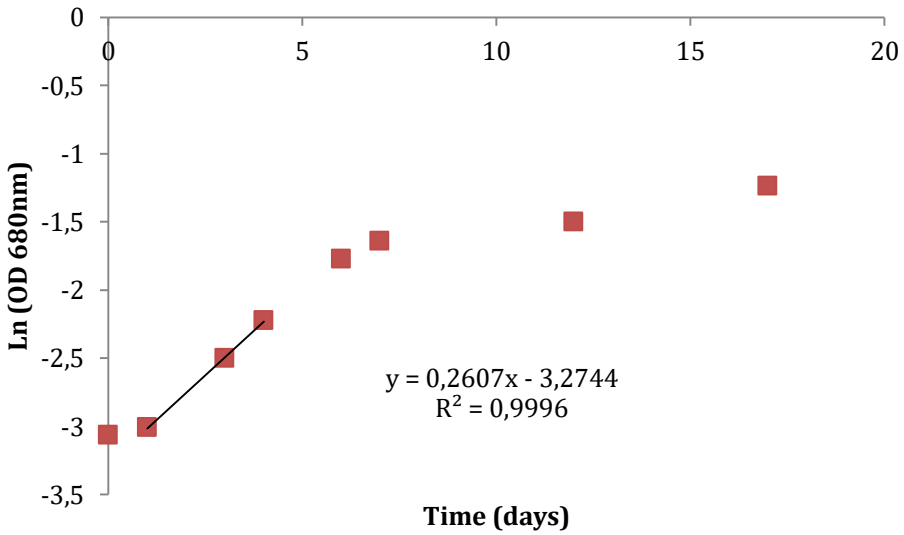


Figure B16: Ln (OD) curve of WCB 4.1 cultivated in Chu#10 medium. The slope of the trend line indicates the growth rate.

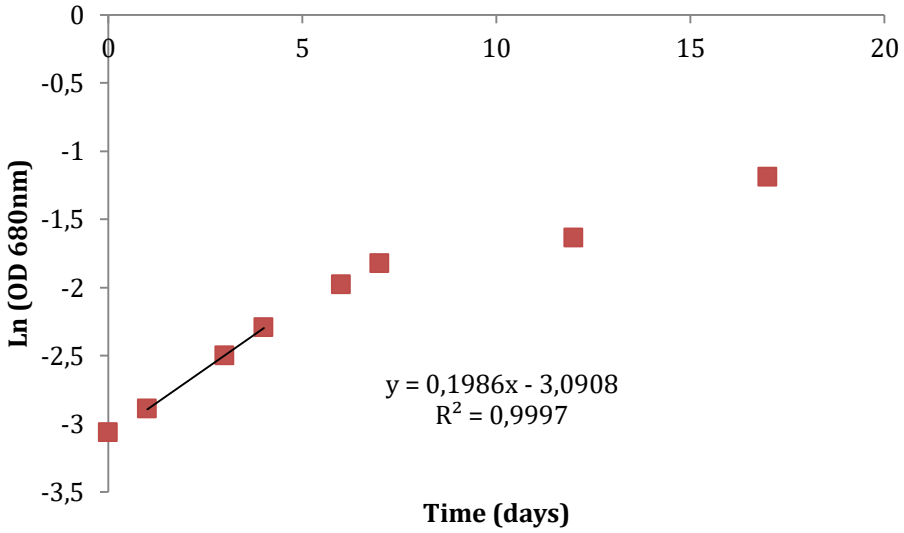


Figure B17: Ln (OD) curve of WCB 4.1 cultivated in DYV medium. The slope of the trend line indicates the growth rate.

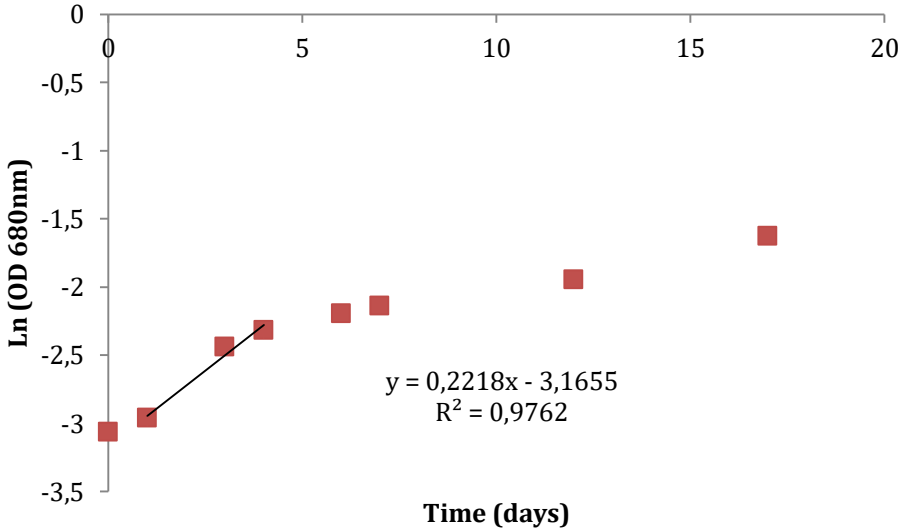


Figure B18: Ln (OD) curve of WCB 4.1 cultivated in Franquil medium. The slope of the trend line indicates the growth rate.

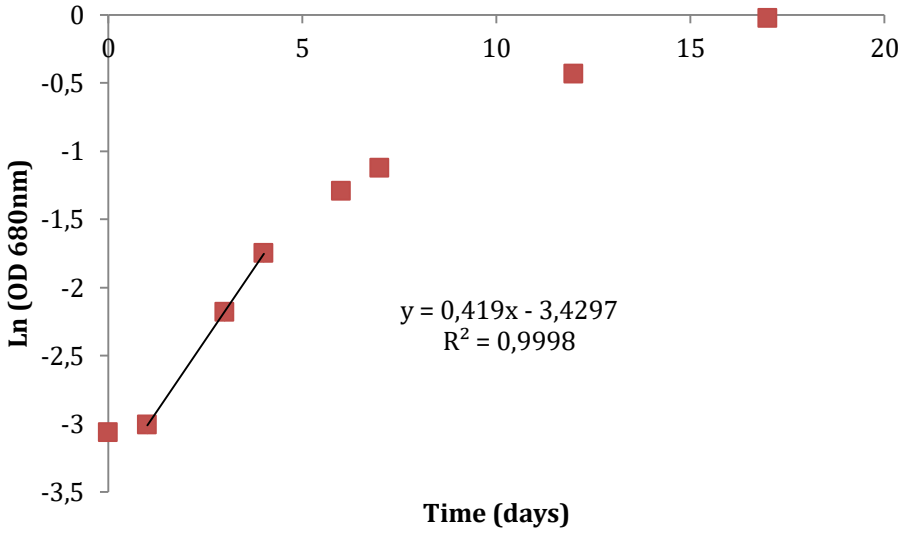


Figure B19: Ln (OD) curve of WCB 4.1 cultivated in Hase medium. The slope of the trend line indicates the growth rate.

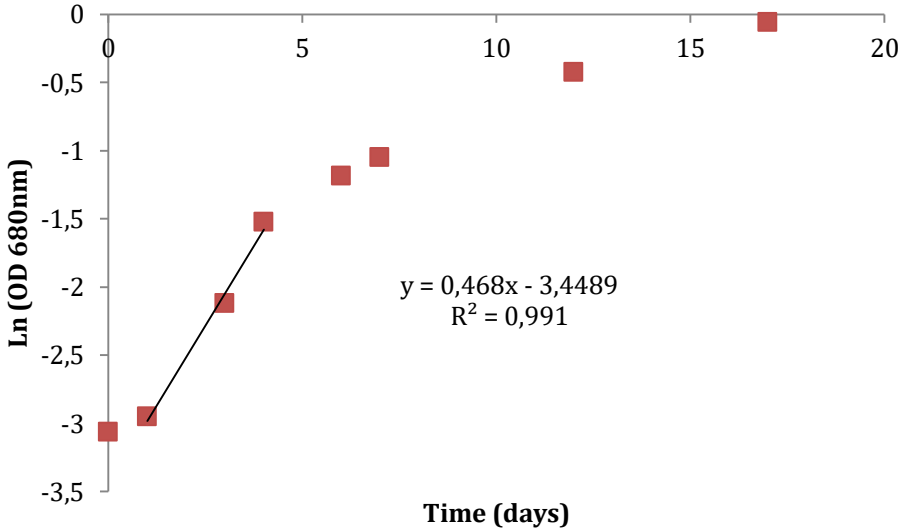


Figure B20: Ln (OD) curve of WCB 4.1 cultivated in JG medium. The slope of the trend line indicates the growth rate.

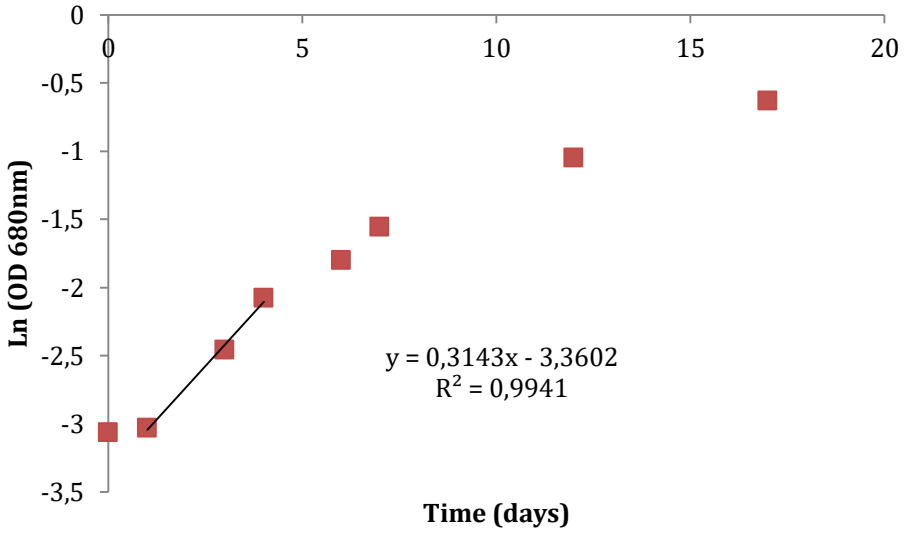


Figure B21: Ln (OD) curve of WCB 4.1 cultivated in Lu medium. The slope of the trend line indicates the growth rate.

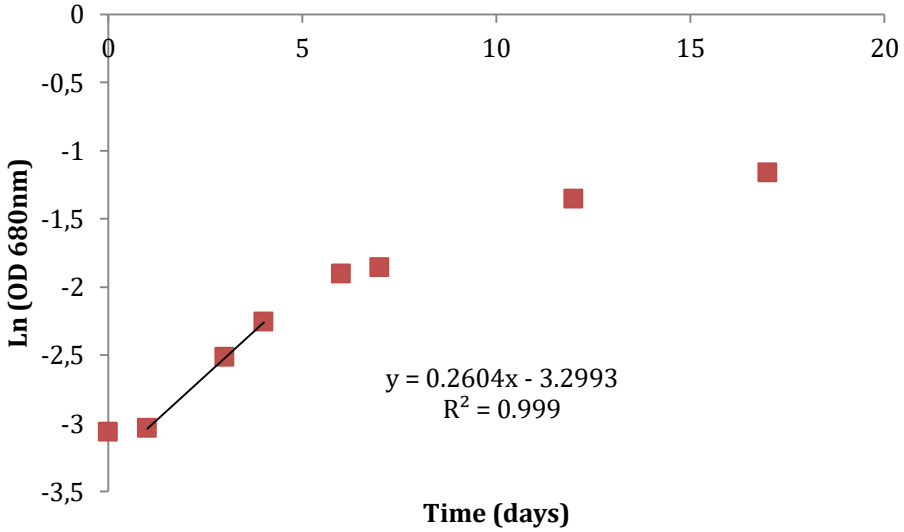


Figure B22: Ln (OD) curve of WCB 4.1 cultivated in WC medium. The slope of the trend line indicates the growth rate.

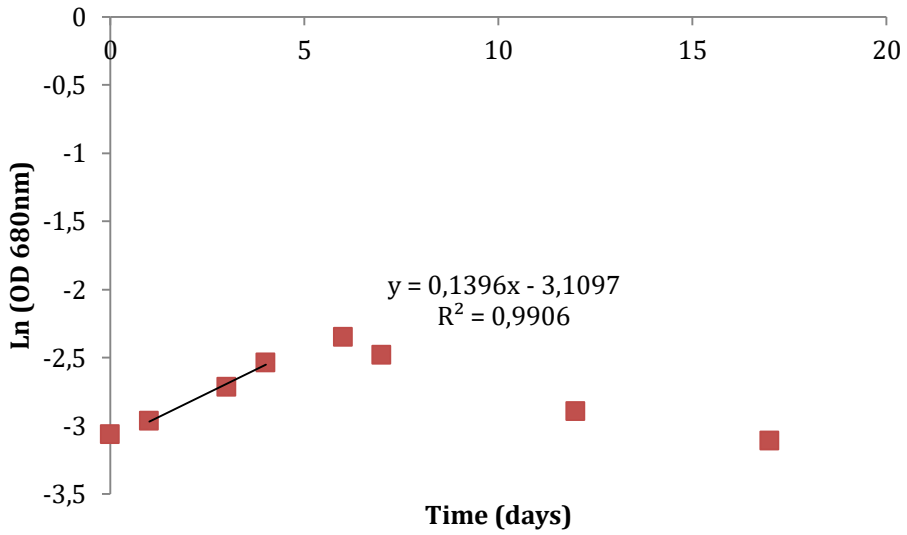


Figure B23: Ln (OD) curve of WCB 4.1 cultivated in Zarrouk medium. The slope of the trend line indicates the growth rate.

Table B3: Medium specific growth rates and yield rates of WCB 4.1

Medium designation	Growth rate (d^{-1})	Growth rate standard deviation	Biomass productivity $mg.L^{-1}.d^{-1}$	Biomass productivity Standard deviation
AF6	0.20	0.031648	21.2	2.657693
BBM	0.12	0.063753	11.1	5.288667
CMEDIUM	0.18	0.03514	26.5	3.098925
CHU 10	0.26	0.036966	20.7	2.145538
DYV	0.20	0.057705	13.8	0.57735
Franquil	0.22	0.069934	7.8	1.006645
Hase	0.42	0.068092	53.1	10.81866
JG	0.47	0.015623	51.1	1.8037
LU	0.31	0.062587	27.4	5.946708
WC	0.26	0.06673	15.7	0.550757
Zarrouk	0.14	0.045929	7.8	2.066398

Appendix C

Chapter 5 data

Fame standard curves

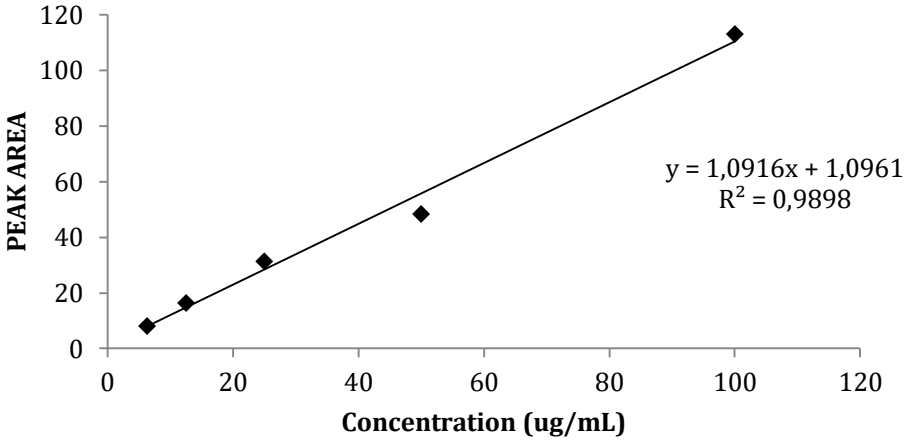


Figure C1: C6:0 FAME-GC standard curve.

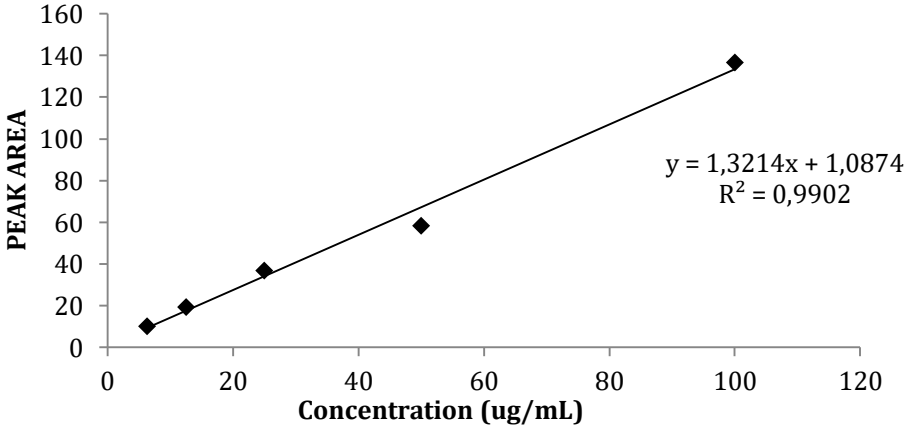


Figure C2: C8:0 FAME-GC standard curve.

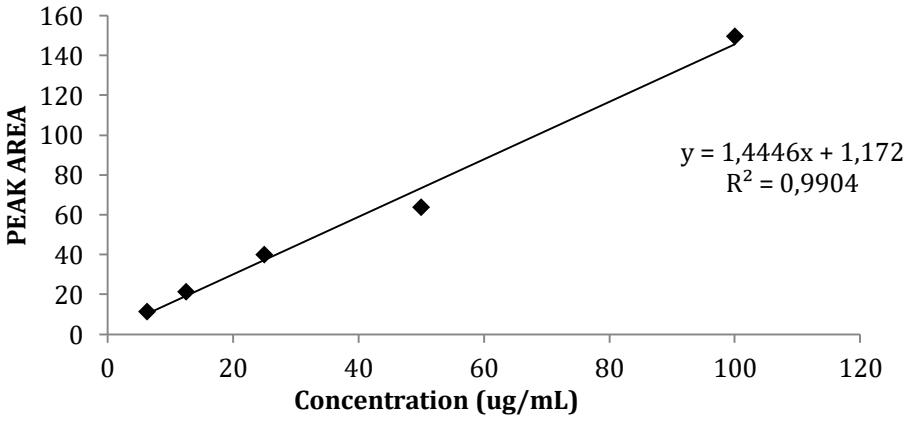


Figure C3: C10:0 FAME-GC standard curve.

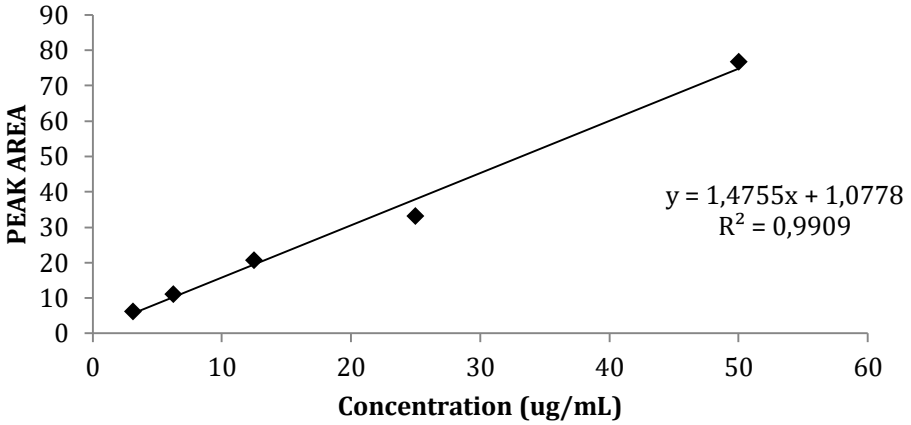


Figure C4: C11:0 FAME-GC standard curve.

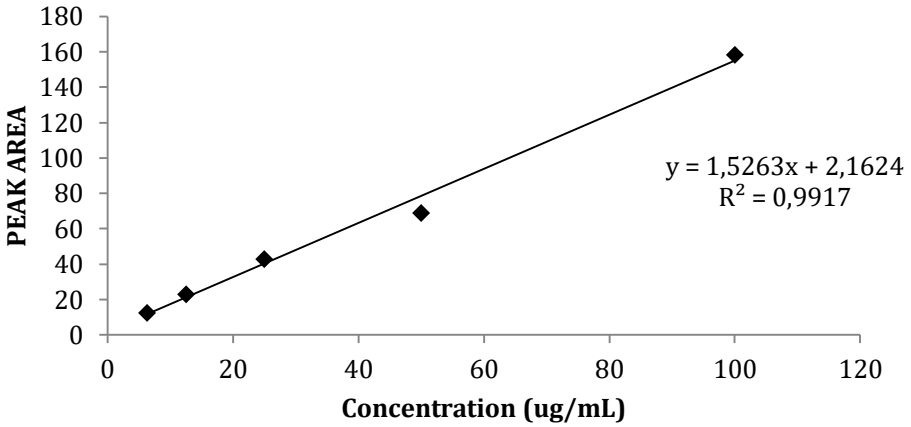


Figure C5: C12:0 FAME-GC standard curve.

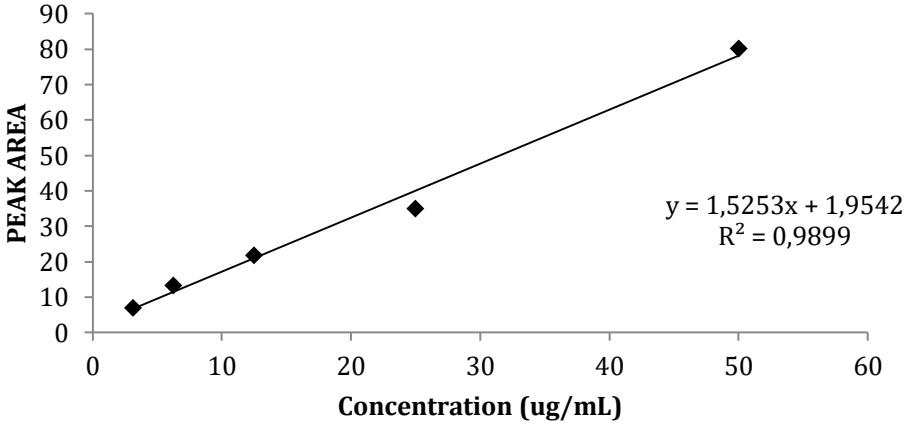


Figure C6: C13:0 FAME-GC standard curve.

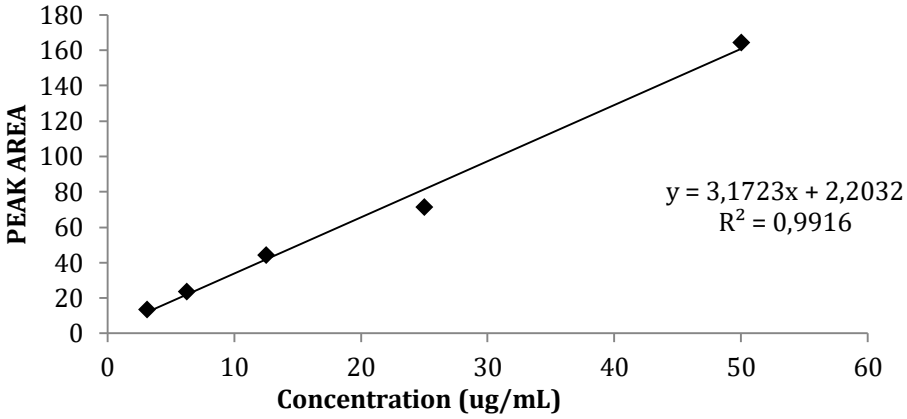


Figure C7: C15:0 FAME-GC standard curve.

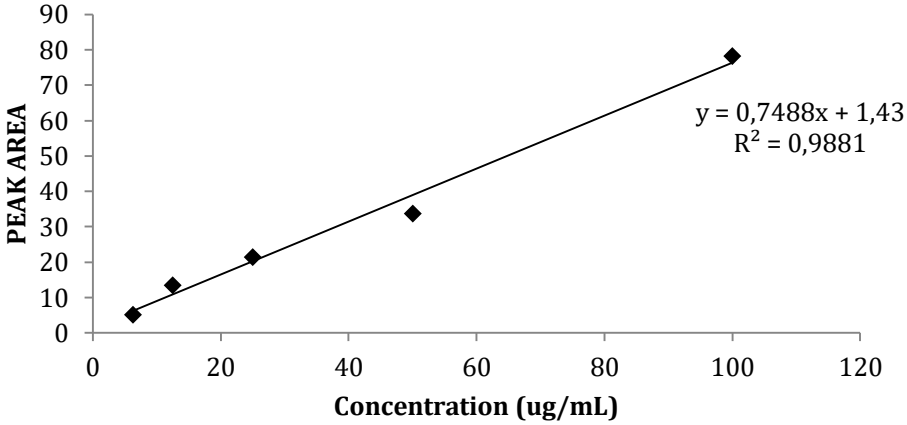


Figure C8: C14:0 FAME-GC standard curve.

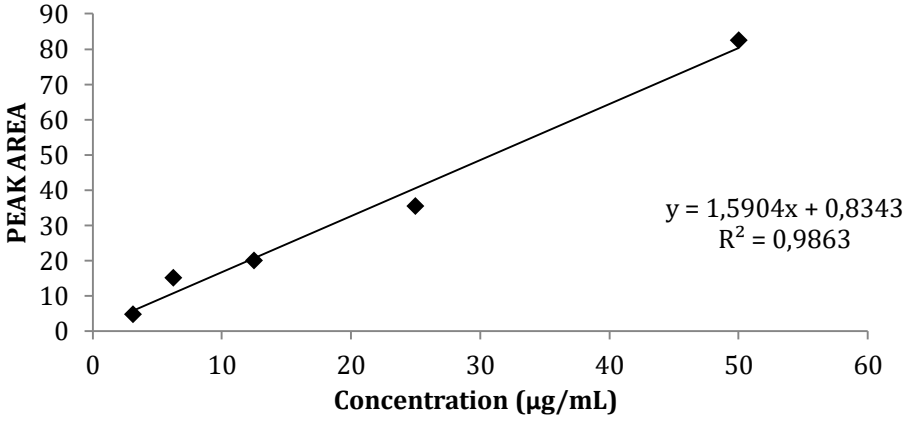


Figure C9: C14:1 FAME-GC standard curve.

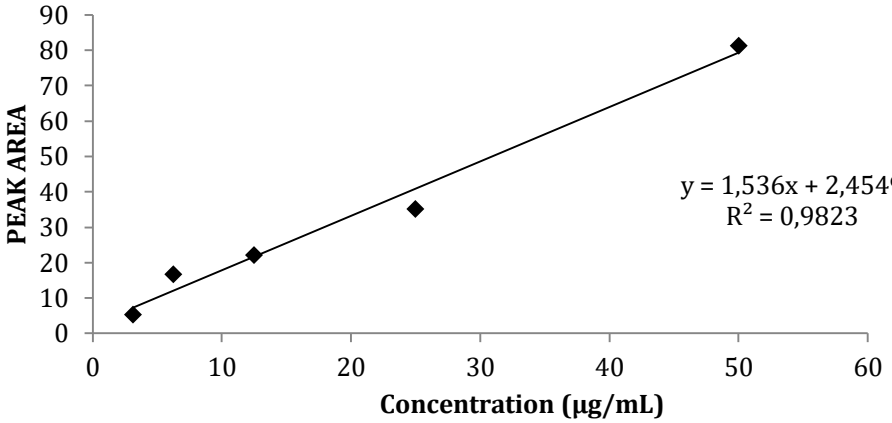


Figure C10: C15:1 FAME-GC standard curve.

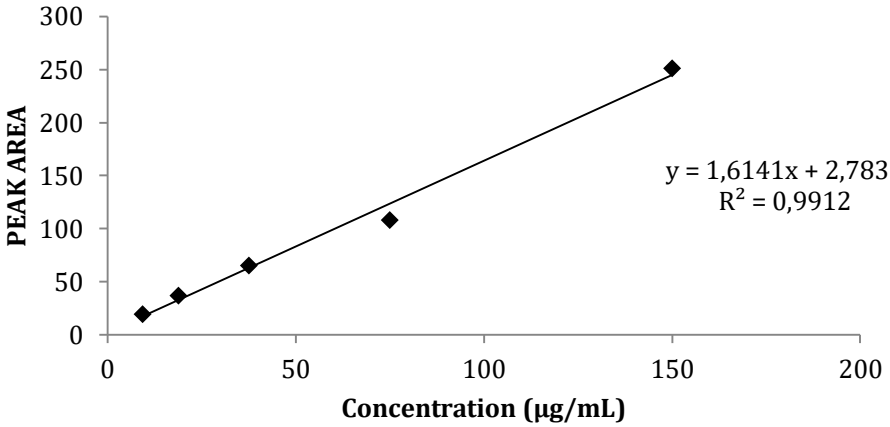


Figure C11: C16:0 FAME-GC standard curve.

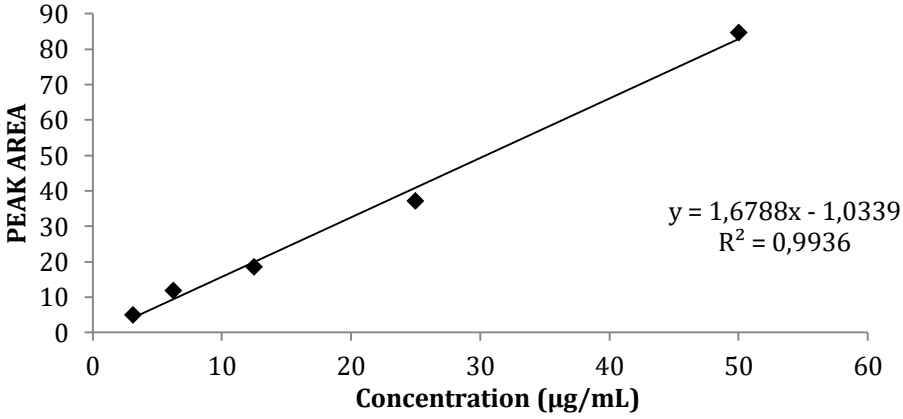


Figure C12: C16:1 FAME-GC standard curve.

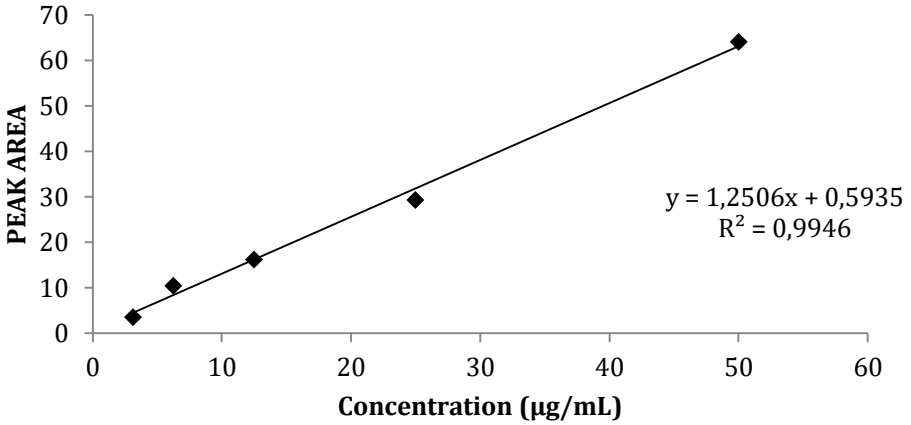


Figure C13: C17:0 FAME-GC standard curve.

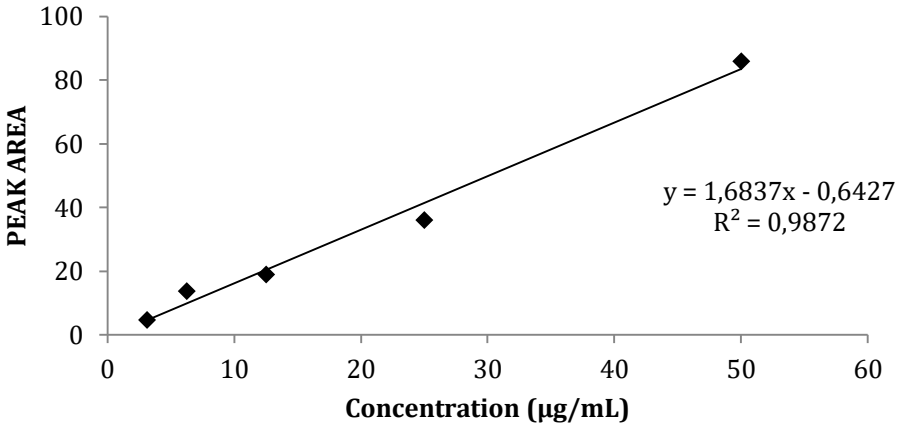


Figure C14: C17:1 FAME-GC standard curve.

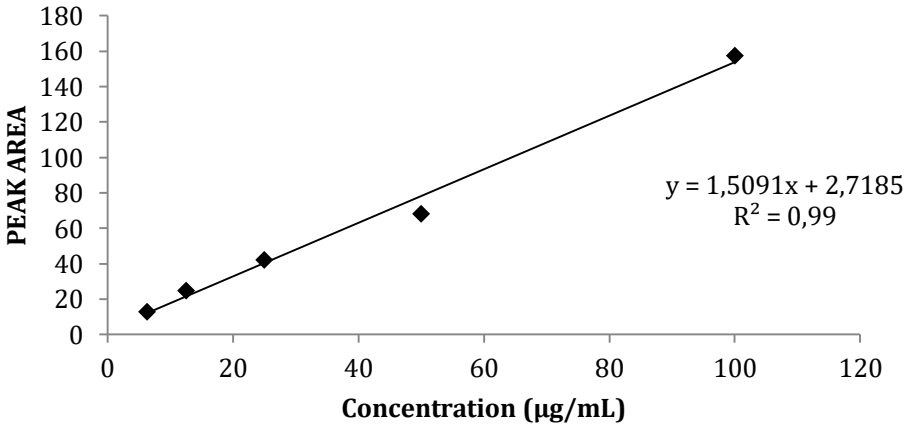


Figure C15: C18:0 FAME-GC standard curve.

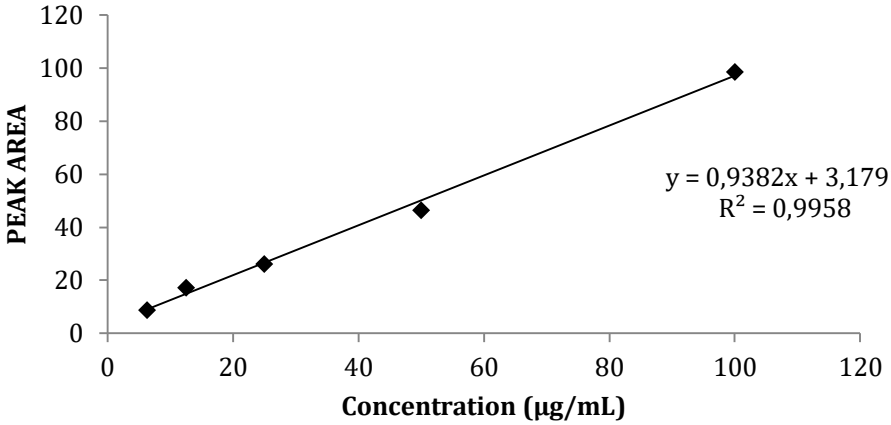


Figure C16: C18:1n9c FAME-GC standard curve.

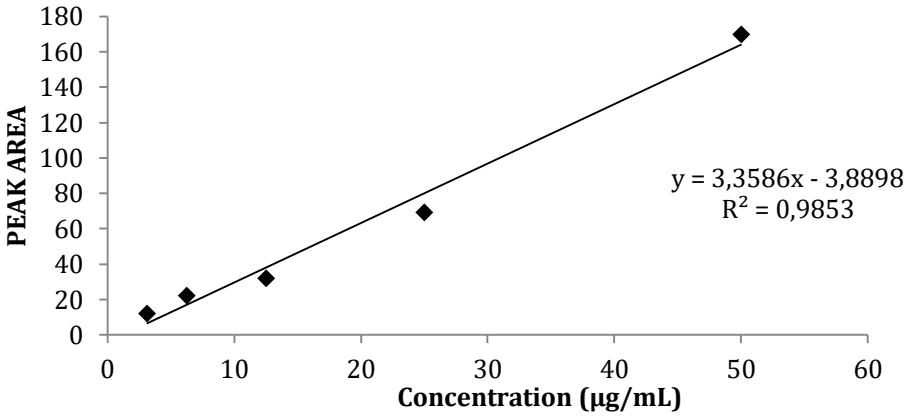


Figure C17: C18:1n9t FAME-GC standard curve.

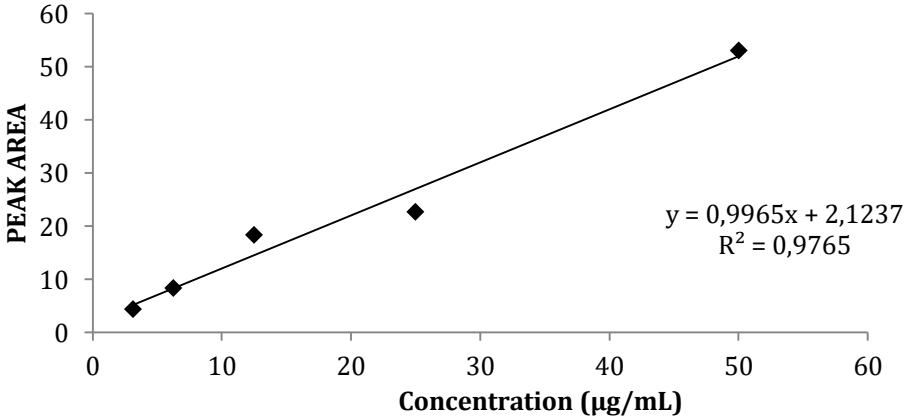


Figure C18: C18:2n6c FAME-GC standard curve.

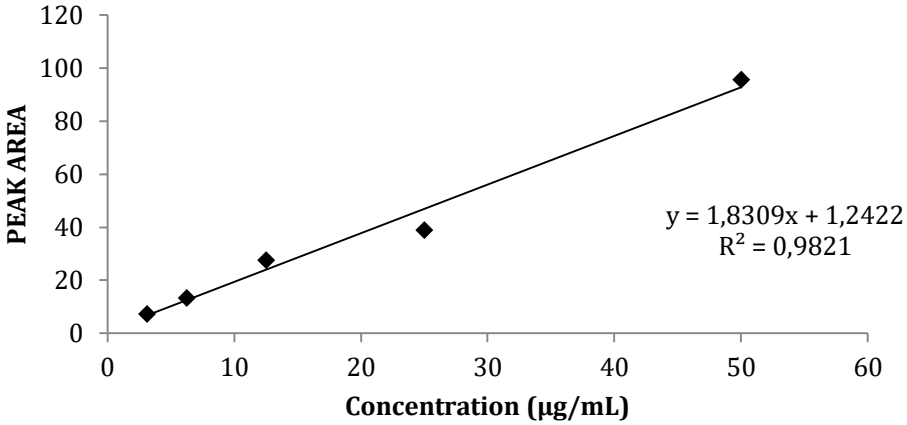


Figure C19: C18:2n6t FAME-GC standard curve.

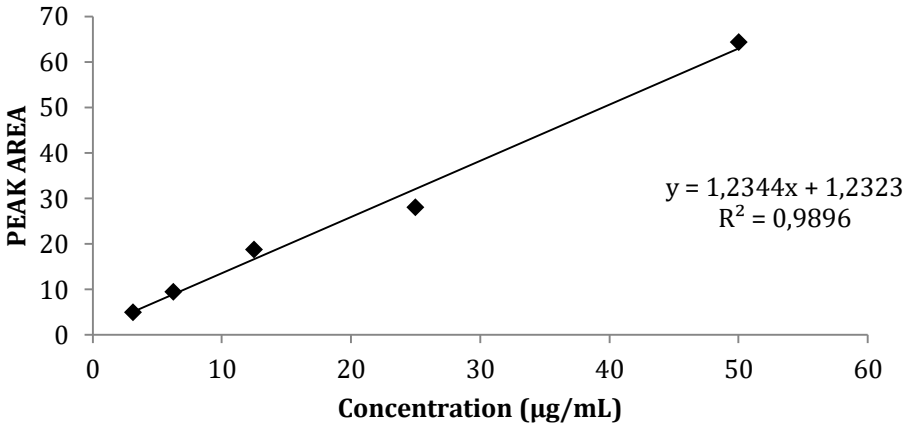


Figure C20: C18:3n6 FAME-GC standard curve.

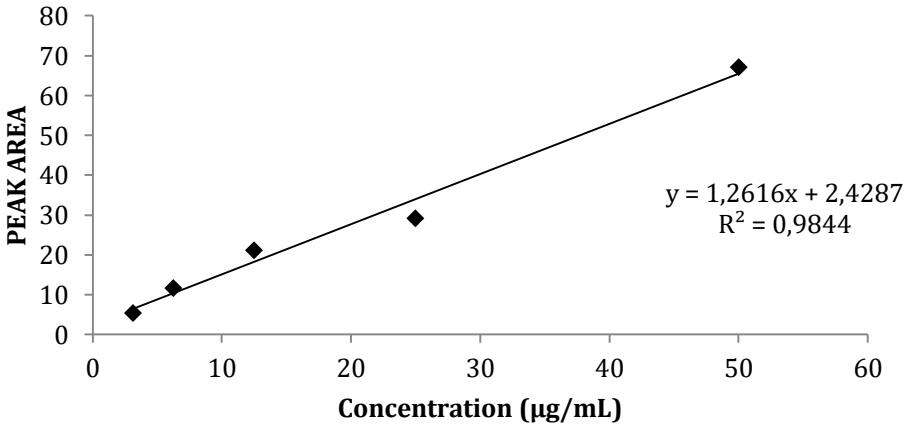


Figure C21: C18:3n3 FAME-GC standard curve.

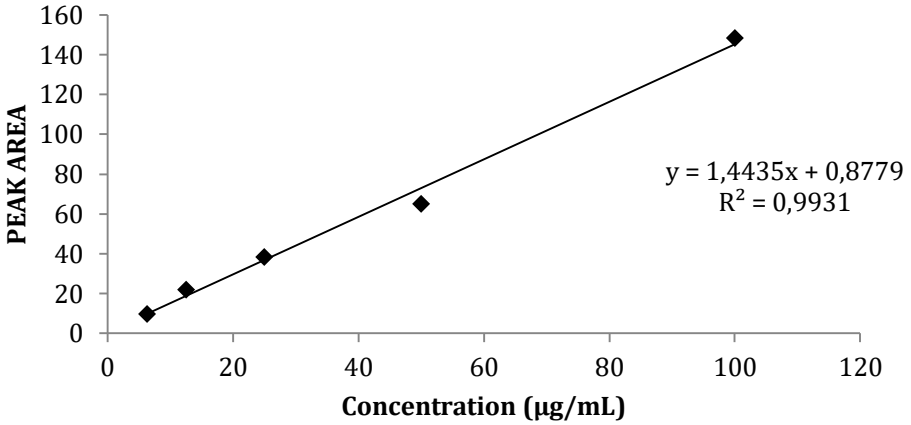


Figure C22: C20:0 FAME-GC standard curve.

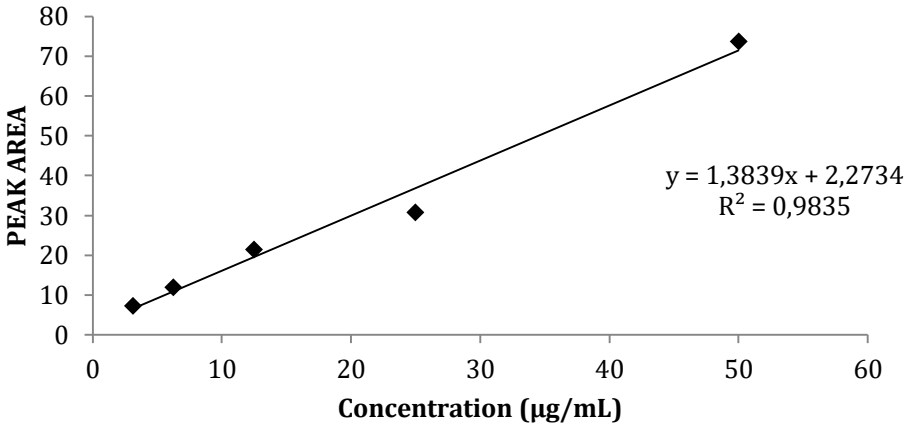


Figure C23: C20:2 FAME-GC standard curve.

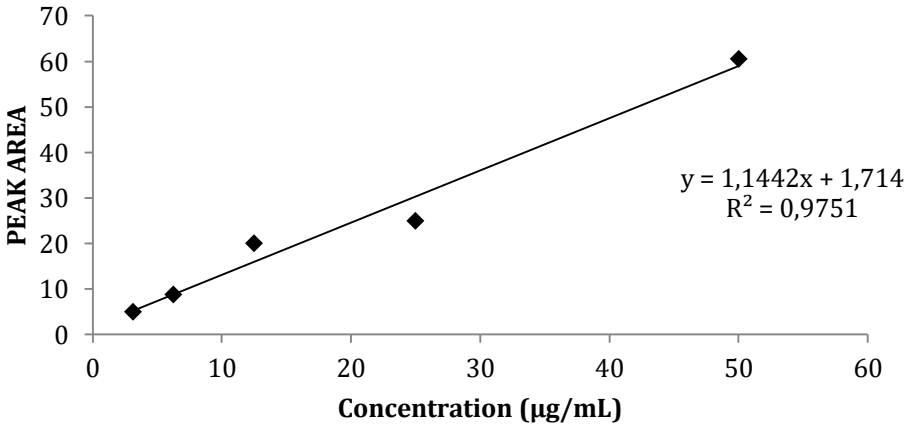


Figure C24: C20:3n6 FAME-GC standard curve.

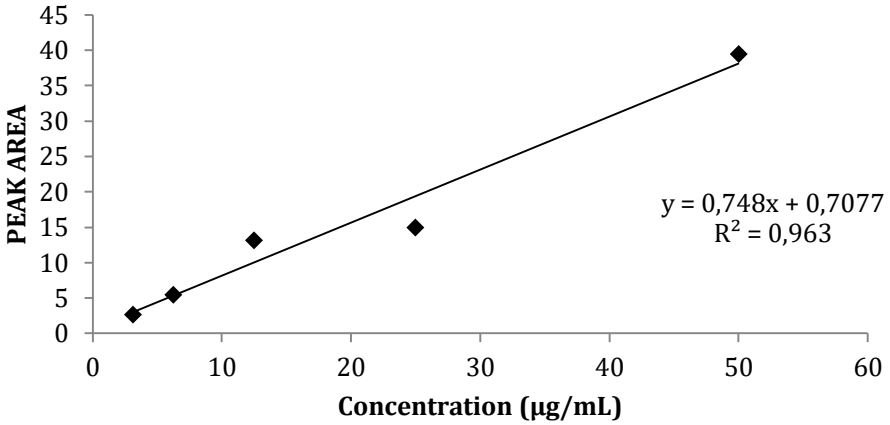


Figure C25: C21:0 FAME-GC standard curve.

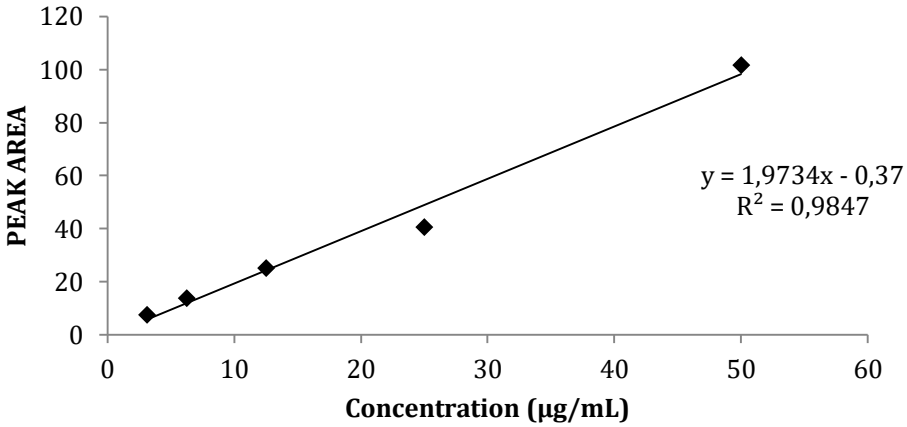


Figure C26: C20:3n3 FAME-GC standard curve.

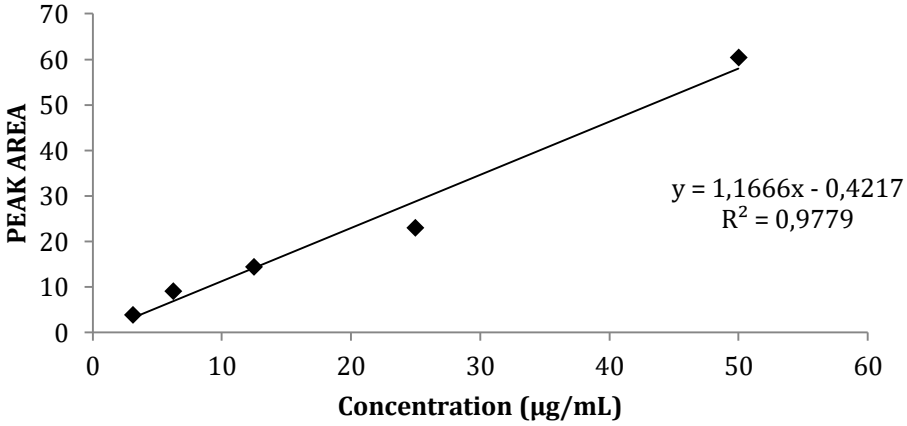


Figure C27: C20:4n6 FAME-GC standard curve.

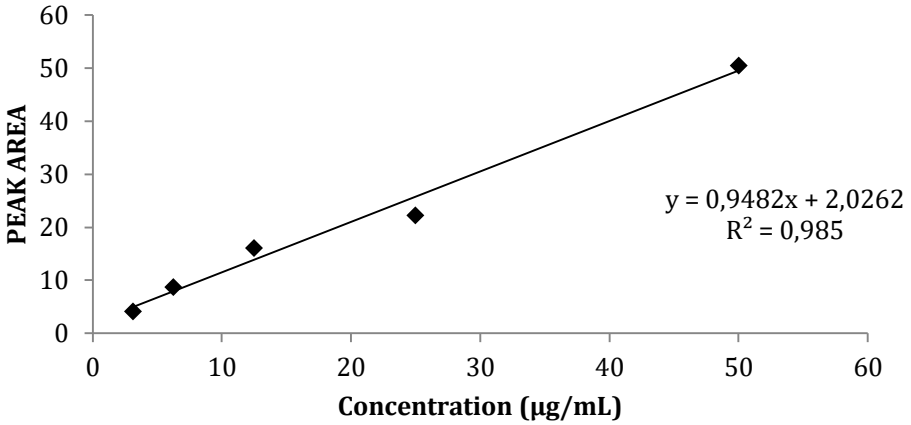


Figure C28: C20:5n3 FAME-GC standard curve.

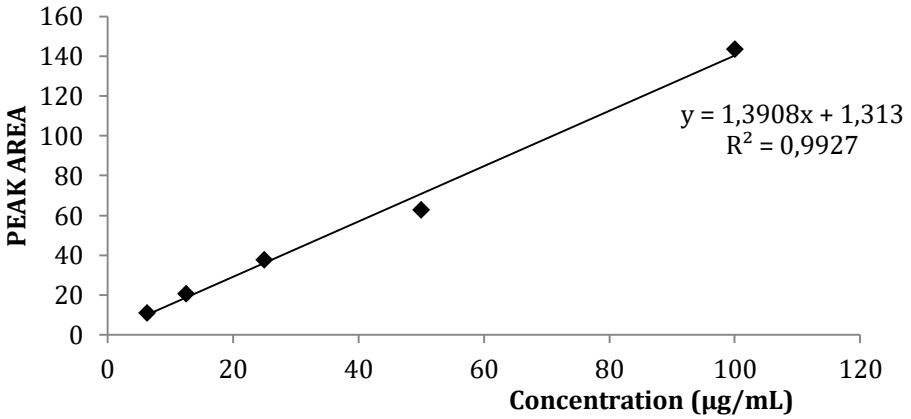


Figure C29: C22:0 FAME-GC standard curve.

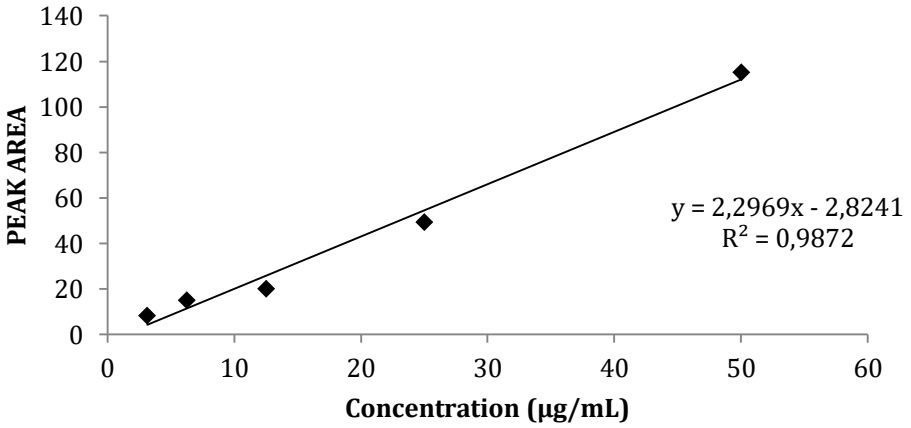


Figure C30: C22:1n9 FAME-GC standard curve.

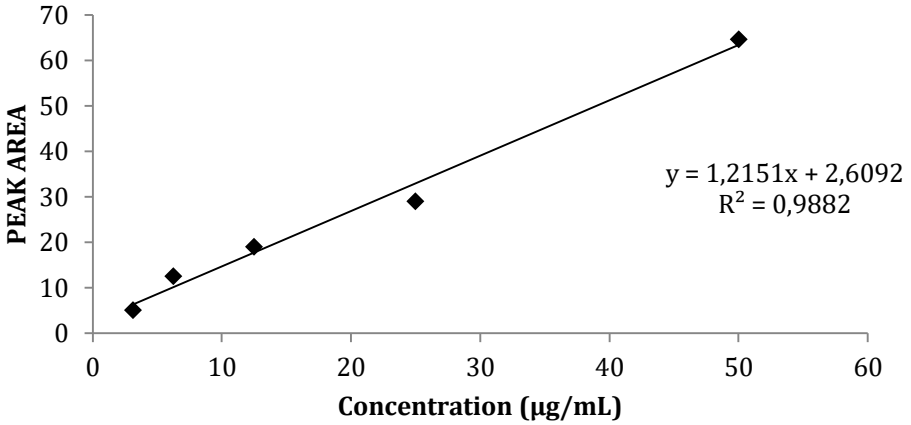


Figure C31: C22:2 FAME-GC standard curve.

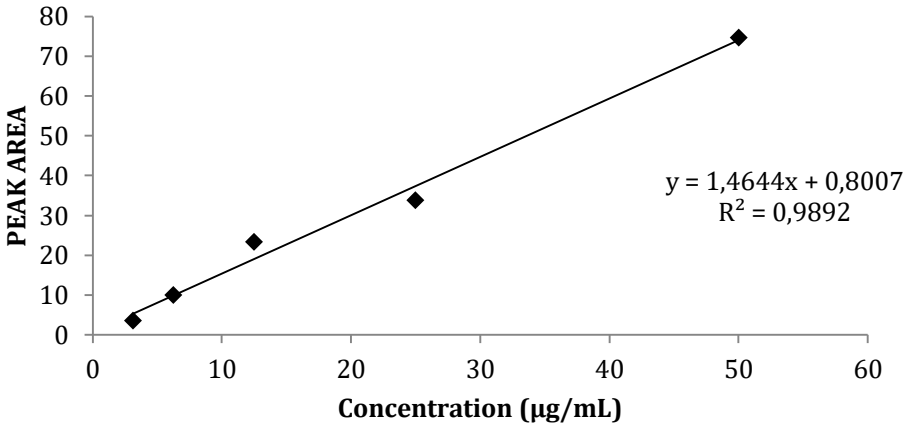


Figure C32: C23:0 FAME-GC standard curve.

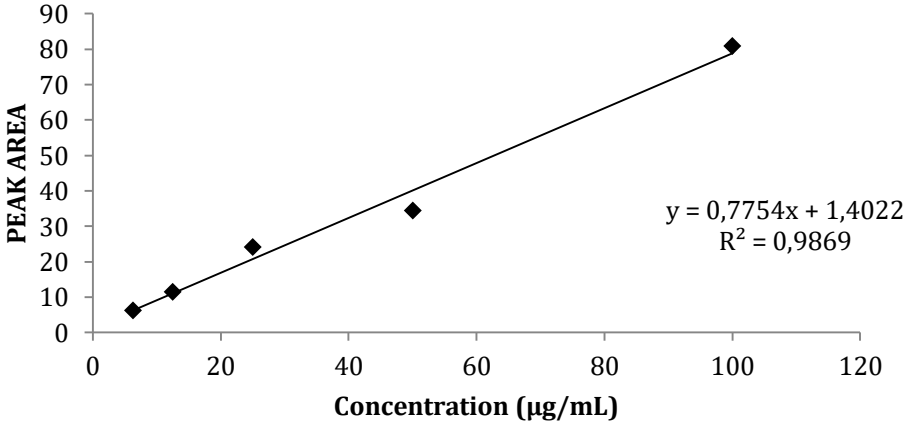


Figure C33: C24:0 FAME-GC standard curve.

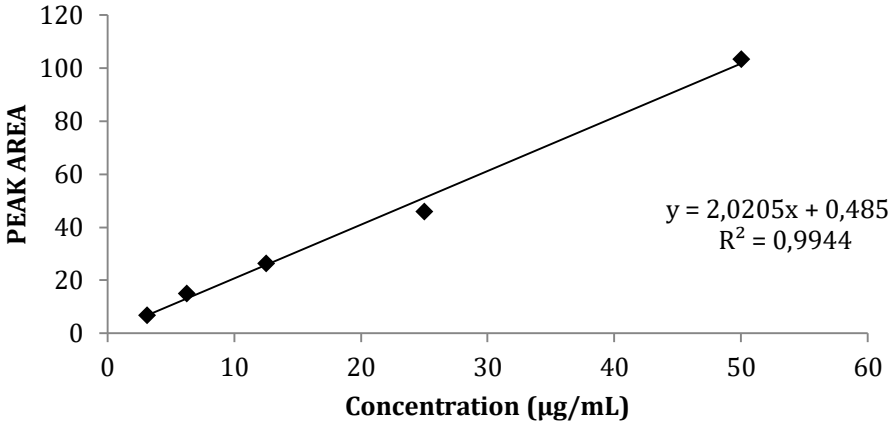


Figure C34: C22:6n3 FAME-GC standard curve.

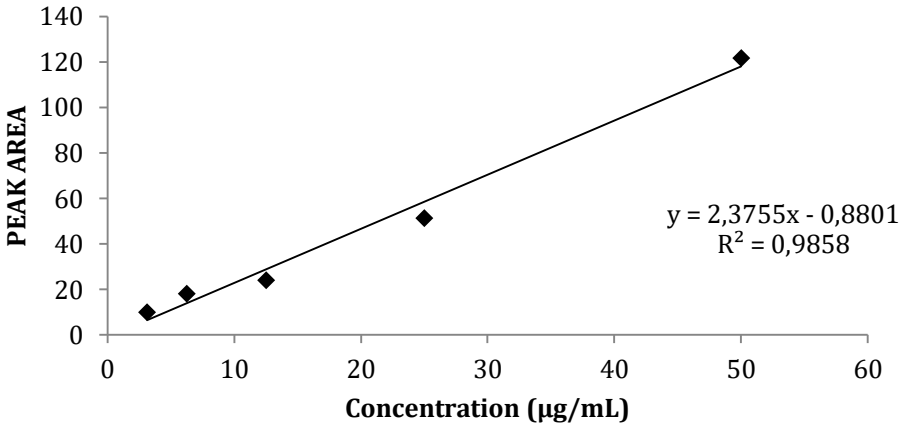


Figure C35: C24:1n9 FAME-GC standard curve.

Lipid content data

Table C1: Lipid yield of WCB 4.1 cultivated in eleven different mediums in triplicate.

Medium designation	Replicate 1 lipid content (g/L)	Replicate 2 lipid content (g/L)	Replicate 3 lipid content (g/L)	Average lipid content (g/L)
AF6	0.093	0.083	0.113	0.096
BBM	0.014	0.010	0.114	0.046
C-medium	0.126	0.126	0.118	0.123
Chu#10	0.379	0.222	0.247	0.283
DYV	0.172	0.246	0.280	0.233
Franquil	0.168	0.153	0.114	0.145
Hase	0.376	0.229	0.131	0.245
JG	0.328	0.332	0.225	0.295
Lu	0.104	0.126	0.169	0.133
WC	0.149	0.125	0.141	0.138
Zarrouk	0.006	0.006	0.006	0.006

Table C2: Estimated cellular lipid percentage of WCB 4.1 cultivated in eleven different mediums in triplicate.

Medium designation	Replicate 1 cellular lipid percentage	Replicate 1 cellular lipid percentage	Replicate 1 cellular lipid percentage	Average cellular lipid percentage
AF6	23.35977	22.45671	30.54189	25.39716
BBM	16.51719	11.14327	23.52035	20.93344
C-medium	25.592	25.14335	26.89769	25.83381
Chu#10	109.357	95.41719	124.9856	109.142
DYV	77.51425	76.33598	101.3924	85.08008
Franquil	88.87199	83.61474	79.26462	84.32004
Hase	36.96971	28.82646	33.41228	33.40556
JG	38.52989	37.30541	26.65222	34.2356
Lu	27.83032	36.12963	22.89899	27.32265
WC	52.39968	39.57592	58.11511	49.22903
Zarrouk	20.48632	21.47144	20.26671	20.74519

Carbohydrate content data

Table C3: Carbohydrate yield of WCB 4.1 cultivated in eleven different mediums in triplicate.

Medium designation	Replicate 1 average carbohydrate content (g/L)	Replicate 2 average carbohydrate content (g/L)	Replicate 3 average carbohydrate content (g/L)	Total average carbohydrate content (g/L)
AF6	0.01708	0.011885	0.012523	0.013829
BBM	0.002811	0.005442	0.025072	0.011108
C-Medium	0.015064	0.016183	0.015351	0.015533
Chu#10	0.035859	0.023199	0.027751	0.028936
DYV	0.021568	0.02665	0.026086	0.024768
Franquil	0.014327	0.015862	0.016721	0.015637
Hase	0.04895	0.043409	0.024638	0.038999
JG	0.044606	0.032964	0.042095	0.039888
LU	0.021187	0.022305	0.025644	0.023045
WC	0.013729	0.014969	0.011995	0.013564
Zarrouk	0.004462	0.00572	0.005333	0.005172

Table C4: Estimated cellular carbohydrate percentage of WCB 4.1 cultivated in eleven different mediums in triplicate.

Medium designation	Replicate 1 cellular carbohydrate percentage	Replicate 1 cellular carbohydrate percentage	Replicate 1 cellular carbohydrate percentage	Average cellular carbohydrate percentage
AF6	4.285098	3.205013	3.386411	3.641791
BBM	3.257484	6.130047	5.187739	5.061849
C-medium	3.060289	3.228699	3.511283	3.257105
Chu#10	10.34484	9.950123	14.06795	11.17157
DYV	9.693228	8.281177	9.461566	9.061193
Franquil	7.600611	8.693896	11.5895	9.104734
Hase	4.807537	5.473377	6.276639	5.308824
JG	5.23587	3.703378	4.995009	4.629604
Lu	5.665376	6.380991	3.470801	4.72765
WC	4.833284	4.734361	4.954052	4.830865
Zarrouk	15.77882	19.09783	17.68409	17.55352

Faculty of Engineering and the Built Environment
Private Bag 3, Wits 2050, South Africa * Telephone (011) 717 – 7007 * Fax: (011) 717 7009

WITS UNIVERSITY

SUBMISSION OF DISSERATION FOR EXAMINATION

1. Name: Jasper
2. Surname: Grobler
3. Student No: 1776234
4. Current Residential Address: 410 Oulandsloop rd, The Willows, Pretoria

Home Telephone Number: _____

Work Telephone Number: _____

Mobile Number: 0761497662

E-mail Address: jas.grobler@gmail.com

5. I hereby submit my Dissertation.
6. I have checked all copies of my Dissertation and declare that no pages are missing or poorly reproduced.
7. Number of copies: 2 (bound) 1 (pdf)
8. I confirm that my signed declaration in terms of Rule G27 is included in each copy of the Dissertation.
9. Title of submitted Dissertation

   Characterisation of South African indigenous microalgae for biofuel production potential

10. Did your research involve animal experimentation or human participants as defined in A.4 of the Senate Standing Orders on Higher degrees?

YES	NO
	X

    If **YES**, please certify that clearance was obtained from the relevant Ethics committee

    Clearance Number: N/A
11. I understand that I may not graduate unless my University fees have been paid in full and I have no Library holds.
12. Name of Supervisor(s)

    Michelle Low School: Chemical and metallurgical engineering

    Kevin Harding School: Chemical and metallurgical engineering

Signature of Candidate: _____

Date: 2019/02/06

FACULTY STAMP

Faculty of Engineering and the Built Environment
Private Bag 3, Wits 2050, South Africa * Telephone (011) 717 – 7007 * Fax: (011) 717 7009

WITS UNIVERSITY

ACQUIESCENCE FORM

Name: Jasper Grobler Student Number: 1776234

Candidate for the degree of: MSc Engineering (ERA00)

has today submitted his/her thesis/dissertation/research report for examination.

Please answer **ALL** questions below by ticking the appropriate box:

Is this research submitted with your acquiescence? (if no attach/submit a separate report to the Faculty Office)

YES	NO

To the best of your knowledge are you able to verify that the candidate has acknowledged wherever any information used in the thesis or other work have been obtained by him or her while employed by, or working under the aegis of any person or organization other than the University or its associated institutions?

YES	NO

Did the students research involve any animal experimentation of human particiapans as defined in A.4 of the Senate Standing Order on Higher Degrees:

YES	NO

If yes, has clearance been obtained rom the relevant Ethics Committee? Provide ethics clearance form.

YES	NO

Name of Supervisor: Michelle Low

Signature:

Date: 30 January 2019

Name of Co-Supervisor:

Signature:

Date: 30/1/2019

Name of Head of School:

Signature:

Date:

FACULTY STAMP

CHANG, E.-H. & YANG, S.-S. 2003. Some characteristics of microalgae isolated in Taiwan for biofixation of carbon dioxide. *Botanical Bulletin of Academia Sinica,* 44.

CHAUDHARY, L., PRADHAN, P., SONI, N., SINGH, P. & TIWARI, A. 2014a. Algae as a feedstock for bioethanol production: new entrance in biofuel world. *Int. J. Chem. Technol. Res,* 6**,** 1381-1389.

CHAUDHARY, L., PRADHAN, P., SONI, N., SINGH, P. & TIWARI, A. 2014b. Algae as a Feedstock for Bioethanol Production: New Entrance in Biofuel World. *Chem. Tech.,* 6**,** 1381-89.

CHAUTON, M. S., REITAN, K. I., NORSKER, N. H., TVETERÅS, R. & KLEIVDAL, H. T. 2015. A techno-economic analysis of industrial production of marine microalgae as a source of EPA and DHA-rich raw material for aquafeed: Research challenges and possibilities. *Aquaculture,* 436**,** 95-103.

CHENA, C., ZHAOB, X., YENC, H., HOD, S., CHENGD, C., LEE, D., BAIB, F. & CHANGA, J. 2013. Microalgae-based carbohydrates for biofuel production. *Biochem. Eng. J.,* 78**,** 1-10.

CHISTI, Y. 2007. Biodiesel from microalgae. *Biotechnol Adv,* 25**,** 294-306.

CHOI, H.-J. & LEE, S.-M. 2015. Biomass and oil content of microalgae under mixotrophic conditions. *Environmental Engineering Research,* 20**,** 25-32.

CHOKSHI, K., PANCHA, I., TRIVEDI, K., GEORGE, B., MAURYA, R., GHOSH, A. & MISHRA, S. 2015. Biofuel potential of the newly isolated microalgae Acutodesmus dimorphus under temperature induced oxidative stress conditions. *Bioresource technology,* 180**,** 162-171.

COBOS, M., PAREDES, J. D., MADDOX, J. D., VARGAS-ARANA, G., FLORES, L., AGUILAR, C. P., MARAPARA, J. L. & CASTRO, J. C. 2017. Isolation and Characterization of Native Microalgae from the Peruvian Amazon with Potential for Biodiesel Production. *Energies,* 10**,** 224.

COLEMAN, J. R. & COLMAN, B. 1981. Inorganic carbon accumulation and photosynthesis in a blue-green alga as a function of external pH. *Plant physiology,* 67**,** 917-921.

COMMISSION, N. P. 2012. Executive Summary–NDP 2030–Our future–make it work. Pretoria, Department: The Presidency.

CONVERTI, A., CASAZZA, A. A., ORTIZ, E. Y., PEREGO, P. & DEL BORGHI, M. 2009. Effect of temperature and nitrogen concentration on the growth and lipid content of Nannochloropsis oculata and Chlorella vulgaris for biodiesel production. *Chemical Engineering and Processing: Process Intensification,* 48**,** 1146-1151.

DE WEVER, A., LELIAERT, F., VERLEYEN, E., VANORMELINGEN, P., VAN DER GUCHT, K., HODGSON, D. A., SABBE, K. & VYVERMAN, W. 2009. Hidden levels of phylodiversity in Antarctic green algae: further evidence for the existence of glacial refugia. *Proceedings of the Royal Society of London B: Biological Sciences,* 276**,** 3591-3599.

DEL CAMPO, J. A., GARCÍA-GONZÁLEZ, M. & GUERRERO, M. G. 2007. Outdoor cultivation of microalgae for carotenoid production: current state and perspectives. *Applied microbiology and biotechnology,* 74**,** 1163-1174.

DEMIRBAS, A. 2010. Use of algae as biofuel sources. *Energy Convers. Manage.,* 51**,** 2738-2749.

DIVAKARAN, R. & PILLAI, V. S. 2002. Flocculation of algae using chitosan. *Journal of Applied Phycology,* 14**,** 419-422.

DOUCHA, J., STRAKA, F. & LÍVANSKÝ, K. 2005. Utilization of flue gas for cultivation of microalgae Chlorella sp.) in an outdoor open thin-layer photobioreactor. *Journal of Applied Phycology,* 17**,** 403-412.

DUBINSKY, Z., MATSUKAWA, R. & KARUBE, I. 1995. Photobiological aspects of algal mass culture. *J. Mar. Biotechnol,* 2**,** 61-65.

DUBOIS, M., GILLES, K. A., HAMILTON, J. K., REBERS, P. T. & SMITH, F. 1956. Colorimetric method for determination of sugars and related substances. *Analytical chemistry,* 28**,** 350-356.

DURAND, P. M., RAOOF, I. & NDHLOVU, A. 2016. Genotypic analysis of 20 isolates in the microalgal culture collection of South Africa (MiCCSA). University of Witwatersrand.

EDWARDS, V. H. 1970. The influence of high substrate concentrations on microbial kinetics. *Biotechnology and Bioengineering,* 12**,** 679-712.

EMERSON, R. & LEWIS, C. M. 1943. The dependence of the quantum yield of Chlorella photosynthesis on wave lenghth of light. *American Journal of Botany***,** 165-178.

FÁBREGAS, J., DOMÍNGUEZ, A., REGUEIRO, M., MASEDA, A. & OTERO, A. 2000. Optimization of culture medium for the continuous cultivation of the microalga Haematococcus pluvialis. *Applied microbiology and biotechnology,* 53**,** 530-535.

FÁBREGAS, J., MASEDA, A., DOMÍNGUEZ, A. & OTERO, A. 2004. The cell composition of Nannochloropsis sp. changes under different irradiances in semicontinuous culture. *World Journal of Microbiology and Biotechnology,* 20**,** 31-35.

FALKOWSKI, P. G. 1997. Evolution of the nitrogen cycle and its influence on the biological sequestration of CO2 in the ocean. *Nature,* 387**,** 272.

FIDALGO, J., CID, A., TORRES, E., SUKENIK, A. & HERRERO, C. 1998. Effects of nitrogen source and growth phase on proximate biochemical composition, lipid classes and fatty acid profile of the marine microalga Isochrysis galbana. *Aquaculture,* 166**,** 105-116.

GINZBURG, M. 1981. Measurements of ion concentrations in Dunaliella parva subjected to hypertonic shock. *Journal of Experimental Botany,* 32**,** 333-340.

GORDILLO, F. J., GOUTX, M., FIGUEROA, F. L. & NIELL, F. X. 1998. Effects of light intensity, CO2 and nitrogen supply on lipid class composition of Dunaliella viridis. *Journal of Applied Phycology,* 10**,** 135-144.

GOUVEIA, L. & OLIVEIRA, A. C. 2009. Microalgae as a raw material for biofuels production. *Journal of industrial microbiology & biotechnology,* 36**,** 269-274.

GRIFFITHS, M., HARRISON, S. T., SMIT, M. & MAHARAJH, D. 2016. Major commercial products from micro-and macroalgae. *Algae Biotechnology.* Springer.

GRIFFITHS, M., VAN HILLE, R. & HARRISON, S. 2010. Selection of direct transesterification as the preferred method for assay of fatty acid content of microalgae. *Lipids,* 45**,** 1053-1060.

GRIFFITHS, M. J., DICKS, R. G., RICHARDSON, C. & HARRISON, S. T. 2011. Advantages and challenges of microalgae as a source of oil for biodiesel. *Biodiesel-feedstocks and processing technologies.* InTech.

GRIFFITHS, M. J. & HARRISON, S. T. 2009. Lipid productivity as a key characteristic for choosing algal species for biodiesel production. *Journal of Applied Phycology,* 21**,** 493-507.

GRIMA, E. M., BELARBI, E.-H., FERNÁNDEZ, F. A., MEDINA, A. R. & CHISTI, Y. 2003. Recovery of microalgal biomass and metabolites: process options and economics. *Biotechnology advances,* 20**,** 491-515.

HAMEED, M. A. 2007. Effect of algal density in bead, bead size and bead concentrations on wastewater nutrient removal. *African Journal of biotechnology,* 6.

HASE, R., OIKAWA, H., SASAO, C., MORITA, M. & WATANABE, Y. 2000. Photosynthetic production of microalgal biomass in a raceway system under greenhouse conditions in Sendai city. *Journal of bioscience and bioengineering,* 89**,** 157-163.

HASHEMI, P. & RAHMANI, Z. 2006. A novel homocystine–agarose adsorbent for separation and preconcentration of nickel in table salt and baking soda using factorial design optimization of the experimental conditions. *Talanta,* 68**,** 1677-1682.

HE, H.-Z., LI, H.-B. & CHEN, F. 2005. Determination of vitamin B1 in seawater and microalgal fermentation media by high-performance liquid chromatography with fluorescence detection. *Analytical and bioanalytical chemistry,* 383**,** 875-879.

HEASMAN, M., DIEMAR, J., O'CONNOR, W., SUSHAMES, T. & FOULKES, L. 2000. Development of extended shelf-life microalgae concentrate diets harvested by centrifugation for bivalve molluscs–a summary. *Aquaculture Research,* 31**,** 637-659.

HOEL, M. & KVERNDOKK, S. 1996. Depletion of fossil fuels and the impacts of global warming. *Resource and energy economics,* 18**,** 115-136.

HSUEH, H., CHU, H. & YU, S.-T. 2007. A batch study on the bio-fixation of carbon dioxide in the absorbed solution from a chemical wet scrubber by hot spring and marine algae. *Chemosphere,* 66**,** 878-886.

HUANG, G., CHEN, F., WEI, D., ZHANG, X. & CHEN, G. 2010. Biodiesel production by microalgal biotechnology. *Applied energy,* 87**,** 38-46.

HUANG, J.-C., CHEN, F. & SANDMANN, G. 2006. Stress-related differential expression of multiple β-carotene ketolase genes in the unicellular green alga Haematococcus pluvialis. *Journal of biotechnology,* 122**,** 176-185.

HUERLIMANN, R., DE NYS, R. & HEIMANN, K. 2010. Growth, lipid content, productivity, and fatty acid composition of tropical microalgae for scale-up production. *Biotechnology and bioengineering,* 107**,** 245-257.

IAGS. 2004. *The Future of Oil* [Online]. Available: http://www.iags.org/futureofoil.html [Accessed 2017/07/09 2017].

IMAHARA, H., MINAMI, E. & SAKA, S. 2006. Thermodynamic study on cloud point of biodiesel with its fatty acid composition. *Fuel,* 85**,** 1666-1670.

IP, P.-F. & CHEN, F. 2005. Employment of reactive oxygen species to enhance astaxanthin formation in Chlorella zofingiensis in heterotrophic culture. *Process biochemistry,* 40**,** 3491-3496.

IQBAL, M. & ZAFAR, S. 1993. Effects of photon flux density, CO 2, aeration rate, and inoculum density on growth and extracellular polysaccharide production byPorphyridium cruentum. *Folia microbiologica,* 38**,** 509-514.

JANAUN, J. & ELLIS, N. 2010. Perspectives on biodiesel as a sustainable fuel. *Renewable and Sustainable Energy Reviews,* 14**,** 1312-1320.

JANET, R., STEIN, E. & STEIN, J. R. 1973. *Handbook of Phycological Methods: Culture Methods and Growth Measurements*, Cambridge University Press.

JIANG, Y., FAN, K.-W., TSZ-YEUNG WONG, R. & CHEN, F. 2004. Fatty acid composition and squalene content of the marine microalga Schizochytrium mangrovei. *Journal of agricultural and food chemistry,* 52**,** 1196-1200.

JORQUERA, O., KIPERSTOK, A., SALES, E. A., EMBIRUCU, M. & GHIRARDI, M. L. 2010. Comparative energy life-cycle analyses of microalgal biomass production in open ponds and photobioreactors. *Bioresour Technol,* 101**,** 1406-13.

JUNEJA, A., CEBALLOS, R. M. & MURTHY, G. S. 2013. Effects of environmental factors and nutrient availability on the biochemical composition of algae for biofuels production: a review. *Energies,* 6**,** 4607-4638.

KLECKA, G. & MAIER, W. 1985. Kinetics of microbial growth on pentachlorophenol. *Applied and environmental microbiology,* 49**,** 46-53.

KNOTHE, G. 2006. Analyzing biodiesel: standards and other methods. *Journal of the American Oil Chemists' Society,* 83**,** 823-833.

KNUCKEY, R. M., BROWN, M. R., ROBERT, R. & FRAMPTON, D. M. 2006. Production of microalgal concentrates by flocculation and their assessment as aquaculture feeds. *Aquacultural Engineering,* 35**,** 300-313.

KONOPKA, A. & BROCK, T. D. 1978. Effect of temperature on blue-green algae (cyanobacteria) in Lake Mendota. *Applied and Environmental Microbiology,* 36**,** 572-576.

LANE, A. E. & BURRIS, J. E. 1981. Effects of environmental pH on the internal pH of Chlorella pyrenoidosa, Scenedesmus quadricauda, and Euglena mutabilis. *Plant physiology,* 68**,** 439-442.

LAPUERTA, M., RODRÍGUEZ-FERNÁNDEZ, J. & DE MORA, E. F. 2009. Correlation for the estimation of the cetane number of biodiesel fuels and implications on the iodine number. *Energy Policy,* 37**,** 4337-4344.

LEE, R. E. 2018. *Phycology*, Cambridge university press.

LELIAERT, F., SMITH, D. R., MOREAU, H., HERRON, M. D., VERBRUGGEN, H., DELWICHE, C. F. & DE CLERCK, O. 2012. Phylogeny and molecular evolution of the green algae. *Critical Reviews in Plant Sciences,* 31**,** 1-46.

LENTON, T. M. & WATSON, A. J. 2000. Redfield revisited: 1. Regulation of nitrate, phosphate, and oxygen in the ocean. *Global biogeochemical cycles,* 14**,** 225-248.

LI, Y., HORSMAN, M., WANG, B., WU, N. & LAN, C. Q. 2008a. Effects of nitrogen sources on cell growth and lipid accumulation of green alga Neochloris oleoabundans. *Applied microbiology and biotechnology,* 81**,** 629-636.

LI, Y., HORSMAN, M., WU, N., LAN, C. Q. & DUBOIS-CALERO, N. 2008b. Biofuels from microalgae. *Biotechnology progress,* 24**,** 815-820.

LIANG, Y., SARKANY, N. & CUI, Y. 2009. Biomass and lipid productivities of Chlorella vulgaris under autotrophic, heterotrophic and mixotrophic growth conditions. *Biotechnology letters,* 31**,** 1043-1049.

LIN, Z., LIN, Z., LI, H. & SHEN, S. 2012. Sequences analysis of ITS region and 18S rDNA of Ulva. *ISRN Botany,* 2012.

LONG, S., HUMPHRIES, S. & FALKOWSKI, P. G. 1994. Photoinhibition of photosynthesis in nature. *Annual review of plant biology,* 45**,** 633-662.

LOPES, J., BOROS, L., KRÄHENBÜHL, M., MEIRELLES, A., DARIDON, J.-L., PAULY, J., MARRUCHO, I. & COUTINHO, J. 2007. Prediction of cloud points of biodiesel. *Energy & Fuels,* 22**,** 747-752.

LU, W., WANG, Z. & YUAN, Z. 2015. Characteristics of lipid extraction from Chlorella sp. cultivated in outdoor raceway ponds with mixture of ethyl acetate and ethanol for biodiesel production. *Bioresource technology,* 191**,** 433-437.

MACKAY, D. & SALUSBURY, T. 1988. Choosing between centrifugation and crossflow microfiltration. *Chemical engineer***,** 45-50.

MALLICK, N. 2002. Biotechnological potential of immobilized algae for wastewater N, P and metal removal: a review. *biometals,* 15**,** 377-390.

MATA, T. M., MARTINS, A. A. & CAETANO, N. S. 2010. Microalgae for biodiesel production and other applications: a review. *Renewable and sustainable energy reviews,* 14**,** 217-232.

MEDLIN, L., ELWOOD, H. J., STICKEL, S. & SOGIN, M. L. 1988. The characterization of enzymatically amplified eukaryotic 16S-like rRNA-coding regions. *Gene,* 71**,** 491-499.

MIYACHI, S., MIYACHI, S. & KAMIYA, A. 1978. Wavelength effects on photosynthetic carbon metabolism in Chlorella. *Plant and Cell Physiology,* 19**,** 277-288.

MOHN, F. 1980. Experiences and strategies in the recovery of biomass from mass cultures of microalgae. *Algae biomass: production and use/[sponsored by the*

National Council for Research and Development, Israel and the Gesellschaft fur Strahlen-und Umweltforschung (GSF), Munich, Germany]; editors, Gedaliah Shelef, Carl J. Soeder.

MONOD, J. 1949. The growth of bacterial cultures. *Annual Reviews in Microbiology,* 3**,** 371-394.

MUNOZ, R. & GUIEYSSE, B. 2006. Algal–bacterial processes for the treatment of hazardous contaminants: a review. *Water research,* 40**,** 2799-2815.

NAGARAJAN, D., LEE, D.-J. & CHANG, J.-S. 2018. Heterotrophic Microalgal Cultivation. *Bioreactors for Microbial Biomass and Energy Conversion.* Springer.

NAKAYAMA, T., MARIN, B., KRANZ, H. D., SUREK, B., HUSS, V. A., INOUYE, I. & MELKONIAN, M. 1998. The basal position of scaly green flagellates among the green algae (Chlorophyta) is revealed by analyses of nuclear-encoded SSU rRNA sequences. *Protist,* 149**,** 367-380.

NASCIMENTO, I. A., MARQUES, S. S. I., CABANELAS, I. T. D., PEREIRA, S. A., DRUZIAN, J. I., DE SOUZA, C. O., VICH, D. V., DE CARVALHO, G. C. & NASCIMENTO, M. A. 2013. Screening Microalgae Strains for Biodiesel Production: Lipid Productivity and Estimation of Fuel Quality Based on Fatty Acids Profiles as Selective Criteria. *Bioenerg. Res.,* 6**,** 1-13.

NIGAM, P. S. & SINGH, A. 2011. Production of liquid biofuels from renewable resources. *Prog. Energy Combust. Sci.,* 37**,** 52-68.

NUR, M. M. A., SETYONINGRUM, T. M. & BUDIAMAN, I. G. S. 2017. Potency of Botryococcus braunii cultivated on palm oil mill effluent wastewater as a source of biofuel. *Environmental Engineering Research,* 22**,** 417-425.

ORCUTT, D. M. & PATTERSON, G. W. 1974. Effect of light intensity upon lipid composition ofNitzschia closterium (Cylindrotheca fusiformis). *Lipids,* 9**,** 1000-1003.

OZKAN, A., KINNEY, K., KATZ, L. & BERBEROGLU, H. 2012. Reduction of water and energy requirement of algae cultivation using an algae biofilm photobioreactor. *Bioresour Technol,* 114**,** 542-8.

PESSOA, M. F. 2012. Harmful effects of UV radiation in algae and aquatic macrophytes-a review. *Emirates Journal of Food and Agriculture,* 24**,** 510.

PETRUSEVSKI, B., BOLIER, G., VAN BREEMEN, A. & ALAERTS, G. 1995. Tangential flow filtration: a method to concentrate freshwater algae. *Water Research,* 29**,** 1419-1424.

PITTMAN, J. K., DEAN, A. P. & OSUNDEKO, O. 2011. The potential of sustainable algal biofuel production using wastewater resources. *Bioresource technology,* 102**,** 17-25.

PRICE, K. & FARAG, I. H. 2013. Resources Conservation in Microalgae Biodiesel Production. *International Journal of Engineering and Technical Research***,** 49-56.

PULZ, O. 2001. Photobioreactors: production systems for phototrophic microorganisms. *Appl Microbiol Biotechnol,* 57**,** 287-93.

RAVEN, J. A. & GEIDER, R. J. 1988. Temperature and algal growth. *New phytologist,* 110**,** 441-461.

REDFIELD, A. C. 1958. The biological control of chemical factors in the environment. *American scientist,* 46**,** 230A-221.

RENAUD, S. & PARRY, D. 1994. Microalgae for use in tropical aquaculture II: Effect of salinity on growth, gross chemical composition and fatty acid composition of three species of marine microalgae. *Journal of applied Phycology,* 6**,** 347-356.

RENAUD, S., PARRY, D., THINH, L.-V., KUO, C., PADOVAN, A. & SAMMY, N. 1991. Effect of light intensity on the proximate biochemical and fatty acid composition of Isochrysis sp. and Nannochloropsis oculata for use in tropical aquaculture. *Journal of Applied Phycology,* 3**,** 43-53.

RENAUD, S. M., THINH, L.-V., LAMBRINIDIS, G. & PARRY, D. L. 2002. Effect of temperature on growth, chemical composition and fatty acid composition of tropical Australian microalgae grown in batch cultures. *Aquaculture,* 211**,** 195-214.

RHEE, G.-Y. 1982. Effects of environmental factors and their interactions on phytoplankton growth. *Advances in microbial ecology.* Springer.

RHEE, G. & GOTHAM, I. J. 1981. The effect of environmental factors on phytoplankton growth: temperature and the interactions of temperature with nutrient limitation. *Limnology and Oceanography,* 26**,** 635-648.

RODOLFI, L., CHINI ZITTELLI, G., BASSI, N., PADOVANI, G., BIONDI, N., BONINI, G. & TREDICI, M. R. 2009. Microalgae for oil: strain selection, induction of lipid synthesis and outdoor mass cultivation in a low-cost photobioreactor. *Biotechnol Bioeng,* 102**,** 100-12.

SACKETT, J. I. 2001. The future of nuclear energy. *Fuel processing technology,* 71**,** 197-204.

SALAMEH, M. G. 2004. Oil Crises, Historical Perspective☆.

SANDNES, J., KÄLLQVIST, T., WENNER, D. & GISLERØD, H. R. 2005. Combined influence of light and temperature on growth rates of Nannochloropsis oceanica: linking cellular responses to large-scale biomass production. *Journal of Applied Phycology,* 17**,** 515-525.

SATYARTHI, J., CHIRANJEEVI, T., GOKAK, D. & VISWANATHAN, P. 2013. An overview of catalytic conversion of vegetable oils/fats into middle distillates. *Catalysis Science & Technology,* 3**,** 70-80.

SCHENK, P. M., THOMAS-HALL, S. R., STEPHENS, E., MARX, U. C., MUSSGNUG, J. H., POSTEN, C., KRUSE, O. & HANKAMER, B. 2008. Second generation biofuels: high-efficiency microalgae for biodiesel production. *Bioenergy research,* 1**,** 20-43.

SHAFIEE, S. & TOPAL, E. 2009. When will fossil fuel reserves be diminished? *Energy policy,* 37**,** 181-189.

SHI, X. M. & CHEN, F. 2002. High-Yield Production of Lutein by the Green Microalga Chlorella protothecoidesin Heterotrophic Fed-Batch Culture. *Biotechnology progress,* 18**,** 723-727.

SHURIN, J. B., ABBOTT, R. L., DEAL, M. S., KWAN, G. T., LITCHMAN, E., MCBRIDE, R. C., MANDAL, S. & SMITH, V. H. 2013. Industrial-strength ecology: trade-offs and opportunities in algal biofuel production. *Ecology letters,* 16**,** 1393-1404.

SMIT, M., GROBLER, J., MALPERMAL, V. & MAHARAJH, D. 2017a. Sub-culture and Establishment of the Microalgae Culture Collection of South Africa, Pretoria, South Africa: CSIR Biosciences.

SMIT, M., MALPERMAL, V., GROBLER, J. & MAHARAJH, D. 2017b. Sub-culture and Consolidation of Indigenous Microalgae into the Microalgae Culture Collection of South Africa, Pretoria, South Africa: CSIR Biosciences.

SOROKIN, C. & KRAUSS, R. W. 1958. The Effects of Light Intensity on the Growth Rates of Green Algae. *Plant physiology,* 33**,** 109.

STANSELL, G. R., GRAY, V. M. & SYM, S. D. 2012. Microalgal fatty acid composition: implications for biodiesel quality. *Journal of Applied Phycology,* 24**,** 791-801.

TALEBNIA, F., KARAKASHEV, D. & ANGELIDAKI, I. 2010. Production of bioethanol from wheat straw: an overview on pretreatment, hydrolysis and fermentation. *Bioresource technology,* 101**,** 4744-4753.

TAMER, E., AMIN, M., OSSAMA, E., BO, M. & BENOIT, G. 2006. Biological treatment of industrial wastes in a photobioreactor. *Water science and technology,* 53**,** 117-125.

TASIĆ, M. B., KONSTANTINOVIĆ, B. V., LAZIĆ, M. L. & VELJKOVIĆ, V. B. 2009. The acid hydrolysis of potato tuber mash in bioethanol production. *Biochemical engineering journal,* 43**,** 208-211.

TJAHJONO, A. E., HAYAMA, Y., KAKIZONO, T., TERADA, Y., NISHIO, N. & NAGAI, S. 1994. Hyper-accumulation of astaxanthin in a green algaHaematococcus pluvialis at elevated temperatures. *Biotechnology letters,* 16**,** 133-138.

TONG, D., HU, C., JIANG, K. & LI, Y. 2011. Cetane number prediction of biodiesel from the composition of the fatty acid methyl esters. *Journal of the American Oil Chemists' Society,* 88**,** 415-423.

TYRRELL, T. 1999. The relative influences of nitrogen and phosphorus on oceanic primary production. *Nature,* 400**,** 525.

ULLMANN, F., GERHARTZ, W., YAMAMOTO, Y. S., CAMPBELL, F. T., PFEFFERKORN, R., ROUNSAVILLE, J. F. & ULLMANN, F. 1985. *Ullmann's encyclopedia of industrial chemistry,* Weinheim, Federal Republic of Germany; Deerfield Beach, FL, USA, VCH.

VAN GERPEN, J. 2009. Biodiesel: small scale production and quality requirements. *Methods Mol Biol,* 581**,** 281-90.

VERGARA-FERNÁNDEZ, A., HERNÁNDEZ, S. & REVAH, S. 2008. Phenomenological model of fungal biofilters for the abatement of hydrophobic VOCs. *Biotechnology and Bioengineering,* 101**,** 1182-1192.

VISVIKI, I. & SANTIKUL, D. 2000. The pH tolerance of Chlamydomonas applanata (Volvocales, Chlorophyta). *Archives of environmental contamination and toxicology,* 38**,** 147-151.

WANG, B., LI, Y., WU, N. & LAN, C. Q. 2008. CO2 bio-mitigation using microalgae. *Applied microbiology and biotechnology,* 79**,** 707-718.

WATANABE, M., KAWACHI, M., HIROKI, M. & KASAI, F. 2000. NIES-collection. list of strains. microalgae and protozoa. microbial culture collection. *National Institute for Environmental Studies, Tsukuba,* 159.

WEN, Z.-Y. & CHEN, F. 2003. Heterotrophic production of eicosapentaenoic acid by microalgae. *Biotechnology advances,* 21**,** 273-294.

WOJTOWICZ, J. A. 2001. The carbonate system in swimming pool water. *Journal of the Swimming Pool and Spa Industry,* 3**,** 54-59.

XU, X.-Q. & BEARDALL, J. 1997. Effect of salinity on fatty acid composition of a green microalga from an antarctic hypersaline lake. *Phytochemistry,* 45**,** 655-658.

YANG, C., HUA, Q. & SHIMIZU, K. 2000. Energetics and carbon metabolism during growth of microalgal cells under photoautotrophic, mixotrophic and cyclic light-autotrophic/dark-heterotrophic conditions. *Biochemical Engineering Journal,* 6**,** 87-102.

YOU, T. & BARNETT, S. M. 2004. Effect of light quality on production of extracellular polysaccharides and growth rate of Porphyridium cruentum. *Biochemical Engineering Journal,* 19**,** 251-258.

ZARROUK, C. 1966. *Influence de divers facteuors physiques et chimiques sur lacroissance et la photosynthese de, Geitle, Spirulina maxima.* Ph. D. thesis, University of Paris, France.

ZHILA, N. O., KALACHEVA, G. S. & VOLOVA, T. G. 2011. Effect of salinity on the biochemical composition of the alga Botryococcus braunii Kütz IPPAS H-252. *Journal of Applied Phycology,* 23**,** 47-52.

ZITTELLI, G. C., BIONDI, N., RODOLFI, L. & TREDICI, M. R. 2013. Photobioreactors for mass production of microalgae. *Handbook of microalgal culture: applied phycology and biotechnology,* 2**,** 225-266.